



**INVESTIGATION OF ROLE OF ENTEROVIRUS A71  
NONSTRUCTURAL 3A PROTEIN AND INTERACTING  
PROTEIN IN VIRAL REPLICATION**

**BY**

**MISS PATHAYA RATTANAKOMOL**

**A DISSERTATION SUBMITTED IN PARTIAL FULFILLMENT  
OF THE REQUIREMENTS FOR THE DEGREE OF THE  
DOCTOR OF PHILOSOPHY (BIOMEDICAL SCIENCES)**

**GRADUATE PROGRAM IN BIOMEDICAL SCIENCES  
FACULTY OF ALLIED HEALTH SCIENCES  
THAMMASAT UNIVERSITY  
ACADEMIC YEAR 2020**

**COPYRIGHT OF THAMMASAT UNIVERSITY**

**INVESTIGATION OF ROLE OF ENTEROVIRUS A71  
NONSTRUCTURAL 3A PROTEIN AND INTERACTING  
PROTEIN IN VIRAL REPLICATION**

**BY**

**MISS PATTHAYA RATTANAKOMOL**

**A DISSERTATION SUBMITTED IN PARTIAL FULFILLMENT  
OF THE REQUIREMENTS FOR THE DEGREE OF THE  
DOCTOR OF PHILOSOPHY (BIOMEDICAL SCIENCES)**

**GRADUATE PROGRAM IN BIOMEDICAL SCIENCES  
FACULTY OF ALLIED HEALTH SCIENCES  
THAMMASAT UNIVERSITY  
ACADEMIC YEAR 2020**

**COPYRIGHT OF THAMMASAT UNIVERSITY**

THAMMASAT UNIVERSITY  
FACULTY OF ALLIED HEALTH SCIENCES

DISSERTATION

BY

MISS PATTHAYA RATTANAKOMOL

ENTITLED

INVESTIGATION OF ROLE OF ENTEROVIRUS A71 NONSTRUCTURAL 3A  
PROTEIN AND INTERACTING PROTEIN IN VIRAL REPLICATION

was approved as partial fulfillment of the requirements for  
the degree of Doctor of Philosophy (Biomedical Sciences)  
on May 17, 2021

Chairman	<u>Sansanee Noisakran</u> (Sansanee Noisakran, Ph.D.)
Member and Advisor	<u>Jeeraphong T.</u> (Assist. Prof. Jeeraphong Thanongsaksrikul, Ph.D.)
Member and Co-Advisor	<u>Pongsri Tongtawe</u> (Assist. Prof. Pongsri Tongtawe, Ph.D.)
Member and Co-Advisor	<u>Potjane</u> (Assist. Prof. Potjane Srimanote, Ph.D.)
Member and Co-Advisor	<u>P. Angkasekwinai</u> (Assoc. Prof. Pornpimon Angkasekwinai, Ph.D.)
Dean	<u>Plaiwan Sattanon</u> (Assoc. Prof. Plaiwan Sattanon, Ph.D.)

Dissertation Title	INVESTIGATION OF ROLE OF ENTEROVIRUS A71 NONSTRUCTURAL 3A PROTEIN AND INTERACTING PROTEIN IN VIRAL REPLICATION
Author	Miss Patthaya Rattanakomol
Degree	Doctor of Philosophy (Biomedical Sciences)
Major	Molecular Immunology and Microbiology
Faculty	Faculty of Allied Health Sciences
University	Thammasat University
Dissertation Advisor	Assistant Professor Jeeraphong Thanongsaksrikul, Ph.D.
Dissertation Co-Advisors	Prof. Wanpen Chaicumpa, D.V.M. (Hons.), Ph.D. Assoc. Prof. Pornpimon Angkasekwinai, Ph.D. Assist. Prof. Pongsri Tongtawe, Ph.D. Assist. Prof. Potjanee Srimanote, Ph.D. Suganya Yongkiettrakul, Ph.D.
Academic Year	2020

## ABSTRACT

Enterovirus A71 (EV-A71) is a positive-sense single-stranded RNA (+ssRNA) virus in the *Picornaviridae* family that causes hand, foot, and mouth disease (HFMD) associated with neurological complications in young children. As yet, there is no specific treatment for EV-A71 infection due to inadequate information on viral neuropathogenesis. Generally, the +ssRNA viruses have strategies for establishing viral replication by remodeling host cell membranes to construct distinct platforms for viral RNA synthesis and virion assembly, termed as replication organelles (ROs). In enteroviruses, the nonstructural 3A protein has been reported as a key player in RO formation. In this study, the cellular factor in human SH-SY5Y neuronal cells interacting with the EV-A71 3A protein was searched for understanding structure and function as well as the role of the 3A protein or its interacting counterpart in neuropathogenesis. Transient expression of recombinant 3A protein in fusion with FLAG and mCherry protein (FLAG-3A-mCherry) was successfully established in human neuronal SH-SY5Y cells. By FLAG pull-down,

proteins in neuronal cell co-purified with FLAG-3A-mCherry were identified by LC-MS/MS. The potential identified EV-A71 3A interacting protein was human PRSS3 (mesotrypsinogen, also known as brain trypsinogen). The transcript variants of PRSS3 were further identified in SH-SY5Y cells. It was shown that only PRSS3 variant 3 (*PRSS3-v3*) was detected. Thus, full-length cDNA of *PRSS3-v3* molecularly fused with the coding sequence of Myc tag (*FL-PRSS3-Myc*) was constructed. The interaction of FLAG-3A-mCherry and FL-PRSS3-Myc was confirmed by co-immunoprecipitation assay using anti-Myc magnetic beads. The role of PRSS3 in EV-A71 replication was subsequently investigated by overexpressing FL-PRSS3-Myc or silencing *PRSS3* by siRNA in EV-A71 infected cells. The results have shown that PRSS3 had a positive effect on EV-A71 replication. The detailed mechanism of human PRSS3 involved in EV-A71 replication and neuropathogenesis warrants further experimental elucidation. In conclusion, this study has discovered a novel EV-A71 3A interacting protein that offers the opportunity to study the neuropathogenesis of EV-A71 infection which paves the way for developing a specific treatment for EV-A71 infection.

**Keywords:** Enterovirus A71, Nonstructural 3A protein, Replication organelles, Neuronal cells, Human PRSS3



## ACKNOWLEDGEMENTS

I would like to thank the following people for helping with this research project, without whom I would not have made it through my Ph.D. degree.

I would like first to thank to my dissertation advisor, Assist. Prof. Jeeraphong Thanongsaksrikul, for his support, encouragement, and patience, and for the thoughtful comments and recommendations on this dissertation.

I would also like to thank to my co-advisors, Prof. Dr. Wanpen Chaicumpa, D.V.M. (Hons.), Assist. Prof. Dr. Pongsri Tongtawe, Assist. Prof. Dr. Potjanee Srیمانote, Assoc. Prof. Dr. Pornpimon Angkasekwinae, and Dr. Suganya Yongkiettrakul whose expertise was invaluable in formulating the research questions and methodology.

I would like to acknowledge my lovely colleagues, Miss Oratai Supasorn or P.Katae, for providing advices, encouragement, smile, and laughter, without her I would not have been able to complete this research. Furthermore to all members of Molecular Immunology and Microbiology; P.Kob, P.Num, P.Nun, P. New, P. Bell, P. Mo, P.Su, N.Pang, N.Em, N. Nun, N.Pam, N.Kred, N.Joy, N.Taa, who have been a great source of support and made my graduate life full of fun and experiences.

I am extremely thankful to my bestie, Sine Wasinee, for providing me emotional support, smile, cute souvenirs from wherever she visited.

I am also thankful to all professors, staffs, and friends in Graduate Program in Biomedical Sciences, Faculty of Allied Health Sciences, Thammasat University.

And my biggest thanks to my family for all support during this period of intense Ph.D. life. I love them so much.

Miss Patthaya Rattanakomol

**TABLE OF CONTENTS**

	Page
ABSTRACT	(1)
ACKNOWLEDGEMENTS	(3)
LIST OF TABLES	(11)
LIST OF FIGURES	(12)
LIST OF ABBREVIATIONS	(18)
CHAPTER 1 INTRODUCTION	1
CHAPTER 2 REVIEW OF LITERATURE	3
2.1 Clinical aspects, virology and genome organization of EV-A71	3
2.2 Epidemiology	5
2.3 Enterovirus 71 life cycle	6
2.3.1 Viral entry	7
2.3.2 Viral genome uncoating	8
2.3.3 Viral translation and polyprotein processing	10
2.3.4 Host cellular membrane remodeling and virus genome replication	11
2.3.5 Virus assembly and egress (morphogenesis)	15
2.4 Pathogenesis	19
CHAPTER 3 OBJECTIVES	21

## TABLE OF CONTENTS (Cont.)

	Page
3.1 Primary objective	21
3.2 Specific objectives	21
3.3 Hypothesis	21
 CHAPTER 4 MATERIALS AND METHODS	 22
4.1 Virus propagation and preparation of genetic material of EV-A71	22
4.1.1 Propagation of EV-A71	22
4.1.2 Determination of the viral titer	22
4.1.3 Preparation and detection of EV-A71 genomic RNA	24
4.2 Determination of EV-A71 infection of human neuronal cells using CCID50 method	25
4.3 Searching interacting counterparts of the EV-A71 nonstructural 3A protein in EV-A71 permissive human neuronal cells	26
4.3.1 Molecular cloning of EV-A71 nonstructural 3A coding sequence	26
4.3.1.1 Construction of recombinant plasmid DNA carrying coding sequence of EV-A71 nonstructural 3A in-frame with FLAG-epitope tag at 5'-end	26
(1) PCR amplification of <i>FLAG-3A</i>	26
(2) Cloning of <i>EcoRI-FLAG-3A-Sall</i> into cloning vector	26
4.3.1.2 Prediction of functional domain/motif of EV-A71 NS3A	27
4.3.1.3 Subcloning of FLAG-3A coding sequence into mammalian expression vector	29



## TABLE OF CONTENTS (Cont.)

	Page
4.3.1.4 Detection of FLAG-3A protein expression in mammalian cells	30
(1) Transfection with pLVX:: <i>FLAG-3A</i>	30
(2) Detection of FLAG-3A protein expression by immunofluorescence (IF) assay	31
4.3.1.5 Expression of FLAG-3A protein in mammalian cells	32
4.3.1.6 Construction of recombinant plasmid DNA carrying coding sequence of EV-A71 nonstructural 3A in-frame with FLAG-epitope tag at 5'-end and red monomeric fluorescent protein mCherry at 3'-end	33
(1) PCR amplification of coding sequence of EV-A71 nonstructural 3A in-frame with FLAG-epitope tag at 5'-end and red monomeric fluorescent protein mCherry at 3'-end	33
(2) Cloning of FLAG-3A-mCherry coding sequence	37
(3) Subcloning of FLAG-3A-mCherry coding sequence to mammalian expression vector	39
4.3.1.7 Examination of FLAG-3A-mCherry protein expression in mammalian cells using fluorescence microscope	39
4.3.1.8 Detection of FLAG-3A-mCherry protein expression in mammalian cells using western blot analysis	39
(1) Transfection with pLVX:: <i>FLAG-3A-mCherry</i>	39
(2) Detection of FLAG-3A-mCherry expression	40
4.3.2 Pull-down of EV-A71 3A interacting proteins in human neuronal SH-SY5Y cells	42

## TABLE OF CONTENTS (Cont.)

	Page
4.3.3 Protein identification by Liquid Chromatography Tandem Mass Spectrometer (LC-MS/MS) and analysis	43
4.4 Investigation of expression profiles of trypsinogens (PRSSs) in mammalian cells	44
4.4.1 Determination of PRSS expression	44
4.4.2 Subtyping of specific PRSS expressed by human SH-SY5Y neuronal cells	45
4.5 Confirmation of direct protein-protein binding between EV-A71 3A protein and the identified interacting protein by immunoprecipitation assay	46
4.5.1 Production of recombinant PRSS3 transcript variant 3 fused with Myc epitope tag at C-terminal end by mammalian expression system	46
4.5.2 Production of recombinant mCherry fused with FLAG epitope tag at N-terminal end by mammalian expression system	48
4.5.3 Confirmation of interaction of EV-A71 3A and PRSS3 proteins using immunoprecipitation assay	49
4.5.3.1 Preparation of total protein lysates	49
4.5.3.2 Immunoprecipitation assay	49
4.6 Determination of role of PRSS3 in EV-A71 replication	51
4.1.1 Examination of permissiveness of HEK293T to EV-A71 infection	51
4.1.2 Determination of role of PRSS3 overexpression in EV-A71 replication	51
4.1.3 Determination of effect of PRSS3 loss-of-function on EV-A71 replication	53
4.6.3.1 Gene knockdown of <i>PRSS3</i> by siRNAs	53

## TABLE OF CONTENTS (Cont.)

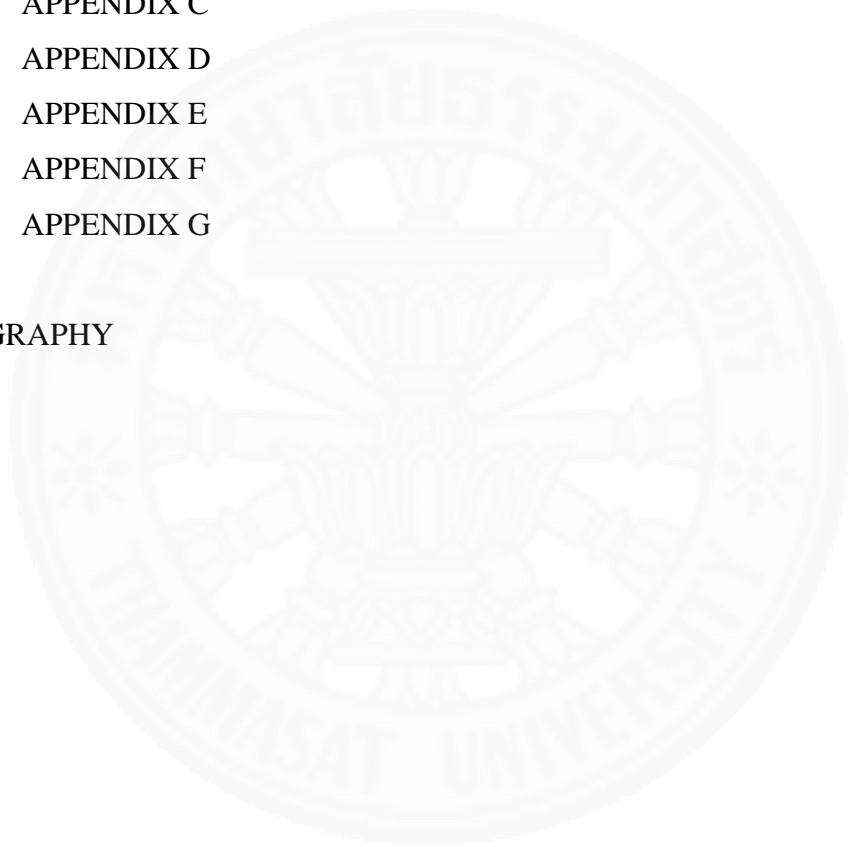
	Page
4.6.3.2 Effect of gene knockdown of <i>PRSS3</i> on EV-A71 replication	55
 CHAPTER 5 RESULTS	 57
5.1 Virus propagation and preparation of genetic material of EV-A71	57
5.2 Selection of human neuronal cells that are permissive to EV-A71 infection	57
5.3 Molecular cloning of EV-A71 nonstructural 3A coding sequence	58
5.3.1 Construction of recombinant plasmid DNA carrying coding sequence of EV-A71 nonstructural 3A in-frame with FLAG-epitope tag at 5'-end	58
5.3.2 Prediction of functional domain/motif EV-A71 NS3A	61
5.3.3 Construction of recombinant mammalian expression plasmid to produce EV-A71 3A protein	67
5.3.4 Construction of recombinant plasmid DNA carrying coding sequence of EV-A71 nonstructural 3A in-frame with FLAG-epitope tag at 5'-end and red monomeric fluorescent protein mCherry at 3'-end	72
5.3.5 Determination of FLAG-3A-mCherry protein expression in mammalian cells using fluorescence microscope	82
5.3.6 Determination of FLAG-3A-mCherry protein expression in mammalian cells using western blot analysis	84

## TABLE OF CONTENTS (Cont.)

	Page
5.3.7 Pull-down of FLAG-3A-mCherry interacting protein using anti-FLAG <sup>®</sup> M2 magnetic beads	86
5.3.8 Protein identification by liquid chromatography mass spectrometer (LC-MS/MS) and analysis	88
5.4 Determination of PRSS gene expression in SH-SY5Y cells	91
5.5 Confirmation of direct protein-protein binding between EV-A71 3A protein and the PRSS3 variant 3 protein by co-immunoprecipitation assay	99
5.5.1 Production of recombinant PRSS3 transcript variant 3 by mammalian expression system	99
5.5.2 Confirmation of direct interaction between EV-A71 3A and PRSS3 protein interaction by co-immunoprecipitation assay	111
5.6 Role of PRSS3 in EV-A71 replication	115
<b>CHAPTER 6 DISCUSSION</b>	<b>121</b>
2.1 The use of human SH-SY5Y neuroblastoma and HEK293T cells as models in CNS-associated EV-A71 infection	122
2.2 Molecular cloning of EV-A71 nonstructural 3A coding sequence	123
2.3 FLAG pull-down and protein identification by liquid chromatography mass spectrometer (LC-MS/MS) and analysis	127
2.4 Role of PRSS3 in EV-A71 replication	129
<b>CHAPTER 7 CONCLUSION AND RECOMMENDATION</b>	<b>133</b>
<b>REFERENCES</b>	<b>134</b>

**TABLE OF CONTENTS (Cont.)**

	Page
APPENDICES	148
APPENDIX A	149
APPENDIX B	152
APPENDIX C	153
APPENDIX D	154
APPENDIX E	156
APPENDIX F	159
APPENDIX G	160
BIOGRAPHY	177



**LIST OF TABLES**

Table		Page
5.1	List of proteins identified by LC-MS/MS	89
5.2	Generated peptide sequences of PRSS1 and PRSS3 by LC-MS/MS	90





## LIST OF FIGURES

Figures	Page
4.1 Genome structure of picornavirus, processed polyprotein and mature proteins	4
4.2 Schematic representation of poliovirus structure, a member of <i>Picornaviridae</i> family.	5
4.3 Geographic distribution of EV-A71 infection	6
4.4 Model of SCARB2-mediated EV-A71 entry and genome uncoating	9
4.5 Picornavirus polyprotein processing mediated by 2A <sup>pro</sup> and 3C <sup>pro</sup>	11
4.6 Morphology of picornavirus replication organelles (ROs)	12
4.7 Morphology of double membrane vesicles (DMVs) of picornavirus replication organelles (ROs).	13
4.8 Model of PV- and CVB3-modified membranes for genome replication mediated by enterovirus 3A proteins	14
4.9 Model of PV assembly and egress.	16
4.10 Picornavirus morphogenesis	18
4.11 Enterovirus 71 (EV-A71) pathogenesis	20
4.1 Schematic map of pJET1.2/blunt cloning vector shows genetic elements and restriction sites in multiple cloning site (MCS)	28
4.2 Schematic map of pLVX-Puro lentiviral expression vector shows genetic elements, and restriction sites and sequences in multiple cloning site (MCS)	30
4.3 Schematic drawing of amplification of <i>EcoRI-FLAG-3A-mCherry-XbaI</i> using overlap extension PCR (OE-PCR)	34
4.4 Schematic map of pGEM <sup>®</sup> -T Easy vector shows elements and restriction sites in the vector	38
4.5 Schematic diagram of pull down of EV-A71 3A interacting proteins using anti-FLAG <sup>®</sup> M2 magnetic beads	43

## LIST OF FIGURES (Cont.)

Figures	Page
4.6 Schematic diagram of transfection of HEK293T cells followed by EV-A71 infection	52
5.1 Determination of permissiveness to EV-A71 infection of SH-SY5Y and SK-N-MC neuronal cells	58
5.2 Agarose gel electrophoresis of <i>FLAG-3A</i> amplicons	59
5.3 Agarose gel electrophoresis of PCR products amplified from colonies of JM109 <i>E. coli</i> transformed with pJET1.2:: <i>FLAG-3A</i> by colony PCR	60
5.4 Nucleotide sequence of <i>FLAG-3A</i> inserted in pJET1.2/blunt cloning vector and the deduced amino acid sequence of <i>FLAG-3A</i> coding sequence	61
5.5 Homology search of the cloned <i>EV-A71 3A</i> sequence using NCBI BLASTx.	63
5.6 Functional domain prediction of EV-A71 3A protein	64
5.7 Homology structure of EV-A71 3A protein modeled by Swiss-Model	65
5.8 Prediction of myristoylation site of the amino acid sequences deduced from the cloned EV-A71 3A nucleotide sequences	66
5.9 Agarose gel electrophoresis of the double digestion of pLVX-Puro and pJET1.2:: <i>FLAG-3A</i> using <i>EcoRI</i> and <i>XbaI</i> endonucleases	68
5.10 Agarose gel electrophoresis of PCR products amplified from colonies of JM109 <i>E. coli</i> transformed with pLVX:: <i>FLAG-3A</i> by colony PCR.	69
5.11 Expression of <i>FLAG-3A</i> protein in HEK293T and SH-SY5Y cells	71
5.12 Agarose gel electrophoresis (1%) of <i>EcoRI-FLAG-3A-mCherry</i> amplicons	73

## LIST OF FIGURES (Cont.)

Figures	Page
5.13 Agarose gel electrophoresis of <i>3A-mCherry-Xba</i> amplification	74
5.14 Agarose gel electrophoresis of the gel-purified <i>EcoRI-FLAG-3A-mCherry</i> and <i>3A-mCherry-XbaI</i>	75
5.15 Agarose gel electrophoresis of the PCR amplicons of the full length <i>EcoRI-FLAG-3A-mCherry-XbaI</i>	76
5.16 Agarose gel electrophoresis of PCR products amplified from 5 randomly selected colonies of JM109 <i>E. coli</i> transformed with pGEM <sup>®</sup> -T:: <i>FLAG-3A-mCherry</i> by colony PCR	78
5.17 Nucleotide sequence of <i>EcoRI-FLAG-3A-mCherry-XbaI</i> inserted in pGEM <sup>®</sup> -T Easy vector and the deduced amino acid sequence of <i>EcoRI-FLAG-3A-mCherry-XbaI</i> coding sequence	79
5.18 Agarose gel electrophoresis of the double digestion of pGEM <sup>®</sup> -T:: <i>FLAG-3A-mCherry</i> using <i>EcoRI</i> and <i>XbaI</i> endonucleases	80
5.19 Agarose gel electrophoresis of PCR products amplified from colonies of JM109 <i>E. coli</i> transformed with pLVX:: <i>FLAG-3A-mCherry</i> by colony PCR	81
5.20 Expression of FLAG-3A-mCherry or mCherry proteins in HEK293T and SH-SY5Y cells	83
5.21 Detection of mCherry and FLAG-3A-mCherry proteins expressed in HEK293T and SH-SY5Y cells	85
5.22 Pull down of proteins with EV-A71 3A in cell lysate prepared from FLAG-3A-mCherry-transfected SH-SY5Y cells	87
5.23 Mutialignment of amino acid sequences of PRSS1 and four PRSS3 transcript variants by DNAMAN program	90

### LIST OF FIGURES (Cont.)

Figures	Page
5.24 Agarose gel electrophoresis of <i>PRSS</i> gene amplification determined in HEK293T and SH-SY5Y cells by RT- PCR	92
5.25 Detection of endogenous <i>PRSS3</i> protein in HEK293T and SH-SY5Y cells	92
5.26 Agarose gel electrophoresis of amplicons of full-length <i>PRSS3</i> transcript variants determined in SH-SY5Y cells by RT-PCR	94
5.27 Agarose gel electrophoresis of PCR products amplified from colonies of JM109 <i>E. coli</i> transformed with pGEM <sup>®</sup> -T:: <i>PRSS3-V3</i> by colony PCR	95
5.28 Nucleotide sequence of <i>PRSS3-V3</i> inserted in pGEM <sup>®</sup> -T Easy vector and the deduced amino acid sequence of <i>PRSS3-V3</i> coding sequence	96
5.29 Homology search of the cloned <i>PRSS3-V3</i> coding sequence inserted in pGEM <sup>®</sup> -T vector by BLASTn.	97
5.30 Homology search of the cloned <i>PRSS3-V3</i> coding sequence inserted in pGEM <sup>®</sup> -T vector by BLASTx.	98
5.31 Agarose gel electrophoresis of PCR amplicons of <i>FL-PRSS3-Myc</i> amplification	100
5.32 Agarose gel electrophoresis of PCR products amplified from colonies of JM109 <i>E. coli</i> transformed with pGEM <sup>®</sup> -T:: <i>FL-PRSS3-Myc</i> by colony PCR	101
5.33 Nucleotide sequence of <i>FL-PRSS3-Myc</i> inserted in pGEM <sup>®</sup> -T Easy vector and the deduced amino acid sequence of <i>FL-PRSS3-Myc</i> coding sequence	102
5.34 Agarose gel electrophoresis of the double digestion of pGEM <sup>®</sup> -T:: <i>FL-PRSS3-Myc</i> and pLVX-Puro using <i>XhoI</i> and <i>XbaI</i> endonucleases	103

## LIST OF FIGURES (Cont.)

Figures		Page
5.35	Agarose gel electrophoresis of PCR products amplified from colonies of JM109 <i>E. coli</i> transformed with pLVX:: <i>FL-PRSS3-Myc</i>	104
5.36	Nucleotide sequence of <i>FL-PRSS3-Myc</i> inserted in pLVX-Puro vector and the deduced amino acid sequence of <i>FL-PRSS3-Myc</i> coding sequence	105
5.37	Micrographs of FL-PRSS3-Myc protein expressed in HEK293T cells visualized by immunofluorescence assay on of FL-PRSS3-Myc protein in HEK293T cells	106
5.38	Agarose gel electrophoresis of <i>FLAG-mCherry</i> amplification and clone selection of <i>FLAG-mCherry</i> inserted in pGEM <sup>®</sup> -T Easy vector by colony PCR	108
5.39	Agarose gel electrophoresis of the double digestion of pGEM <sup>®</sup> -T:: <i>FLAG-mCherry</i> by <i>Xho</i> I and <i>Xba</i> I endonucleases and clone selection of <i>FLAG-mCherry</i> inserted in pLVX-Puro vector by colony PCR	109
5.40	Alignment of the verified <i>FLAG-mCherry</i> sequence with sequence of <i>FLAG-mCherry</i> template	110
5.41	Micrographs of FLAG-mCherry protein expressed in HEK293T cells visualized by fluorescence microscopy	111
5.42	Western blot analysis of FLAG-mCherry, FLAG-3A-mCherry, and FL-PRSS3-Myc expressed in HEK293T cells	113
5.43	Co-immunoprecipitation (IP) assay for determining direct protein-protein interaction of FLAG-3A-mCherry and FL-PRSS3-Myc	114
5.44	Determination of permissiveness of HEK293T cells to EV-A71 infection	116

**LIST OF FIGURES (Cont.)**

Figures		Page
5.45	Determination of relative fold-change of <i>EV-A71 RNA</i> copy number by semi-quantitative real-time RT-PCR in response to overexpression of neuron-derived <i>PRSS3</i> in pLVX:: <i>FL-PRSS3-Myc</i> -transfected HEK293T cells	118
5.46	Determination of relative fold-change of <i>EV-A71 RNA</i> copy number by semi-quantitative real-time RT-PCR in response to the knockdown of <i>PRSS3</i>	119
6.1	Prediction of <i>EV-A71 3A</i> protein structure compared to the poliovirus 3A-N	127



## LIST OF ABBREVIATIONS

<b>Symbols/Abbreviations</b>	<b>Terms</b>
ACAD9	Acyl-CoA dehydrogenase family member 9
ACBD3	Acyl-CoA binding domain containing 3
ACTB	Actin beta
ACN	Acetonitrile
AD	Alzheimer's disease
AP	Alkaline phosphatase
APS	Ammonium persulfate
ALS	Amyotrophic lateral sclerosis
Arf1	ADP-ribosylation factor 1
bp	Base pair
BBB	Blood-brain barrier
BSA	Bovine serum albumin
cDNA	Complementary DNA
CCID50	Median cell culture infectious dose
CDS	Coding sequence
CERT	Ceramide transfer protein
CNS	Central nervous system
CPE	Cytopathic effect
Ct	Cycle threshold
CVB3	Coxsackievirus B3
DENV	Dengue virus
DMVs	Double-membrane vesicles
DNA	Deoxyribonucleic acid
eIFs	Eukaryotic initiation factors
EBV	Epstein-Barr virus
ER	Endoplasmic reticulum
EV-A71	Enterovirus A71

**LIST OF ABBREVIATIONS (Cont.)**

<b>Symbols/Abbreviations</b>	<b>Terms</b>
EV-D68	Enterovirus D68
FAPP1/FAPP2	Four-phosphate-adaptor protein 1 and 2
FBS	Fetal bovine serum
GAPDH	Glyceraldehyde 3-phosphate dehydrogenase
GBF1	Golgi brefeldin A resistant guanine nucleotide exchange factor 1
GEF	Guanine nucleotide exchange factor
GFP	Green fluorescent protein
h.p.i.	hour post-infection
h.p.t.	hour post-transfection
HAV	Hepatitis A virus
HCV	Hepatitis C virus
HEV	Hepatitis E virus
HEK293T cells	Human embryonic kidney 293T cells
HFMD	Hand, foot, and mouth disease
HIV	Human immunodeficiency virus
HRP	Horseradish peroxidase
Hsp90	Heat shock protein 90
IRES	Internal ribosome entry site
ITAFs	IRES-specific <i>trans</i> -acting factors
JEV	Japanese encephalitis virus
kb	Kilobase
kDa	Kilodalton
LC-MS/MS	Liquid chromatography mass spectrometer
LIMP2	Lysosome integral membrane protein 2
MCS	Multiple cloning site
MHC	Major histocompatibility complex
MOI	Multiplicity of infection

**LIST OF ABBREVIATIONS (Cont.)**

<b>Symbols/Abbreviations</b>	<b>Terms</b>
mRNA	Messenger RNA
MW	Molecular weight
NS3A	Nonstructural 3A protein
OD	Optical density
OE-PCR	Overlap extension polymerase chain reaction
ORF	Open reading frame
OSBP	Oxysterol-binding protein
pI	Isoelectric point
PARs	Protease-activated receptors
PBS	Phosphate buffered saline
PBS-T	Phosphate buffered saline with Tween 20
PCR	Polymerase chain reaction
PD	Parkinson's disease
PFA	Paraformaldehyde
PH	Pleckstrin-homology domain
PI	Phosphatidylinositol
PI4P	Phosphatidylinositol-4-phosphate
PI4KIII $\beta$	Phosphatidylinositol-4-kinase type III $\beta$
PS	Phosphatidylserine
PSGL-1	P-selectin glycoprotein ligand-1
PTMs	Post-translational modifications
PV	Poliovirus
P3A	Poliovirus 3A-like domain
RCs	Replication complexes
RdRP	RNA-dependent RNA polymerase
RD cells	Rhabdomyosarcoma cells
ROs	Replication organelles
RNA	Ribonucleic acid

**LIST OF ABBREVIATIONS (Cont.)**

<b>Symbols/Abbreviations</b>	<b>Terms</b>
RT-PCR	Reverse transcription polymerase chain reaction
+RNA	Positive-sense RNA
siRNA	Small interference RNA
SCARB2	Human scavenger receptor class B member 2
SDS	Sodium dodecyl sulfate
SDS-PAGE	Sodium dodecyl sulfate polyacrylamide gel electrophoresis
TFA	Trifluoroacetic acid
UDW	Ultrapure distilled water
UTRs	Untranslated regions
vRNA	Viral RNA
VPg	Viral protein genome-linked
ZIKA	Zika virus

## CHAPTER 1

### INTRODUCTION

Hand, foot and mouth disease (HFMD) is an illness mostly found in children at the age under 5 years caused by viruses classified in the family *Picornaviridae*. The HFMD has become a public health problem in Asia-Pacific countries including China, Hong Kong, Taiwan, Japan, Malaysia, Singapore, Vietnam, Cambodia and also Thailand.<sup>1-15</sup> The Asia-Pacific region has experienced the cyclical large outbreaks of HFMD that occur every 1-2 years and potentially become an endemic viral infection.<sup>16, 17</sup> Enterovirus A71 (EV-A71) is one of the main causative agents of HFMD. The symptoms range from mild or typical HFMD to severe HFMD.<sup>18</sup> The typical HFMD symptoms are blisters or sores in the mouth and rash on the hands, feet, and buttocks as well as legs which they are actually self-limited within seven to ten days after the symptoms onset. While, the severe HFMD involves the ability of EV-A71 to invade central nervous system (CNS) resulting in neurological complications such as meningitis, brainstem encephalitis, acute flaccid paralysis, neurogenic cardio-respiratory failure and even death. The neurological complications of the CNS are consequences of the viral replication and inflammation of viral-infected tissues.<sup>19</sup> However, the pathogenesis mechanism of viral infection in the CNS is poorly understood, leading to a lack of preventive vaccines and also antiviral drugs for treatment.

The positive-sense RNA genome of EV-A71 contains a single open reading frame (ORF) encoding for a polyprotein that is subsequently processed into structural proteins (VP1-VP4), and nonstructural proteins (2A, 2B, 2BC, 2C, 3A, 3AB, 3B, 3C, 3CD, and 3D which play diverse roles in viral replication.<sup>20-23</sup> To establish successful infection, the virus has to produce a number of viral progenies throughout time of infection, and at the same time, virus has to evade or protect itself from recognition by intracellular immune sensing. Among viral proteins, enterovirus 3A protein has been reported as a key player in modulation of host cellular membranes to construct platforms for viral genome replication and assembly, termed as replication organelles (ROs).<sup>24, 25</sup> Utilization of host cellular proteins and lipids for formation of replication organelles (ROs) are various depending on host cell and

preferential location of ROs. The 3A protein is highly conserved among enteroviruses.<sup>26</sup> Even though the roles and functions of 3A protein have been intensively studied, the data on EV-A71 3A protein, especially in neuronal cells, is still limited. Since the viral nonstructural proteins might contribute to viral pathogenesis. The study of 3A protein by searching its interacting counterpart in neuronal cells would guide for the involved host cellular pathway as well as role in viral replication. The gained knowledge would provide more understanding on pathogenesis mechanism in the EV-A71 infection associated with severe neurological complications which might lead to the development of effective drugs and vaccine.





## CHAPTER 2

### REVIEW OF LITERATURE

#### 2.1 Clinical aspects, virology and genome organization of EV-A71

Human enterovirus 71 (EV-A71) is one of the causative agents for hand, foot and mouth disease (HFMD). The spectrum of HFMD clinical outcomes ranges from mild to severe as fatal. The hallmarks of mild or typical HFMD are the presence of blisters or sores in the mouth and rash on the hands, feet, and buttocks as well as legs which they are actually self-limited within seven to ten days after the symptoms onset.<sup>18</sup> In the case of a fatality, it has been reported that severe HFMD associated with an EV-A71 infection which has the ability to invade central nervous system (CNS) resulting in neurological complications such as meningitis, brainstem encephalitis, acute flaccid paralysis, neurogenic cardio-respiratory failure and even death. The neurological complications of CNS are consequences of the viral replication and inflammation of the viral-infected brain tissues.<sup>19,27</sup>

The EV-A71 belongs to family *Picornaviridae*, genus *Enterovirus*, species A. It is a non-enveloped, 22-30 nm icosahedral particle which contains a single-stranded, positive-sense RNA genome which is approximately 7.4 kb in length (**Figure 2.1**).<sup>28, 29</sup> The EV-A71 genome contains a single open reading frame (ORF) which is translated into a polyprotein that subsequently processed by viral proteases to produce mature viral proteins. The EV-A71 ORF is flanked with 5' and 3' untranslated regions (UTRs). A viral protein genome-linked; i.e. VPg or nonstructural 3B protein, is attached covalently by phosphodiester bond at 5' end of the genome to function as a primer for initiating viral RNA synthesis. The 5' UTR contains secondary structures of a *cis*-replicating element called the cloverleaf (a stem-loop A-D) and the internal ribosomal entry site (IRES) at which C-rich region of spacer located between them. There are terminal stem, type 1 pseudoknot and poly(A) at the 3' UTR. The genetics elements appear on both the 5' and 3' UTRs play important roles in viral genome replication and translation.

The EV-A71 ORF could be organized into three regions which are responsible for encoding three precursors (P1-P3) of the polyprotein which are subsequently processed into mature proteins by viral proteases. P1 is cleaved into four structural proteins; i.e. VP1-VP4, which are viral capsid proteins. An EV-A71 icosahedral particle consisting of 60 copies of each of VPs are assembled to form 2-, 3- and 5-fold rotational symmetry axes capsid (**Figure 2.2**).<sup>30</sup> VP1 to VP3 are displayed on the outer surface of the virion, while VP4 is inside the particle. There is a depression region called the canyon locates around each icosahedral 5-fold axis on the surface of the viral capsid. The canyon is a site for cellular receptor binding. The P2 and P3 are cleaved into nonstructural proteins 2A-2C and 3A-3D, respectively. The roles of these viral nonstructural proteins have been reported in viral replication and host immune evasion.<sup>24, 31, 32</sup>

Based on *VP1* gene sequence homology, EV-A71 are divided into five genotypes; i.e. A, B, C, D and E. Within genotype B and C, they are further divided into five subgenotypes; i.e. B1-B5 and C1-C5, respectively.<sup>33, 34</sup>

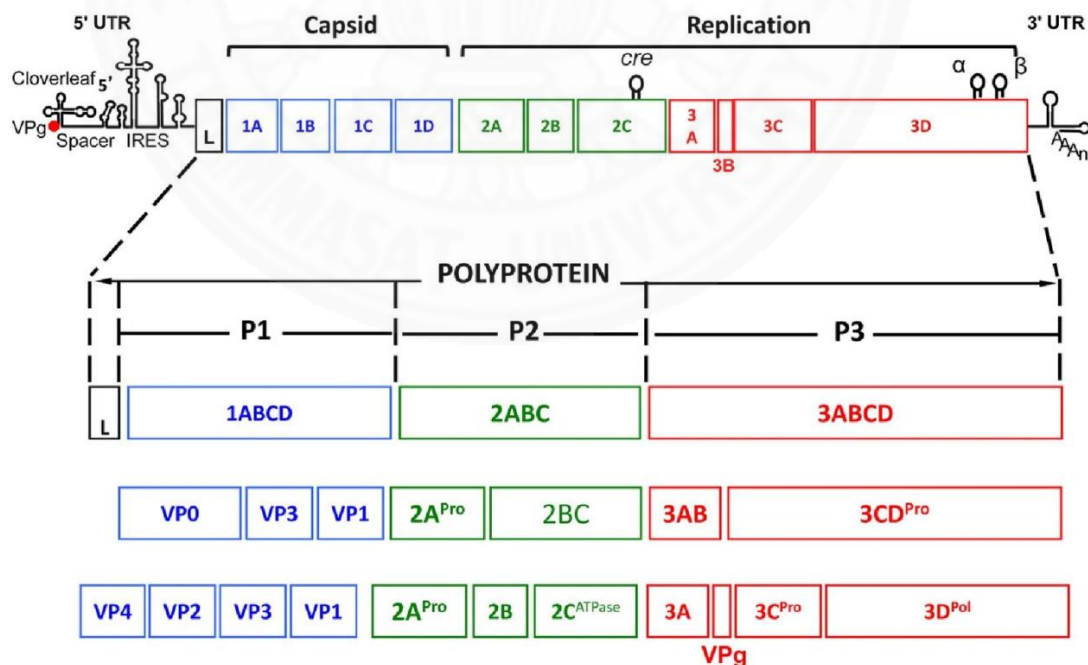


**Figure 2.1** Genome structure of picornavirus, processed polyprotein and mature proteins. The picornavirus genome size of approximately 7.4 kb consists of viral protein genome-linked (VPg) at 5' end, *cis*-replicating element called cloverleaf, C-

rich spacer region, internal ribosome entry site (IRES), a single open reading frame (ORF) encoding for viral polyprotein, and poly (A) tail at 3'end, respectively. The viral polyprotein is processed by viral proteases into three precursors; P1-P3, and subsequently processed into four structural proteins; VP1-VP4, and seven nonstructural proteins; 2A-2C and 3A-3D, respectively.<sup>29</sup>

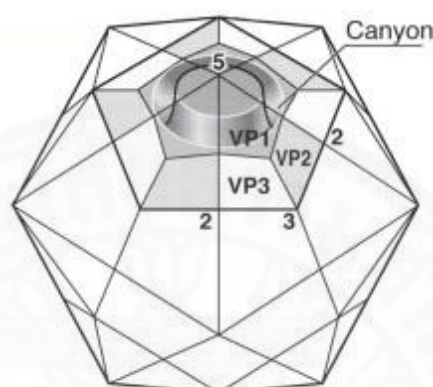


**Figure 2.2** Schematic representation of poliovirus structure, a member of *Picornaviridae* family. Viral capsid proteins VP1, VP2, and VP3 are displayed on the outer surface of the virion, whereas VP4 is located inside the particle. The numbers; 5, 3 and 2, represent the 5-fold, 3-fold and 2-fold axes of icosahedral symmetry. The depression region called the canyon locates around each icosahedral 5-fold axis on the surface of the viral capsid.<sup>30</sup>

## 2.2 Epidemiology

The EV-A71 infection has become a public health problem worldwide (**Figure 2.3**).<sup>35</sup> It is the causative agent of several large outbreaks of HFMD in Asia-Pacific countries such as in Malaysia in 1997, China in 1998-2008, Taiwan in 1998, 2000, 2003, and 2007-2008, Japan and Singapore in 2000, Vietnam in 2005, and Thailand in 2008-2009 with higher frequencies since 2011.<sup>1, 2, 4-7, 9, 11, 14, 15, 34, 35</sup> In Thailand, HFMD caused by EV-A71 was firstly reported in 2001 by the Bureau of Epidemiology, Department of Disease Control. In 2007, EV-A71 was reported as minor species causing the large outbreak of HFMD. During 2008-2009, EV-A71 was responsible for 47.9% of HFMD cases. Even though the majority of HFMD in the

large outbreak in 2010 was caused by other enterovirus species, the prevalence of EV-A71 infection has been increased since 2011 onwards.<sup>14</sup> In the large outbreak of HFMD in 2012, there were three confirmed fatal cases with EV-A71-B5 genome positive. One of the fatal cases was reported involving in neurological complications.<sup>13</sup>

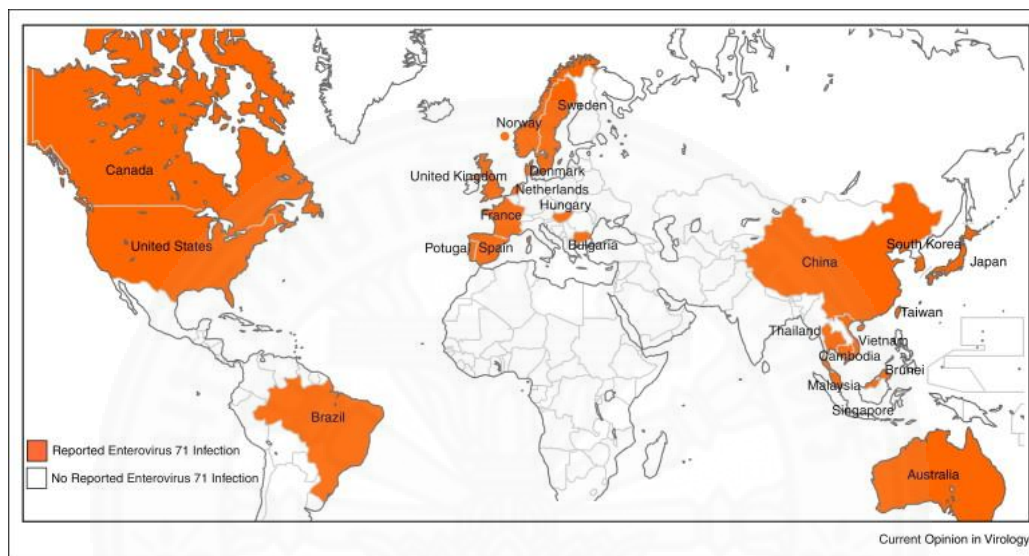


**Figure 2.3** Geographic distribution of EV-A71 infection.<sup>35</sup>

### 2.3 Enterovirus 71 life cycle

Because viruses are obligate intracellular pathogens, they need a host cell to accomplish their life cycle for producing their progeny. The viral life cycle is multistep process composed of viral entry, genome uncoating, genome translation and replication, as well as particle assembly and egression.<sup>36</sup> After the virus gets into the host cell, its genome is directly translated and processed into viral proteins which subsequently take control of cellular metabolism and biosynthesis processes that favor for establishing a productive viral infection. During viral replication, host cellular homeostasis is disturbed leading to pathological changes of the infected cells or even cell death.<sup>37</sup> Moreover, there is plenty of pathogens sensors present in host cytoplasm.<sup>38</sup> These molecular sensors can recognize viral genome and activate host immune responses, resulting in the intervening of virus life cycle. Nevertheless,

viruses oppose host immune responses by several antagonistic strategies using virally encoded nonstructural proteins in order to maintain an infectious cycle in the host.<sup>21, 22, 39–41</sup>

### 2.3.1 Viral entry

For EV-A71 which is a non-enveloped virus, it initially recognizes and attaches to host cellular receptors on cell surface. Recently, there are two human transmembrane proteins including P-selectin glycoprotein ligand-1 (PSGL-1) or CD162 and human scavenger receptor class B member 2 (SCARB2), a type III glycoprotein which is also known as lysosome integral membrane protein 2 (LIMP2) or CD36b like-2, have been identified as a functional receptor for EV-A71 entry.<sup>42</sup> Virus binding to host cell receptors promotes viral entry *via* clathrin- or caveolar-dependent endocytosis.<sup>43, 44</sup> PSGL-1 is expressed on myeloid cells, all types of lymphoid cells, dendritic lineage, epithelium of the fallopian tube, lamina propria of mouth and esophagus, the muscularis mucosae of stomach and intestine, pneumocytes, and alveolar macrophage.<sup>45</sup> Because it is involved in the leukocyte rolling and interacting with vascular endothelial cells, PSGL-1 has been postulated to play an important role in the dissemination of EV-A71 into CNS by exploiting immune cell as a Trojan horse.<sup>46</sup> However, some EV-A71 strains do not require PSGL-1 for their entry suggesting specificity of EV-A71 strains to immune cells.<sup>47</sup> It has been reported that amino acid residue at position 145 of VP1, which is either glycine (G) or glutamine (Q), determines the binding capability of EV-A71 to PSGL-1.<sup>48</sup> Post-translational modification by tyrosine sulfation at the N-terminus of PSGL-1 is also critical for binding to EV-A71.<sup>49</sup> Moreover, it was reported that PSGL-1-independent EV-A71 infection can cause death in cynomolgus monkey.<sup>50</sup> The SCARB2 is a functional entry receptor for all EV-A71 strains. It is widely expressed in various tissues, particular in mucosal epithelium and granular ducts in the gastrointestinal tract, supporting the principle sites of EV-A71 infection.<sup>51, 52</sup> Both PSGL-1 and SCARB2 have also been found to be expressed in neurons and microglia, suggesting the ability of EV-A71 to infect cells in CNS and cause neuropathologies.<sup>53</sup> This notion has been supported by a histopathological study in monkey model which demonstrated that neuron progenitor, mature neuron, and glia could be EV-A71 cellular targets which consequently result in neuropathological changes.<sup>54</sup>

### 2.3.2 Viral genome uncoating

The SCARB2, or lysosome integral membrane protein 2 (LIMP-2), one of the major lysosomal membrane proteins, is also responsible for viral genome uncoating (**Figure 2.4**).<sup>55</sup> After binding of EV-A71 to SCARB2 and internalization *via* clathrin- or caveolar-dependent endocytosis, the interaction of SCARB2 with the canyon makes the hydrophobic pocket of EV-A71 VP1 capsid containing pocket factors lie adjacent to the lipid-transfer tunnel of SCARB2.<sup>56-58</sup> Upon acidification of endosome (pH<5.5), SCARB2 changes its conformation leading to the lipid-transfer tunnel opening which allows the expulsion of pocket factors from the cavities.<sup>57, 59-61</sup> The dislodging of pocket factors from the cavity results in destabilization of the viral capsid. Therefore, the viral capsid undergoes a conformational change and then dissociates from the SCARB2 receptor. Eventually, the EV-A71 uses VP1 N-terminus and VP4 to form the channel in the membrane and releases its RNA genome out to the cytoplasm.<sup>62-64</sup>



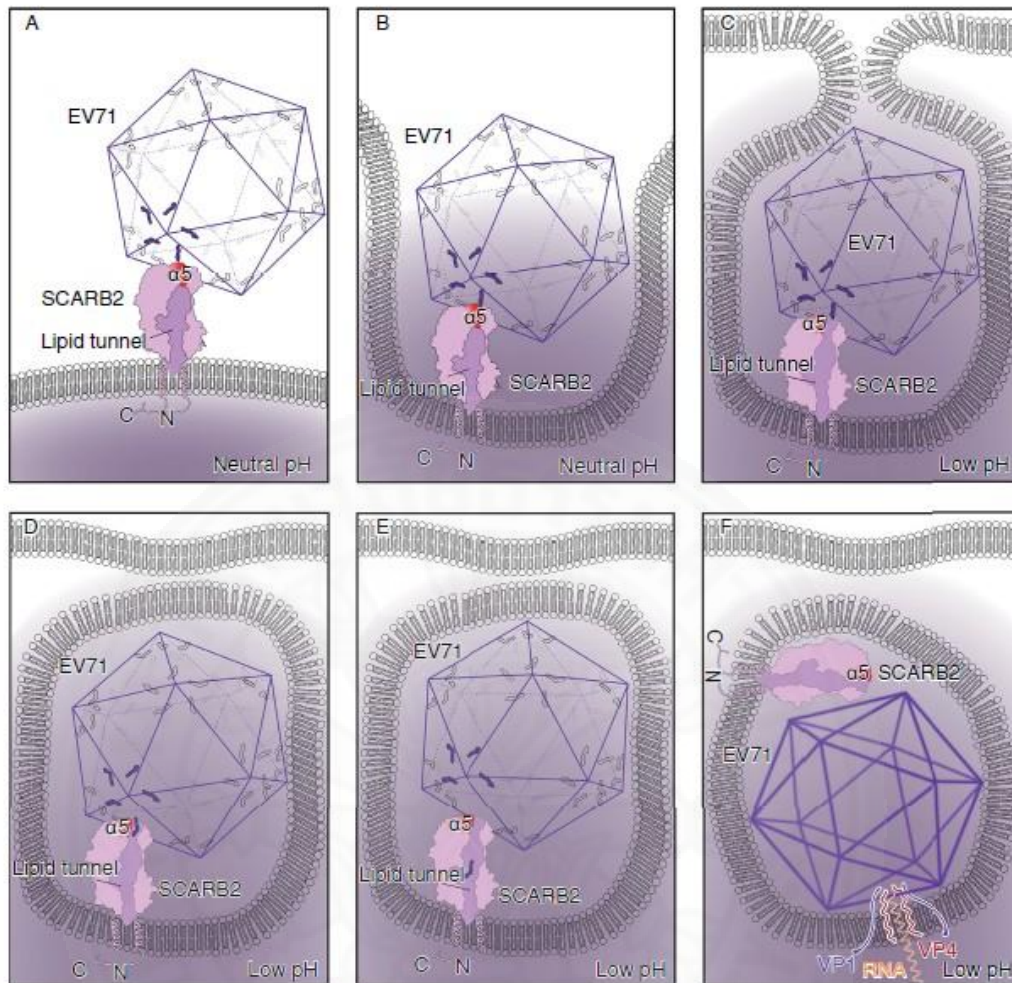


**Figure 2.4** Model of SCARB2-mediated EV-A71 entry and genome uncoating. SCARB2 is expressed on host cellular membrane. Pocket factors in VP1 represent as a “red worm”. The EV-A71 mature virion is shown as a purple icosahedral particle, and the deep-purple bigger icosahedral particle represents the EV-A71 uncoating intermediate. (A) Attachment of EV-A71 to SCARB2 receptor. (B) Binding of EV-A71 to SCARB2 receptor triggers the internalization *via* clathrin- or caveolar-dependent endocytosis. (C) SCARB2 is conformationally changed uncover its lipid-transfer tunnel at low pH. (D) The expulsion of pocket factors *via* a lipid-transfer tunnel. (E) While pocket factors are transferred to the membrane, EV-A71 undergoes a conformational change of viral capsid. (F) Then, EV-A71 dissociates from the SCARB2 receptor and use VP1 and VP4 to form the channel in the membrane releasing viral genomic RNA out to the cytoplasm.<sup>56</sup>

### 2.3.3 Viral translation and polyprotein processing

EV-A71 genome is a positive-sense RNA containing type I internal ribosome entry site (IRES) at the 5' UTR upstream of a single ORF encoding for viral polyprotein.<sup>65</sup> Type I IRES is approximately 450 nucleotides in length containing five domains designated as dVII-dVI. The IRES is the *cis*-acting RNA sequence that recruits various eukaryotic initiation factors (eIFs) and IRES-specific *trans*-acting factors (ITAFs) which are required for initiating viral protein translation.<sup>66</sup> The positive-sense EV-A71 RNA is like an mRNA that can be directly translated into a viral polyprotein by the cap-independent, IRES-driven manner (**Figure 2.5**). The growing polyprotein is subsequently processed by its proteases; 2A<sup>pro</sup> and 3C<sup>pro</sup>.<sup>67</sup> The cleavages of polyprotein take place at the specific cleavage sites recognized by the 2A<sup>pro</sup> and 3C<sup>pro</sup> which located between the amino-terminus and carboxy-terminus of the adjacent viral proteins.<sup>68</sup> The polyprotein processing is comprised of three consecutive events including primary, secondary, and maturation cleavages. The step of polyprotein processing is common to all picornavirus but differ in the detailed mechanisms at a level of genera.<sup>37</sup> Primary polyprotein processing is a co-translational reaction taking place almost as soon as the translation is complete. In enterovirus, as ribosomes traverse the genome until reaching P2 region, a self-contained protease 2A<sup>pro</sup> within the context of nascent polyprotein primarily cleave in *cis* at its own N-terminus to separate P1 from the growing P2/P3 precursor. As such followed by secondary processing, the cleavages at the junctions within P1 and between P2/P3 are mediated by 3C<sup>pro</sup> protease in *cis* which is common in all picornaviruses.<sup>37, 67</sup> Those intermediate viral protein forms are subsequently cleaved into functional proteins in maturation polyprotein processing mediated by 3C<sup>pro</sup>.

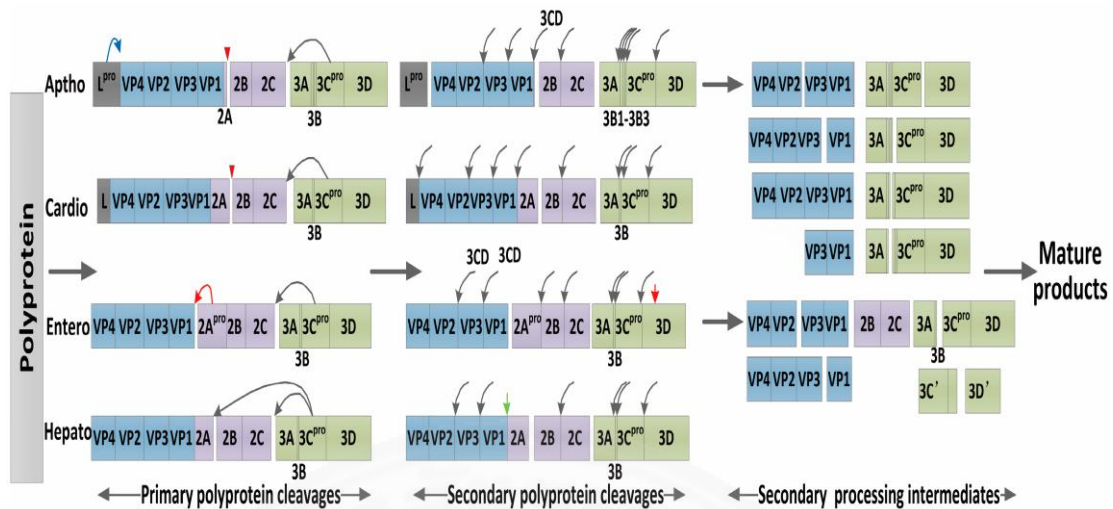


**Figure 2.5** Picornavirus polyprotein processing mediated by 2A<sup>pro</sup> and 3C<sup>pro</sup>.<sup>67</sup>

### 2.3.4 Host cellular membrane remodeling and virus genome replication

Many RNA viruses, like picornaviruses, hijack and remodel host intracellular membrane to generate the distinct structural platform for their genome replication and viral assembly termed as replication organelles (ROs).<sup>24, 69–71</sup> *Picornaviridae* is a large family containing several genera; such as *Enterovirus*, *Cardiovirus*, *Kobuvirus*, *Hepatovirus*, and *etc.*, which are diverse in some biological aspects. The viruses from different genera utilize different strategies and molecules for their genome replication.<sup>24, 69, 71</sup> The remodeling of host intracellular membrane to generate virally-induced ROs is mediated by the concerted actions of both viral nonstructural proteins and host cellular components from a variety of sources, depending on the type of virus, such as endoplasmic reticulum (ER), Golgi apparatus, peroxisomes, endosomes, mitochondria or plasma membrane.<sup>69, 71–74</sup> The formation of ROs is like 'cut and stitch' the components from the secretory pathway to build the distinct structures that facilitate their genome replication. In poliovirus (PV) and coxsackievirus B3 (CVB3), belonging to *Picornaviridae* family, their ROs are derived from Golgi apparatus.<sup>24, 69</sup> The morphology of ROs of enteroviruses could be both of single and double membrane vesicles.<sup>75, 76</sup> At the early infection phase, around first 2-hours post-infection, the majority of replication membranes are single-membrane convoluted tubular-vesicular structures (**Figure 2.6**).<sup>75</sup> Later, they are subsequently

transformed into double-membrane vesicles (DMVs) and larger multilamellar structures upon a course of infection (**Figure 2.7**).<sup>76</sup> The inner membrane of DMVs is a closed compartment, the import and export of substrates or viral RNA genome are still unclear.

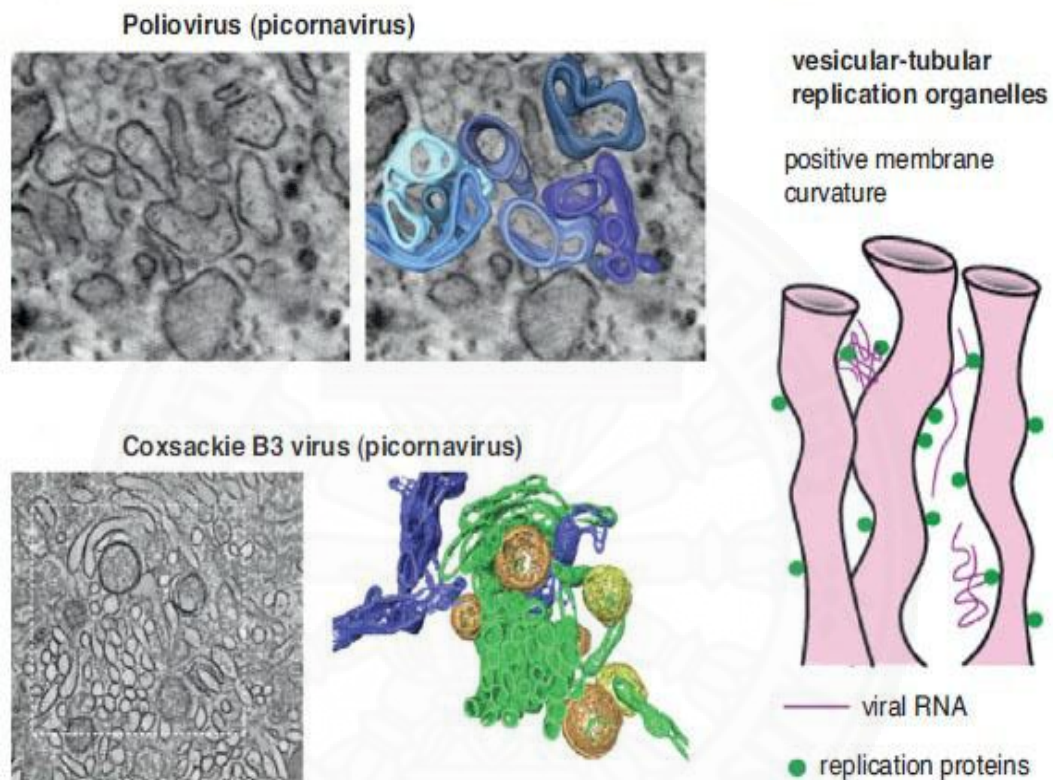


**Figure 2.6** Morphology of picornavirus replication organelles (ROs). At the early infection phase, ROs are formed as single-membrane convoluted tubular-vesicular structures.<sup>75</sup>



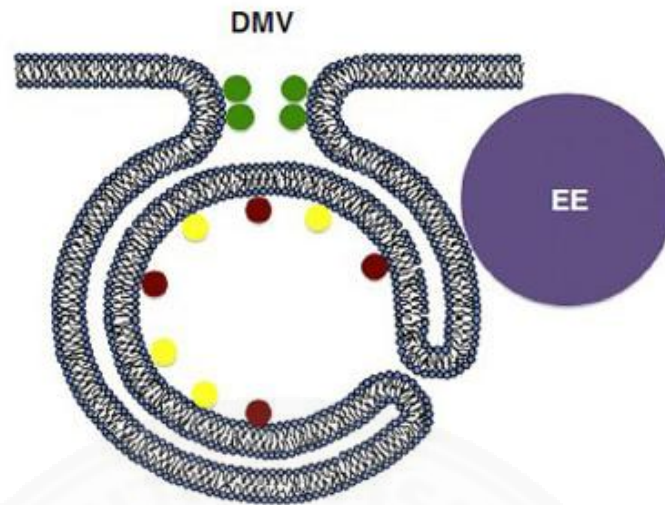


**Figure 2.7** Morphology of double membrane vesicles (DMVs) of picornavirus replication organelles (ROs). Green, yellow and brown circles represent some host proteins involving in the modulation of membrane curvature such as reticulon. EE: early endosome.<sup>76</sup>

At these sites, many viral nonstructural proteins such as 2C, 3A, 3B (VPg), 3AB, 3CD, and 3D are concentrated at ROs and participate in viral genome replication.<sup>69</sup> It has been reported that 3A protein; an 86 amino acid membrane-bound viral protein with the unstructured regions at N-termini, plays a key role in the formation of ROs. The reorganization of host secretory pathway happens over the course of infection (**Figure 2.8**).<sup>69</sup> PV and CVB3 3A proteins recruit many host secretory factors to build up the ROs, *e.g.*, Golgi brefeldin A resistant guanine nucleotide exchange factor 1 (GBF1) which is a guanine nucleotide exchange factor (GEF) of the small ADP-ribosylation factor 1 (Arf1) GTPase.<sup>24, 69, 77-79</sup> They actually localize at ER, ERGIC, and Golgi apparatus. GBF1/Arf1-GTP functions in the recruitment of many effectors including membrane coat proteins COPI and clathrin, cytoskeleton effectors and lipid modifying enzymes such as phosphatidylinositol-4-kinase type III $\beta$  (PI4KIII $\beta$ ) to their localized sites. PV and CVB3 3A proteins bind to GBF1 and block the activation of Arf1, interfering recruitment of COPI protein to the replication membrane platform.<sup>77</sup> On the other hand, PV 3A protein has also been reported to recruit GBF1 and Arf1, then Arf1 is activated and turns to recruit other effectors like PI4KIII $\beta$ .<sup>24, 79</sup> The function of GBF1 in viral replication is still unclear.

Moreover, many picornaviruses, but not EV-A71, 3A proteins have been reported to interact with the acyl-CoA binding domain containing 3 (ACBD3) to recruit PI4KIII $\beta$  to the membrane.<sup>80-82</sup> For EV-A71, the interesting candidate for interaction with 3A protein is an acyl-CoA dehydrogenase family member 9 (ACAD9). PI4KIII $\beta$  functions in the generation of phosphatidylinositol-4-phosphate (PI4P) by phosphorylation of phosphatidylinositol (PI). Picornaviruses generate the ROs that enrich with PI4P for providing the interaction of viral RNA-dependent RNA polymerase (RdRp) 3D protein or 3D<sup>pol</sup>.<sup>69, 83</sup> Various cellular proteins such as oxysterol-binding protein (OSBP), ceramide transfer protein (CERT), four-phosphate-adaptor protein 1 and 2 (FAPP1/FAPP2), contain the PI4P-binding domain, called the pleckstrin-homology domain (PH), that can sense and specifically bind to PI4P lipids.<sup>71</sup> OSBP has been reported to be recruited to the ROs *via* PI4P.<sup>71, 84</sup> OSBP plays a key role in the transport of cholesterol and PI4P between the ER and Golgi.<sup>85</sup>

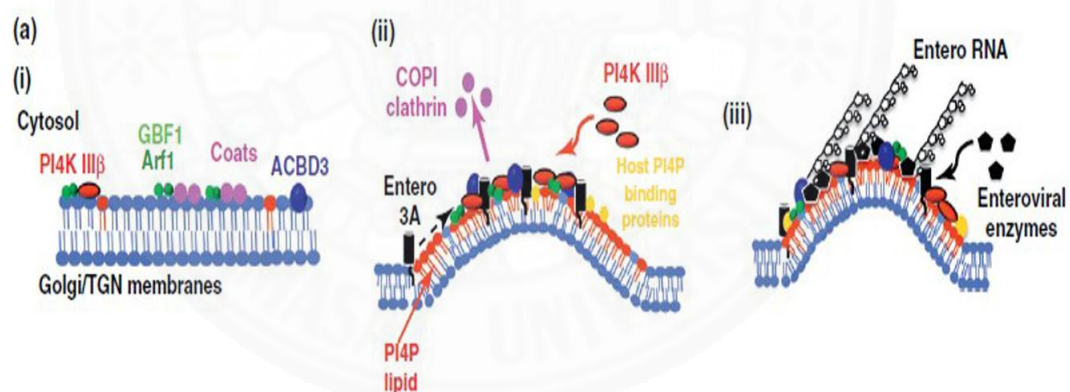


**Figure 2.8** Model of PV- and CVB3-modified membranes for genome replication mediated by enterovirus 3A proteins.<sup>83</sup>

Thus, in the picornavirus-infected cell, OSBP functions in cholesterol shuttling, exchanging cholesterol with PI4P from ER to ROs. Cholesterol is another factor that plays a crucial role in viral replication in which cholesterol serves membrane fluidity and lipid raft.<sup>86</sup> CVB3 3A protein has been reported to recruit Rab11-positive recycling endosome containing cholesterol to the ROs in PI4P-independent manner.<sup>25</sup> Cholesterol does not only play a role in the regulation of

assembly and function of membrane-based protein/lipid complexes like a viral replication complex but also functions in attenuation of viral polyprotein processing by facilitating the proper conformation of 3CD<sup>pro</sup> for autocatalytic processing.<sup>25</sup> At these ROs, viral nonstructural proteins and co-opted host factors coordinately synthesize negative-sense RNA from the input positive-sense RNA genome. Then, negative-sense RNA molecule further serves as a template for replicating a new positive-sense RNA molecule, cyclically.<sup>37</sup> The newly synthesized positive-sense RNA molecules are destined for either viral encapsidation generating the new progeny for subsequent infection or viral translation producing more viral proteins which turn back to play roles in genome replication, viral encapsidation as well as modulation of host cellular responses. So far, this process of EV-A71 replication cycle has not been elucidated yet. Since the formation of ROs mediated by viral nonstructural 3A protein disturbs the assembly of host secretory pathway, leading to accumulation of vesicles at ER-exit sites, many proteins such as cytokines and major histocompatibility complex (MHC) class I molecule are suppressed for secretion or expression on the cell surface.<sup>32, 87</sup> It seems that nonstructural 3A protein might also play a role in host immune evasion.

### 2.3.5 Virus assembly and egress (morphogenesis)

After viral RNA genome is replicated, it might be suddenly incorporated into the icosahedral capsid to form mature virion and released out from host cell *via* the unwell-defined mechanism.<sup>29</sup> Although non-enveloped virus might rely on host cell lysis to egress, it has been reported some non-enveloped viruses were spread non-lytically.<sup>88-92</sup> For example, CVB3 was shed from CVB3-infected cells *via* extracellular microvesicles (EMVs), PV could be spread non-lytically by utilizing some host components in autophagy pathway, the enveloped form of hepatitis A virus (HAV) and hepatitis E virus (HEV) were observed in supernatant of infected cell cultures and, surprisingly, in blood of acute hepatitis A and E patients, respectively, causing resistance to neutralizing antibody.<sup>91, 93</sup> Moreover, viral spreading *via* phosphatidylserine (PS)-enriched vesicle and reliance on PS receptor to infection was reported in several viruses, both enveloped and non-enveloped viruses, including HAV, PV, HIV, Ebola, Dengue (DENV) and Vaccinia virus (**Figure 2.9**).<sup>94</sup> Meanwhile, CVB3, HIV, hepatitis C virus (HCV), Epstein-Barr virus (EBV), as well

as EV-A71, were also reported to be transferred *via* exosomes.<sup>95</sup> By these mechanisms, it seems to provide more efficiency for virus transmission and infection.

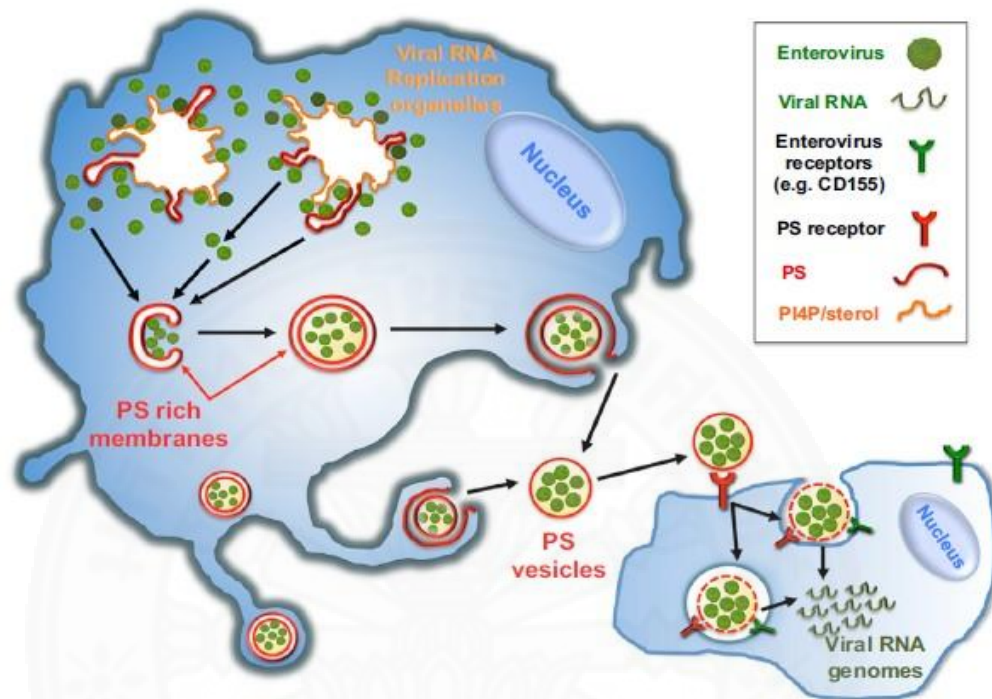


**Figure 2.9** Model of PV assembly and egress. After viral genome replication and encapsidation at replication organelles (ROs), a cluster of PV particles are assembled into phosphatidylserine (PS)-enriched double membrane vesicles. These double membrane vesicles fuse with the plasma membrane releasing out the unilamellar vesicles containing PV particles that subsequently promote virus infection.<sup>94</sup>

### Morphogenesis<sup>29</sup>

Positive-sense RNA plays an important role in three mechanisms of the viral life cycle: being as an mRNA for viral protein translation, as a template for viral replication, and as a genome for viral encapsidation. These three mechanisms are tightly regulated serving as a proofreading for each other. After translation and polyprotein processing, many non-structural proteins play a role in viral replication, while structural proteins form the capsid in the processing of encapsidation (**Figure 2.10**). Upon translation, the polyprotein processing which is a co-translational action



is primarily mediated by 2A<sup>pro</sup> cleaving the P1 from the rest of polyprotein. Then, P1 is modified by covalent linkage to myristic acid, called myristoylation. The myristoylated P1 interacts with heat shock protein 90 (Hsp90) making a processing-competent conformation. P1 is subsequently cleaved by 3CD<sup>pro</sup> into VP0, VP1, and VP3 capsid proteins, and then dissociate from Hsp90, followed by viral morphogenesis which is Hsp90-independent. The VP0, VP1, and VP3 are immediately assembled into 5S protomer. Myristoylation targets P1 to replication organelles (ROs) and provides the moiety enhancing the assembly of five protomers into 14S pentamer. At the replication organelles containing many viral non-structural proteins, 2C<sup>ATPase</sup> interacts with VP3 or VP1 recruiting 14S pentamers to the site of assembly. At this stage, based on the currently accepted model, twelve pentamers are likely to condense around viral RNA genome to produce 150S provirion. However, the roles of 2C<sup>ATPase</sup> in the condensation of viral RNA is still undefined. Finally, to develop into a mature viral particle, VP0 is autocatalytically cleaved into VP2 and VP4 in RNA-dependent manner. Cleavage of VP0 triggers the rearrangement of viral capsid proteins producing stable icosahedral viral particle.

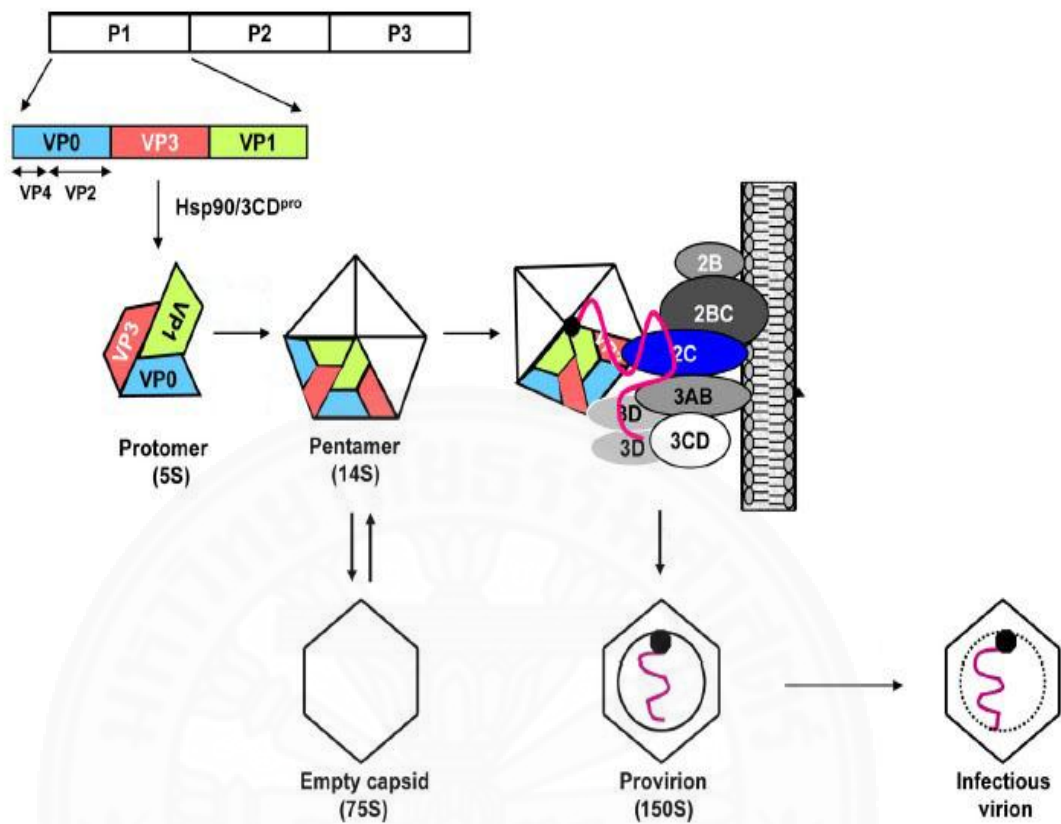


**Figure 2.10** Picornavirus morphogenesis. Myristoylated precursor 1 (P1) of polyprotein is processed into viral capsid protein VP0, VP3 and VP1 by 3CD<sup>PRO</sup> with the facilitation of Hsp90. Then, VP0, VP1, and VP3 are immediately assembled into 5S protomer. Five protomers are assembled into 14S pentamer and translocate to ROs recruited by 2C<sup>ATPase</sup>. Then, twelve pentamers condense around newly synthesized viral RNA to produce 150S provirion. The alternative model is the formation of 75S empty capsid without RNA. The 150S provirion undergoes maturation by autocatalytic cleavage of VP0 to VP2 and VP4 generating mature icosahedral viral particle.<sup>29</sup>

## 2.4 Pathogenesis<sup>96</sup>

Enterovirus 71 (EV-A71) is transmitted *via* the fomite-oral route through closing contact to an infected person or contaminated surface or objects and then ingesting (**Figure 2.11**). After viruses get into the human body by ingestion, the ingested viruses infect cells of the oropharyngeal mucosa and regional lymphoid tissue such as tonsils where they replicate and spread into the alimentary tract. Viruses may go further down to the gastrointestinal tract. EV-A71 is a non-enveloped virus which they are tolerant to the acid in the stomach. Thus, they can pass into the intestine and set up infections in the intestinal lymphoid tissue like Peyer's patches, underlying the intestinal mucosa. Based on the high expression of PSGL-1 and SCARB2 receptor along the gastrointestinal tract, here is the principle site of viral replication.<sup>54, 61</sup> Viruses are either shed into the feces or disseminate into blood circulation, causing viremic phase. During the viremic phase, pro-inflammatory cytokines are induced to express causing fever and related clinical signs and symptoms in the affected patients. Viruses then further infect tissues that express the cognate receptors and replicate there. At mucosae like oral cavity and skin, the replicating viruses trigger inflammation leading to the formation of skin lesions.<sup>97</sup> The EV-A71 has been identified as a neurotropic virus since they can invade and infect CNS resulting in neurological complications upon the infection. However, the mechanism of neuropathogenesis is still unknown. It is postulated that viruses may get into the CNS by hypothetical mechanisms including retrograde axonal transport and hematogenous transmission *via* blood-brain barrier (BBB).<sup>98-101</sup> Because of a lack of suitable small lab animal models to study neuropathogenesis of EV-A71, the knowledge is still limited. Only suckling mouse which is difficult to handle, and transgenic mouse and non-human primate which need sophisticated animal husbandry facilities are available as EV-A71 animal models. It has been known that viral pathogenesis relies on establishing successful productive infection in the target tissues.<sup>55</sup> Many viral factors have been considered for contributing to neuropathogenesis mediated by EV-A71 infection, including the ability to invade CNS, genetic determinant variations of the virus that encode for factors involving in receptor binding, virus-host interaction and immune evasion which allow it to

establish a productive infection in the CNS. Consequently, the virus replication may induce pathological changes in the affected tissues.<sup>27, 55</sup>

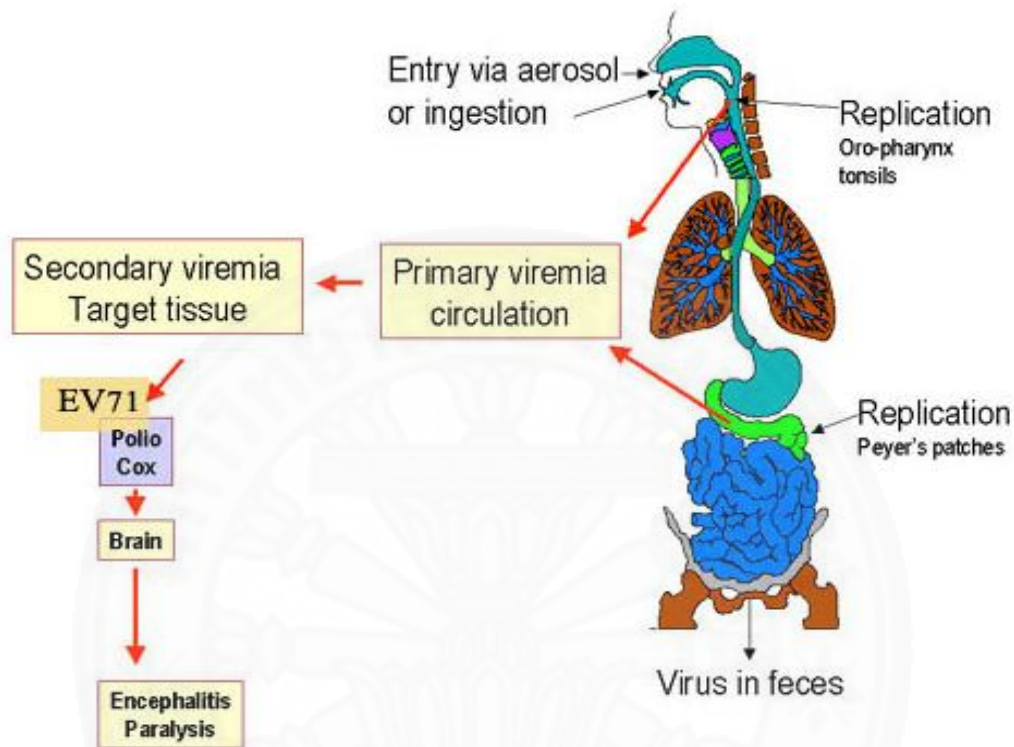


**Figure 2.11** Enterovirus 71 (EV-A71) pathogenesis. EV-A71 are transmitted *via* the fomite-oral route. First, viruses infect cells of the oropharyngeal mucosa and lymphoid tissue, like tonsils, where they replicate and shed into the alimentary tract. Viruses may go further down to the intestine and set up the infection in Peyer's patches. Then, they replicate and shed into the feces or disseminate into blood circulation, causing viremic phase. Subsequently, viruses infect tissues that express the cognate receptors by hypothetical mechanisms including retrograde axonal transport and hematogenous transmission *via* blood-brain barrier (BBB). The viruses get an entry into CNS resulting in neurological pathologies.<sup>96</sup>

## **CHAPTER 3**

### **OBJECTIVES**

#### **3.1 Primary objective**

The main objective of this study is to investigate interaction of enterovirus A71 (EV-A71) nonstructural 3A protein with cellular proteins in human neuronal cells and its roles in EV-A71 infection.

#### **3.2 Specific objectives**

1. To screen human neuronal cells that are permissive to EV-A71 infection
2. To search interacting counterparts of the EV-A71 nonstructural 3A protein in the permissive human neuronal cells
3. To predict functional domain/motifs on EV-A71 3A protein
4. To produce polyclonal antibodies to EV-A71 3A proteins and/or the 3A-interacting protein candidates
5. To study roles of the EV-A71 3A protein in infected cells

#### **3.3 Hypothesis**

Nonstructural 3A protein of EV-A71 modulates host cellular proteins in order to facilitate the virus genome replication and evade host immune response. Investigation of interactions between the 3A protein with cellular proteins in neuronal cells will elucidate the host cellular pathway involved in EV-A71 replication cycle and roles of EV-A71 3A nonstructural protein in EV-A71 infection.

## CHAPTER 4

### MATERIALS AND METHODS

#### 4.1 Virus propagation and preparation of genetic material of EV-A71

**Objective:** To propagate enterovirus A71 (EV-A71) and prepare viral genomic RNA used for molecular cloning of EV-A71 nonstructural 3A protein (NS3A).

##### 4.1.1 Propagation of EV-A71

The viral stock of EV-A71 (Thai clinical isolate, genotype B5) kindly given by Prof. Yong Poovorawan, M.D., Faculty of Medicine, Chulalongkorn University, Bangkok, Thailand, designated as TUCU001/B5 isolate was propagated in 90-95% confluence of cell monolayer of human skeletal muscle cell line; i.e., human rhabdomyosarcoma (RD) cells (CCL-136<sup>TM</sup>), a standard cell for EV-A71 infection. Human RD cells were grown in Corning<sup>®</sup> 75-cm<sup>2</sup> flask containing Dulbecco's Modified Eagle's Medium (DMEM) (Biochrom GmbH, Germany) supplemented with 10% fetal bovine serum (FBS) (Hyclone<sup>TM</sup>, GE Healthcare Life Sciences), 2 mM L-glutamine (Gibco<sup>TM</sup>, Thermo Fisher Scientific, US), and 1× penicillin-streptomycin (Gibco<sup>TM</sup>, Thermo Fisher Scientific, US), at 37 °C in 5% CO<sub>2</sub> incubator. At 90% cell confluence, the viral stock was diluted 1/100 in 2 mL pre-warmed serum-free DMEM and added to the cell monolayer. The inoculated monolayer cell was incubated at 37 °C in 5% CO<sub>2</sub> for 1 hour for viral adsorption. Then, the medium was discarded and 12 mL pre-warmed completed DMEM was added into the monolayer cell. The culture was incubated for 48-96 hours with a daily observation of cytopathic effects (CPEs) including cell rounding and detaching. The virus was collected using the freeze-thaw method.<sup>102</sup> The cell homogenate was centrifuged to remove cellular debris. The supernatant containing the virus was collected, aliquoted, and kept at -80 °C as a stock for use in the experiments throughout this study.

##### 4.1.2 Determination of the viral titer

The titer of the virus was determined by cell culture infectious dose-50 (CCID50) method and calculated using the Kärber following the WHO Polio

Laboratory Manual.<sup>102</sup> Human RD cells were harvested from 90% confluent culture, prepared as cell suspension containing  $1 \times 10^5$  cells/mL in completed DMEM. One hundred microliters of the RD cell suspension containing  $1 \times 10^4$  cells were added in all wells of a 96-well culture plate except columns 9 and 10 as shown in the plate layout below. The cell culture supernatant was 10-fold serially diluted in serum-free DMEM from  $10^{-1}$  to  $10^{-8}$ . On columns 1 to 8, 100  $\mu$ L of each dilution of the virus were added into 8 replicate wells of the respective column containing RD cells. On columns 11 and 12, 100  $\mu$ L of DMEM were added to cell suspension instead of viral inoculum served as uninfected cell control. The plate was mixed gently by tapping and returned to 5% CO<sub>2</sub> incubator. CPEs were observed daily using an inverted light microscope for 5 days. Culture medium was aspirated from the wells. Monolayer cells were washed once with 200  $\mu$ L of  $1 \times$  PBS and fixed with 200  $\mu$ L of ice-cold absolute methanol for 30 minutes at room temperature. Cells were washed twice with 200  $\mu$ L of  $1 \times$  PBS and stained with 200  $\mu$ L of 1:30 diluted Giemsa dye solution for 30-60 minutes at room temperature. Cells were rinsed gently with tap water and air-dried. The titer of the virus was calculated using the Kärber formula expressed as the median cell culture infectious dose (CCID<sub>50</sub>/100  $\mu$ L). The formula is as follows;

$$\text{Log CCID}_{50} = L - [d(S - 0.5)]$$

where;

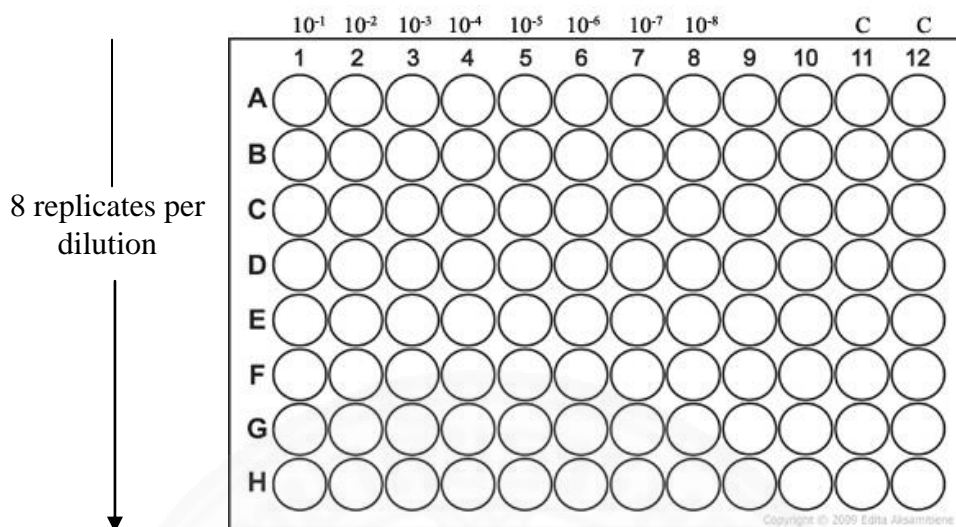
L = log of the lowest dilution used in the test

d = difference between log dilution steps

S = sum of the proportion of the positive test (i.e., cultures showing CPEs)



### Plate layout for virus titration



#### 4.1.3 Preparation and detection of EV-A71 genomic RNA

EV-A71 genomic RNA was extracted from 500  $\mu\text{L}$  of the viral stock using TRIzol™ reagent (Thermo Fisher Scientific, US). The extraction was done following the manufacturer's instruction. The concentration of the extracted RNA was determined by optical density (OD) at absorbance 260 nm measured by spectrophotometer (NanoDrop 2000/2000c, Thermo Fisher Scientific, USA). The purity of the extracted RNA was determined by OD ratios of 260/280 nm and 260/230 nm for protein and salt contamination, respectively. RNA with OD ratios of 260/280 nm and 260/230 nm greater than 1.8 and 2, respectively, was the high-quality genetic material. Moreover, the extracted RNA was verified for the presence of EV-A71 genome by one-step SYBR Green-based real-time reverse transcription PCR (real-time qRT-PCR) (Agilent Technologies, Brilliant II SYBR® Green QRT-PCR Master Mix Kit, USA) using *VPI* specific primers as listed in **Appendix A**. The PCR reaction mixture was made from all components as follows.

Component	Volume/amount
EV-F2760 (10 $\mu\text{M}$ )	1 $\mu\text{L}$
EV-R3206 (10 $\mu\text{M}$ )	1 $\mu\text{L}$
RT-RNase block enzyme mixture	0.5 $\mu\text{L}$
Brilliant II SYBR Green qRT-PCR Master Mix	6.25 $\mu\text{L}$



Total RNA	50-200 ng
Total volume	12.5 $\mu$ L

The thermal cycle was consisted of the consecutive steps as follows.

Step	Temperature ( $^{\circ}$ C)	Time	Cycle
Reverse transcription	42	60 minutes	1 cycle
	95	10 minutes	1 cycle
Denaturation	95	30 seconds	} 40 cycles
Annealing	57	30 seconds	
Extension	68	30 seconds	
Melt curve analysis			

#### 4.2 Determination of EV-A71 infection of human neuronal cells using CCID50 method

**Objective:** To select human neuronal cells that are permissive to EV-A71 infection to be used as model for studying role of EV-A71 NS3A protein.

Two lines of human neuronal cells consisting of human SH-SY5Y (ATCC<sup>®</sup> No. CRL-2266<sup>TM</sup>) and human SK-N-MC (ATCC<sup>®</sup> HTB-10<sup>TM</sup>) were examined for permissibility to EV-A71 infection using CCID50 method. Human RD cells were used as a control of maximum EV-A71 infection. SH-SY5Y cells were maintained in 1:1 mixture of DMEM and Ham's F-12 (DMEM/F-12). SK-N-MC cells were maintained in Ham's F-12. RD cells were maintained in DMEM. The culture media were supplemented with 10% FBS, 1 $\times$  penicillin-streptomycin, and 2 mM L-glutamine. At 90% cell confluence, cells were harvested, made for cell suspension, and plated into wells of a 96-well plate. SK-N-MC and RD cells were plated at seeding density of 1 $\times$ 10<sup>4</sup> cells/well while SH-SY5Y cells were plated at seeding density of 2.5 $\times$ 10<sup>4</sup> cells/well. EV-A71 viral stock prepared from RD cells as described in **Section 4.1.1** was made for 10-fold serial dilutions and inoculated with the cells in wells to determine CCID50 as described in **Section 4.1.2**. The permissibility to EV-A71 infection of SH-SY5Y and SK-N-MC neuronal cells was determined by comparing CCID50 with those of RD cells.

### 4.3 Searching interacting counterparts of the EV-A71 nonstructural 3A protein in EV-A71 permissive human neuronal cells

**Objective:** To produce recombinant EV-A71 3A protein to use as a bait for searching its interacting protein in permissive human neuronal cells.

#### 4.3.1 Molecular cloning of EV-A71 nonstructural 3A coding sequence

##### 4.3.1.1 Construction of recombinant plasmid DNA carrying coding sequence of EV-A71 nonstructural 3A in-frame with FLAG-epitope tag at 5'-end

###### (1) PCR amplification of *FLAG-3A*

EV-A71 genomic RNA prepared from the **Section 4.1.3** was reverse-transcribed to complementary DNA (cDNA) using AccuPower<sup>®</sup> RT Premix (AccuPower<sup>®</sup> RT Premix, Bioneer, Republic of Korea) and used as template for PCR amplification of EV-A71 3A coding sequence fused 5'-end in-frame with FLAG-tag coding sequence. The PCR was performed using *ProFi Taq* DNA polymerase which harbors proof-reading activity and capability to generate 3'-adenosine (A) overhang. The nucleotide sequence of restriction sites of *EcoRI* and *Sall* endonucleases were incorporated at 5' ends of the Outer1-MamNS3A forward and R-pQE30pGEX4T1-NS3A reverse primers, respectively. The primer sequences were shown in **Appendix A**. Two extra-bases, i.e., AT, were also added into 5' ends of each primer to increase efficiency of restriction enzyme digestion. Conventional PCR was performed as described in **Appendix E** using annealing temperature at 50 °C for 45 seconds and extension step lasted for 1 minute for each cycle. The PCR amplicons of *EcoRI-FLAG-3A-Sall* were detected by agarose gel electrophoresis and purified from agarose gel as described in **Appendix E**.

###### (2) Cloning of *EcoRI-FLAG-3A-Sall* into cloning vector

The purified *EcoRI-FLAG-3A-Sall* DNA fragments were ligated with pJET1.2/blunt cloning vector (CloneJET PCR Cloning Kit, Thermo Fisher Scientific, US) (**Figure 4.1**) following blunt-end cloning protocol. The *EcoRI-FLAG-3A-Sall* amplicons were blunted for 5 minutes at 70 °C by thermostable DNA

blunting enzyme prior to ligation. The blunting reaction mixture was made from all components as follows.

<b>Component</b>	<b>Volume</b>
2× Reaction Buffer	5 µL
Ultrapure distilled water (UDW)	Variable
Purified <i>FLAG-3A</i> amplicon	15 ng (for 300-bp PCR product)
DNA blunting enzyme	0.5 µL
Total volume	8 µL

After DNA blunting, the ligation reaction was set on ice by adding component as follows.

<b>Component</b>	<b>Volume</b>
pJET1.2/blunt cloning vector (50 ng/µL)	1 µL
T4 DNA Ligase	1 µL
Total volume	10 µL

The ligation was done at 16 °C for overnight and then transformed into bacterial competent cells using heat-shock method as described in **Appendix E**. The presence of the recombinant plasmid DNA inserted with *EcoRI-FLAG-3A-Sall* designated as pJET1.2::*FLAG-3A* was detected using colony PCR. The primers for detection were pJET1.2 forward sequencing and pJET1.2 reverse sequencing primers. The PCR amplification was done using annealing temperature at 60 °C for 30 seconds and extension step lasted for 30 seconds for each cycle. The plasmid containing the inserted target coding sequence were subsequently isolated from the positive bacterial clones and verified by DNA sequencing (Bioneer, Korea).

#### **4.3.1.2 Prediction of functional domain/motif of EV-A71 NS3A**

The obtained nucleotide sequences were analyzed using DNAMAN program and Applied Biosystems Sequence Scanner Software 2. The nucleotide sequence analysis of the cloned EV-A71 3A sequence was performed by BLAST program to compare with sequences deposited in the GenBank database. The protein domain homology and tertiary structure of the cloned EV-A71 3A sequence was predicted by BLASTx and Swiss-Model (<https://swissmodel.expasy.org/>), respectively.

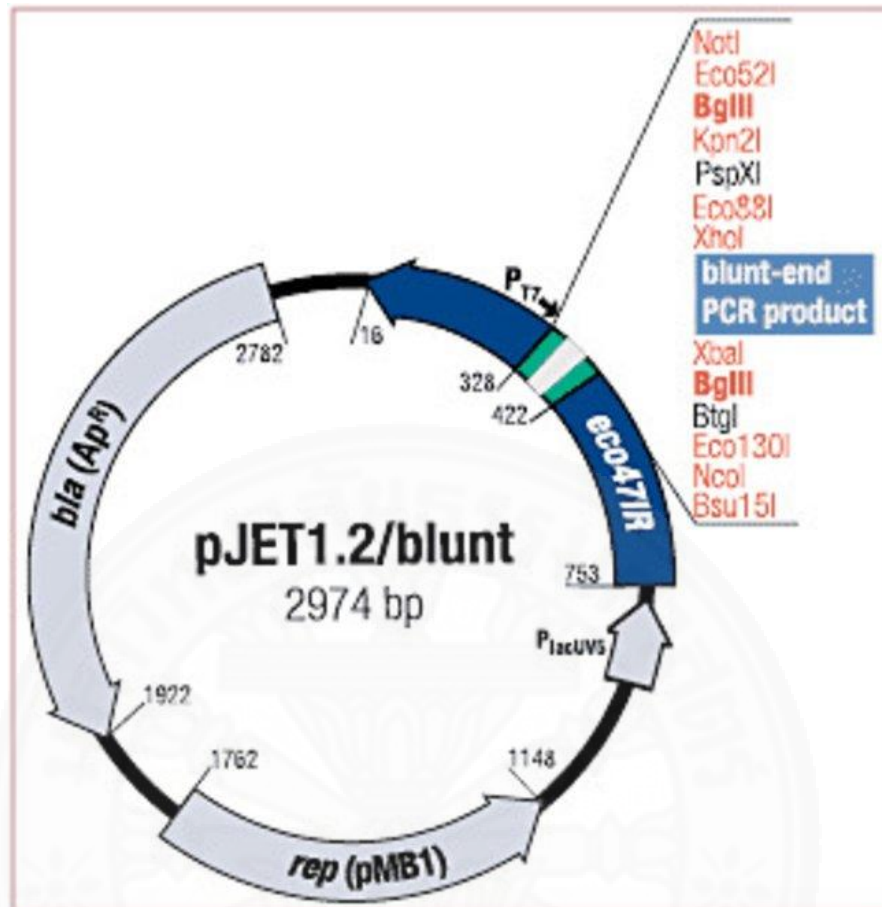


**Figure 4.1** Schematic map of pJET1.2/blunt cloning vector shows genetic elements and restriction sites in multiple cloning site (MCS).

#### 4.3.1.3 Subcloning of FLAG-3A coding sequence into mammalian expression vector

The FLAG-3A coding sequence in pJET1.2/blunt cloning vector and pLVX-Puro expression vector (**Figure 4.2**) were double-digested using restriction endonucleases; *EcoRI* and *XbaI* (Thermo Fisher Scientific, US). The digestion reaction mixture was prepared from all ingredients as shown below.

Component	Volume
<i>EcoRI</i> (10 U/ $\mu$ L)	1 $\mu$ L
<i>XbaI</i> (10 U/ $\mu$ L)	2 $\mu$ L
1 $\times$ Tango Buffer	4 $\mu$ L
DNA fragment / Plasmid DNA target	1 $\mu$ g
Ultrapure distilled water (UDW)	Variable
Total volume	20 $\mu$ L

Digestion mixtures were incubated at 37 °C in water bath for overnight. Subsequently, the digestion reaction was detected using 1% agarose gel electrophoresis. The digested *FLAG-3A* DNA fragment and pLVX-Puro vector were purified from the gel following Bioneer's AccuPrep<sup>®</sup> Gel Purification Kit protocol. The purified fragments were detected using 1% agarose gel electrophoresis and ethidium bromide staining, and estimated the DNA concentration by comparing the DNA band intensity to that of standard DNA marker.

The insert:vector molecular ratio used in ligation of *FLAG-3A* and pLVX-Puro vector was 3:1. The ligation was performed. Transformation and positive clone selection were done as described in **Appendix E**. The plasmid harboring *FLAG-3A* inserted sequence (pLVX::*FLAG-3A*) was verified by DNA sequencing and bioinformatic analysis.

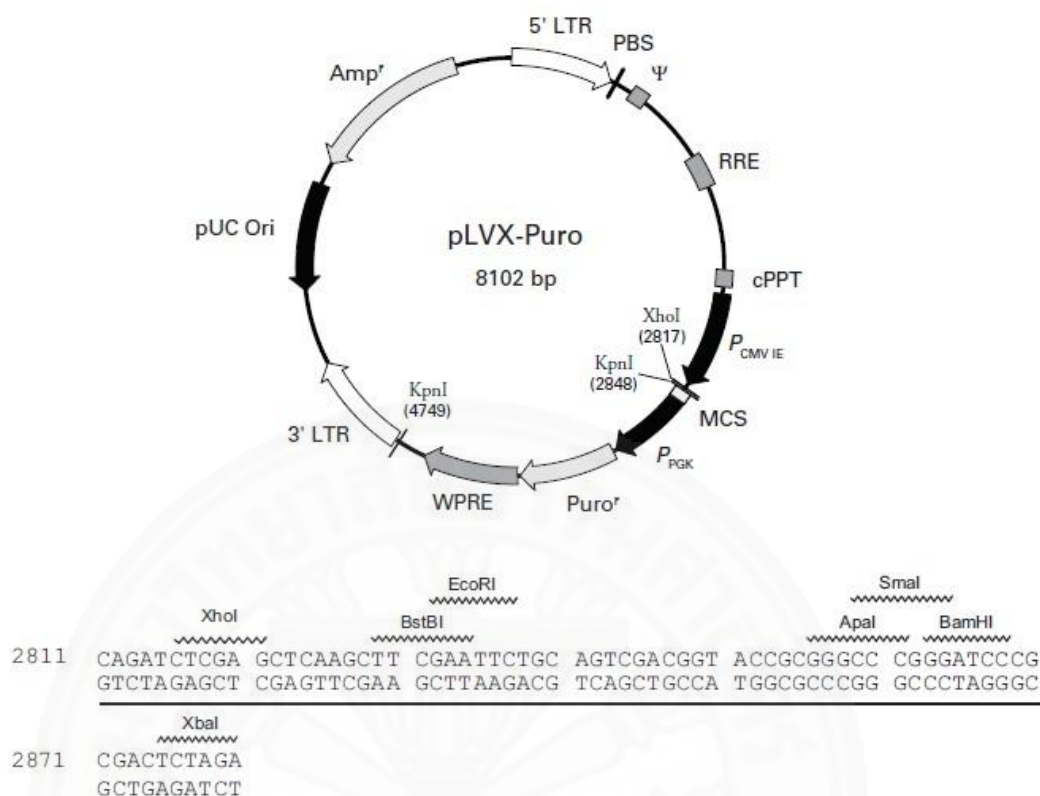


**Figure 4.2** Schematic map of pLVX-Puro lentiviral expression vector shows genetic elements, and restriction sites and sequences in multiple cloning site (MCS).

#### 4.3.1.4 Detection of FLAG-3A protein expression in mammalian cells

##### (1) Transfection with pLVX::FLAG-3A

Human embryonic kidney 293T cells (Lenti-X™ HEK293T cell line, cat. no. 632180, CloneTech, CA, USA) were maintained in Dulbecco's Modified Eagle Medium (DMEM) (Gibco™, Thermo Fisher Scientific, US) while human SH-SY5Y cells were maintained in 1:1 mixture of DMEM and Ham's F-12 (DMEM/F-12) (Gibco™, Thermo Fisher Scientific, US). The culture media were supplemented with 10% fetal bovine serum (FBS), 2 mM L-glutamine (Gibco™, Thermo Fisher Scientific, US), and 1× penicillin-streptomycin (Gibco™, Thermo Fisher Scientific, US). At 90-95% cell confluence, Menzel™ Microscope 12-mm round coverslips were flamed and pre-placed into the well of 24-well plate. HEK293T cells were plated at seeding density of  $5 \times 10^4$  cells/well while SH-SY5Y were plated

at seeding density of  $1 \times 10^5$  cells/well in the 24-well culture plate. The plate was incubated at 37°C with 5% CO<sub>2</sub> until cells reached 50-70% cell confluence. The pLVX::*FLAG-3A* plasmids were prepared and extracted from the bacterial host cells as described in **Appendix E**. The purified pLVX::*FLAG-3A* plasmids were introduced into mammalian cells using Lipofectamine<sup>TM</sup> 3000 Transfection Reagent (Invitrogen, Thermo Fisher Scientific) following the instruction manual protocol. Transfection reaction mixture was separately prepared into 2 tubes namely DNA mixture and Lipofectamine mixture. The main component the DNA mixture tube was pLVX::*FLAG-3A* while of those Lipofectamine mixture was transfection reagent. Each mixture tube was made of the ingredients listed below by mixing them together.

#### **DNA mixture tube**

<b>Component</b>	<b>Volume/amount</b>
Opti-MEM <sup>®</sup> I Reduced-Serum Medium	Fill to 25 µL
pLVX:: <i>FLAG-3A</i>	1 µg/reaction
P3000 <sup>TM</sup> Reagent	2 µL
Total	25 µL

#### **Lipofectamine mixture tube**

<b>Component</b>	<b>Volume</b>
Opti-MEM <sup>®</sup> I Reduced-Serum Medium	23.5 µL
Lipofectamine <sup>TM</sup> 3000 Reagent	1.5 µL
Total	25 µL

The entire volume of the DNA mixture tube was added into Lipofectamine mixture tube and vigorously mixed using vortex. The mixture was incubated at room temperature for 20 minutes. The DNA-Lipid complex mixture was added dropwise to the monolayer cells. The plate was incubated at 37°C with 5% CO<sub>2</sub> for 24 hours.

#### **(2)Detection of FLAG-3A protein expression by immunofluorescence (IF) assay**

At 24 hours post-transfection (h.p.t.), the monolayer cells were washed gently with 1× PBS and fixed with 4% paraformaldehyde (PFA) (**Appendix C**) for 20 minutes at room temperature. The monolayer cells were washed



with 1× PBS and permeabilized by 0.1% Triton X-100 (**Appendix C**) for 10 minutes at room temperature. Cells were washed with 1× PBS and blocked with 5% bovine serum albumin (BSA) (**Appendix C**) for 1 hour at room temperature. Cells were washed twice with 1× PBS, incubated with 1:1000 mouse monoclonal anti-FLAG<sup>®</sup> M2 antibody (cat. F3165, Sigma-Aldrich, USA) diluted in 1% BSA for 1 hour at room temperature, and continued overnight incubation at 4 °C. The monolayer cells were washed twice with 1× PBS and incubated with 1:1600 goat anti-Mouse IgG (H+L) antibody conjugated with Alexa Fluor 488 (cat. A11001, Invitrogen, Thermo Fisher Scientific, US) diluted in 1% BSA for 1 hour at 4 °C, protected from light. Cells were washed 3 times with 1× PBS. For mounting, a small drop of 80% (v/v) glycerol was placed on clean glass slide. The coverslip was picked up from the well and placed upside-down on glycerol drop, avoiding generation of bubbles. The edge of coverslip was sealed with nail polish. The cells were visualized under fluorescence microscope.

#### **4.3.1.5 Production and purification of recombinant EV-A71 3A protein for polyclonal antibody generation**

To produce recombinant EV-A71 3A protein to be used as immunogen for generation of polyclonal antibody specific to EV-A71 3A, HEK293T cells were grown in DMEM supplemented with 10% fetal bovine serum (FBS), 2 mM L-glutamine, and 1× penicillin-streptomycin. At 90-95% cell confluence, cells were plated in 2 wells of 6-well plate at seeding density of  $3 \times 10^5$  cells/well. Cells were transfected with pLVX::FLAG-3A as described above but scaled-up the amount of plasmid to 5 µg per reaction. Transfection was done in the scale of 6-well plate following instruction manual.

After 24 hours of transfection, cell lysate was prepared by adding 1× lysis buffer (**Appendix D**) containing 1× protease inhibitor cocktails (Promega, US) to the cells. To complete cell lysis, ultrasonication was done setting pulse at 0.5:0.5, 30% amplitude, for 30 second. To remove cellular debris, centrifugation was done at 12,000 rpm, at 4°C for 20 minutes. The supernatant was transferred to new 1.5-mL microcentrifuge tube. Expression of FLAG-3A protein was determined by 12% SDS-PAGE and western blot analysis using anti-FLAG<sup>®</sup> M2 antibody. However, the expression level of recombinant 3A protein was too low and



purity was too poor even several attempts of optimization was performed (**data not shown**). Thus, the production of polyclonal antibody specific to EV-A71 3A protein was not further performed in this study.

#### **4.3.1.6 Construction of recombinant plasmid DNA carrying coding sequence of EV-A71 nonstructural 3A in-frame with FLAG-epitope tag at 5'-end and red monomeric fluorescent protein mCherry at 3'-end**

##### **(1) PCR amplification of coding sequence of EV-A71 nonstructural 3A in-frame with FLAG-epitope tag at 5'-end and red monomeric fluorescent protein mCherry at 3'-end**

Because the expression level of the FLAG-3A protein in HEK293T cells was too low, fusion of fluorescence protein mCherry with NS3A was performed aiming to enhance the protein expression. Coding sequences of FLAG-epitope and red monomeric fluorescent protein mCherry were molecularly fused in-frame with EV-A71 nonstructural 3A coding sequence at 5'- and at 3'-end, respectively. To generate *FLAG-3A-mCherry* gene fusion, two overlapping DNA sequences including *EcoRI-FLAG-3A-mCherry* and *3A-mCherry-XbaI* were amplified separately to subsequently generate full-length fragment of *EcoRI-FLAG-3A-mCherry-XbaI* using overlap extension polymerase chain reaction (OE-PCR), as showed in the schematic drawing (**Figure 4.3**).

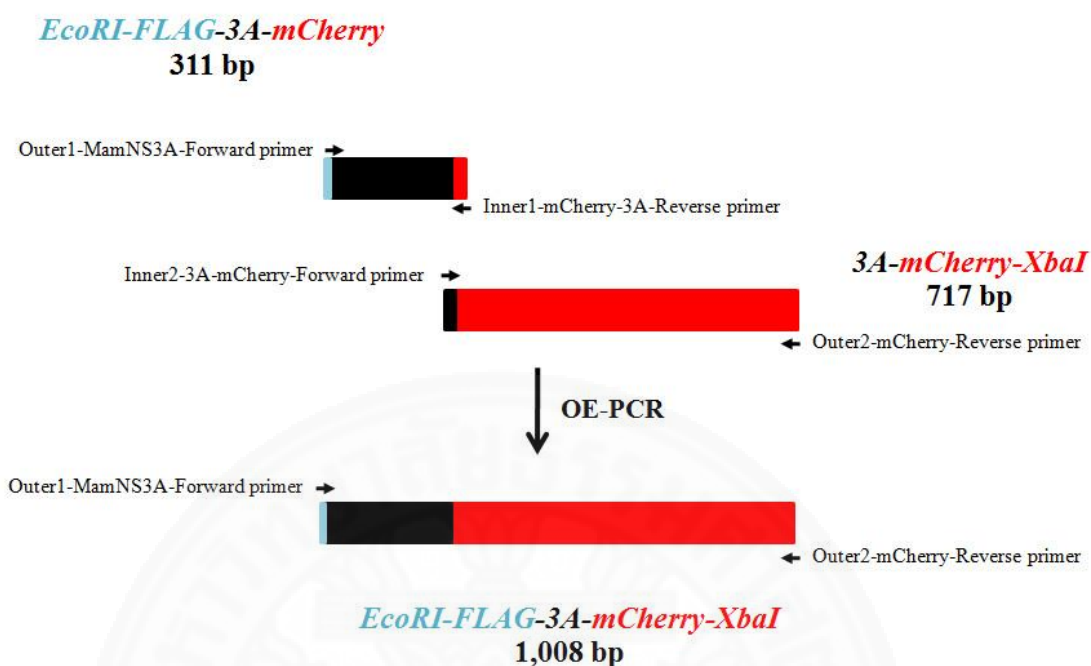


**Figure 4.3** Schematic drawing of amplification of *EcoRI-FLAG-3A-mCherry-XbaI* using overlap extension PCR (OE-PCR).

To generate *EcoRI-FLAG-3A-mCherry*, the sequence-verified pLVX::*FLAG-3A* was used as a template for amplifying *FLAG-3A* incorporated with restriction sequence of *EcoRI* endonuclease at 5'-end and the first 20 nucleotides of mCherry coding sequence at 3'-end using Outer1-MamNS3A-Forward primer and Inner1-mCherry-3A-Reverse primer (**Appendix A**). The PCR reaction mixture for *EcoRI-FLAG-3A-mCherry* amplification was prepared by mixing components as described below together.

Component	Volume
Ultrapure distilled water (UDW)	10.9 $\mu$ L
10 $\times$ reaction buffer	2 $\mu$ L
20 mM MgCl <sub>2</sub>	2 $\mu$ L
10 mM dNTPs (2.5 mM each)	2 $\mu$ L
Outer1-MamNS3A primer (10 $\mu$ M)	1 $\mu$ L
Inner1-mCherry-3A-Reverse (10 $\mu$ M)	1 $\mu$ L

<i>ProFi Taq</i> DNA polymerase (5 units/ $\mu$ L)	0.1 $\mu$ L
pLVX::FLAG-3A (10 ng/ $\mu$ L)	1 $\mu$ L
Total volume	20 $\mu$ L

Amplification of *EcoRI-FLAG-3A-mCherry* DNA fragment was performed at various annealing temperatures including 52, 56, 60, 65, and 68 °C for 30 seconds to find the optimal condition using gradient PCR. The steps of thermal cycle were performed as follows, consecutively.

Step	Temperature (°C)	Time	Cycle
Pre-denaturation	95	5 minutes	1 cycle
Denaturation	95	30seconds	} 30 cycles
Annealing	Gradient from 52 to 68	30seconds	
Extension	72	30 seconds	
Final extension	72	2 minutes	1 cycle

To generate *3A-mCherry-XbaI*, pLV-mCherry (Addgene plasmid #36084) was used as a template for amplifying mCherry coding sequence incorporated with the last 20 nucleotides of EV-A71 3A coding sequence at 5'-end and sequence of restriction site of *XbaI* endonuclease at 3'-end using Inner2-3A-mCherry-Forward primer and Outer2-mCherry-Reverse primer (**Appendix A**). The PCR reaction mixture for *3A-mCherry-XbaI* amplification was prepared by mixing all components as shown below together.

Component	Volume
Ultrapure distilled water (UDW)	10.9 $\mu$ L
10 $\times$ reaction buffer	2 $\mu$ L
20 mM MgCl <sub>2</sub>	2 $\mu$ L
10 mM dNTPs (2.5 mM each)	2 $\mu$ L
Inner2-3A-mCherry-Forward (10 $\mu$ M)	1 $\mu$ L
Outer2-mCherry-Reverse (10 $\mu$ M)	1 $\mu$ L
<i>ProFi Taq</i> DNA polymerase (5 units/ $\mu$ L)	0.1 $\mu$ L
pLV-mCherry (10 ng/ $\mu$ L)	1 $\mu$ L
Total volume	20 $\mu$ L

The amplification was performed using three annealing temperatures to find the optimal condition which were 60, 68, and 70 °C for 30 seconds. The steps of thermal cycle were performed as follows, consecutively.

Step	Temperature (°C)	Time	Cycle
Pre-denaturation	95	5 minutes	1 cycle
Denaturation	95	30 seconds	} 30 cycles
Annealing	Gradient from 66 to 70°C	30 seconds	
Extension	72	1 minute	
Final extension	72	3 minutes	1 cycle

Then, the two overlapping sequences of *EcoRI-FLAG-3A-mCherry* and *3A-mCherry-XbaI* were resolved in 1% agarose gel and purified to further use as templates for generating the full-length sequence of *EcoRI-FLAG-3A-mCherry-XbaI*. The PCR reaction mixture for assembling the *EcoRI-FLAG-3A* and *3A-mCherry-XbaI* to generate *EcoRI-FLAG-3A-mCherry-XbaI* was prepared as follows.

Component	Volume
Ultrapure distilled water (UDW)	9.9 µL
10× reaction buffer	2 µL
20 mM MgCl <sub>2</sub>	2 µL
10 mM dNTPs (2.5 mM each)	2 µL
<i>ProFi Taq</i> DNA polymerase (5 units/µL)	0.1 µL
The purified 5'-FLAG-3A (10 ng/µL)	1 µL
The purified mCherry-3' (10 ng/µL)	1 µL
Total volume	18 µL

The PCR program consisted of two phases. Phase 1 was touchdown step for overlap extension and phase 2 was a conventional thermocycling program for DNA amplification. At phase 1, the PCR mixture without primers was heated at 95 °C for 5 minutes to denature the DNA double-strands of the templates; *EcoRI-FLAG-3A-mCherry* and *3A-mCherry-XbaI*. Then, the temperature was brought down gradually from 95 °C to 45 °C with decrement rate at -1 °C per minute for 2 minutes. In this step, the *EcoRI-FLAG-3A-mCherry* and *3A-mCherry-XbaI* were

slowly annealed at the overlapping sites and the overhang termini of them then were extended by filling with deoxynucleotides at 68 °C for 1 minute. Consequently, the full-length DNA template of *EcoRI-FLAG-3A-mCherry-XbaI* coding sequences was generated. Immediately, the thermal cycle was paused and 1 µL of each Outer1-MamNS3A primer (10 µM) and Outer2-mCherry-Reverse (10 µM) (**Appendix A**) was added into the reaction mixture to top the volume up to 20 µL. Afterward, the thermal cycle was resumed to amplify *EcoRI-FLAG-3A-mCherry-XbaI* coding sequences by the PCR protocol; 95 °C, 30 seconds; 55 °C, 1 minute; 68 °C, 1 minute; 30 cycles with final extension at 68 °C for 3 minutes. The PCR amplicons of *EcoRI-FLAG-3A-mCherry-XbaI* were resolved by 1% agarose gel electrophoresis, and subsequently gel purified following AccuPrep<sup>®</sup> Gel Purification Kit protocol. The purified product was detected using 1% agarose gel electrophoresis and ethidium bromide staining.

## **(2)Cloning of FLAG-3A-mCherry coding sequence**

The purified *EcoRI-FLAG-3A-mCherry-XbaI* DNA fragments were ligated with pGEM<sup>®</sup>-T Easy vector (Promega, USA) (**Figure 4.4**) in ratio 3:1 at 16 °C for overnight. The transformation was done using heat-shock method. The sequence of *FLAG-3A-mCherry* was verified by DNA sequencing (Bioneer, Korea).

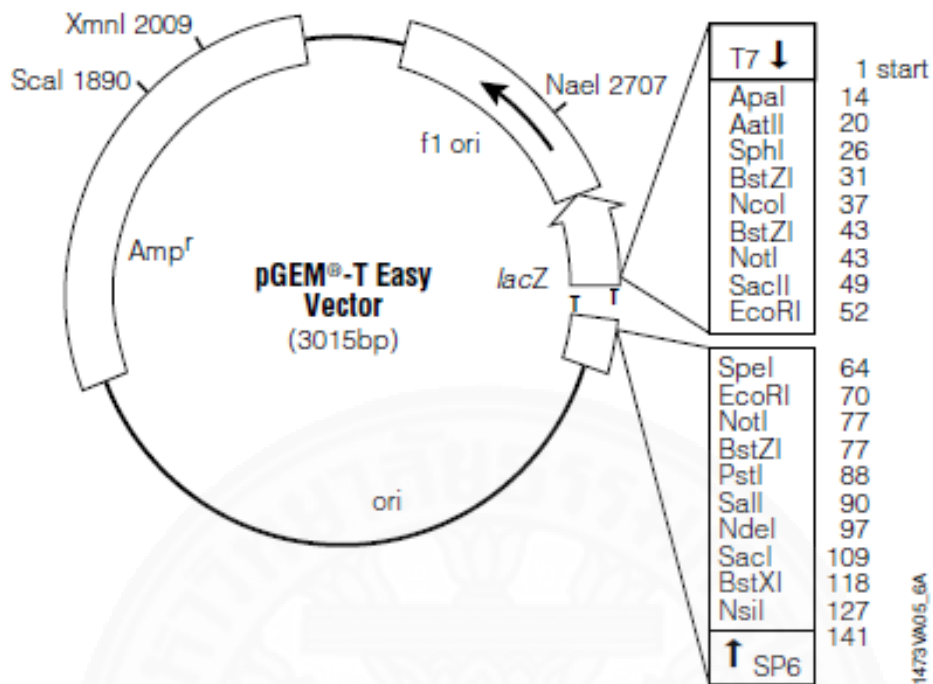


**Figure 4.4** Schematic map of pGEM<sup>®</sup>-T Easy vector shows elements and restriction sites in the vector.

### **(3) Subcloning of FLAG-3A-mCherry coding sequence to mammalian expression vector**

The sequence-verified *FLAG-3A-mCherry* inserted in pGEM<sup>®</sup>-T Easy vector was double-digested using *EcoRI* and *XbaI* endonucleases. The digested *FLAG-3A-mCherry* was resolved and purified from agarose gel, and then directionally cloned into pLVX-Puro expression vector. The ligation was done at 16 °C for overnight before transforming into bacterial competent cells using heat-shock method as described in **Appendix E**. The sequence of *FLAG-3A-mCherry* in pLVX-Puro vector (pLVX::*FLAG-3A-mCherry*) was verified using DNA sequencing (Bioneer, Korea).

#### **4.3.1.7 Examination of FLAG-3A-mCherry protein expression in mammalian cells using fluorescence microscope**

Detection of expression of FLAG-3A-mCherry protein was performed by transfection of the HEK293T cells in 24-well plate as described in the section **4.3.1.3**. The DNA-Lipid complex mixture was added dropwise to the cells. The plate was incubated at 37 °C with 5% CO<sub>2</sub> for 24 hours. Fusion of FLAG-3A with red fluorescent mCherry protein allows direct detection of protein expression by fluorescence microscope. At 24 hours post-transfection (h.p.t.), cells were washed with 1× PBS and fixed with 4% PFA at room temperature for 20 minutes. Cells were washed twice with 1× PBS. The coverslips were mounted and visualized under fluorescent microscope.

#### **4.3.1.8 Detection of FLAG-3A-mCherry protein expression in mammalian cells using western blot analysis**

According to vastly different transfection efficiency of HEK293T and SH-SY5Y cells, expression of FLAG-3A-mCherry protein in these two cells were performed in different scales aiming to obtain the same number of transfected cells enough to be detected by western blot analysis.

##### **(1) Transfection with pLVX::*FLAG-3A-mCherry***

HEK293T and SH-SY5Y cells were cultured as mentioned previously. For cell seeding, HEK293T cells were plated into 2 wells of 6-well plate at seeding density of  $3 \times 10^5$  cells/well. Human SH-SY5Y cells were plated into 5

plates of 6-well plate at seeding density of  $1 \times 10^6$  cells/well. At 70-80% cell confluence, transfection was carried out as described in the **Section 4.3.1.3** with increasing of plasmid DNA quantity to 6  $\mu$ g per reaction. Transfection was done in the scale of 6-well plate following Lipofectamine™ 3000 reagent instruction manual.

At 24 hours post-transfection (h.p.t), cells were harvested by trypsinization and washed once with  $1 \times$  PBS. Cells were resuspended in 1 mL of  $1 \times$  lysis buffer containing protease inhibitor cocktail (Promega, US) (**Appendix D**). To allow complete cell lysis, the suspension was incubated at 4 °C on roller shaker for 30 minutes and further lysed by ultra-sonication set as; pulse 0.5:0.5, 1 minutes, and 30% amplitude. The suspension was centrifuged at 12,000 rpm, 4 °C, 20 minutes. Cell lysate was collected and kept at  $-20$  °C until use.

### (2) Detection of FLAG-3A-mCherry expression

The proteins were resolved by sodium dodecyl sulfate polyacrylamide gel electrophoresis (SDS-PAGE). Denaturing, discontinuous polyacrylamide gel comprised of 2 layers; 4% stacking and 12% resolving gels, was set by using SE245 Hoefer® Dual Gel Caster gel casting apparatus. Each layer of the gel was prepared by mixing ingredients as shown below.

<b>Polyacrylamide gel</b>	<b>Component</b>	<b>Volume (for 2 gels)</b>
12 % Resolving gel	Ultrapure distilled water (UDW)	3.2 mL
	100% Glycerol	0.1 mL
	Gel buffer 1.5 M Tris-HCl, pH 8.8	2.5 mL
	30% Acrylamide/Bis Solution (Bio-Rad, US)	4 mL
	10% SDS	0.1 mL
	10% Ammonium persulfate (APS)	0.2 mL
	TEMED	10 $\mu$ L
<b>Polyacrylamide gel</b>	<b>Component</b>	<b>Volume (for 2 gels)</b>
4% Stacking gel	Ultrapure distilled water (UDW)	3.05 mL



Gel buffer 0.5 M Tris-HCl, pH 6.8	1.25 mL
30% Acrylamide/Bis Solution (Bio-Rad, US)	0.65 mL
10% SDS	50 $\mu$ L
10% Ammonium persulfate (APS)	75 $\mu$ L
TEMED	10 $\mu$ L

The cell lysate was mixed with 6 $\times$  SDS sample buffer (**Appendix D**) to final concentration 1 $\times$  and boiled for 10 minutes. The solution was cooled down to room temperature and spun down for 10 seconds. Proteins were loaded by normalizing total protein amount at 10  $\mu$ g per well. Electrophoresis was performed using SE250 Hoefer<sup>®</sup> vertical electrophoresis unit (Hoefer, MA, USA). Electrophoresis was first set at 10 mA until the dye front entered the stacking gel, then electricity was increased to 20 mA until dye font reached the bottom of the resolving gel.

The SDS-PAGE-separated proteins were transferred to nitrocellulose membrane by horizontal electrophoresis using Hoefer<sup>®</sup> standard electrophoresis blotting unit (Hoefer, MA, USA). The electricity was applied at 100 voltages for 1 hour. The blotted membrane was soaked in 1 $\times$  PBS for 5 minutes and immersed in 5% fetal bovine serum (FBS) in PBS for 1 hour. The blocking solution was removed and the blotted membrane was washed with PBS-tween (PBS-T) for 3 times. The blotted membrane was incubated with rabbit anti-mCherry polyclonal antibody (cat. 5993-100, Biovision, USA) diluted 1:3000 in 0.2% FBS in PBS-T at 4  $^{\circ}$ C for overnight. The antibody solution was removed and the membrane was washed 3 times with PBS-T. The blotted membrane was then incubated with goat anti-mouse IgG (H+L) antibody labeled with alkaline phosphatase (AP) (cat. 0751-1806, SeraCare, USA) diluted 1:3000 in 0.2% FBS in PBS-T for 1 hour at room temperature. The membrane was washed 3 times with PBS-T and equilibrated in 0.15M Tris-HCl pH 9.6 for at least 15 minutes. Each step was done on rotating platform. To develop signal, the membrane was immersed in KPL BCIP/NBT substrate solution (cat. 5420-0030, SeraCare, USA) protected from light for 5-10

minutes. The reaction was stopped by washing the membrane with tap water for several times.

#### **4.3.2 Pull-down of EV-A71 3A interacting proteins in human neuronal SH-SY5Y cells**

Expression of FLAG-3A-mCherry in human SH-SY5Y cells was performed as previously described in **Section 4.3.1.5**. After 24 hours of transfection, cells were harvested and washed with 1× PBS. To prepare cell lysate, cells were resuspended in 1 mL of 1× lysis buffer containing 1× protease inhibitor cocktail (**Appendix D**) and mixed thoroughly by pipetting. Then, the resuspended cells were incubated at room temperature on roller shaker for 1 hour. To complete cell lysis, ultrasonication was done briefly at 30% amplitude with pulse 0.5:0.5 and setting time for 30 seconds. To remove cellular debris, centrifugation was done at 12,000 rpm at 4°C for 20 minutes. Cell lysate was transferred to a sterile 1.5-mL microcentrifuge tube and kept on ice. To pull down the EV-A71 3A interacting proteins, anti-FLAG<sup>®</sup> M2 Magnetic Beads (Sigma-Aldrich, US) was used. As shown in **Figure 4.5**, magnetic beads were equilibrated with 1× lysis buffer and separated on DynaMag<sup>™</sup>-Spin magnet (Life technologies, UK), this step was repeated 3 times. Then, 500 µL of cell lysate prepared from pLVX::FLAG-3A-mCherry transfected SH-SY5Y cells were added to the equilibrated magnetic beads, and rotated at 4 °C for 2 hours. The magnetic beads were captured on DynaMag<sup>™</sup>-Spin magnet, the unbound fraction was kept in a sterile 1.5-mL microcentrifuge tube. The beads were washed 3 times with 500 µL Wash buffer 1 (**Appendix D**) and washed 3 times with 500 µL Wash buffer 2 (**Appendix D**). The last washing fraction was collected. To elute bound proteins from the beads, 200 µL of elution buffer containing 3× FLAG peptide (**Appendix D**) was added. The mixture was incubated for 30 minutes on rotating platform. The elution step was done repeatedly two more times. The concentration of each protein fraction was measured using Bradford protein assay. The loading amount of protein fractions per well were normalized and resolved in 12% SDS-PAGE. The bands of resolved proteins were double-stained with Coomassie brilliant blue and silver dye following the manufacturer's instruction to enhance sensitivity of the visualization.

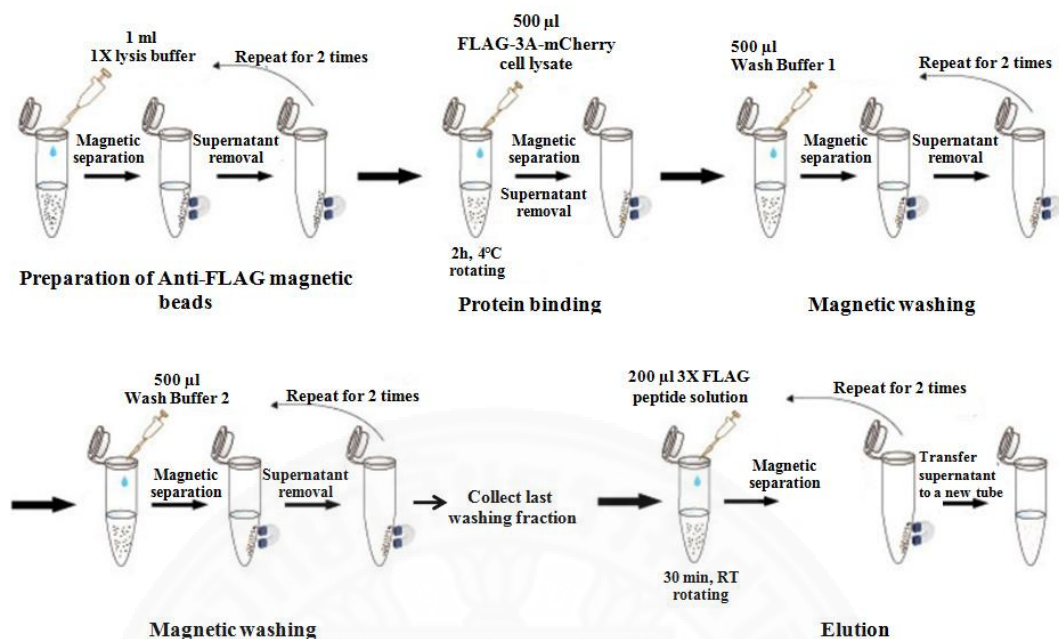


**Figure 4.5** Schematic diagram of pull down of EV-A71 3A interacting proteins using anti-FLAG<sup>®</sup> M2 magnetic beads.

### 4.3.3 Protein identification by Liquid Chromatography Tandem Mass Spectrometry (LC-MS/MS) and analysis

The protein bands counterstained with silver dye of the pull-down of the FLAG-3A-mCherry transfected SH-SY5Y cells were compared to the protein bands in controls including cell lysate prepared from untransfected SH-SY5Y cells, cell lysate prepared from pLV-mCherry transfected SH-SY5Y cells, and washing fraction. The distinguishable protein bands were excised from the SDS-PAGE gel. The gel plugs were sent to service unit of Proteomics International, Australia for protein identification by LC-MS/MS. To de-stain silver dye, the gel pieces of silver-stained bands were incubated with a 1:1 solution of 30 mM potassium ferricyanide and 100 mM sodium thiosulfate for 10 minutes, 2 times. Then, the gel pieces were washed 2 times with water for 1 hour and washed with 25 mM ammonium bicarbonate in 50:50 acetonitrile (ACN):water for 10 minutes. The de-stained and washed gel pieces were vacuum-dried. To perform trypsin digestion, the gel pieces were incubated with trypsin digest solution (12.5 mg/mL trypsin, 25 mM ammonium bicarbonate) at 37 °C for overnight. The digested peptides were extracted by

incubating with ACN containing 1% trifluoroacetic acid (TFA) for 20 minutes, 2 times. The pooled extracts were dried by rotary evaporation and stored at  $-20\text{ }^{\circ}\text{C}$  for further mass spectrometric analysis. Peptides were analyzed by LC-MS analysis using the Agilent 1260 Infinity HPLC system (Agilent) coupled to an Agilent 1260 ChipcubeNanospray interface (Agilent) on an Agilent 6540 mass spectrometer (Agilent). Peptides were loaded onto a ProtID-Chip-150 C18 column (Agilent) and separated with a linear gradient of water/acetonitrile/0.1% formic acid (v/v). Spectra were analyzed to identify proteins of interest using Mascot sequence matching software (Matrix Science) with MSPnr100 database. Protein identification was performed on the basis of statistically significant Mascot score ( $p < 0.05$ ).

#### **4.4 Investigation of expression profiles of trypsinogens (PRSSs) in mammalian cells**

**Objective:** To further characterize the transcriptional expression profile of the EV-A71 3A interacting proteins identified by pull-down assay and LC-MS/MS

##### **4.4.1 Determination of PRSS expression**

Gene expression profiles of human trypsinogens PRSS1 and PRSS3 which are EV-A71 3A interacting proteins identified by pull-down assay and LC-MS/MS as well as closely related PRSS2 were determined by conventional reverse-transcription PCR (RT-PCR). The gene expression of *PRSS1*, *PRSS2*, and *PRSS3* were determined in human SH-SY5Y neuronal cells comparing with HEK293T cells. The HEK293T cells served as a positive control of *PRSS1*, *PRSS2*, and *PRSS3* gene expression as reported by the related article.<sup>103</sup> The total RNA was extracted from the cells using easy-spin™ [DNA free] Total RNA Extraction Kit (iNtRON Bio, Korea) following instruction protocol. Complementary DNA (cDNA) was synthesized using Maxime RT PreMix Oligo (dT)<sub>18</sub> primer (iNtRON Bio, Korea). The sequences of primers used for amplifying PRSS genes were obtained from the previously published work as described by [Hideki Hayashi et al., 2018](#) and listed in **Appendix A**.<sup>103</sup> The primers amplified the specific nucleotide sequences which differentiate each *PRSS* gene. The conventional RT-PCR was performed using protocol as follows;  $95\text{ }^{\circ}\text{C}$ , 5

minutes; 95 °C, 30 seconds, 57 °C, 45 seconds; 72 °C, 40 seconds; 72 °C, 2 minutes; 30 cycles. PCR amplicons were detected by 1% agarose gel electrophoresis.

The expression of the specific PRSS protein was verified by immunofluorescence assay. Human SH-SY5Y cells were grown in completed DMEM/F-12 while HEK293T cells were grown in completed DMEM. At 80% cell confluence, cells were harvested and plated in 24-well plate containing round glass coverslip. SH-SY5Y cells were plated at seeding density of  $2.5 \times 10^4$  cells/well, while HEK293T cells were plated at seeding density of  $1 \times 10^4$  cells/well. At 50-70% cell confluence, culture media were removed and cells were washed with  $1 \times$  PBS. Cells were fixed with 4% PFA at room temperature for 20 minutes and washed with  $1 \times$  PBS. Then, cells were permeabilized with 0.1% (v/v) Triton X-100 at room temperature for 10 minutes, and washed with  $1 \times$  PBS. To block irrelevant proteins, cells were incubated with 5% BSA for 1 hour at room temperature, then washed with  $1 \times$  PBS for two times. Cells were incubated with type-specific anti-PRSS primary antibody diluted in 1% BSA, at 4 °C for overnight. Cells were washed with  $1 \times$  PBS twice, then incubated with 1:1000 Alexa Fluor<sup>®</sup> 488 goat anti-mouse IgG (H+L) (Thermo Fisher Scientific, US) diluted in 1% BSA, at 4 °C for 1 hour, protected from light. Cells were washed three times with  $1 \times$  PBS. To visualize, a small drop of 80% glycerol was placed on glass slide. The round glass coverslips were then transferred to glass slide, sealed with nail polish, and observed under fluorescence microscope.

#### **4.4.2 Subtyping of specific PRSS expressed by human SH-SY5Y neuronal cells**

Because each human PRSS contains several transcript variants, the verified human PRSS expressed by human SH-SY5Y neuronal cells was subtyped by amplifying the full-length cDNA, and verifying by DNA sequencing and bioinformatic analysis. Variant-specific primers were designed according to the coding sequences (CDSs) of *homo sapiens* PRSSs deposited in the Genbank database. The sequences of restriction sites of *Xho*I and *Xba*I endonucleases were incorporated in the primers for further cloning purpose. The sequences of primers were listed in **Appendix A**. The PCR reaction was prepared following the procedure described in **Appendix E**. PCR protocol was as follows; 95 °C, 5 minutes; 95 °C, 30 seconds; gradient temperature at 50, 55, 60 °C, 45 seconds; 72 °C, 1 minute; 30 cycles. PCR

amplicons were detected by 1% agarose gel electrophoresis, purified from the gel using AccuPrep<sup>®</sup> Gel Purification Kit protocol (Bioneer, Korea) and cloned into pGEM<sup>®</sup>-T Easy vector for sequence verification by DNA sequencing and bioinformatic analysis.

#### **4.5 Confirmation of direct protein-protein binding between EV-A71 3A protein and the identified interacting protein by immunoprecipitation assay**

**Objective:** To produce recombinant protein of the EV-A71 3A interacting protein which identified by pull-down assay and LC-MS/MS and verified by gene and protein expression profiling and to confirm direct protein-protein binding with the recombinant EV-A71 3A by immunoprecipitation assay.

##### **4.5.1 Production of recombinant PRSS3 transcript variant 3 fused with Myc epitope tag at C-terminal end by mammalian expression system**

To generate full-length sequence of PRSS3 transcript variant 3 in-frame with Myc coding sequence at 3'-end, the primers were designed according to the sequence of the verified pGEM<sup>®</sup>-T::*prss3v3*. Nucleotide sequences of Myc protein tag, GAGCAGAACTCATCTCAGAAGAGGATCTG, were incorporated into reverse primer at 3'-end. To directionally clone into mammalian expression vector, nucleotide sequences of restriction endonucleases, *Xho*I and *Xba*I, were incorporated at 5'-end of forward primer named 1-prss3v3-forward and reverse primer named 783-Myc-prss3v3-reverse, respectively. The sequences of primers were shown in **Appendix A**. The verified pGEM<sup>®</sup>-T::*prss3v3* was used a template for amplifying the target sequence to generate full-length *PRSS3-Myc (FL-PRSS3-Myc)* DNA fragment. PCR protocol was as follows; 95 °C, 10 minutes; 95 °C, 30 seconds; 62 °C, 45 seconds; 72 °C, 1 minute; 72 °C, 3 minutes, 30 cycles. PCR amplicons were detected by 1% agarose gel electrophoresis and purified from the gel using AccuPrep<sup>®</sup> Gel Purification Kit protocol (Bioneer, Korea). The purified *FL-PRSS3-Myc* fragment was cloned into pGEM<sup>®</sup>-T Easy vector (Promega, US). The ligation was set at 3:1 insert to vector ratio and performed at 16 °C for overnight. Ligation reaction was then transformed into bacterial competent cells JM109 *E. coli* using heat-shock method as



described in **Appendix E**. The presence of *FL-PRSS3-Myc* inserted in pGEM<sup>®</sup>-T (pGEM<sup>®</sup>-T::*FL-PRSS3-Myc*.) was detected by colony PCR using M13 primers. To verify sequence of the inserted *FL-PRSS3-Myc* in positive transformants, overnight bacterial cultures of the positive clones were prepared. Plasmid DNA was isolated using AccuPrep<sup>®</sup> Nano-Plus Plasmid Mini Extraction Kit protocol (Bioneer, Korea) and sent for DNA sequencing conducted by Bioneer, Korea. The obtained nucleotide sequences were analyzed using Applied Biosystems Sequence Scanner Software 2 and DNAMAN program.

The sequence-verified *FL-PRSS3-Myc* fragments were subcloned from pGEM<sup>®</sup>-T cloning vector to pLVX-Puro mammalian expression vector. The pGEM<sup>®</sup>-T::*FL-PRSS3-Myc* and pLVX-Puro plasmids were double-digested with *Xho*I and *Xba*I (Thermo Fisher Scientific, US). The digestion reaction mixture was set by mixing the components as follows together.

<b>Component</b>	<b>Volume</b>
<i>Xho</i> I (10 U/ $\mu$ L)	1 $\mu$ L
<i>Xba</i> I (10 U/ $\mu$ L)	2 $\mu$ L
10 $\times$ Tango buffer	4 $\mu$ L
pGEM <sup>®</sup> -T:: <i>FL-PRSS3-Myc</i> or pLVX-Puro	0.5 $\mu$ g
Ultrapure distilled water (UDW)	Top up to 20 $\mu$ L

The digestion reactions were incubated at 37 °C in water bath for overnight. The digested DNA fragments were detected by 1% agarose gel electrophoresis and purified from the gel using AccuPrep<sup>®</sup> Gel Purification Kit protocol (Bioneer, Korea). The purified *FL-PRSS3-Myc* fragments were ligated with the purified pLVX-Puro vector at 16 °C for overnight before transforming into bacterial competent cells JM109 *E. coli* using heat-shock method. Bacterial transformants were screened by colony PCR using pLVX primers (**Appendix A**). The nucleotide sequence of the *FL-PRSS3-Myc* inserted in pLVX-Puro (pLVX::*FL-PRSS3-Myc*) was verified by DNA sequencing and analyzed by DNAMAN and Sequence scanner (Applied Biosystems). To examine *FL-PRSS3-Myc* protein expression in mammalian cells, the verified clone of pLVX::*FL-PRSS3-Myc* was introduced to HEK293T cells using Lipofectamine<sup>™</sup> 3000 transfection reagent. Mock

and pLVX-Puro transfections were controls in the experiment. Expression was determined at 6- and 24-hours post-transfection (h.p.t.). HEK293T cells were plated at seeding density of  $5 \times 10^4$  cells/well on round coverslip had been placed in the wells of 24-well plate. At 80% cell confluence, transfection was performed as described previously in the **Section 4.3.1.3**.

At the determining time point, cells were washed once with 500  $\mu$ L of  $1 \times$  PBS and fixed with 4% PFA, 250  $\mu$ L/well, at room temperature for 20 minutes. Cells were washed with  $1 \times$  PBS and permeabilized with 250  $\mu$ L of 0.1% Triton X-100 at room temperature for 10 minutes. After washing with  $1 \times$  PBS, cells were incubated with 250  $\mu$ L of 5% BSA at room temperature for 1 hour for blocking nonspecific binding. Then, cells were washed twice with  $1 \times$  PBS. To detect FL-PRSS3-Myc, 1:500 mouse monoclonal anti-cMyc antibody (Biorad, US) was added and incubated at 4 °C for overnight. Cells were washed twice with  $1 \times$  PBS and incubated with 1:1000 goat anti-mouse IgG conjugated with Alexa Fluor 488 for 1 hour at 4 °C, protected from light. Cells were washed 3 times with  $1 \times$  PBS before transferring the round coverslip to slide for mounting and observing under fluorescence microscope.

#### **4.5.2 Production of recombinant mCherry fused with FLAG epitope tag at N-terminal end by mammalian expression system**

Recombinant mCherry fused with FLAG epitope tag at N-terminal end (FLAG-mCherry) would serve as irrelevant interacting protein in the subsequent immunoprecipitation assay. To construct recombinant plasmid DNA carrying coding sequence of FLAG-mCherry, the forward primer for previously amplifying mCherry coding sequence was incorporated with FLAG coding sequence; ATGGATTACAAGGATGACGATGACAAG, at 5'-end. To facilitate directional cloning, nucleotide sequences of restriction sites for *Xho*I and *Xba*I endonucleases were added at 5'-end of forward and reverse primers, respectively. To amplify *FLAG-mCherry* sequence, pLV-mCherry was used as a template. The PCR protocol was as follows; 95 °C, 10 minutes; 95 °C, 30 seconds; 55 °C, 45 seconds; 72 °C, 1 minute; 72 °C, 3 minutes, 30 cycles. Cloning procedure for constructing *FLAG-mCherry* coding plasmid and expression of the recombinant protein was done in the same way as construction of *FL-PRSS3-Myc* coding plasmid described previously. Detection of



the FLAG-mCherry expression in the transfected HEK293T cells was performed using fluorescence microscope

#### **4.5.3 Confirmation of interaction of EV-A71 3A and PRSS3 proteins using immunoprecipitation assay**

##### **4.5.3.1 Preparation of total protein lysates**

Expression of recombinant FLAG-mCherry, FLAG-3A-mCherry, and FL-PRSS3-Myc proteins determined by fluorescence-based techniques showed different expression levels in HEK293T cells in which  $\text{FLAG-mCherry} > \text{FLAG-3A-mCherry} \geq \text{FL-PRSS3-Myc}$ . To obtain roughly fair amounts of the proteins to be used for immunoprecipitation, the scale of expression of each protein was adjusted. For transfection experiments, FLAG-mCherry, FLAG-3A-mCherry, and FL-PRSS3-Myc plasmid constructs were transfected separately in HEK293T cells using Lipofectamine™ 3000 transfection reagent (Invitrogen). Expression of FLAG-mCherry was performed in 2 wells of 6-well plate while expressions of FLAG-3A-mCherry and FL-PRSS3-Myc were performed in 6 wells. After 24 hours of transfection, cell lysates of each protein were prepared in 500  $\mu\text{L}$  ice-cold  $1\times$  lysis buffer (**Appendix D**) containing  $1\times$  protease inhibitor cocktail (Promega). Total protein was measured by Bradford protein assay (Bio-Rad) and normalized amount of protein per well for western blot analysis. Recombinant FLAG-mCherry and FLAG-3A-mCherry proteins were detected by mouse monoclonal anti-FLAG® M2 antibody (Sigma-Aldrich) while FL-PRSS3-Myc protein was detected by mouse monoclonal anti-cMyc antibody (Bio-Rad). Protein lysates were kept at  $-80\text{ }^{\circ}\text{C}$  until use.

##### **4.5.3.2 Immunoprecipitation assay**

To confirm direct protein-protein interaction of EV-A71 3A and PRSS3 proteins in reverse way from FLAG pull-down experiment in **Section 4.3.2**, magnetic beads conjugated with anti-Myc-Tag (9B11) mouse monoclonal antibody (Cell signaling technology) were used to precipitate FL-PRSS3-Myc protein. Immunoprecipitation was performed at 1:1 protein-protein amount ratio. Twenty microliters of the beads were washed 3 times with 500  $\mu\text{L}$  of  $1\times$  lysis buffer. Three hundred micrograms of FL-PRSS3-Myc protein lysate were mixed with 300  $\mu\text{g}$  of FLAG-3A-mCherry protein lysate, and added into the pre-washed beads. To ensure that protein-protein interaction did not cause by protein tags, the same amount of FL-

PRSS3-Myc protein lysate was mixed with 100 µg of FLAG-mCherry protein lysate. To determine binding of the beads to Myc protein, FL-PRSS3-Myc protein lysate and protein lysate prepared from untransfected HEK293T cells were included as controls. The precipitation reactions were incubated at 4 °C with constant mixing on roller shaker for overnight. Unbound fractions were collected. The beads were washed 3 times with Wash buffer 1 (**Appendix D**) and washed 3 more times with Wash buffer 2 (**Appendix D**). Last washing fractions were collected. One hundred microliters of 1× SDS buffer were added to the beads and boiled for 10 minutes to elute bound proteins. The boiled beads were left at room temperature to cool down before spinning down to collect all volume of supernatant. Every magnetic separating step was performed on DynaMag<sup>TM</sup>-Spin magnet (Life technologies, UK).

To detect EV-A71 3A and PRSS3 protein interaction, all precipitation fractions were resolved in 12% SDS-PAGE and transferred to nitrocellulose membrane. The membranes were blocked with 5% FBS at room temperature for 1 hour and washed with PBS-T 3 times, 5 minutes each time. The membranes were incubated with 1:3000 rabbit anti-mCherry polyclonal antibody (BioVision) or 1:6000 mouse monoclonal anti-cMyc antibody (Bio-Rad) at room temperature for 1 hour or 4 °C for overnight. The membranes were washed 3 times with PBS-T, 5 minutes each time, then incubated with secondary antibodies; 1:3000 goat anti-mouse IgG conjugated with alkaline phosphatase or 1:3000 goat anti-mouse IgG conjugated with alkaline phosphatase, at room temperature for 1 hour. The membranes were washed 3 times with PBS-T, 5 minutes each time and equilibrated in 0.15 M Tris-HCl pH 9.6 for 15-30 minutes. Every step was done on rocking platform. To develop colorimetric signals, BCIP/NBT substrate mixture was added to the membrane and incubated at room temperature, protected from light, for 5 minutes. The reaction was stopped by washing with water.

## 4.6 Determination of role of PRSS3 in EV-A71 replication

**Objective:** To determine role of PRSS3 variant 3 in EV-A71 replication by two approaches including overexpression of exogenous protein and gene silencing using small interference RNA (siRNA).

### 4.6.1 Examination of permissiveness of HEK293T cells to EV-A71 infection

Due to low transfection efficiency in SH-SY5Y cells, HEK293T cells were selected to be used as model in this experiment for determining role of neuronal-derived PRSS3 variant 3 in EV-A71 replication. Because *PRSSI*, *PRSS2*, *PRSS3* expressions were low in HEK293T cells as described in result **Section 5.4**, this cell was chosen as a host for overexpressing the exogenous PRSS3 variant 3 and determined the role of PRSS3 in EV-A71 replication. Moreover, HEK293T cells are considered as a highly transfectable cell line. Therefore, the HEK293T cells were considered as a cell that suitable for transfection with mammalian expression vector and siRNA for gene silencing experiment. Prior to performing the infection, HEK293T cells were tested for permissiveness to EV-A71 infection by CCID50 method. RD cells were used as control of maximum EV-A71 infection. Both HEK293T and RD cells were maintained in completed DMEM and plated at seeding density of  $1 \times 10^4$  cells/well into wells of 96-well plate. EV-A71 viral stock with titer  $10^{6.125}$  CCID50/100  $\mu$ L was 10-fold serially diluted from  $10^{-1}$  to  $10^{-8}$  to determine CCID50 in HEK293T cells as aforementioned protocol in **Section 4.1.2**. The permissiveness of HEK293T cells to EV-A71 infection was determined by comparing CCID50 to those of derived from the RD cells.

### 4.6.2 Determination of role of PRSS3 overexpression in EV-A71 replication

HEK293T cells were plated at seeding density of  $4 \times 10^5$  cells/well into wells of 6-well plate. At 60-70% cell confluence, cells were transfected with pLVX::*FL-PRSS3-Myc*. Monolayer cells transfected with pLVX-Puro vector served as negative control. Cells treated with transfection reagent alone served as mock control. The transfection was carried out using Lipofectamine™ 3000 reagent. Transfection was performed as described previously in the **Section 4.3.1.3**.

As shown in the schematic diagram (**Figure 4.6**), at 6 h.p.t., the transfected and mock cells were infected with EV-A71 at MOI 10. To determine EV-A71 replication at 24 hours post-infection (h.p.i.), total RNA was isolated from each sample using TRIzol™ Reagent following instruction protocol. EV-A71 RNA was determined by one-step SYBR Green-based real-time RT-PCR. The PCR protocol was as follows; 42 °C, 1 hour; 95 °C, 10 minutes; 95 °C, 1 minute; 57 °C, 45 seconds; 72 °C, 45 seconds; 40 total cycles with melting temperature analysis. The sequences of EV-A71 specific primers were listed in **Appendix A**.

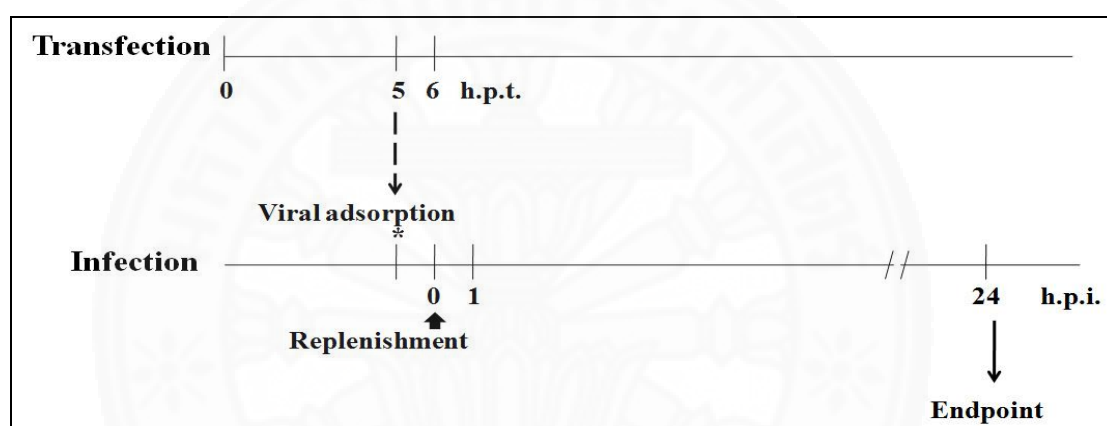


**Figure 4.6** Schematic diagram of transfection of HEK293T cells followed by EV-A71 infection.

To investigate the effect of PRSS3 protein overexpression on EV-A71 replication, the levels of viral genome were semi-quantified using the  $\Delta\Delta\text{CT}$  method to determine fold change ( $2^{-\Delta\Delta\text{CT}}$ ) in copy number of EV-A71 genome.<sup>104</sup> To calculate the fold change of EV-A71 genome copy number, the Ct value of EV-A71 RNA of PRSS3-, pLVX-Puro-transfected cells, and mock control cells were normalized with the internal house-keeping gene *GAPDH*. The normalized EV-A71 Ct ( $\Delta\text{Ct}$ ) values of the PRSS3- and pLVX-Puro-transfected cells were subtracted with EV-A71 normalized Ct of mock control cells ( $\Delta\Delta\text{Ct}$ ). The relative fold-change of EV-A71 genome copy number in the transfected cells were calculated using formula as below.

### Fold change of EV-A71 genome copy number in PRSS3-transfected cells:

$$\begin{aligned} \Delta Ct_{\text{EV-A71 infected PRSS3-transfected cells}} &= Ct_{\text{EV-A71-infected PRSS3-transfected cells}} - Ct_{\text{its GAPDH}} \\ \Delta Ct_{\text{EV-A71-infected mock cells}} &= Ct_{\text{EV-A71-infected mock cells}} - Ct_{\text{its GAPDH}} \\ \Delta\Delta Ct_{\text{EV-A71-infected PRSS3-transfected cells}} &= \Delta Ct_{\text{EV-A71 infected PRSS3-transfected cells}} - \Delta Ct_{\text{EV-A71-infected}} \\ &\text{mock cells} \\ \text{Fold change} &= 2^{-\Delta\Delta Ct_{\text{EV-A71-infected PRSS3-transfected cells}}} \end{aligned}$$

### Fold change of EV-A71 genome copy number in pLVX-Puro-transfected cells:

$$\begin{aligned} \Delta Ct_{\text{EV-A71-infected pLVX-transfected cells}} &= Ct_{\text{EV-A71-infected pLVX-transfected cells}} - Ct_{\text{its GAPDH}} \\ \Delta Ct_{\text{EV-A71-infected mock cells}} &= Ct_{\text{EV-A71-infected mock cells}} - Ct_{\text{its GAPDH}} \\ \Delta\Delta Ct_{\text{EV-A71-infected pLVX-transfected cells}} &= \Delta Ct_{\text{EV-A71-infected pLVX-transfected cells}} - \Delta Ct_{\text{EV-A71-infected mock cells}} \\ \text{Fold change} &= 2^{-\Delta\Delta Ct_{\text{EV-A71-infected pLVX-transfected cells}}} \end{aligned}$$

The Ct values of test and control samples were from 3 independent experiments performed with triplicate wells of real-time RT-PCR (N = 9).

## 4.6.3 Determination of effect of PRSS3 loss-of-function on EV-A71 replication

### 4.6.3.1 Gene knockdown of PRSS3 by siRNAs

HEK293T at number of  $5 \times 10^4$  cells were seeded per well of 24-well plate and cultured in 500  $\mu\text{L}$  of completed DMEM without antibiotics. At 70-80% cell confluence, cells were transfected with equally pooled of three siRNA constructs targeting *PRSS3* including Silencer<sup>®</sup> Select pre-designed ID s194719, s11259, and s11260 (ambion<sup>®</sup>, life technologies<sup>™</sup>) at final concentration 30 nM in the culture medium. Cells incubated with 10 nM siRNA targeting *GAPDH* house-keeping gene (Silencer<sup>®</sup> Select *GAPDH* siRNA, ambion<sup>®</sup>, life technologies<sup>™</sup>) were served as control for siRNA transfection and irrelevant gene knockdown. The sequences of siRNAs used in this study were shown in **Appendix A**. Mock transfection control was also included in the experiment. Transfection reaction mixtures of each assayed groups were prepared into 2 separate tubes as described in the **Section 4.3.1.3**.

#### Tube 1 siRNA mixture

Component	Mock	<i>GAPDH</i>	<i>PRSS3</i>
Opti-MEM <sup>®</sup> I Reduced-Serum	25 $\mu\text{L}$	24.5 $\mu\text{L}$	23.5 $\mu\text{L}$

Medium			
siGAPDH (10 pmol/ $\mu$ L or 10 $\mu$ M)	-	0.5 $\mu$ L	-
3 constructs of siPRSS3 (10 pmol/ $\mu$ L or 10 $\mu$ M)	-	-	0.5 + 0.5 + 0.5 $\mu$ L
Total	25 $\mu$ L	25 $\mu$ L	25 $\mu$ L

### **Tube 2 Lipofectamine mixture**

<b>Component</b>	<b>Volume per reaction</b>		
Opti-MEM <sup>®</sup> I Reduced-Serum Medium	23.5 $\mu$ L	23.5 $\mu$ L	23.5 $\mu$ L
Lipofectamine <sup>™</sup> 3000 reagent	1.5 $\mu$ L	1.5 $\mu$ L	1.5 $\mu$ L
Total	25 $\mu$ L	25 $\mu$ L	25 $\mu$ L

The entire volume of siRNA mixture (Tube 1) was added to Lipofectamine mixture (Tube 2) and mixed thoroughly using vortex, and then incubated at room temperature for 20 minutes. Transfection mixture was added dropwise 50  $\mu$ L per well. At 72 h.p.t., total RNA samples were isolated from the cells using TRIzol<sup>™</sup> reagent following instruction protocol. Concentration and purity of total RNA were measured using spectrophotometer. One microgram of total RNA of each sample was treated with DNase I (Thermo Fisher Scientific, US) prepared as follows.

<b>Component</b>	<b>Volume or amount</b>
Total RNA	1 $\mu$ g
10 $\times$ Reaction buffer with MgCl <sub>2</sub>	2 $\mu$ L
DNase I, RNase-free	1 $\mu$ L (1 U)
UltraPure <sup>™</sup> DNase/RNase-free distilled water	to 20 $\mu$ L

The gene knockdown efficiency was determined by semi-quantitative real-time RT-PCR using the  $\Delta\Delta$ CT method to determine fold change ( $2^{-\Delta\Delta$ CT}) of *PRSS3* and *GAPDH* expression. To calculate the fold change of *PRSS3* and *GAPDH* expression, the Ct values of those two genes of siRNA-treated and mock cells were normalized with the internal actin house-keeping gene (*ACTB*). The normalized Ct ( $\Delta$ Ct) values of *PRSS3* and *GAPDH* were subtracted with Ct of the

respective genes of mock control cells ( $\Delta\Delta Ct$ ). The relative fold-change of the *PRSS3* and *GAPDH* in the transfected cells were calculated using formula as below.

**Fold change of *PRSS3* gene expression in siRNA-treated and mock cells:**

$$\begin{aligned}\Delta Ct_{\text{siPRSS3-transfected cells}} &= Ct_{\text{siPRSS3-transfected cells}} - Ct_{\text{its ACTB}} \\ \Delta Ct_{\text{mock transfected cells}} &= Ct_{\text{mock transfected cells}} - Ct_{\text{its ACTB}} \\ \Delta\Delta Ct_{\text{siPRSS3-transfected cells}} &= \Delta Ct_{\text{siPRSS3-transfected cells}} - \Delta Ct_{\text{mock transfected cells}} \\ \text{Fold change} &= 2^{-\Delta\Delta Ct_{\text{siPRSS3-transfected cells}}}\end{aligned}$$

**Fold change *GAPDH* gene expression in siRNA-treated and mock cells:**

$$\begin{aligned}\Delta Ct_{\text{siGAPDH-transfected cells}} &= Ct_{\text{siGAPDH-transfected cells}} - Ct_{\text{its ACTB}} \\ \Delta Ct_{\text{mock transfected cells}} &= Ct_{\text{mock transfected cells}} - Ct_{\text{its ACTB}} \\ \Delta\Delta Ct_{\text{siGAPDH-transfected cells}} &= \Delta Ct_{\text{siGAPDH-transfected cells}} - \Delta Ct_{\text{mock transfected cells}} \\ \text{Fold change} &= 2^{-\Delta\Delta Ct_{\text{siGAPDH-transfected cells}}}\end{aligned}$$

The Ct values of test and control samples were from 3 independent experiments performed with triplicate wells of real-time RT-PCR (N = 9).

**4.6.3.2 Effect of gene knockdown of *PRSS3* on EV-A71 replication**

Monolayer cells of HEK293T were prepared and silenced the expression of *PRSS3* target gene and *GAPDH* control gene described in the **Section 4.6.3.1**. Cells treated with transfection reagent alone served as mock control. At 48 h.p.t., three hundred microliters of the diluted virus solution yielding EV-A71 MOI 10 were added to the siRNA-transfected and mock cells, and incubated at 37 °C for 1 hour for viral adsorption. The siRNA-transfected and mock cells were not inoculated with EV-A71 served as negative infection control. At 24 hours post-infection (h.p.i.), both total protein and RNA were isolated from the same samples using TRIzol™ reagent following instruction protocol. For protein, concentration of the prepared protein lysates was measured by Bradford protein assay. Concentration and purity of total RNA was measured using spectrophotometer. The total RNA samples were treated with DNase I as described previously. The fold change of *PRSS3* and *GAPDH* expression in response to EV-A71 was determined as described above. To investigate the effect of *PRSS3* and *GAPDH* gene knockdown on EV-A71 replication, the levels of viral genome were semi-quantified using the  $\Delta\Delta Ct$  method described in the



**Section 4.6.2.** The relative fold-change of EV-A71 genome copy number in the transfected cells were calculated using formula as below.

**Fold change of EV-A71 genome copy number in siPRSS3-transfected cells:**

$$\begin{aligned} \Delta Ct_{\text{EV-A71-infected siPRSS3-transfected cells}} &= Ct_{\text{EV-A71-infected siPRSS3-transfected cells}} - Ct_{\text{its ACTB}} \\ \Delta Ct_{\text{EV-A71-infected mock cells}} &= Ct_{\text{EV-A71-infected mock cells}} - Ct_{\text{its ACTB}} \\ \Delta \Delta Ct_{\text{EV-A71-infected siPRSS3-transfected cells}} &= \Delta Ct_{\text{EV-A71-infected siPRSS3-transfected}} - \Delta Ct_{\text{EV-A71-infected mock cells}} \\ \text{Fold change} &= 2^{-\Delta \Delta Ct_{\text{EV-A71-infected siPRSS3-transfected cells}}} \end{aligned}$$

**Fold change of EV-A71 genome copy number in siGAPDH-transfected cells:**

$$\begin{aligned} \Delta Ct_{\text{EV-A71-infected siGAPDH-transfected cells}} &= Ct_{\text{EV-A71-infected siGAPDH-transfected cells}} - Ct_{\text{its ACTB}} \\ \Delta Ct_{\text{EV-A71-infected mock cells}} &= Ct_{\text{EV-A71-infected mock cells}} - Ct_{\text{its ACTB}} \\ \Delta \Delta Ct_{\text{EV-A71-infected siGAPDH-transfected cells}} &= \Delta Ct_{\text{EV-A71-infected siGAPDH-transfected cells}} - \Delta Ct_{\text{EV-A71-infected cells}} \\ \text{Fold change} &= 2^{-\Delta \Delta Ct_{\text{EV-A71-infected siGAPDH-transfected cells}}} \end{aligned}$$

The Ct values of test and control samples were from 3 independent experiments performed with triplicate wells of real-time RT-PCR (N = 9).

Not only genome replication, but also the EV-A71 protein levels were examined in the siRNA-treated cells and controls by western blot analysis. The amount of protein loading was normalized as 1 µg per well. The prepared protein lysates were resolved in 12% SDS-PAGE before transferring to nitrocellulose membrane. The membrane was blocked with 5% FBS for 1 hour, then washed with PBS-T 3 times, 5 minutes each time. The membrane was incubated with 1:3000 mouse anti-enterovirus 71 VP2 antibody (cat. 4175-0127, Bio-Rad) at 4 °C for overnight and washed 3 times with PBS-T. The membrane was then incubated with 1:3000 goat anti-mouse IgG (H+L) conjugated with HRP at room temperature for 1 hour and washed 3 times with PBS-T, 5 minutes each time. Every step was done on rocking platform. To visualize protein bands, the membrane was incubated with Clarity western ECL substrate (Bio-Rad) at room temperature for 10 minutes and imaged by ChemiDoc™ XRS+ with Image Lab™ Software (Bio-Rad). To show normalization, detection of β-actin protein band was also done simultaneously using mouse anti-beta Actin antibody (cat. BF0198, Affinity Biosciences).



## CHAPTER 5

### RESULTS

#### 5.1 Virus propagation and preparation of genetic material of EV-A71

EV-A71 (Thai clinical isolate, genotype B5) designated as TUCU001/B5 isolate was successfully propagated in rhabdomyosarcoma (RD) cells. After 24 hours of infection, the infected cells initially showed explicit cytopathic effects (CPEs), the hallmarks of EV-A71 infection, including cell rounding, aggregation, and detachment. The CPEs increasingly occurred upon the time of infection and reached a maximum at day 5 post-infection. The viral titer was  $1 \times 10^{8.125}$  CCID<sub>50</sub>/100  $\mu$ L.

Total RNA was extracted from 500  $\mu$ L of the viral stock. The concentration of the extracted RNA was 106.0 ng/ $\mu$ L with an OD ratio of 260/280 and 260/230 were 1.83 and 1.34, respectively. The EV-A71 genomic RNA was detected from the extracted total RNA using real-time qRT-PCR at cycle threshold (Ct) 21. The specific PCR products of EV-A71 *VPI* were verified by determining melting temperature which was 81.5-82.5  $^{\circ}$ C. Taken together, it was found that the quality and quantity of viral RNA were eligible for further use in the subsequent experiments.

#### 5.2 Selection of human neuronal cells that are permissive to EV-A71 infection

The permissiveness to EV-A71 infection of SH-SY5Y and SK-N-MC neuronal cells was determined by comparing CCID<sub>50</sub> with those of RD cells. The 10-fold serially diluted viral inoculum was made from EV-A71 viral stock with starting titer at  $10^{8.125}$  CCID<sub>50</sub>/100  $\mu$ L and tested with the human neuronal cells comparing with standard RD cells. It was found that CCID<sub>50</sub> of tested EV-A71 inoculum in SH-SY5Y cells was comparable to those of RD cells of which  $10^7$  and  $10^{8.125}$  CCID<sub>50</sub>/100  $\mu$ L from the former and latter, respectively (**Figure 5.1**). While the SK-N-MC cells were refractory to EV-A71 infection as none of dilution of virus stock could cause CPEs. It was concluded that SH-SY5Y was suitable model for

investigating the interaction of EV-A71 3A protein and cellular factor in human neuronal cell.

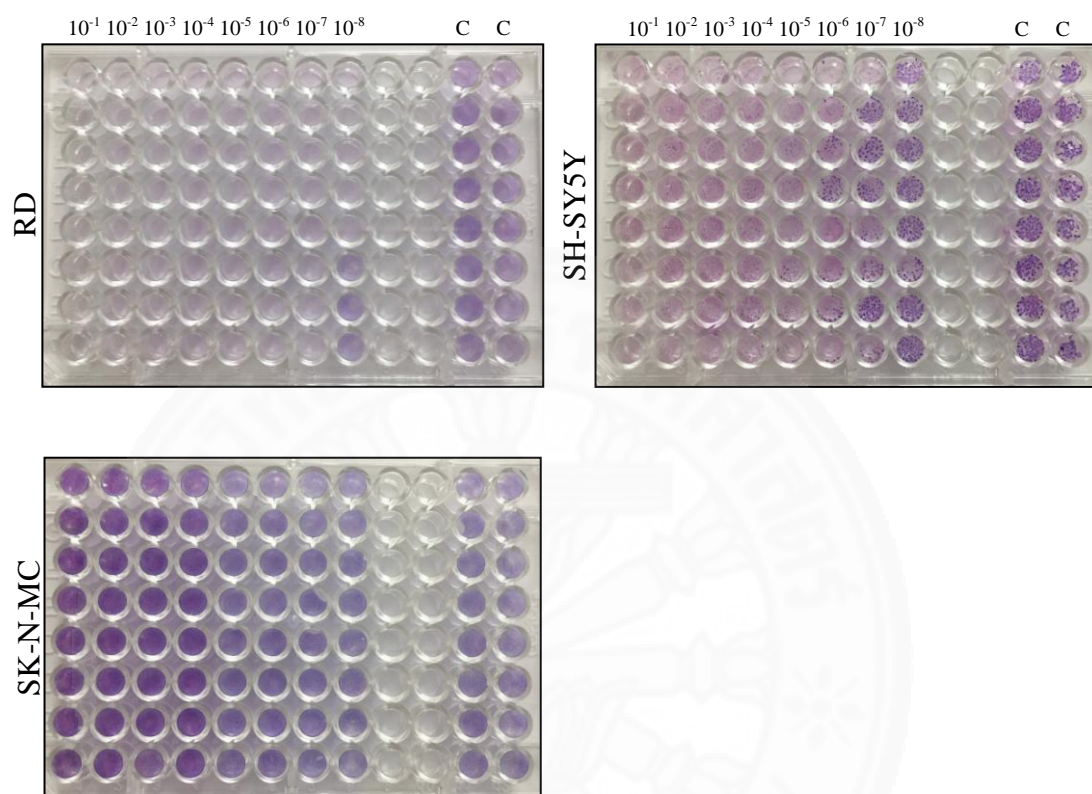


**Figure 5.1** Determination of permissiveness to EV-A71 infection of SH-SY5Y and SK-N-MC neuronal cells by comparing CCID50 with those of RD cells. Dilutions of the tested EV-A71 viral stock ( $10^{-1}$  to  $10^{-8}$ ) were indicated above each row of 96-well plate. Monolayer cells were stained with Giemsa dye. Wells with cell detachment showing clear well or less stained cells were positive for CPE. C; Cell control.

### 5.3 Molecular cloning of EV-A71 nonstructural 3A coding sequence

#### 5.3.1 Construction of recombinant plasmid DNA carrying coding sequence of EV-A71 nonstructural 3A in-frame with FLAG-epitope tag at 5'-end

The coding sequence of EV-A71 3A incorporated with FLAG-epitope tag at 5'-end (*FLAG-3A*) was successfully amplified by RT-PCR (**Figure 5.2**). After ligation and transformation, the insertion of EV-A71 *FLAG-3A* coding sequence

in the pJET1.2/blunt cloning vector was screened from the colonies of *E. coli* transformant by direct colony PCR. It was found that 11 out of 12 randomly selected transformants were detected for the recombinant plasmid harboring the *FLAG-3A* insertion designated as pJET1.2::*FLAG-3A* (**Figure 5.3**). The insertion of *FLAG-3A* sequence was verified by DNA sequencing and bioinformatic analysis. It was showed that the FLAG tag coding sequence was successfully incorporated upstream of EV-A71 3A coding sequence (**Figure 5.4A**). The deduced amino acid sequence of *FLAG-3A* showed that FLAG amino acid sequences were correct and in the same reading frame with EV-A71 3A (**Figure 5.4B**).

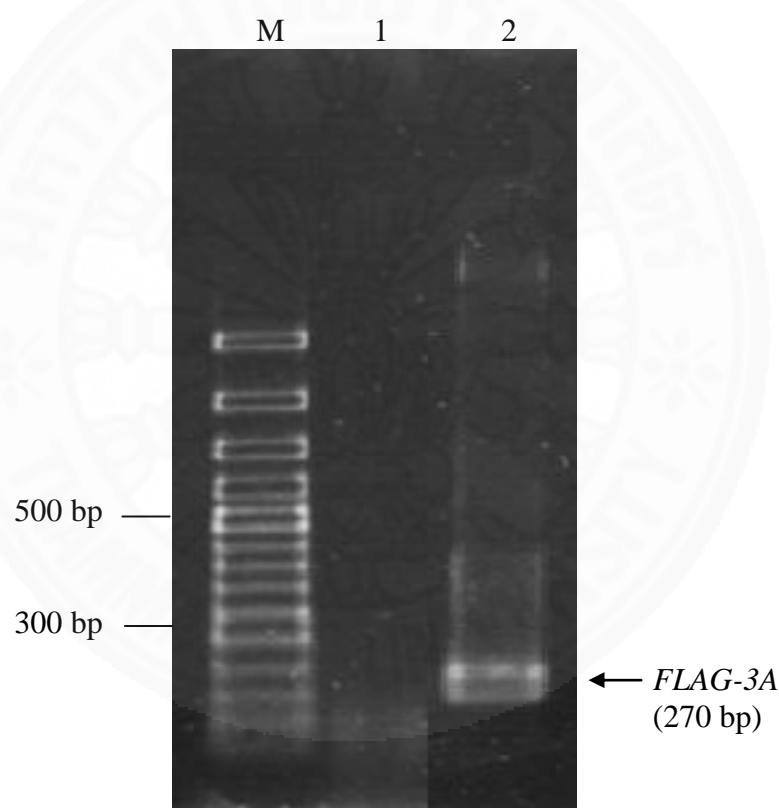


**Figure 5.2** Agarose gel electrophoresis of *FLAG-3A* amplicon. Lane M; 100 bp DNA ladder (in base pairs, bp), lane 1; non-template control, lane 2; PCR amplicons of *FLAG-3A* as indicated by arrow with expected size (bp).

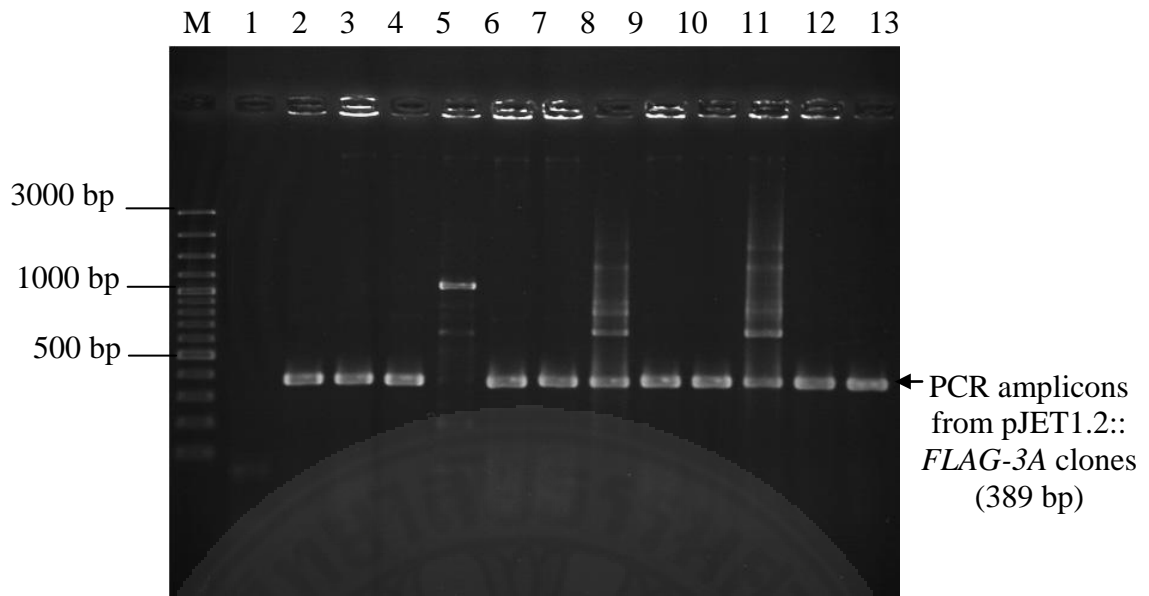


**Figure 5.3** Agarose gel electrophoresis of PCR products amplified from colonies of JM109 *E. coli* transformed with pJET1.2::*FLAG-3A* by colony PCR. Lane M; 100 bp Plus DNA ladder (in base pairs, bp), lane 1; non-template control, lanes 2-13; PCR amplicons from 12 colonies of the transformed *E. coli*, respectively. Lanes 2-4 and 6-13 showed positive PCR amplicons at expected size of 389 bp which is *FLAG-3A* together with flanking DNA region generated by primer extension indicated by arrow.

A

<i>EcoRI</i>	<i>FLAG</i>	<i>3A</i>
ATATGAATTC	ATGGATTACA	AGGATGACGA
TAGAATCAGT	AGCCAGCCCC	AGATGCTATT
TGACAGTGAG	GGAGCAAGGT	TGGATCATCC
CACCAATGTT	TCAACAGAGC	ATGCAATCCA
GGTGGCAGTT	TGTATGTCAT	TTTGCAGGGT
CGACATATCT	TTCTAGAAGA	TTCAATAGGT
<i>SalI</i>	<i>XbaI</i>	

B

<i>FLAG</i>	<i>3A</i>
MDYKDDDDKG	PPKFRPIRIS
ERHLNRAVLV	MQSIATVVAV
	VSLVYVIYKL
	FAGFQ*

**Figure 5.4** Nucleotide sequence of *FLAG-3A* inserted in pJET1.2/blunt cloning vector (A) and the deduced amino acid sequence of *FLAG-3A* coding sequence (B). Light grey highlight indicates FLAG sequence. Underline indicates restriction sites. Red letters and asterisk indicate stop codon.

### 5.3.2 Prediction of functional domain/motif EV-A71 NS3A

Protein homology search of the cloned EV-A71 3A coding sequence was performed by NCBI BLASTx using a translated nucleotide query to search protein databases (<https://blast.ncbi.nlm.nih.gov/Blast.cgi>, assessed on 8/6/2021). It was found that 3A protein shared high sequence identity among the EV-A71 (97.67% to 100% identity) and across members in genus *Enterovirus* such as coxsackievirus A2 (98.84% identity), A10 (100% identity), and A16 (100% identity) (**Figure 5.5**). Protein domain homology of the cloned EV-A71 3A sequence was predicted from the deduced amino acid sequence. It was found that the nucleotide sequence of EV-A71 3A at position 22-132 contains poliovirus 3A protein-like domain or P3A (accession number pfam08727), and the nucleotide sequence at 91-159 contains FGGY\_RhuK, the L-rhamnulokinase domain (accession number cd07771) (**Figure 5.6A**). The nucleotides 22-132 of EV-A71 3A were translated and aligned with the full-length EV-A71 3A to annotate this domain in the protein (**Figure 5.6B**). It was found that

the P3A domain is located at amino acid positions 8 to 45 of the EV-A71 3A. The deduced amino acid sequence of the cloned EV-A71 3A was aligned with the poliovirus P3A accession number 1NG7 for annotating additional functional domains. It was found that the cloned EV-A71 3A contains soluble N-terminal domain, hydrophobic C-terminal domain, and additional residues which located at amino acid residues 1-58, 59-80, and 81-85, respectively (**Figure 5.6C**). And it has been reported that 3A proteins of enteroviruses contains 58-residue N-terminus, 22-residue C-terminus and the additional residues at C-terminus.<sup>26</sup> In addition, homology structure of EV-A71 3A protein analyzed by Swiss-Model showed that amino acid residues 16-83 were modeled with cyclin-dependent kinase 5 activator 1 (model 1) while amino acid residues 1-58 were modeled with P3A accession number 1NG7 (model 2) corresponding to the BLASTx results (**Figure 5.7**). By model 1, it was found that three amphipathic alpha-helices were predicted at amino acid residues 16-38, 57-61, and 64-82 on the EV-A71 3A, respectively. While model 2 could predict two amphipathic alpha-helices at amino acid positions 22-28 and 31-40 on the EV-A71 3A, respectively. It has been reported that the P3A, also known as N-soluble poliovirus 3A (or 3A-N), is likely to form symmetric homodimer in which each monomer is composed of two amphipathic alpha-helices spanning residues 23-29 and 32-41 with the loop between them bending 180° to form a helical hairpin.<sup>26</sup> It could be postulated that the EV-A71 3A might share homologous structure with the P3A as showed by the model 2.

Myristoylation were detected at N-terminal region of some picornaviral 3A proteins including 3A proteins of Aichi virus, bovine kobuvirus, and klassevirus.<sup>82</sup> However, in poliovirus and enteroviruses, myristoylation was found at N-terminus of viral capsid protein 4 (VP4) instead of the 3A proteins.<sup>105, 106</sup> To verify the myristoylation site in EV-A71 3A protein, prediction of myristoylation site of the deduced amino acid sequences of the cloned EV-A71 3A protein was performed using Myristoylator (<https://web.expasy.org/myristoylator/>) and NMT program (<http://mendel.imp.ac.at/myristate/SUPLpredictor.htm>). As expected, it was found that the EV-A71 3A was predicted as non-myristoylated protein (**Figure 5.8A and B**).



**Sequences producing significant alignments**

Download  Select columns  Show 100  GenPept  Graphics

select all 100 sequences selected

Description	Scientific Name	Max Score	Total Score	Query Cover	E value	Per. Ident	Acc. Len	Accession
3A protein [Coxsackievirus A2]	Coxsackievirus...	139	139	100%	5e-41	98.84%	86	YP_009508937.1
3A protein [Enterovirus A71]	Enterovirus A71	139	139	100%	5e-41	98.84%	86	AOX45788.1
3A [Enterovirus A]	Enterovirus A	139	139	100%	8e-41	97.67%	86	NP_740533.1
TPA_hypothetical protein [Shigella sonnei]	Shigella sonnei	139	139	100%	4e-39	96.51%	228	HAY9402748.1
Uncharacterized protein T05_2797 [Trichinella murrai]	Trichinella murrai...	144	144	100%	1e-37	100.00%	780	KRX33122.1
polyprotein [Enterovirus A71]	Enterovirus A71	144	144	100%	2e-37	100.00%	2063	ANTI96633.1
polyprotein [Coxsackievirus A10]	Coxsackievirus...	143	143	100%	2e-37	100.00%	2193	AXE74046.1
RecName: Full=Genome polyprotein; Contains: RecName: Full=Capsid...	Human enterovirus...	143	143	100%	2e-37	100.00%	2193	C68879.3
polyprotein [Coxsackievirus A16]	Coxsackievirus...	143	143	100%	2e-37	100.00%	2193	ABX55895.1
polyprotein [Coxsackievirus A16]	Coxsackievirus...	143	143	100%	2e-37	100.00%	2193	ACI25595.1

Alignment view Pairwise  Restore defaults  Download

100 sequences selected

---

**3A protein [Coxsackievirus A2]**  
Sequence ID: YP\_009508937.1 Length: 86 Number of Matches: 1

Range 1: 1 to 86  GenPept  Graphics

Score	Expect	Method	Identities	Positives	Gaps	Frame
139 bits (351)	5e-41	Compositional matrix adjust.	85/86 (99%)	86/86 (100%)	0/86 (0%)	+1

Query 1 GPKFRPRTISLLEEKQAPDQATSDLLASVDSSEVROVCREQGITDEPTINVERHLNRAVL 180  
 GPKFRPRTISLLEEKQAPDQATSDLLASVDSSEVROVCREQGITDEPTINVERHLNRAVL 180  
 Sbjct 1 GPKFRPRTISLLEEKQAPDQATSDLLASVDSSEVROVCREQGITDEPTINVERHLNRAVL 60

Query 181 VMQSIATVAAVWSLVVYIKLFAFGQ 258  
 VMQSIATVAAVWSLVVYIKLFAFGQ 86  
 Sbjct 61 VMQSIATVAAVWSLVVYIKLFAFGQ 86

**Related Information**  
Gene - associated gene details

---

**3A protein, partial [Enterovirus A71]**  
Sequence ID: AOX45788.1 Length: 86 Number of Matches: 1

Range 1: 1 to 86  GenPept  Graphics

Score	Expect	Method	Identities	Positives	Gaps	Frame
139 bits (351)	5e-41	Compositional matrix adjust.	85/86 (99%)	86/86 (100%)	0/86 (0%)	+1

Query 1 GPKFRPRTISLLEEKQAPDQATSDLLASVDSSEVROVCREQGITDEPTINVERHLNRAVL 180  
 GPKFRPRTISLLEEKQAPDQATSDLLASVDSSEVROVCREQGITDEPTINVERHLNRAVL 180  
 Sbjct 1 GPKFRPRTISLLEEKQAPDQATSDLLASVDSSEVROVCREQGITDEPTINVERHLNRAVL 60

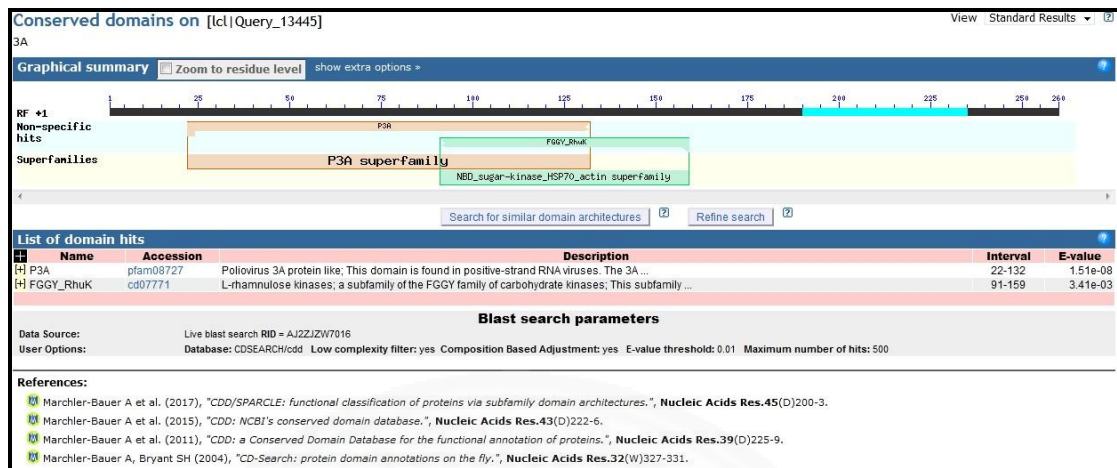
Query 181 VMQSIATVAAVWSLVVYIKLFAFGQ 258  
 VMQSIATVAAVWSLVVYIKLFAFGQ 86  
 Sbjct 61 VMQSIATVAAVWSLVVYIKLFAFGQ 86

**Next**  **Previous**  **Descriptions**

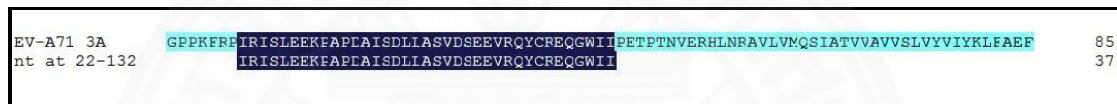
**Figure 5.5** Homology search of the cloned *EV-A71* 3A sequence using NCBI BLASTx.



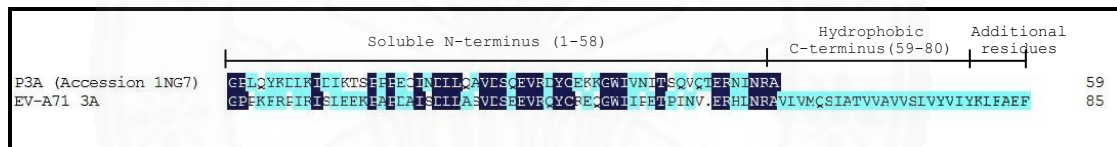
A



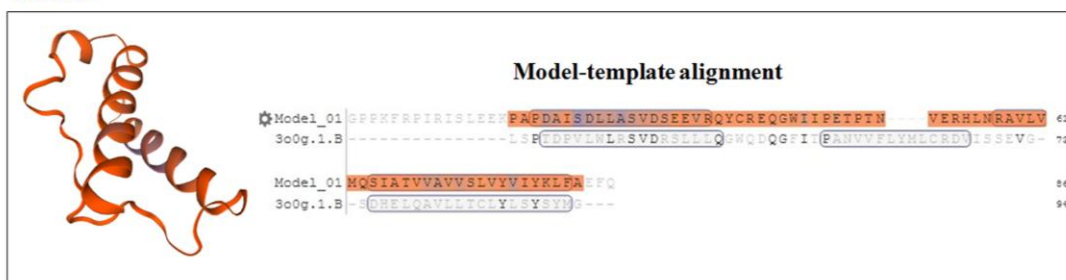
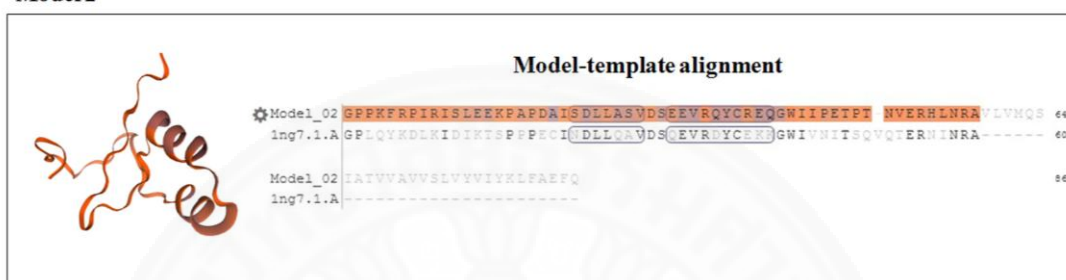
B



C



**Figure 5.6** Functional domain prediction of EV-A71 3A protein. **(A)** The conserved domains of the cloned EV-A71 3A analyzed by BLASTx. **(B)** Sequence alignment of the deduced amino acids of EV-A71 3A from nucleotide sequence at 12-132 with the full-length EV-A71 3A. **(C)** Sequence alignment of the cloned EV-A71 3A with poliovirus 3A protein-like domain (P3A), accession number 1NG7.

**Model 1****Model 2**

**Figure 5.7** Homology structure of EV-A71 3A protein modeled by Swiss-Model. **Model 1**; amino acids 16-83 of EV-A71 3A (Model\_01, orange shaded residues) were modeled with cyclin-dependent kinase 5 activator 1 (PDB 3o0g.1.B). Three amphipathic alpha-helices were predicted at 16-38, 57-61, and 64-82 on the EV-A71 3A, respectively (orange shaded residues indicated by boxes). **Model 2**; amino acids 1-58 of EV-A71 3A (Model\_02, orange shaded residues) were modeled with core protein P3A accession 1NG7 (PDB 1ng7.1.A). Two amphipathic alpha-helices were predicted at amino acid positions 22-28 and 31-40 on the EV-A71 3A, respectively (orange shaded residues indicated by boxes).

A



**Myristoylator**

Documentation is available.

The entered sequence is:

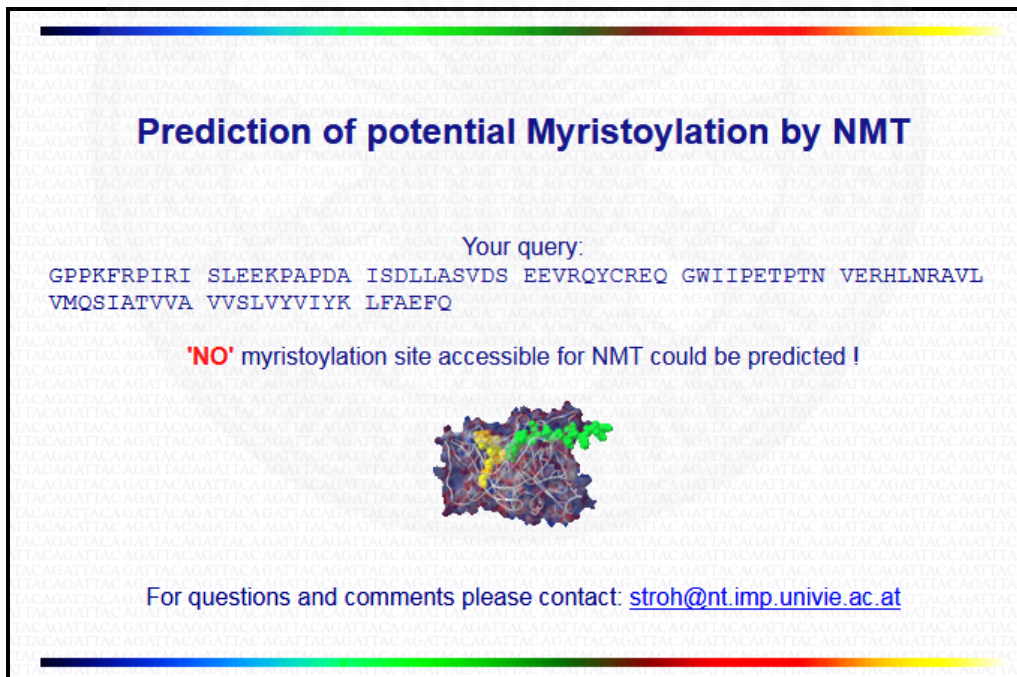
```
GPPKFRPIRI SLEEKPA PDA ISDLLASVDS EEVRQYCREQ GWIIPETPTN VERHLNRAVL
VMQSIATVVA VVSLVYVIYK LFAEFQ
```

This protein is predicted as **non-myristoylated**:

	Positive	Negative
Average response of 25 neural networks	0.0151248	0.984957
Counters	0	25

Score = 0.0151248 - 0.984957 = -0.9698322

B



**Prediction of potential Myristoylation by NMT**

Your query:

```
GPPKFRPIRI SLEEKPA PDA ISDLLASVDS EEVRQYCREQ GWIIPETPTN VERHLNRAVL
VMQSIATVVA VVSLVYVIYK LFAEFQ
```

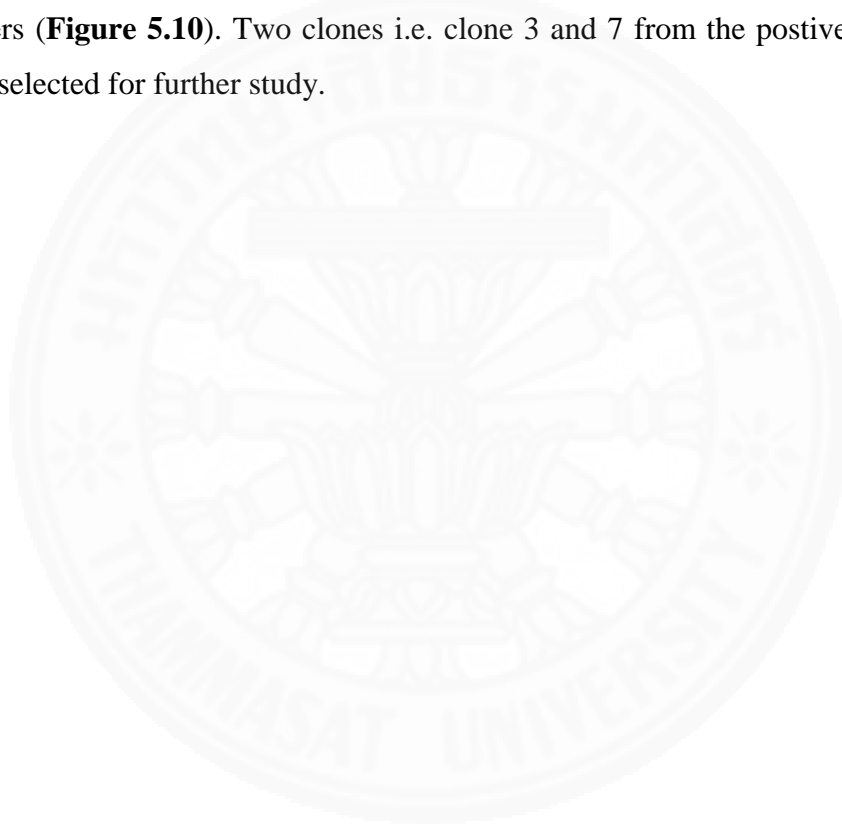
**'NO'** myristoylation site accessible for NMT could be predicted !

For questions and comments please contact: [stroh@nt.imp.univie.ac.at](mailto:stroh@nt.imp.univie.ac.at)

**Figure 5.8** Prediction of myristoylation site of the amino acid sequences deduced from the cloned EV-A71 3A nucleotide sequence using Myristoylator (<https://web.expasy.org/myristoylator/>) (A) and NMT-The MYR Predictor (<http://mendel.imp.ac.at/myristate/SUPLpredictor.htm>) (B).

### 5.3.3 Construction of recombinant mammalian expression plasmid to produce EV-A71 3A protein

To subclone *FLAG-3A* into pLVX-Puro mammalian expression vector, pLVX-Puro (**Figure 5.9A**) and pJET1.2::*FLAG-3A* (**Figure 5.9B**) were double-digested with *EcoRI* and *XbaI* endonucleases. The digested pLVX-Puro and *FLAG-3A* were ligated and transformed into JM109 *E. coli*. Nine out of ten randomly selected *E. coli* clones were positive screening for *FLAG-3A* inserted in pLVX-Puro plasmid (pLVX::*FLAG-3A*) as determined by direct colony PCR using sequencing primers (**Figure 5.10**). Two clones i.e. clone 3 and 7 from the positive transformants were selected for further study.



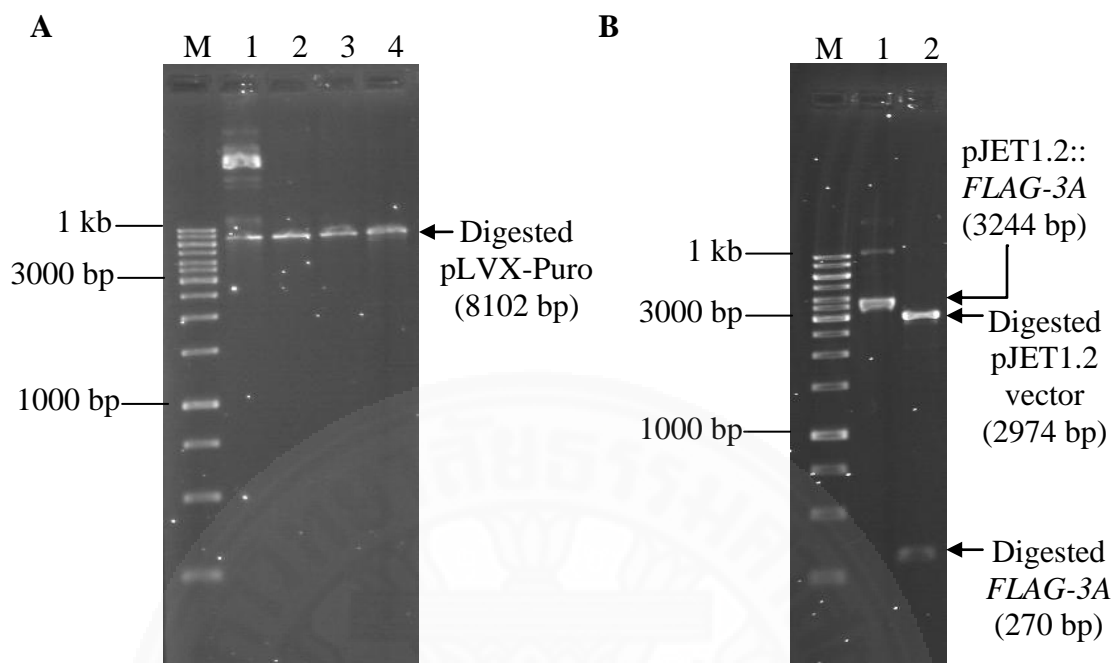


**Figure 5.9** Agarose gel electrophoresis of the double digestion of pLVX-Puro (**A**) and pJET1.2::*FLAG-3A* (**B**) using *EcoRI* and *XbaI* endonucleases. **A**; lane M; 1kb DNA ladder (in base pairs, bp), lane 1; undigested pLVX-Puro vector, lane 2; *EcoRI*-digested pLVX-Puro, lane 3; *XbaI*-digested pLVX-Puro, lane 4; Double-digested pLVX-Puro. **B**; lane M; DNA ladder (in base pairs, bp), lane 1; undigested pJET1.2::*FLAG-3A*, lane 2; double-digested *FLAG-3A*. The sizes of molecular weight are indicated on the left of the figure. The sizes of the bands of interest are indicated by arrows on the figure.

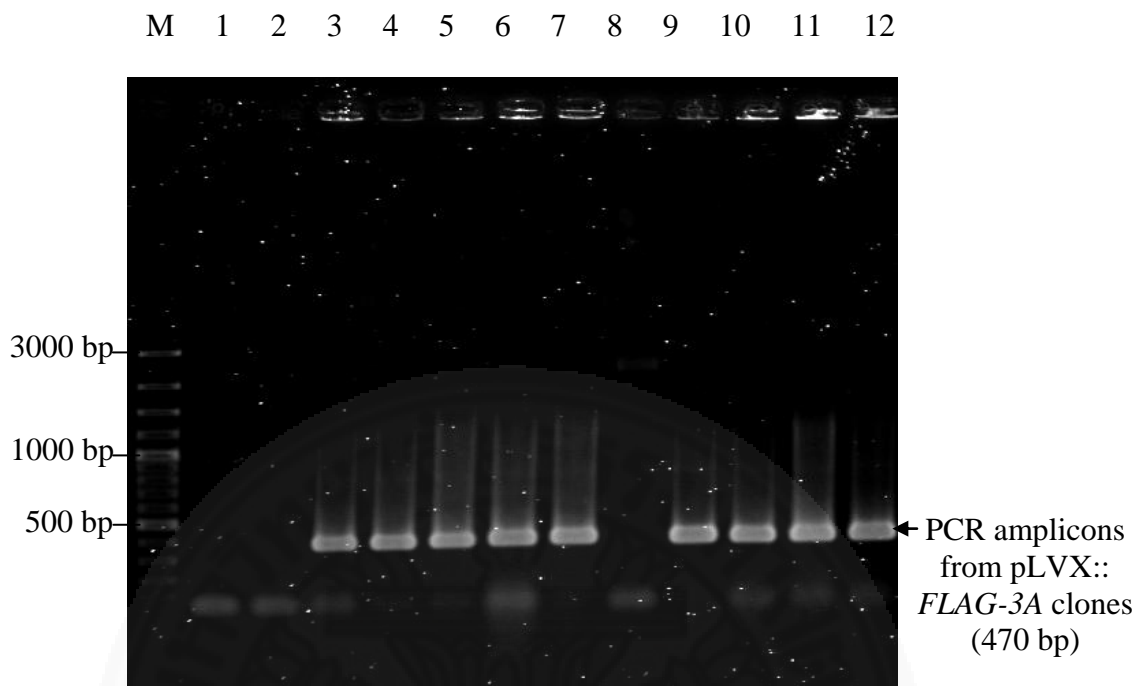


**Figure 5.10** Agarose gel electrophoresis of PCR products amplified from colonies of JM109 *E. coli* transformed with pLVX::*FLAG-3A* by colony PCR. Lane M; 100 bp Plus DNA ladder (in base pairs, bp), lane 1; non-template control, lanes 2-12; PCR amplicons from 11 colonies of the transformed *E. coli*. Lanes 3-7 and 9-12 showed positive PCR amplicons at expected size of 470 bp which is *FLAG-3A* together with flanking DNA region generated by primer extension. The sizes of molecular weight are indicated on the left of the figure. The sizes of the bands of interest are indicated by arrow on the figure.

The FLAG-3A coding sequence was successfully subcloned into pLVX-Puro mammalian expression vector designated as pLVX::*FLAG-3A*, and verified the coding sequence by DNA sequencing and NCBI blast analysis (**data not shown**). To determine FLAG-3A protein expression in mammalian cells including HEK293T, a highly transfectable cells, and SH-SY5Y, the target cell of study, transfection of the cells with pLVX::*FLAG-3A* was performed. After 24 hours of transfection, the expression of FLAG-3A protein could be detected in HEK293T cells (**Figure 5.11A**) but not in SH-SY5Y cells (**Figure 5.11B**), compared to mock and pLVX vector transfection, served as negative controls. It has been reported that expression of viral protein in the mammalian cells could be improved by fusion with fluorescent protein.<sup>107</sup> Therefore, the EV-A71 3A coding sequence in-frame with mCherry coding sequence was constructed.



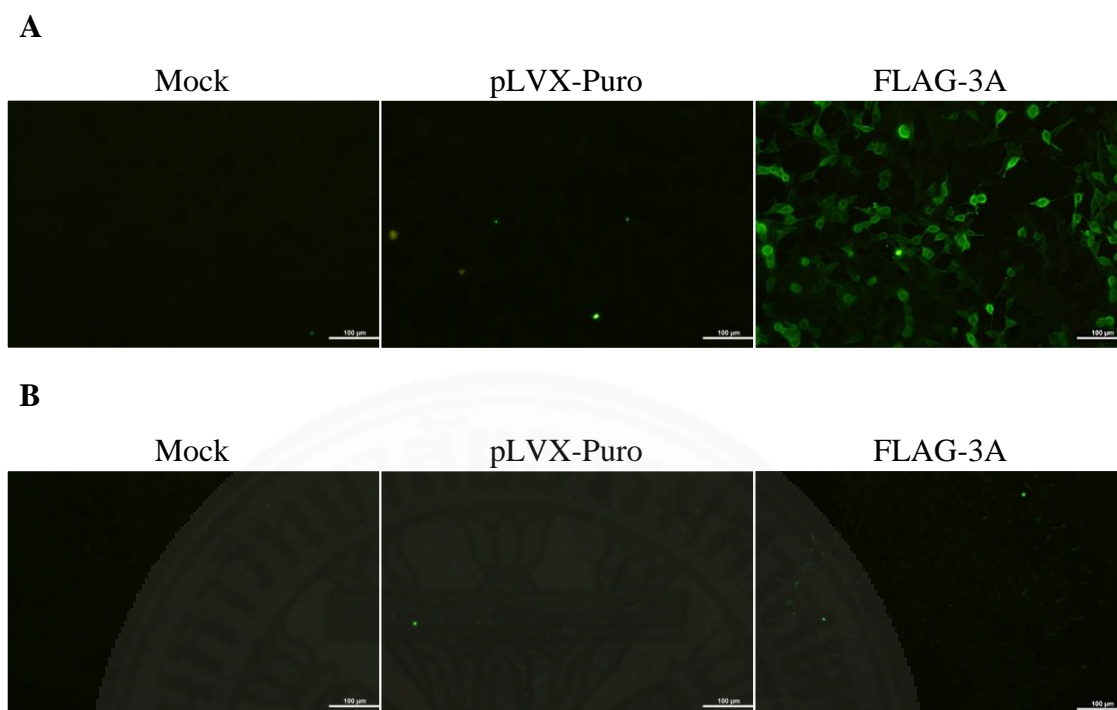


**Figure 5.11** Expression of FLAG-3A protein in HEK293T (**A**) and SH-SY5Y (**B**) cells. FLAG-3A plasmid or pLVX-Puro vector was transfected in HEK293T and SH-SY5Y cells. At 24 h.p.t., cells were fixed, stained for FLAG using Alexa Fluor 488-conjugated secondary antibody, and observed under fluorescence microscopy. Mock and pLVX transfection served as negative controls. The positive signals were detected in bright green fluorescence. The scale bar represents 100 μm.

#### **5.3.4 Construction of recombinant plasmid DNA carrying coding sequence of EV-A71 nonstructural 3A in-frame with FLAG-epitope tag at 5'-end and red monomeric fluorescent protein mCherry at 3'-end**

PCR amplicons of the two overlapping sequences, *EcoRI-FLAG-3A-mCherry* (expected size at 311 base pairs) and *3A-mCherry-XbaI* (expected size at 717 base pairs) were successfully amplified from pLVX::*FLAG-3A* and pLV-mCherry lentiviral vector, respectively. Amplification of *EcoRI-FLAG-3A-mCherry* or *3A-mCherry-XbaI* performed at all annealing temperatures tested gave high product yield of the correct PCR amplicons (**Figures 5.12 and 5.13**). The PCR amplicons were purified from agarose gel (**Figure 5.14**) before using as templates for amplifying the full-length *EcoRI-FLAG-3A-mCherry-XbaI* (expected size at 1,008 base pairs) (**Figure 5.15**) by overlapping-extension PCR. The PCR amplicon of *EcoRI-FLAG-3A-mCherry-XbaI* was purified from agarose gel.

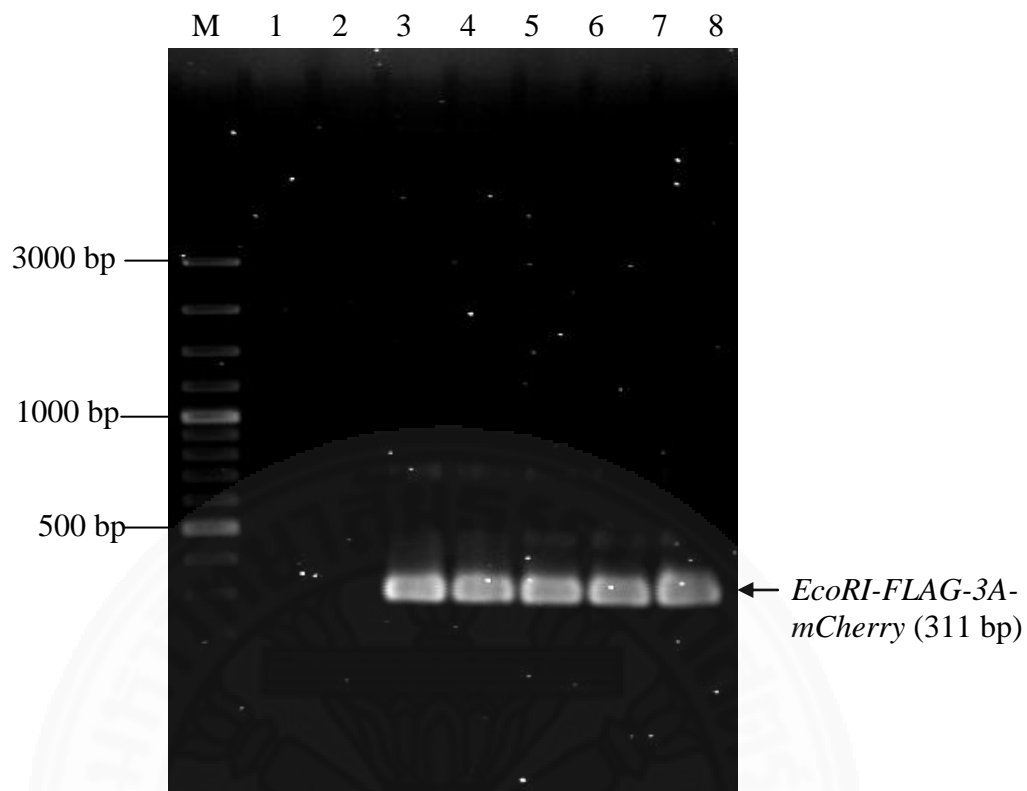


**Figure 5.12** Agarose gel electrophoresis of *EcoRI-FLAG-3A-mCherry* amplicons. Lane M; 100 bp Plus DNA ladder (in base pairs, bp), lane 1; non-template control, lanes 2-6; PCR amplicons of the *EcoRI-FLAG-3A-mCherry* (311 bp) amplified using annealing temperature at 52, 56, 60, 65, and 68 °C, respectively. The sizes of molecular weight are indicated on the left of the figure. The sizes of the bands of interest are indicated by arrow on the figure.

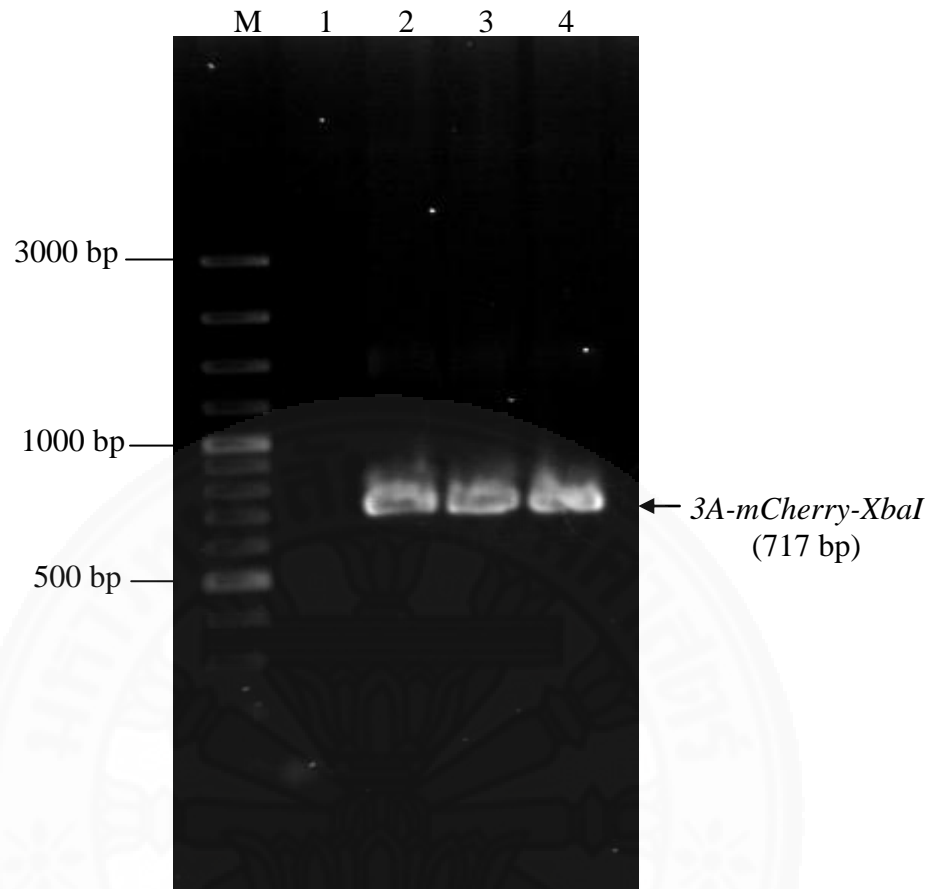


**Figure 5.13** Agarose gel electrophoresis of *3A-mCherry-Xba* amplification. Lane M; 100 bp Plus DNA ladder (in base pairs, bp), lane 1; non-template control, lanes 2-4; PCR amplicons of the *3A-mCherry-XbaI* (717 bp) amplified using annealing temperature at 66, 68, and 70 °C, respectively. The sizes of molecular weight are indicated on the left of the figure. The sizes of the bands of interest are indicated by arrow on the figure.

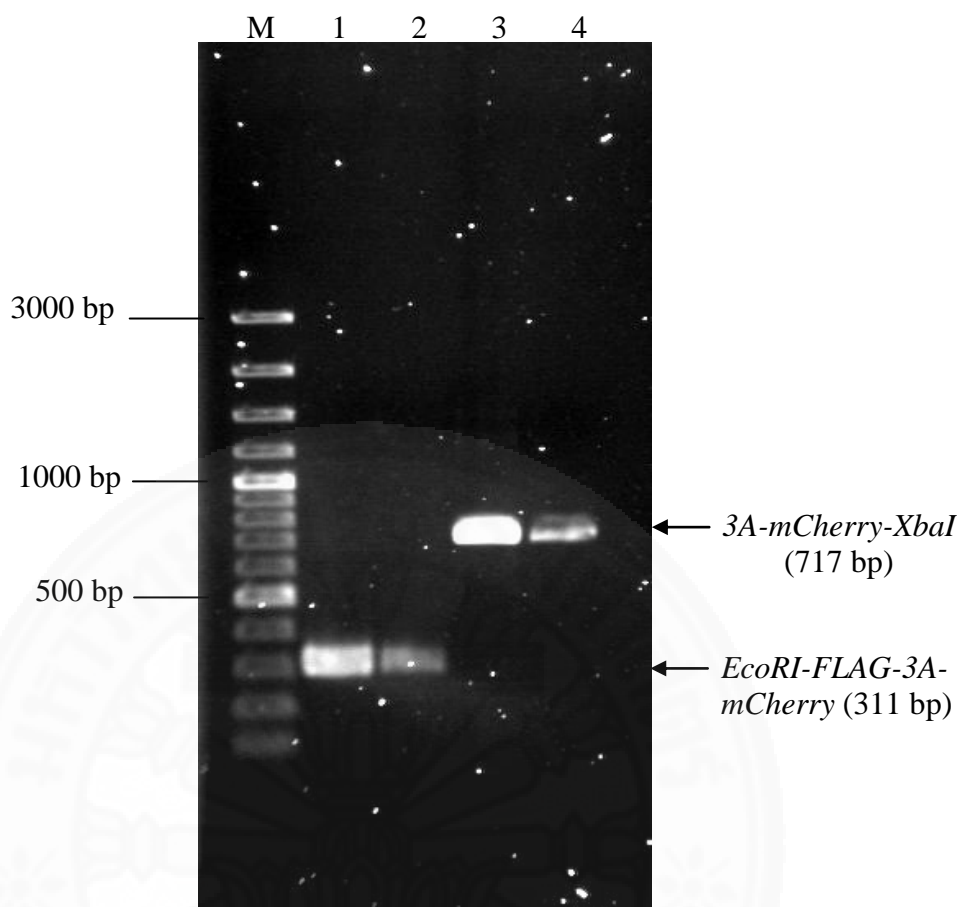


**Figure 5.14** Agarose gel electrophoresis of the gel-purified *EcoRI-FLAG-3A-mCherry* and *3A-mCherry-XbaI*. Lane M; 100 bp Plus DNA ladder (in base pairs, bp), lane 1; eluted *EcoRI-FLAG-3A-mCherry* fraction 1, lane 2; eluted *EcoRI-FLAG-3A-mCherry* fraction 2, lane 3; eluted *3A-mCherry-XbaI* fraction 1, lane 4; eluted *3A-mCherry-XbaI* fraction 2. The sizes of molecular weight are indicated on the left of the figure. The sizes of the bands of interest are indicated by arrow on the figure.

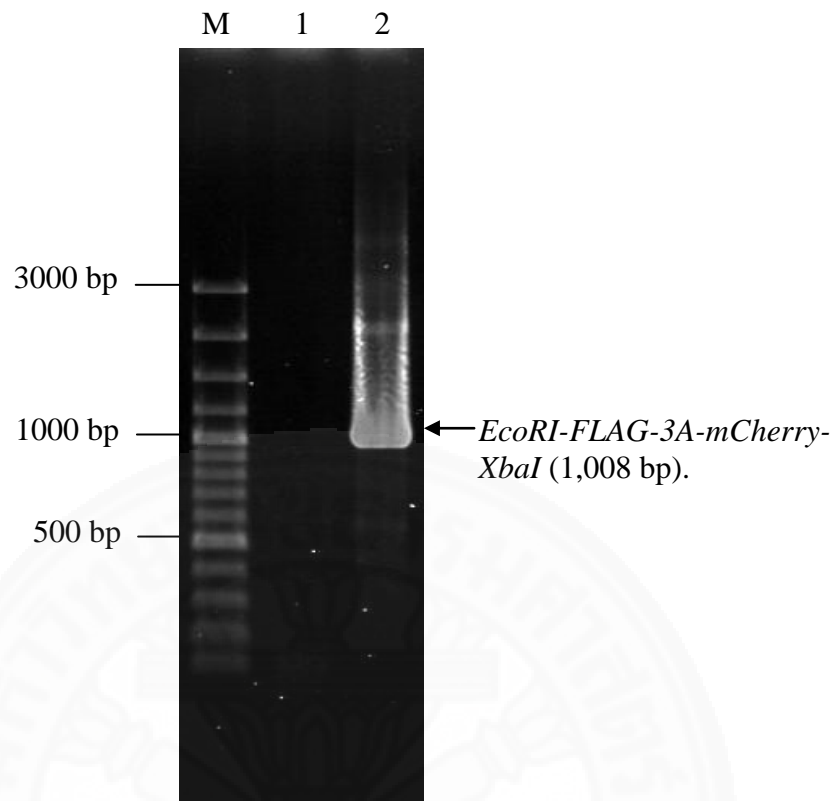


**Figure 5.15** Agarose gel electrophoresis of the PCR amplicons of the full length *EcoRI-FLAG-3A-mCherry-XbaI* (1,008 bp). Lane M; 100 bp Plus DNA ladder (in base pairs, bp), lane 1; non-template control, lane 2; PCR amplicon of the full-length *EcoRI-FLAG-3A-mCherry-XbaI*. The sizes of molecular weight are indicated on the left of the figure. The sizes of the bands of interest are indicated by arrow on the figure.

The purified DNA fragment of *EcoRI-FLAG-3A-mCherry-XbaI* was ligated with pGEM<sup>®</sup>-T Easy vector designated as pGEM<sup>®</sup>-T::*FLAG-3A-mCherry* and transformed into competent JM109 *E.coli* by heat-shock method. By blue-white colony screening, the white colonies of the transformants were randomly selected to screen for the presence of the insertion of *EcoRI-FLAG-3A-mCherry-XbaI* fragment by direct colony PCR. Five colonies were picked up. The result showed that all picked colonies gave the PCR amplicons at size corresponding to the expected size of *EcoRI-FLAG-3A-mCherry-XbaI* flanked with DNA region of the plasmid which is 1,209 base pairs (**Figure 5.16**).

Some of the positive clones were selected to verify by DNA sequencing. The result showed that generation of FLAG-3A coding sequence incorporated with mCherry coding sequence at 3'-end was successful in which the translated sequence of the mCherry was in the same reading frame with the translated sequence of FLAG-3A (**Figure 5.17**).

The sequence-verified pGEM<sup>®</sup>-T::*FLAG-3A-mCherry* was digested with *EcoRI* and *XbaI* endonucleases to release *EcoRI-FLAG-3A-mCherry-XbaI* fragment (**Figure 5.18**). The fragment was purified from agarose gel and directionally ligated with pLVX-Puro which was previously digested with the same restriction enzymes generating the recombinant plasmid construct designated as pLVX::*FLAG-3A-mCherry*. The ligation was transformed into JM109 competent *E. coli* by heat-shock method. Five colonies of transformant *E. coli* were randomly screened for the insertion of the fragment by direct colony PCR. The results showed that only one transformant clone gave the PCR amplicon at size corresponding to the size of *EcoRI-FLAG-3A-mCherry-XbaI* flanked with DNA region of pLVX-Puro vector which is 1,272 base pairs (**Figure 5.19A**). The plasmid of the positive clone was extracted (**Figure 5.19B**).



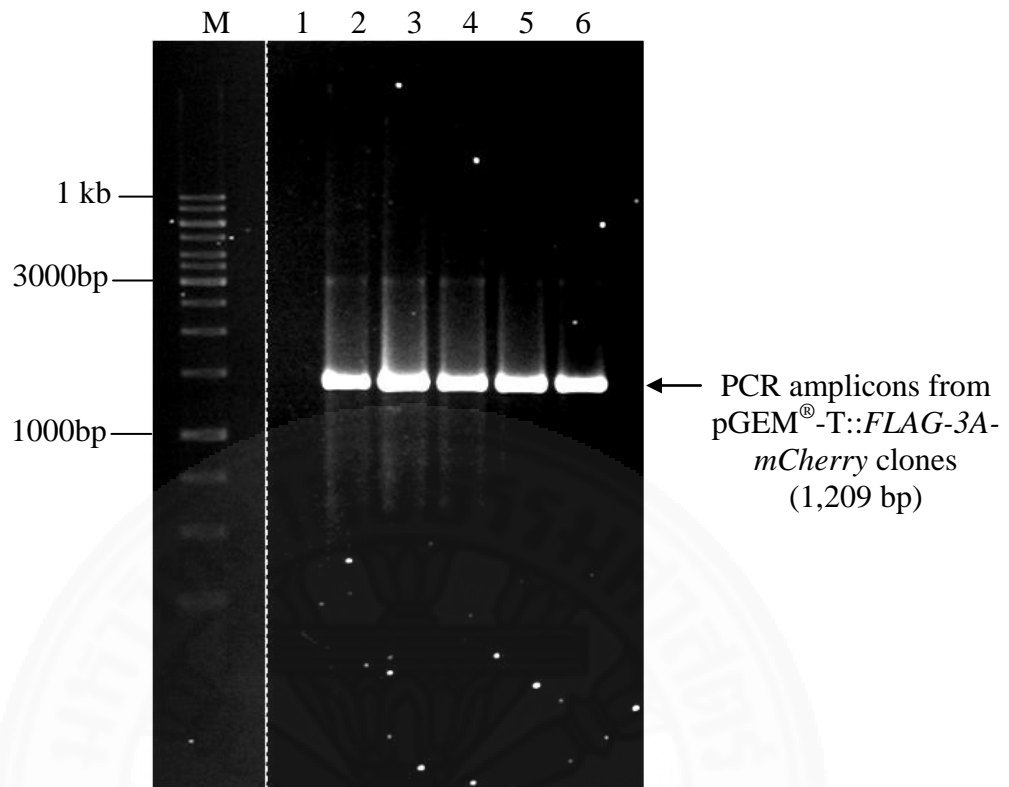


**Figure 5.16** Agarose gel electrophoresis of PCR products amplified from 5 randomly selected colonies of JM109 *E. coli* transformed with pGEM<sup>®</sup>-T::*FLAG-3A-mCherry* by colony PCR. Lane M; 1 kb DNA ladder (in base pairs, bp), lane 1; non-template control, lanes 2-6; PCR amplicons from 5 colonies of the transformed *E. coli*. All selected colonies were positive transformants giving the PCR amplicons at size of 1,209 bp which is *FLAG-3A-mCherry* with flanking region from the vector. The sizes of molecular weight are indicated on the left of the figure. The sizes of the bands of interest are indicated by arrow on the figure.

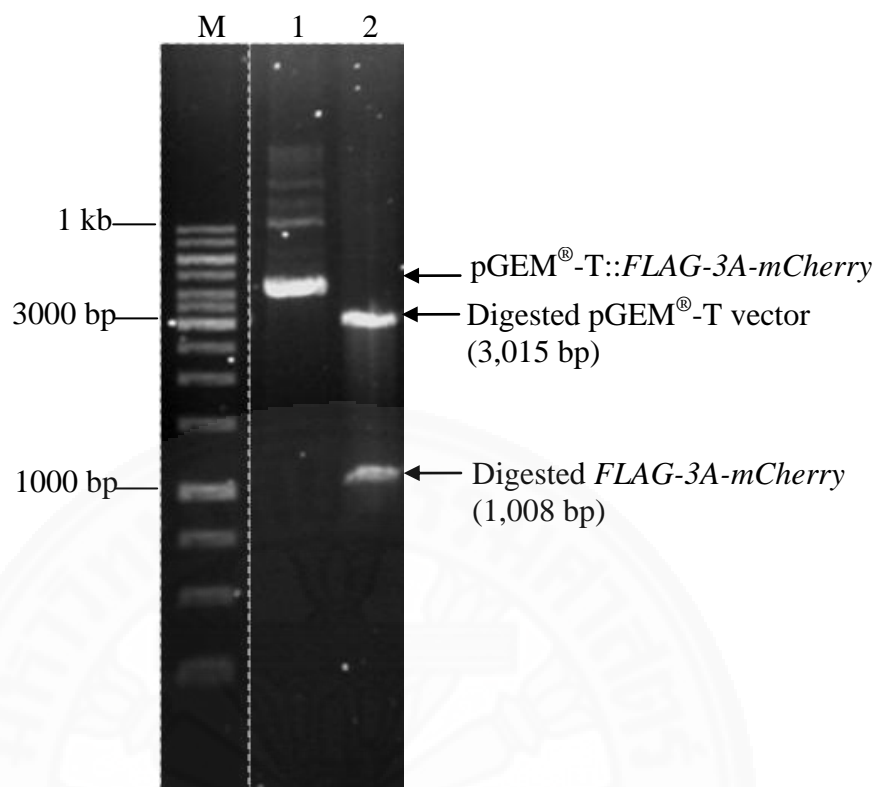
A

<i>EcoRI</i>	<i>EcoRI</i>	<i>FLAG</i>	<i>3A</i>
<u>CGCGGGAATT</u>	<u>CGATTATGAA</u>	<b>TTCATGGATT ACAAGGATGA CGATGACAAG</b>	GGCCCCGCCA
AGTTCAGACC	AATTAGAATC	AGTCTTGAGG	AGAAGCCAGC
CCCAGATGCT	ATTAGTGATC	TCCTCGCTAG	TGTTGACAGT
GAGGAAGTGC	GCCAATACTG	TAGGGAGCAA	GGTTGGATCA
TCCCTGAAAC	TCCCACCAAT	GTTGAACGAC	ATCTCAACAG
AGCAGTGCTA	GTTATGCAAT	CCATCGCTAC	TGTGGTGGCA
GTTGTCTCAC	TGGTGTATGT	CATTTACAAG	CTCTTTGCGG
GGTTTCAAAT	GGTGAGCAAG	GGCGAGGAGG	ATAACATGGC
CATCATCAAG	GAGTTCATGC	GCTTCAAGGT	GCACATGGAG
GGCTCCGTGA	ACGGCCACGA	GTCGAGATC	GAGGGCGAGG
GCGAGGGCCG	CCCCTACGAG	GGCAGCCAGA	CCGCCAAGCT
GAAGGTGACC	AAGGGTGGCC	CCCTGCCCTT	CGCCTGGGAC
ATCCTGTCCC	CTCAGTTCAT	GTACGGCTCC	AAGGCCTACG
TGAAGCAGCC	CGCCGACATC	CCCGACTACT	TGAAGCTGTC
CTTCCCCGAG	GGCTTCAAGT	GGGAGCGCGT	GATGAACTTC
GAGGACGGCG	GCGTGGTGAC	CGTGACCCAG	GACTCCTCCC
TGCAGGACGG	CGAGTTCATC	TACAAGGTGA	AGCTGCGCGG
CACCAACTTC	CCCTCCGACG	GCCCCGTAAT	GCAGAAGAAG
ACCATGGGCT	GGGAGGCCTC	CTCCGAGCGG	ATGTACCCCG
AGGACGGCGC	CCTGAAGGGC	GAGATCAAGC	AGAGGCTGAA
GCTGAAGGAC	GGCGGCCACT	ACGACGCTGA	GGTCAAGACC
ACCTACAAGG	CCAAGAAGCC	CGTGCAGCTG	CCCGGCGCCT
ACAACGTCAA	CATCAAGTTG	GACATCACCT	CCCACAACGA
GGACTACACC	ATCGTGGAAC	AGTACGAACG	CGCCGAGGGC
CGCCACTCCA	CCGGCGGCAT	GGACGAGCTG	TACAAG
<b>TAAT</b>			
<u>CTAGAATCAC</u>	<u>TAGTGAATTC</u>	<i>mCherry</i>	
<i>XbaI</i>	<i>EcoRI</i>		

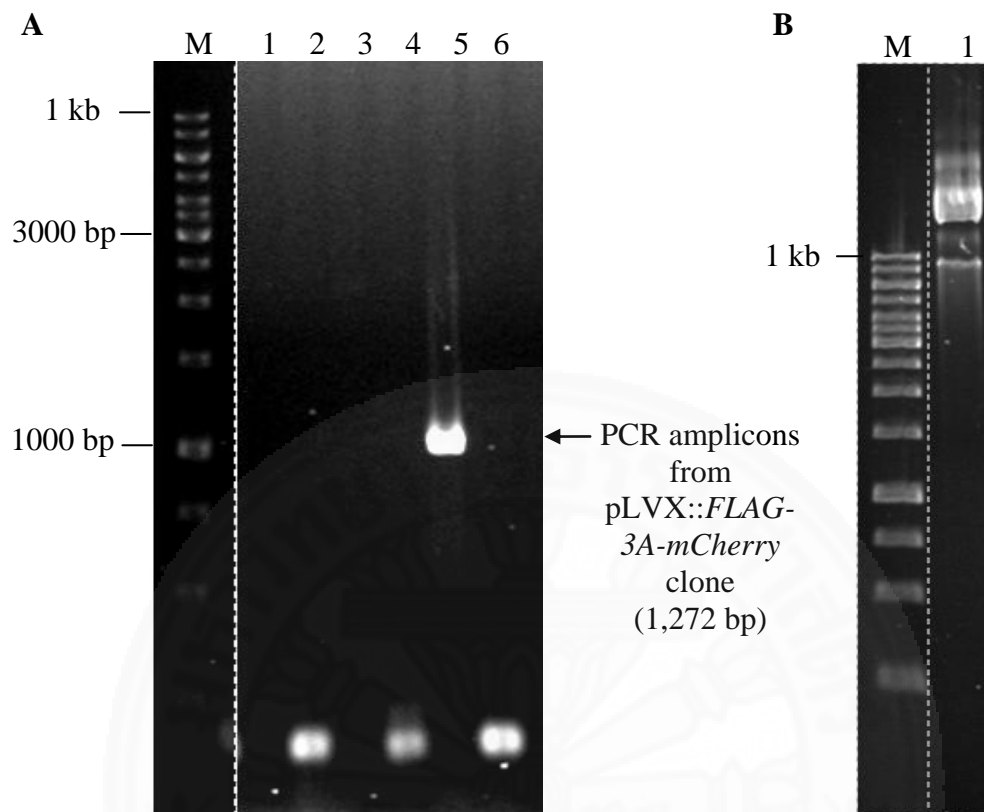
B

<i>FLAG</i>	<i>3A</i>
<b>MDYKDDDDK</b> G	PPKFRPIRIS
LEEKPAIDAI	SDLLASVDSE
EVRQYCREQG	WIIPETPTNV
ERHLNRAVLV	MQSIATVVAV
VSLVYVIYKL	FAGFQMVSKG
EEDNMAIIE	FMRFKVHMEG
SVNGHEFEIE	GEGEGRPYEG
TQTAKLKVTK	GGPLPFAWDI
LSPQFMYGSK	AYVKHPADIP
DYLLKLSFPEG	FKWERVMNFE
DGGVVTVTQD	SSLQDGEFIY
KVKLRGTNFP	SDGPVMQKKT
MGWEASSERM	YPEDGALKGE
IKQRLKLDG	GHYDAEVKTT
YKAKKPVQLP	GAYNVNIKLD
ITSHNEDYTI	VEQYERAAGR
HSTGGMDELY	K*
	<i>mCherry</i>

**Figure 5.17** Nucleotide sequence of *EcoRI-FLAG-3A-mCherry-XbaI* inserted in pGEM<sup>®</sup>-T Easy vector (A) and the deduced amino acid sequence of *EcoRI-FLAG-3A-mCherry-XbaI* coding sequence (B). Black highlight indicates FLAG sequence. Dark grey highlight indicates EV-A71 3A sequence. Light grey indicates mCherry sequence. Underline indicates restriction sites. Red letters and asterisk indicate stop codon.



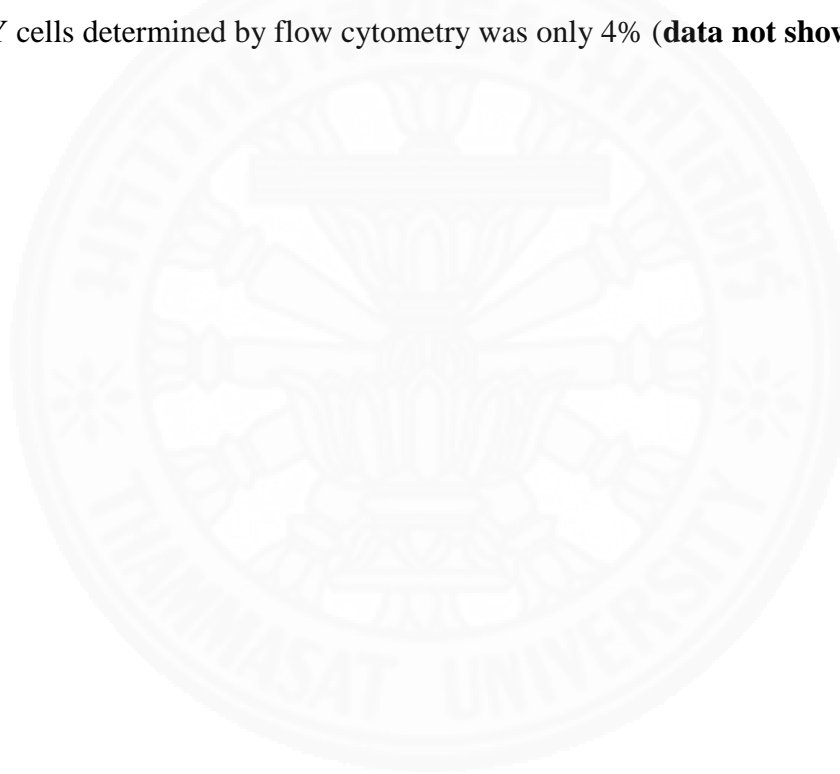
**Figure 5.18** Agarose gel electrophoresis of the double digestion of pGEM<sup>®</sup>-T::*FLAG-3A-mCherry* using *EcoRI* and *XbaI* endonucleases. Lane M; 1 kb DNA ladder (in base pairs, bp), lane 1; undigested pGEM<sup>®</sup>-T::*FLAG-3A-mCherry*, lane 2; Digested pGEM<sup>®</sup>-T::*FLAG-3A-mCherry* showing 2 fragments including digested pGEM<sup>®</sup>-T vector (3,015 bp) and digested *FLAG-3A-mCherry* (1,008 bp). The sizes of molecular weight are indicated on the left of the figure. The sizes of the bands of interest are indicated by arrow on the figure.



**Figure 5.19** Agarose gel electrophoresis of PCR products amplified from colonies of JM109 *E. coli* transformed with pLVX::*FLAG-3A-mCherry* by colony PCR (**A**) and the purified DNA plasmid of the positive clone (**B**). **A**; lane M; 1 kb DNA ladder (in base pairs, bp), lane 1: non-template control, lanes 2-6; PCR amplicons from 5 colonies of the transformed *E. coli*, respectively. One out of five randomly selected colonies gave the PCR amplicons of *FLAG-3A-mCherry* flanked with the nucleotide region of the plasmid with size of 1,272 bp. **B**; lane M; 1kb DNA ladder (in base pairs, bp), lane 1; the purified DNA plasmid of the positive clone. The sizes of molecular weight are indicated on the left of the figure. The sizes of the bands of interest are indicated by arrow on the figure.

### 5.3.5 Determination of FLAG-3A-mCherry protein expression in mammalian cells using fluorescence microscope

Transfection using Lipofectamine™ 3000 reagent tested by manufacturer demonstrates >80% transfection efficiency in HEK293T cells and <30% in human SH-SY5Y cells. Mock transfection served as negative control while pLV-mCherry transfected cells were served as positive control for fluorescent protein expression. Recombinant FLAG-3A-mCherry could be expressed in both HEK293T and SH-SY5Y cell (**Figure 5.20**). But the higher expression level was observed in the HEK293T cells. In this study, it was found that transfection of efficiency of SH-SY5Y cells determined by flow cytometry was only 4% (**data not shown**).



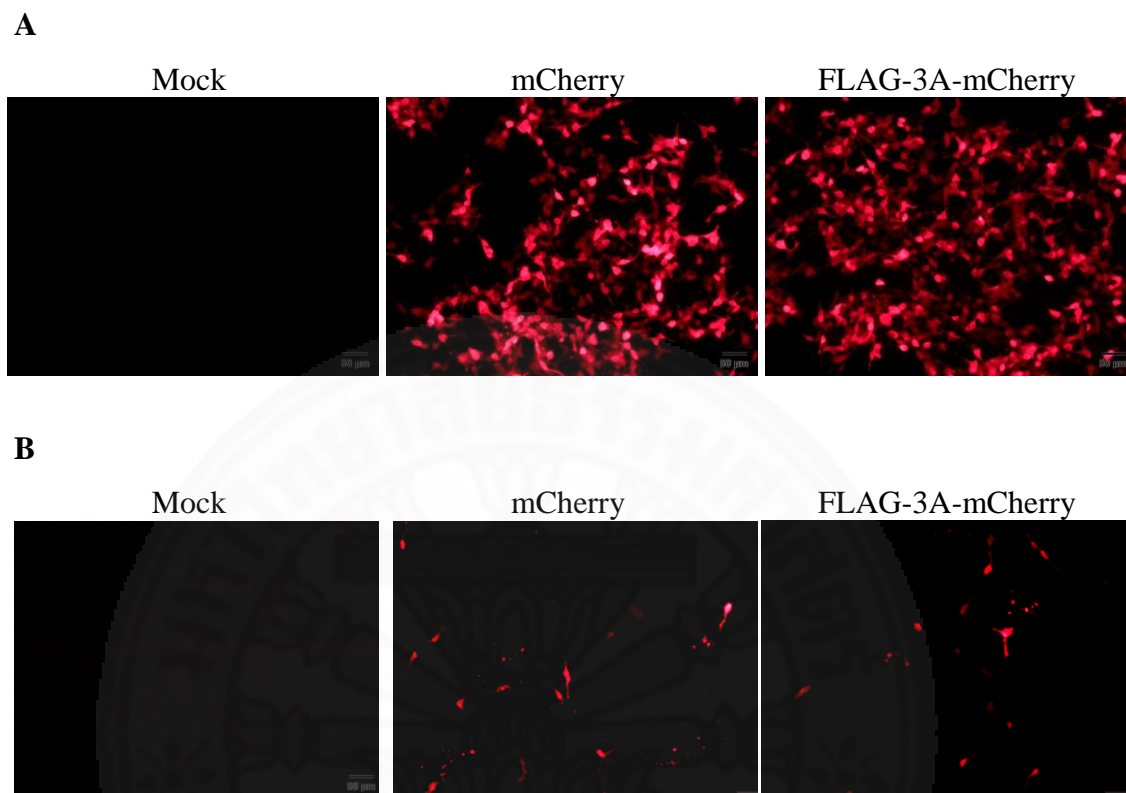


**Figure 5.20** Expression of FLAG-3A-mCherry or mCherry proteins in HEK293T (**A**) and SH-SY5Y (**B**) cells. FLAG-3A-mCherry plasmid or pLV-mCherry vector was transfected in HEK293T and SH-SY5Y cells. At 24 h.p.t., cells were fixed and visualized by fluorescence microscope. Mock transfection i.e. transfection reagent alone served as negative control. Expression of mCherry from pLV-mCherry plasmid served as positive control.

### 5.3.6 Determination of FLAG-3A-mCherry protein expression in mammalian cells using western blot analysis

By estimating from the number of transfected cells as determined by immunofluorescence assay, the replicates of culture plate of transfected SH-SY5Y cells were done to produce the comparable amounts of protein to that of from HEK239T cells. The expression of mCherry protein in both cells served as control expression. To detect protein expression, cell lysates prepared from the transfected cells were loaded 10 µg of total protein per well. Polyclonal anti-mCherry antibody was used. It was found that recombinant FLAG-3A-mCherry and mCherry proteins could be expressed in both cell types (**Figure 5.21**). The relative migration in denaturing condition of mCherry protein expressed from pLV-mCherry was corresponding to its molecular weight which is 26.7 kDa. Interestingly, the migration of recombinant FLAG-3A-mCherry was slower than that of the mCherry and did not correlate to its predicted molecular size which is 38 kDa. In addition, there were 3 distinct bands of FLAG-3A-mCherry protein which were slightly different in their relative molecular sizes. It has been reported that enterovirus 3A proteins may form homodimer.<sup>26, 108</sup> Hence, the top 3 distinct bands of FLAG-3A-mCherry might be formed by homodimer resulting in aberrant electrophoretic mobility. Taken together, the FLAG-3A-mCherry protein was successfully produced in high amount from HEK293T and SH-SY5Y cells. It was suitable for further experiments.



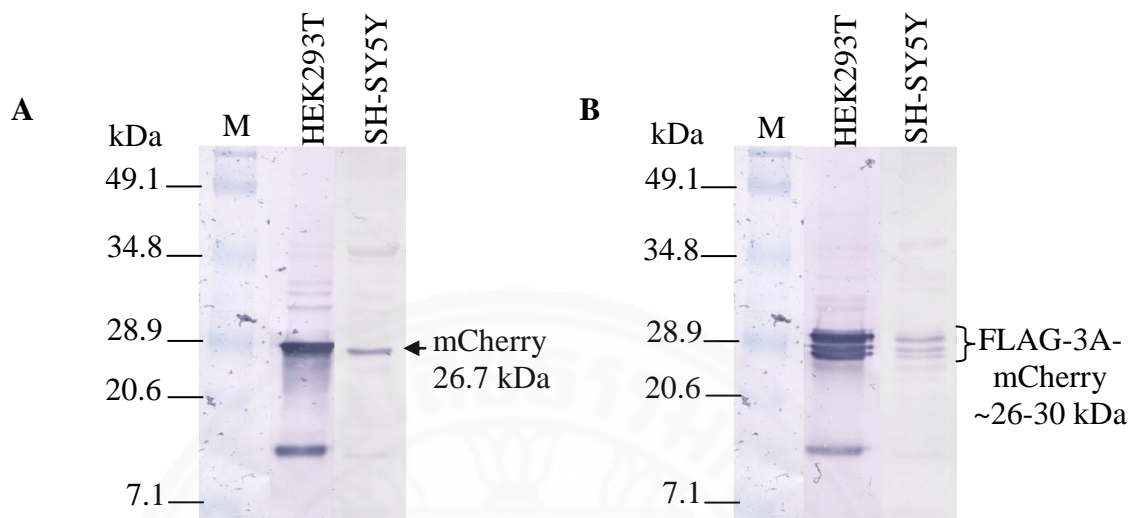


**Figure 5.21** Detection of mCherry (A) and FLAG-3A-mCherry (B) proteins expressed in HEK293T and SH-SY5Y cells by western blot analysis. Cell lysates prepared from transfected cells were immunoblotted with antibody against mCherry. The band of mCherry protein (molecular size = 26.7 kDa) is indicated by arrow. The triplet bands of FLAG-3A-mCherry (molecular size = 38 kDa) showing aberrant relative mobility at ~26-30 kDa are indicated by bracket. The molecular mass markers (in kilodaltons, kDa) are indicated at the left of the membranes.

### 5.3.7 Pull-down of FLAG-3A-mCherry interacting protein using anti-FLAG<sup>®</sup> M2 magnetic beads

To investigate EV-A71 3A interacting proteins in human neuronal cells, eluates from the FLAG pull-down of SH-SY5Y transfected with FLAG-3A-mCherry were resolved by 12% SDS-PAGE and detected by Coomassie brilliant blue followed by counterstaining with silver dye. The presence of FLAG-3A-mCherry in the eluted fractions from pull down was detected by monoclonal mouse anti-FLAG<sup>®</sup> M2 antibody which verified the transfection and expression of the protein as shown in **Appendix F**. The distinguishable protein bands present in eluates (**Figure 5.22, lanes 3-5**) were compared with the protein bands present in washing fraction (**Figure 5.22, lane 6**), cell lysate prepared from untransfected SH-SY5Y cells (**Figure 5.22, lane 1**), and cell lysate prepared from pLV-mCherry transfected SH-SY5Y cells (**Figure 5.22, lane 2**) which served as protein background controls. Five distinguishable bands (indicated by red arrows) were selected and excised in order to subject to trypsin digestion and protein identification by LC-MS/MS. By using Gene Tools program, the predicted relative molecular weight of the selected protein bands was approximately 22-26 kDa.

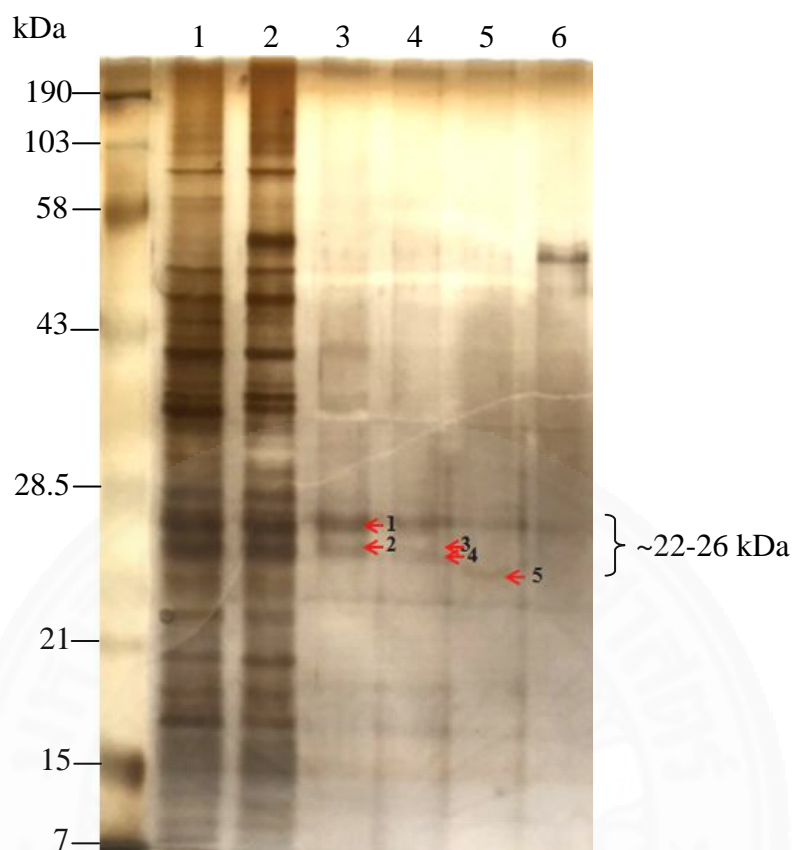


**Figure 5.22** Pull down of proteins with EV-A71 3A in cell lysate prepared from FLAG-3A-mCherry-transfected SH-SY5Y cells. Lane 1; cell lysate prepared from untransfected SH-SY5Y cells, lane 2; cell lysate prepared from pLV-mCherry transfected SH-SY5Y cells, lanes 3-5; eluted fractions from pull down by anti-FLAG<sup>®</sup>M2 magnetic beads, lane 6; last washing fraction. The proteins were resolved in 12% SDS-PAGE and stained with Coomassie brilliant blue followed by counterstaining with silver dye. Red arrows indicate distinguishable protein bands.

### 5.3.8 Protein identification by liquid chromatography mass spectrometer (LC-MS/MS) and analysis

Analysis of mass spectral data using Mascot software identified potential EV-A71 3A interacting proteins with 95% confidence listed in the **Table 5.1**. PRSS3 (mesotrypsinogen), PRSS1 (cationic trypsinogen), putative protein N-methyltransferase FAM86B1, and proteasome subunit alpha type-7 were predicted from the selected protein bands. Meanwhile, the PRSS3 (mesotrypsinogen) and PRSS1 (cationic trypsinogen) were in our interest. Because Mascot scores of them were higher than other identified proteins, the molecular weights of them are also close to the predicted molecular weight of the selected protein bands resolved in SDS-PAGE gel (approximately 22-26 kDa). Human trypsinogen PRSS1 and PRSS3 show high sequence homology as analyzed by sequence alignment (**Figure 5.23**). Therefore, protein identification by LC-MS/MS generated peptide sequences, listed in **Table 5.2**, that were able to be interpreted as PRSS1 or PRSS3.

Moreover, PRSS3 has been reported to play role in influenza A virus infection.<sup>103</sup> PRSS1 (cationic trypsinogen) was identified as one of EV-A71 IRES interacting proteins.<sup>109</sup> Hence, the PRSS3 (mesotrypsinogen) and PRSS1 (cationic trypsinogen) were further characterized in the subsequent experiments as they are closely related.

**Table 5.1** List of proteins identified by LC-MS/MS

Identified protein	MW (kDa)	Accession number	Band number	Mascot score
PRSS3 protein [ <i>Homo sapiens</i> ]	26.5	A1A508	1	63
			2	77
			3	65
			4	57
			5	51
Cationic trypsinogen, partial [ <i>Homo sapiens</i> ]	9.1	AAG30948.1	1	61
			2	78
			3	68
			4	60
			5	51
Proteasome subunit alpha type-7 [ <i>Homo sapiens</i> ]	27.9	O14818	1	48
Putative protein N- methyltransferase FAM86B1 [ <i>Homo sapiens</i> ]	48.3	R4GN25	2	49

PRSS1	.....MNFLLILTFVAAA	13
PRSS3-v1	MCGPDDRCPARWPGPGRAVKCKGKGLAAARPRVERGGAQRGGAGLELHPLLGGRTWRAARDADGCEALGT	70
PRSS3-v2	.....MNFLLILAFVGAA	13
PRSS3-v3	.....MHMRETSGFTLKKGRSAPLVFHPFDAL	27
PRSS3-v4	.....MGPAGE	6
PRSS1	IAPFDDDDKIVGGYNCEENSVPYQVSLNSGYHFCGGSLINEQWVVSAGHCYKRIQVRLGEHNIKVLG	83
PRSS3-v1	VAVPFDDDDKIVGGYTCEENSLPYQVSLNSGSHFCGGSLISEQWVVSAAHCYKRIQVRLGEHNIKVLG	140
PRSS3-v2	VAVPFDDDDKIVGGYTCEENSLPYQVSLNSGSHFCGGSLISEQWVVSAAHCYKRIQVRLGEHNIKVLG	83
PRSS3-v3	IAPFDDDDKIVGGYTCEENSLPYQVSLNSGSHFCGGSLISEQWVVSAAHCYKRIQVRLGEHNIKVLG	97
PRSS3-v4	VAVPFDDDDKIVGGYTCEENSLPYQVSLNSGSHFCGGSLISEQWVVSAAHCYKRIQVRLGEHNIKVLG	76
PRSS1	NEQFINAAKIIRHICYDRKTLNNDIMLKLSSRAVINARVSTISLPTAPPATGTECLISGWGNTASSGAD	153
PRSS3-v1	NEQFINAAKIIRHKYNRDTLNDIMLKLSSPAVINARVSTISLPTAPPAAAGTECLISGWGNTLSEFAD	210
PRSS3-v2	NEQFINAAKIIRHKYNRDTLNDIMLKLSSPAVINARVSTISLPTAPPAAAGTECLISGWGNTLSEFAD	153
PRSS3-v3	NEQFINAAKIIRHKYNRDTLNDIMLKLSSPAVINARVSTISLPTAPPAAAGTECLISGWGNTLSEFAD	167
PRSS3-v4	NEQFINAAKIIRHKYNRDTLNDIMLKLSSPAVINARVSTISLPTAPPAAAGTECLISGWGNTLSEFAD	146
PRSS1	YPDELQCLDAPVLSQAKCEASYPGKITNSMFCVGFLEGGKDSQQRDSGGPVVVCNGQLQGVVSWGHGCAIK	223
PRSS3-v1	YPDELKCLDAPVLTQAECKASYPGKITNSMFCVGFLEGGKDSQQRDSGGPVVVCNGQLQGVVSWGHGCAIK	280
PRSS3-v2	YPDELKCLDAPVLTQAECKASYPGKITNSMFCVGFLEGGKDSQQRDSGGPVVVCNGQLQGVVSWGHGCAIK	223
PRSS3-v3	YPDELKCLDAPVLTQAECKASYPGKITNSMFCVGFLEGGKDSQQRDSGGPVVVCNGQLQGVVSWGHGCAIK	237
PRSS3-v4	YPDELKCLDAPVLTQAECKASYPGKITNSMFCVGFLEGGKDSQQRDSGGPVVVCNGQLQGVVSWGHGCAIK	216
PRSS1	KNKPGVYTKVINYVDWIKDTIAAN	246
PRSS3-v1	NRPGVYTKVINYVDWIKDTIAAN	303
PRSS3-v2	NRPGVYTKVINYVDWIKDTIAAN	246
PRSS3-v3	NRPGVYTKVINYVDWIKDTIAAN	260
PRSS3-v4	NRPGVYTKVINYVDWIKDTIAAN	239

**Figure 5.23** Mutialignment of amino acid sequences of PRSS1 and four PRSS3 transcript variants by DNAMAN program. Highlight homology level; blue = 100%, pink  $\geq 75\%$ , cyan  $\geq 50\%$ , yellow  $\geq 33\%$ . Yellow box indicates the peptide sequences generated by LC-MS/MS as listed in **Table 5.2**.

**Table 5.2** Generated peptide sequences of PRSS1 and PRSS3 by LC-MS/MS

Identified protein	Accession number	Generated peptide sequence
PRSS1	AAG30948.1	RIQVRL and KTLNNDIMLIKL
PRSS3	A1A508	KTLNNDIMLIKL and KNKPGVYTKV

#### 5.4 Determination of PRSS gene expression in SH-SY5Y cells

To clarify which isoform of human trypsinogen i.e. PRSS1 or PRSS3 was expressed in SH-SY5Y cells, isoform-specific primers were used to determine *PRSS* gene expression by RT-PCR. Expression profiles of human *PRSS* genes including *PRSS1*, *PRSS2*, and *PRSS3* were examined. It was found that SH-SY5Y cells expressed only PRSS3, while positive control HEK293T expressed all three *PRSS*s (**Figure 5.24**). Since the antibody specific to PRSS3 protein is commercially available, the expression of the PRSS3 protein in SH-SY5Y was confirmed by immunofluorescence assay (**Figure 5.25**). Because *PRSS3* contains 4 transcript variants, the subtyping was performed by gradient RT-PCR using variant-specific primers to amplify the full-length *PRSS3* transcript variants in SH-SY5Y cells. Variant-specific primers were designed according to the coding sequences (CDSs) of *homo sapiens PRSS3* NCBI reference sequences (accession numbers; NM\_007343.3, NM\_002771.3, NM\_001197097.2, and NM\_001197098.1) deposited in NCBI database. The sequences of restriction sites of *XhoI* and *XbaI* endonuclease were incorporated in the primers for further cloning purpose. It was found that only *PRSS3* transcript variant 3 (*PRSS3-V3*) could be amplified with its correct size at 798 bp (**Figure 5.26**). The *PRSS3-V3* fragment was purified from the gel and cloned in pGEM<sup>®</sup>-T vector, named pGEM<sup>®</sup>-T::*PRSS3-V3*. Clone selection by blue-white colony screening and amplifying using M13 primers showed that 6 out of 10 randomly selected colonies gave the correct size of PCR amplicons of *PRSS3-V3* flanked with sequences from M13 primer binding site which is 1,062 bp. PCR amplicons generated from empty pGEM<sup>®</sup>-T, used as control, is 264 bp (**Figure 5.27**). The nucleotide sequence of the suspected *PRSS3-V3* was verified by DNA sequencing and analyzed by DNAMAN and Applied Biosystems Sequence Scanner Software 2 (**Figure 5.28**). By searching on nucleotide BLAST (BLASTn), the insert sequence verified by DNA sequencing showed 100% identity of the sequence to *homo sapiens* serine protease 3 (PRSS3), transcript variant 3 (NCBI reference sequence accession number NM\_001197097.3), and also *homo sapiens* protease serine 4 isoform B mRNA, complete cds, accession number AY052783.1 (**Figure 5.29**). By BLASTx, the insert sequence showed 100% identity of the sequence to serine protease 3



(mesotrypsin), isoform CRA\_c [*Homo sapiens*], accession number EAW58483 deposited in NCBI database (**Figure 5.30**). It was confirmed that the EV-A71 3A interacting proteins identified in human SH-SY5Y neuronal cells by pull-down assay and LC-MS/MS was PRSS3 variant 3.

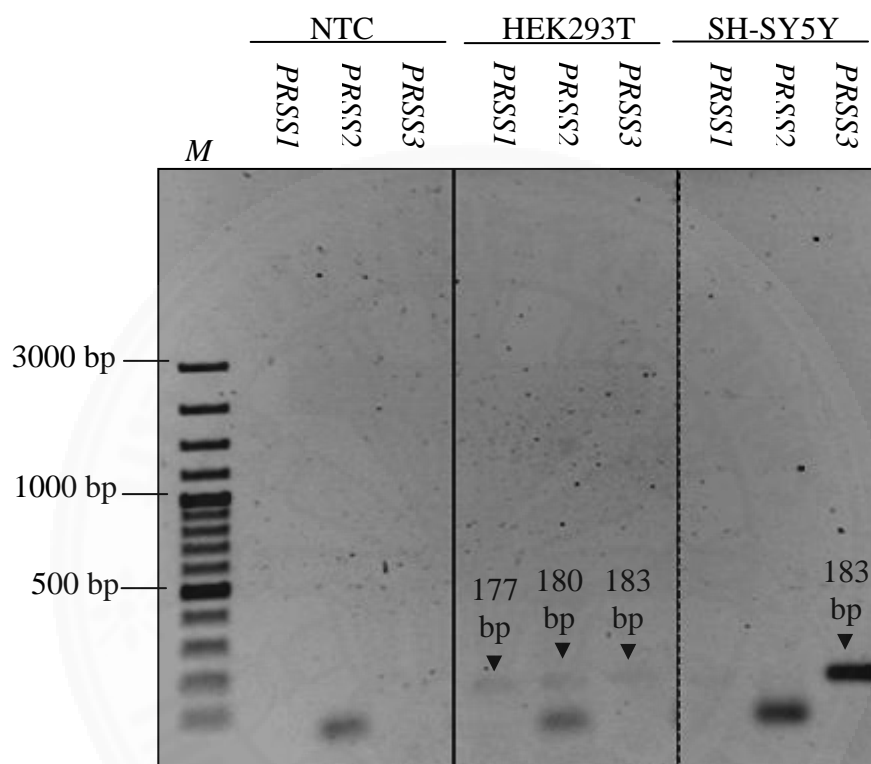


**Figure 5.24** Agarose gel electrophoresis of *PRSS* amplicons determined in HEK293T and SH-SY5Y cells by RT-PCR using subtype-specific primers. Sizes of PCR amplicons of site-specific of *PRSS1*, *PRSS2*, and *PRSS3* are 177, 180, and 183 bp, respectively. Lane M; 100 bp Plus DNA ladder (in base pairs, bp). NTC; non-template control. HEK293T cells express all *PRSSs* while SH-SY5Y cells express only *PRSS3*. The sizes of molecular weight are indicated on the left of the figure. The sizes of the bands of interest are indicated by arrow on the figure.

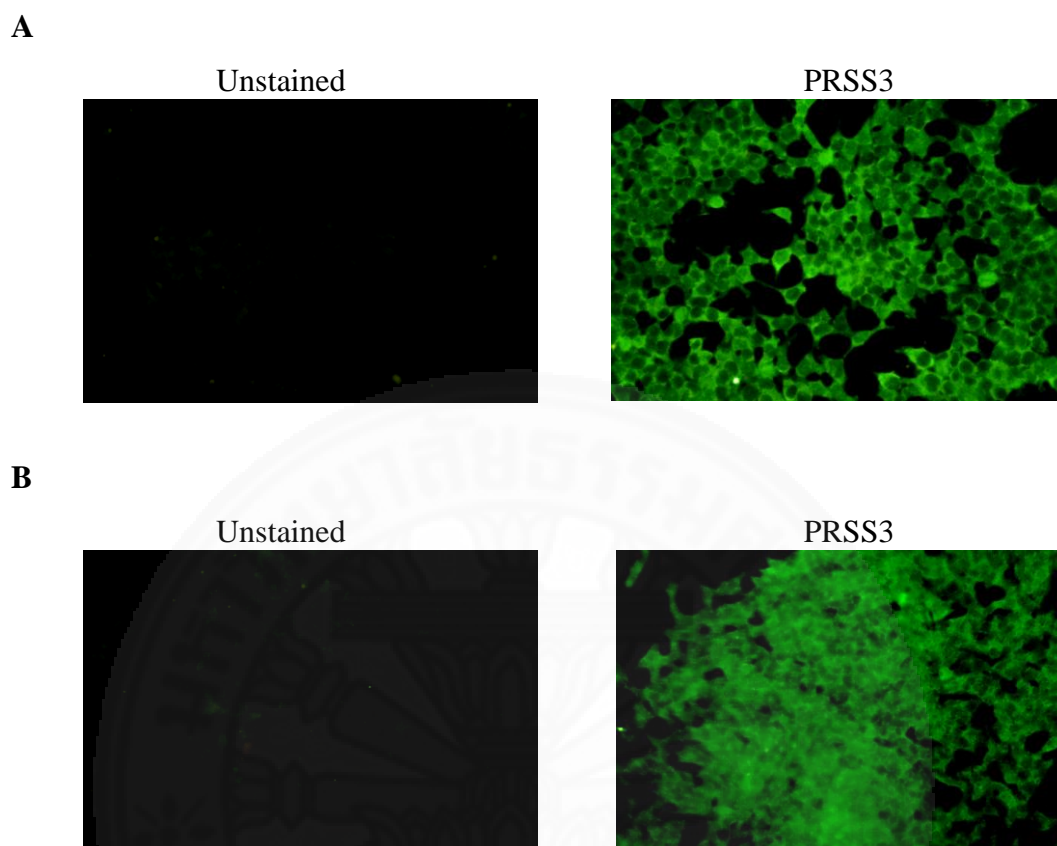


**Figure 5.25** Detection of endogenous PRSS3 protein expression in HEK293T (**A**) and SH-SY5Y (**B**) cells by immunofluorescence assay. Cells were fixed and stained for PRSS3 by 1:100 rabbit anti-PRSS3 polyclonal antibody (PA5-23991, Thermo Fisher Scientific, US). Unstained cells served as negative control.

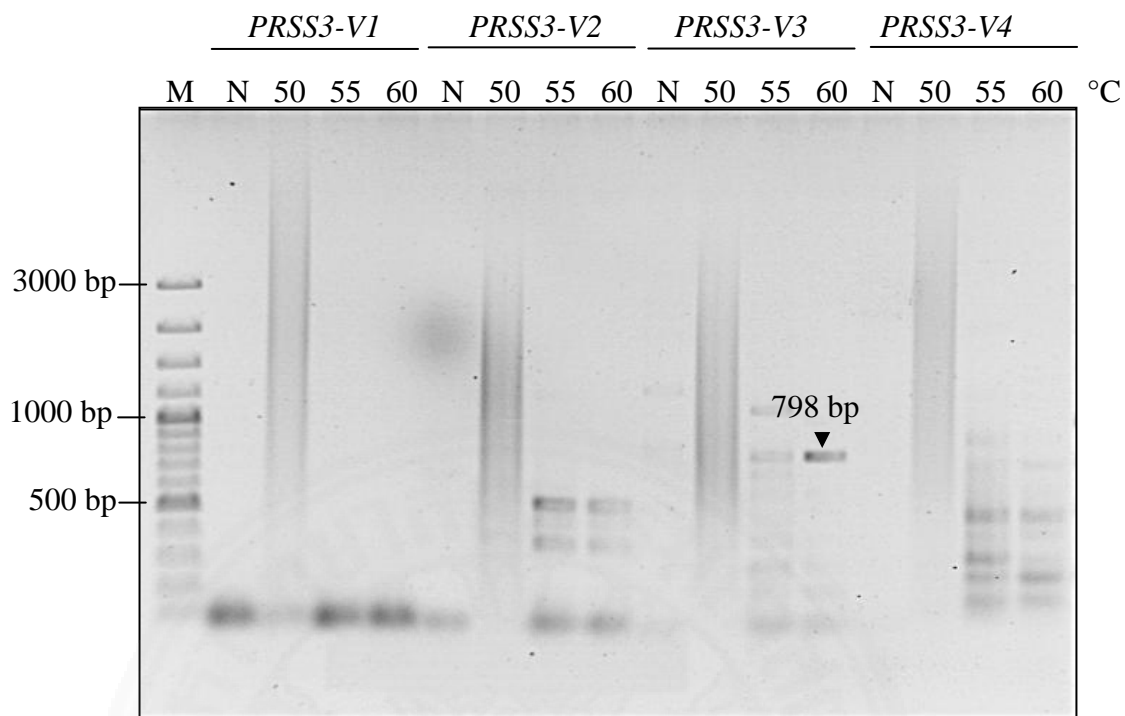


**Figure 5.26** Agarose gel electrophoresis of amplicons of full-length *PRSS3* transcript variants determined in SH-SY5Y cells by RT-PCR. Each full-length transcript variants of *PRSS3* were amplified by RT-PCR using annealing temperatures at 50, 55, and 60 °C. Lane M; 100 bp Plus DNA ladder (in base pairs, bp), lanes N; non-template control of each transcript variant. Only *PRSS3* transcript variant 3 (*PRSS3-V3*) at size of 798 bp could be amplified using annealing temperature at 60 °C as indicated by arrow. The sizes of molecular weight are indicated on the left of the figure. The sizes of the bands of interest are indicated by arrow on the figure.

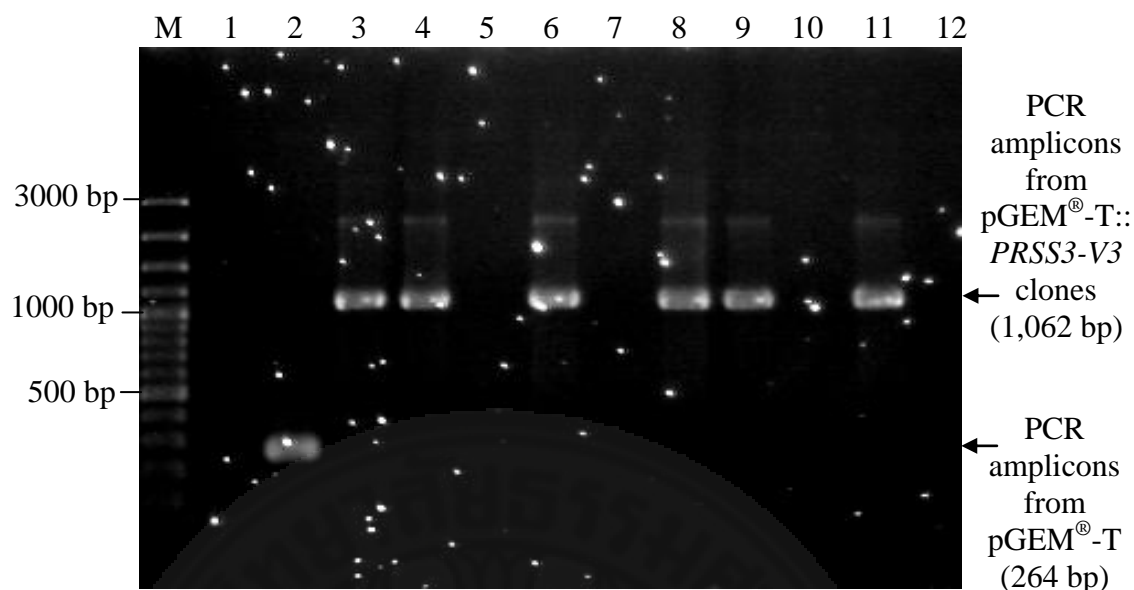


**Figure 5.27** Agarose gel electrophoresis of PCR products amplified from colonies of JM109 *E. coli* transformed with pGEM<sup>®</sup>-T::PRSS3-V3 by colony PCR. Lane M; 100 bp Plus DNA ladder (in base pairs, bp), lane 1; non-template control, lane 2; PCR amplicons from pGEM<sup>®</sup>-T vector without insert (264 bp), lanes 3-12; PCR amplicons from 10 colonies of the transformed *E. coli*, respectively. Six out of ten colonies as shown in lane 3, 4, 6, 8, 9, and 11 were positive transformant producing PCR amplicons at size of 1,062 bp which is PRSS3-V3 with flanking region from the vector. The sizes of molecular weight are indicated on the left of the figure. The sizes of the bands of interest are indicated by arrow on the figure.

A

<i>XhoI</i>				<i>PRSS3-V3</i>			
<u>CTCGAGATGC</u>	ACATGAGAGA	GACAAGTGGC	TTCACATTGA	AGAAGGGGAG	GAGTGCGCCA		
TTGGTTTTCC	ATCCTCCAGA	TGCACTGATT	GCTGTCCCCT	TTGACGATGA	TGACAAGATT		
GTTGGGGGCT	ACACCTGTGA	GGAGAATTCT	CTCCCCTACC	AGGTGTCCCT	GAATTCTGGC		
TCCCCTTCT	GCGGTGGCTC	CCTCATCAGC	GAACAGTGGG	TGGTATCAGC	AGCTCACTGC		
TACAAGACCC	GCATCCAGGT	GAGACTGGGA	GAGCACAACA	TCAAAGTCCT	GGAGGGGAAT		
GAGCAGTTCA	TCAATGCGGC	CAAGATCATC	CGCCACCCTA	AATACAACAG	GGACACTCTG		
GACAATGACA	TCATGCTGAT	CAAACCTCTC	TCACCTGCCG	TCATCAATGC	CCGCGTGTCC		
ACCATCTCTC	TGCCACCAGC	CCCTCCAGCT	GCTGGCACTG	AGTGCCTCAT	CTCCGGCTGG		
GGCAACACTC	TGAGCTTTGG	TGCTGACTAC	CCAGACGAGC	TGAAGTGCCT	GGATGCTCCG		
GTGCTGACCC	AGGCTGAGTG	TAAAGCCTCC	TACCCTGGAA	AGATTACCAA	CAGCATGTTC		
TGTGTGGGCT	TCCTTGAGGG	AGGCAAGGAT	TCCTGCCAGC	GTGACTCTGG	TGGCCCTGTG		
GTCTGCAACG	GACAGCTCCA	AGGAGTTGTC	TCCTGGGGCC	ATGGCTGTGC	CTGGAAGAAC		
AGGCCTGGAG	TCTACACCAA	GGTCTACAAC	TATGTGGACT	GGATTAAGGA	CACCATCGCT		
GCCAACAGCT	<u>AATCTAGA</u>						
	<i>XbaI</i>						

B

<i>PRSS3-V3</i>					
MHMRETSGFT	LKKGRSAPLV	FHPPDALIAV	PFDDDDKIVG	GYTCEENSLP	YQVSLNSGSH
FCGGSLISEQ	WVVSAAHCYK	TRIQVRLGEH	NIKVLEGNEQ	FINAAKIIRH	PKYNRDTLDN
DIMLIKLSPP	AVINARVSTI	SLPTAPPAAG	TECLISGWGN	TLSFGADYPD	ELKCLDAPVL
TQAECKASYP	GKITNSMFCV	GFLEGGKDSC	QRDSGGPVVC	NGQLQGVVSW	GHGCAWKNRP
GVYTKVYNYV	DWIKDTIAAN	S*			

**Figure 5.28** Nucleotide sequence of *PRSS3-V3* inserted in pGEM<sup>®</sup>-T Easy vector (A) and the deduced amino acid sequence of *PRSS3-V3* coding sequence (B). Underline indicates restriction sites. Red letters and asterisk indicate stop codon.



**Sequences producing significant alignments**

Download  Select columns  100

select all 100 sequences selected

GenBank  Distance tree of results

Description	Scientific Name	Max Score	Total Score	Query Cover	E value	Per. Ident	Acc. Len	Accession
<input checked="" type="checkbox"/> <a href="#">Homo sapiens serine protease 3 (PRSS3)_transcript variant 3_mRNA</a>	<a href="#">Homo sapiens</a>	1447	1447	100%	0.0	99.87%	932	<a href="#">NM_001197097.3</a>
<input checked="" type="checkbox"/> <a href="#">Homo sapiens protease serine 4 isoform B mRNA_complete cds</a>	<a href="#">Homo sapiens</a>	1424	1424	100%	0.0	99.36%	928	<a href="#">AY052783.1</a>
<input checked="" type="checkbox"/> <a href="#">PREDICTED: Pan troglodytes serine protease 3 (PRSS3)_transcript variant X2_mRNA</a>	<a href="#">Pan troglodytes</a>	1415	1415	100%	0.0	99.24%	1880	<a href="#">XM_016960743.2</a>
<input checked="" type="checkbox"/> <a href="#">PREDICTED: Gorilla gorilla serine protease 3 (PRSS3)_transcript variant X1_mRNA</a>	<a href="#">Gorilla gorilla go...</a>	1375	1375	100%	0.0	98.22%	886	<a href="#">XM_03104904.1</a>
<input checked="" type="checkbox"/> <a href="#">PREDICTED: Sturnira hondurensis trypsin-3 (LOC118980724)_mRNA</a>	<a href="#">Sturnira hondure...</a>	1301	1301	90%	0.0	99.86%	744	<a href="#">XM_037037374.1</a>
<input checked="" type="checkbox"/> <a href="#">Homo sapiens serine protease 3 (PRSS3)_transcript variant 4_mRNA</a>	<a href="#">Homo sapiens</a>	1301	1301	89%	0.0	100.00%	803	<a href="#">NM_001197098.1</a>
<input checked="" type="checkbox"/> <a href="#">Homo sapiens PRSS3 mRNA for trypsinogen 4_complete cds</a>	<a href="#">Homo sapiens</a>	1301	1301	90%	0.0	99.72%	1032	<a href="#">AB298285.1</a>
<input checked="" type="checkbox"/> <a href="#">Homo sapiens protease_serine_3_mRNA (cDNA clone IMAGE_4537998)_partial cds</a>	<a href="#">Homo sapiens</a>	1301	1301	90%	0.0	99.72%	821	<a href="#">BC030238.1</a>
<input checked="" type="checkbox"/> <a href="#">Homo sapiens mRNA for trypsinogen IV a-form</a>	<a href="#">Homo sapiens</a>	1301	1301	90%	0.0	99.72%	853	<a href="#">X72781.1</a>
<input checked="" type="checkbox"/> <a href="#">Homo sapiens protease_serine_3_mRNA (cDNA clone MGC-97026 IMAGE_7282235)_complete cds</a>	<a href="#">Homo sapiens</a>	1301	1301	90%	0.0	99.86%	807	<a href="#">BC069494.1</a>
<input checked="" type="checkbox"/> <a href="#">Synthetic construct Homo sapiens clone IMAGE:100071592; CCSEB013878_04_protease_serine_3 (mesotr...synthetic constr...</a>		1299	1299	89%	0.0	99.86%	843	<a href="#">HQ448195.1</a>

**Figure 5.29** Homology search of the cloned *PRSS3-V3* coding sequence inserted in pGEM<sup>®</sup>-T vector by BLASTn.

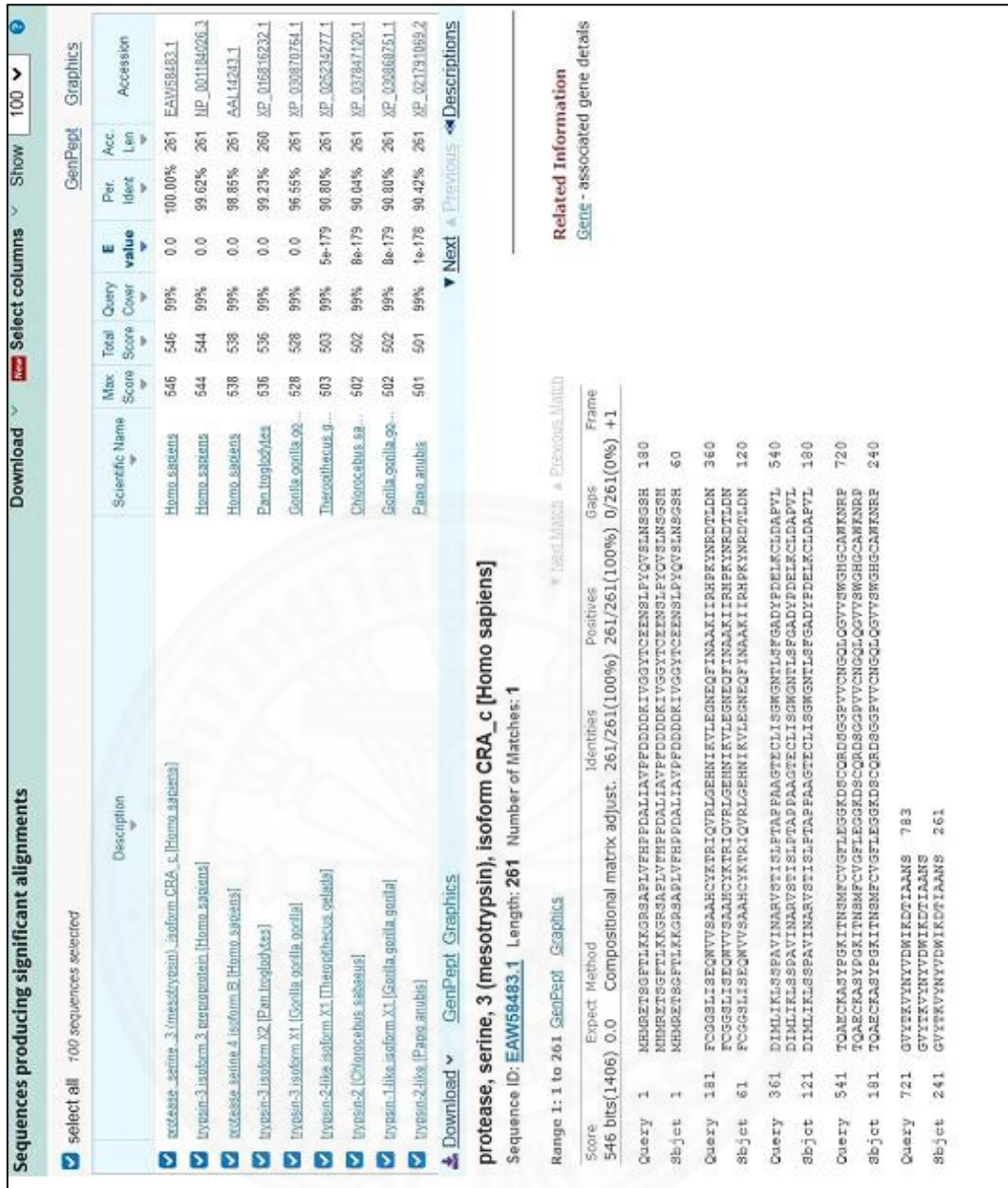


**Figure 5.30** Homology search of the cloned *PRSS3-V3* coding sequence inserted in pGEM<sup>®</sup>-T vector by BLASTx.



## 5.5 Confirmation of direct protein-protein binding between EV-A71 3A protein and the PRSS3 variant 3 protein by co-immunoprecipitation assay

### 5.5.1 Production of recombinant PRSS3 transcript variant 3 by mammalian expression system

Coding sequence of full-length PRSS3 variant 3 in-frame with coding sequence of Myc protein tag at 3'-end (designated as *FL-PRSS3-Myc*) given product size at 828 bp was successfully amplified (**Figure 5.31**) and cloned into pGEM<sup>®</sup>-T Easy vector. By blue-white screening and direct colony PCR using M13 primers, the presence of inserted *FL-PRSS3-Myc* was detected in 5 out of 6 randomly selected colonies (**Figure 5.32**). Size of the PCR amplicons generated from pGEM<sup>®</sup>-T::*FL-PRSS3-Myc* was 1,092 bp, while size of the PCR amplicons produced from pGEM<sup>®</sup>-T Easy empty vector was 264 bp. Verification by DNA sequencing showed correct nucleotide sequences of *FL-PRSS3-Myc* and translation of the sequence by DNAMAN program showed correct reading frame of the amino acid sequences (**Figure 5.33**). To release *FL-PRSS3-Myc* from pGEM<sup>®</sup>-T and clone directionally to pLVX-Puro mammalian expression vector, pGEM<sup>®</sup>-T::*FL-PRSS3-Myc* and pLVX-Puro were successfully digested with *Xho*I and *Xba*I endonucleases (**Figure 5.34**). The successful subcloning of *FL-PRSS3-Myc* into pLVX-Puro vector was detected by colony PCR using pLVX sequencing primers. It was found that 2 out of 6 randomly selected colonies were positive giving the PCR amplicons at size of 1,028 bp while the PCR products amplified from the empty pLVX-Puro vector was 200 bp (**Figure 5.35**). Nucleotide sequence, translational reading-frame, and deduced amino acid sequence of the *FL-PRSS3-Myc* were verified by DNA sequencing and bioinformatic analysis. (**Figure 5.36**). At 6 hours post-transfection (h.p.t.), the recombinant FL-PRSS3-Myc protein could be fairly detected in HEK293T cells. At 24 h.p.t., level of expression of FL-PRSS3-Myc protein was increased (**Figure 5.37**). It could be concluded that the recombinant FL-PRSS3-Myc protein was successfully produced in mammalian cells.

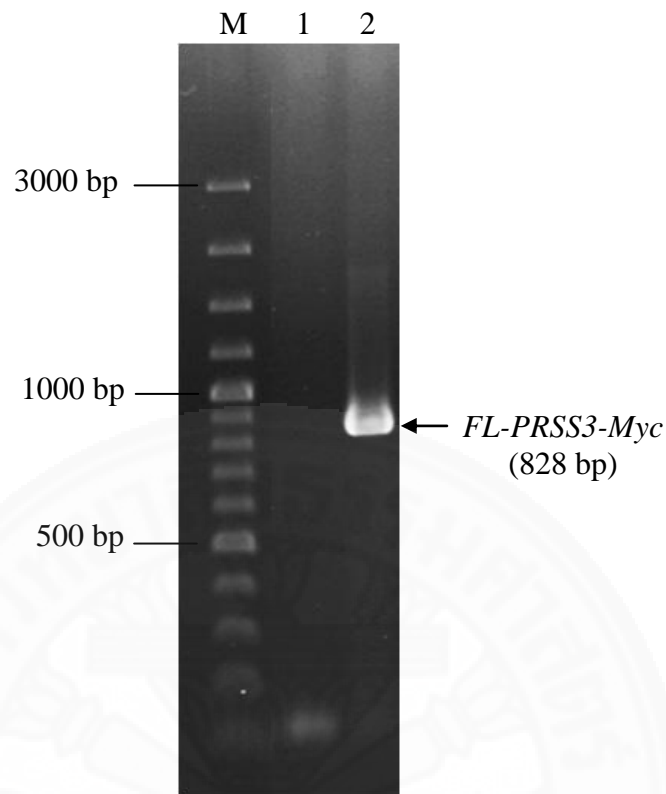


**Figure 5.31** Agarose gel electrophoresis of PCR amplicons of *FL-PRSS3-Myc*. Lane M; 100 bp Plus DNA ladder (in base pairs, bp), lane 1; non-template control, lane 2; PCR amplicons of *FL-PRSS3-Myc* (828 bp). The sizes of molecular weight are indicated on the left of the figure. The sizes of the bands of interest are indicated by arrow on the figure.

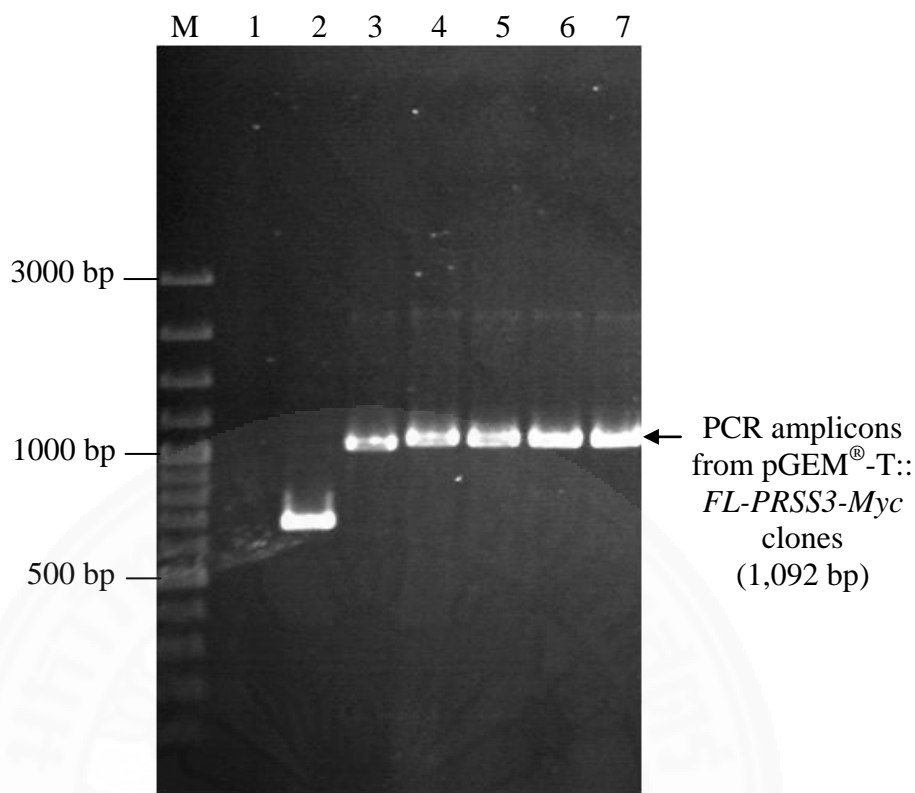


**Figure 5.32** Agarose gel electrophoresis of PCR products amplified from colonies of JM109 *E. coli* transformed with pGEM<sup>®</sup>-T::*FL-PRSS3-Myc* by colony PCR. Lane M; 100 bp Plus DNA ladder (in base pairs, bp), lane 1; non-template control, lanes 2-7; PCR amplicons from 6 colonies of the transformed *E. coli*, respectively. Five out of six colonies as shown in lanes 3-7 were positive transformants producing PCR amplicons at correct size of 1,092 bp which is *PRSS3-V3* with flanking region from the vector. The sizes of molecular weight are indicated on the left of the figure. The sizes of the bands of interest are indicated by arrow on the figure.

A

<i>XhoI</i>			<i>FL-PRSS3</i>		
<u>CTCGAGATGC</u>	ACATGAGAGA	GACAAGTGGC	TTCACATTGA	AGAAGGGGAG	GAGTGCGCCA
TTGGTTTTCC	ATCCTCCAGA	TGCACTGATT	GCTGTCCCCT	TTGACGATGA	TGACAAGATT
GTTGGGGGCT	ACACCTGTGA	GGAGAATTCT	CTCCCCTACC	AGGTGTCCCT	GAATTCTGGC
TCCCACTTCT	GCGGTGGCTC	CCTCATCAGC	GAACAGTGGG	TGGTATCAGC	AGCTCACTGC
TACAAGACCC	GCATCCAGGT	GAGACTGGGA	GAGCACAACA	TCAAAGTCCT	GGAGGGGAAT
GAGCAGTTCA	TCAATGCGGC	CAAGATCATC	CGCCACCCTA	AATACAACAG	GGACACTCTG
GACAATGACA	TCATGCTGAT	CAAACCTCTC	TCACCTGCCG	TCATCAATGC	CCGCGTGTCC
ACCATCTCTC	TGCCACCAGC	CCCTCCAGCT	GCTGGCACTG	AGTGCCTCAT	CTCCGGCTGG
GGCAACACTC	TGAGCTTTGG	TGCTGACTAC	CCAGACGAGC	TGAAGTGCCT	GGATGCTCCG
GTGCTGACCC	AGGCTGAGTG	TAAAGCCTCC	TACCCTGGAA	AGATTACCAA	CAGCATGTTC
TGTGTGGGCT	TCCTTGAGGG	AGGCAAGGAT	TCCTGCCAGC	GTGACTCTGG	TGGCCCTGTG
GTCTGCAACG	GACAGCTCCA	AGGAGTTGTC	TCCTGGGGCC	ATGGCTGTGC	CTGGAAGAAC
AGGCCTGGAG	TCTACACCAA	GGTCTACAAC	TATGTGGACT	GGATTAAGGA	CACCATCGCT
GCCAACAGCG	<u>AGCAGAAACT</u>	<u>CATCTCAGAA</u>	<u>GAGGATCTGT</u>	<u>AACTAGAA</u>	
		<i>Myc</i>		<i>XbaI</i>	

B

<i>FL-PRSS3</i>					
MHMRETSGFT	LKKGRSAPLV	FHPPDALIAV	PFDDDDKIVG	GYTCEENSLP	YQVSLNSGSH
FCGGSLLISEQ	WVVSAAHCYK	TRIQVRLGEH	NIKVLEGNEQ	FINAAKIIRH	PKYNRDTLDN
DIMLIKLSPP	AVINARVSTI	SLPTAPPAAG	TECLISGWGN	TLSFGADYPD	ELKCLDAPVL
TQAECKASYP	GKITNSMFCV	GFLEGGKDSC	QRDSGGPVVC	NGQLQGVVSW	GHGCAWKNRP
GVYTKVYNYV	DWIKDTIAAN	<u>SEQKLISEED</u>	<u>L*</u>		
		<i>Myc</i>			

**Figure 5.33** Nucleotide sequence of *FL-PRSS3-Myc* inserted in pGEM<sup>®</sup>-T Easy vector (A) and the deduced amino acid sequence of *FL-PRSS3-Myc* coding sequence (B). Underline indicates restriction sites. Grey highlight indicates Myc sequence. Red letters and asterisk indicate stop codon. Grey highlight indicates Myc sequence. Underline indicates restriction sites. Red letters and asterisk indicate stop codon.

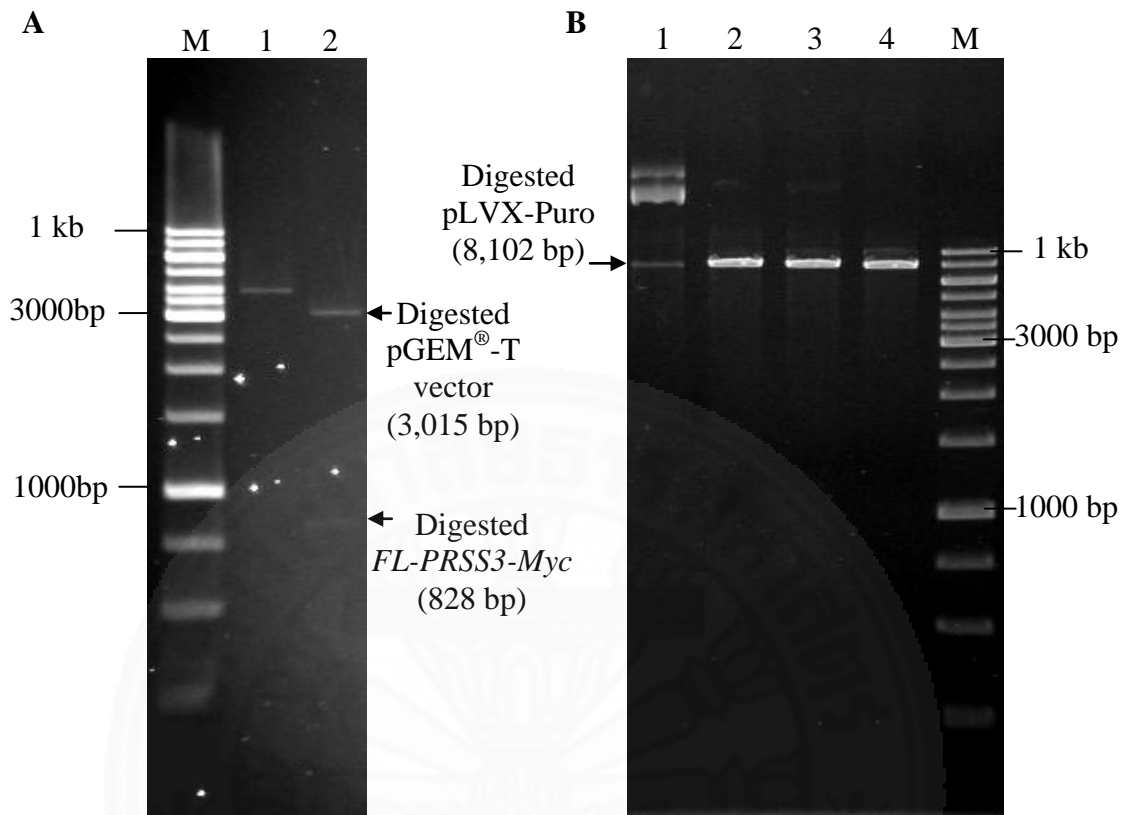


**Figure 5.34** Agarose gel electrophoresis of pGEM<sup>®</sup>-T::*FL-PRSS3-Myc* (**A**) and pLVX-Puro (**B**) double-digested with *XhoI* and *XbaI* endonucleases. **A**; lane M; 1 kb DNA ladder (in base pairs, bp), lane 1; undigested pGEM<sup>®</sup>-T::*FL-PRSS3-Myc*, lane 2; *XhoI/XbaI* digested pGEM<sup>®</sup>-T::*FL-PRSS3-Myc* showing 2 fragments including digested pGEM<sup>®</sup>-T vector (3,015 bp) and digested *FL-PRSS3-Myc* (828 bp). **B**; lane M; 1 kb DNA ladder (in base pairs, bp), lane 1; undigested pLVX-Puro vector, lane 2; *XhoI* digested pLVX-Puro, lane 3; *XbaI* digested pLVX-Puro, lane 4; *XhoI/XbaI* digested pLVX-Puro. The sizes of molecular weight are indicated on the left (**A**) or right (**B**) of the figure. The sizes of the bands of interest are indicated by arrow on the figure.

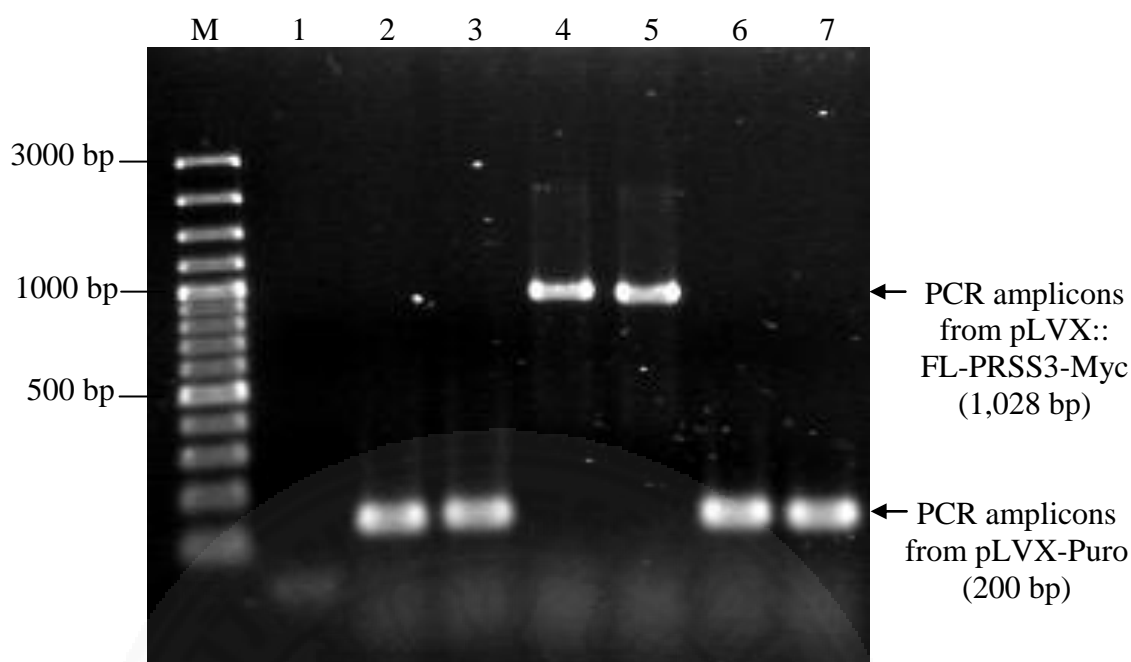


**Figure 5.35** Agarose gel electrophoresis of PCR products amplified from colonies of JM109 *E. coli* transformed with pLVX::*FL-PRSS3-Myc*. Lane M; 100 bp Plus DNA ladder (in base pairs, bp), lane 1; non-template control, lanes 2-7; PCR amplicons from 6 randomly selected colonies of the transformed *E. coli*, respectively. Two out of six colonies as shown in lanes 4 and 5 were positive transformants producing PCR amplicons at size of 1,028 bp which is *FL-PRSS3-Myc* with flanking region from the vector. Lanes 2, 3, 6, and 7 were PCR amplicons from pLVX-Puro without insert (200 bp). The sizes of molecular weight are indicated on the left of the figure. The sizes of the bands of interest are indicated by arrow on the figure.



A

<i>XhoI</i>			<i>FL-PRSS3</i>		
<u>CTCGAGATGC</u>	ACATGAGAGA	GACAAGTGGC	TTCACATTGA	AGAAGGGGAG	GAGTGCGCCA
TTGGTTTTCC	ATCCTCCAGA	TGCACTGATT	GCTGTCCCCT	TTGACGATGA	TGACAAGATT
GTTGGGGGCT	ACACCTGTGA	GGAGAATTCT	CTCCCCTACC	AGGTGTCCCT	GAATTCTGGC
TCCCACTTCT	GCGGTGGCTC	CCTCATCAGC	GAACAGTGGG	TGGTATCAGC	AGCTCACTGC
TACAAGACCC	GCATCCAGGT	GAGACTGGGA	GAGCACAACA	TCAAAGTCCT	GGAGGGGAAT
GAGCAGTTCA	TCAATGCGGC	CAAGATCATC	CGCCACCCTA	AATACAACAG	GGACACTCTG
GACAATGACA	TCATGCTGAT	CAAACCTCTC	TCACCTGCCG	TCATCAATGC	CCGCGTGTCC
ACCATCTCTC	TGCCACCAGC	CCCTCCAGCT	GCTGGCACTG	AGTGCCTCAT	CTCCGGCTGG
GGCAACACTC	TGAGCTTTGG	TGCTGACTAC	CCAGACGAGC	TGAAGTGCCT	GGATGCTCCG
GTGCTGACCC	AGGCTGAGTG	TAAAGCCTCC	TACCCTGGAA	AGATTACCAA	CAGCATGTTC
TGTGTGGGCT	TCCTTGAGGG	AGGCAAGGAT	TCCTGCCAGC	GTGACTCTGG	TGGCCCTGTG
GTCTGCAACG	GACAGCTCCA	AGGAGTTGTC	TCCTGGGGCC	ATGGCTGTGC	CTGGAAGAAC
AGGCCTGGAG	TCTACACCAA	GGTCTACAAC	TATGTGGACT	GGATTAAGGA	CACCATCGCT
GCCAACAGCG	<u>AGCAGAAACT</u>	<u>CATCTCAGAA</u>	<u>GAGGATCTGT</u>	<u>AATCTAGA</u>	
		<i>Myc</i>		<i>XbaI</i>	

B

<i>FL-PRSS3</i>					
MHMRETSGFT	LKKGRSAPLV	FHPPDALIAV	PFDDDDKIVG	GYTCEENSLP	YQVSLNSGSH
FCGGSLLISEQ	WVVSAAHCYK	TRIQVRLGEH	NIKVLEGNEQ	FINAAKIIRH	PKYNRDTLDN
DIMLIKLSPP	AVINARVSTI	SLPTAPPAAG	TECLISGWGN	TLSFGADYPD	ELKCLDAPVL
TQAECKASYP	GKITNSMFCV	GFLEGGKDSC	QRDSGGPVVC	NGQLQGVVSW	GHGCAWKNRP
GVYTKVYNYV	DWIKDTIAAN	<u>SEQKLISEED</u>	<u>L*</u>		
		<i>Myc</i>			

**Figure 5.36** Nucleotide sequence of *FL-PRSS3-Myc* inserted in pLVX-Puro vector (A) and the deduced amino acid sequence of *FL-PRSS3-Myc* coding sequence (B). Underline indicates restriction sites. Grey highlight indicates Myc sequence. Red letters and asterisk indicate stop codon. Grey highlight indicates Myc sequence. Underline indicates restriction sites. Red letters and asterisk indicate stop codon.



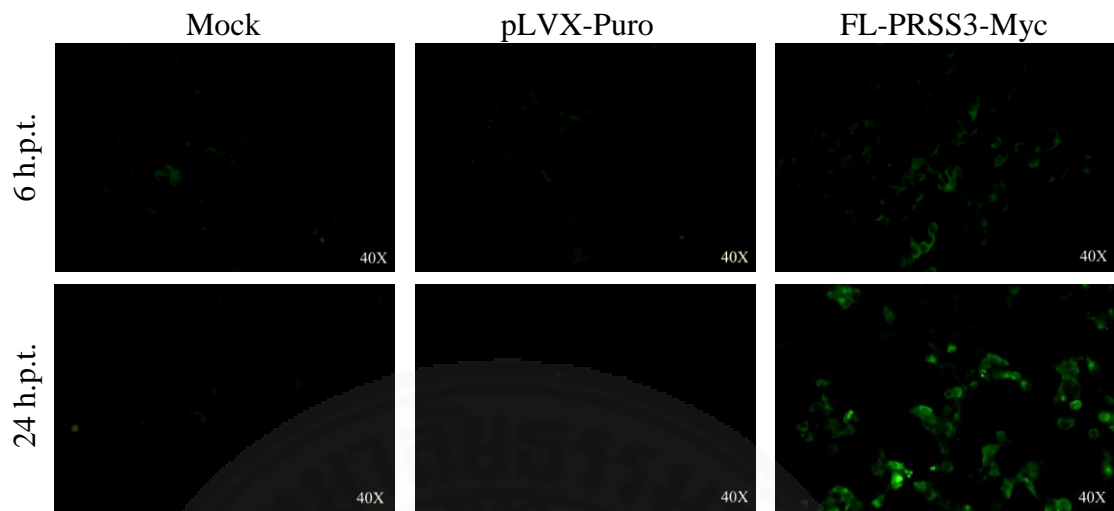


**Figure 5.37** Micrographs of FL-PRSS3-Myc protein expressed in HEK293T cells visualized by immunofluorescence assay using anti-Myc and Alexa Fluor 488-conjugated antibody. The expression of FL-PRSS3-Myc in the transfected HEK293T cells was determined at 6 and 24 h.p.t. Cells transfected with pLVX-Puro vector and only transfection reagent served as negative and mock control, respectively.

FLAG-mCherry would be used as irrelevant interacting protein control in immunoprecipitation assay. To construct the mammalian expressing vector producing recombinant FLAG-mCherry, the coding sequence of *FLAG-mCherry* was successfully amplified demonstrating at its correct size which is 747 bp (**Figure 5.38A**). The *FLAG-mCherry* fragments were ligated with pGEM<sup>®</sup>-T Easy vector. The positive clones of transformed *E. coli* were screened by blue-white screening and M13 sequencing primers. It was found that 4 out of 5 randomly selected colonies gave the correct size of the insert which is 1,011 bp, compared to the PCR amplicons amplified from blue colony or transformant carrying pGEM<sup>®</sup>-T vector with no insert (264 bp) (**Figure 5.38B**). The cloning vector carrying *FLAG-mCherry* (pGEM<sup>®</sup>-T::*FLAG-mCherry*.) was successfully generated. To transfer coding sequence of *FLAG-mCherry* to mammalian expression vector, pGEM<sup>®</sup>-T::*FLAG-mCherry* was double-digested with *Xho*I and *Xba*I endonucleases. The fragment was released from pGEM<sup>®</sup>-T (**Figure 5.39A**), purified, and cloned directionally to pLVX-Puro vector named as pLVX::*FLAG-mCherry*. One out of four colonies showed the size of the insertion which is 947 bp (**Figure 5.39B**). The insertion of *FLAG-mCherry* was verified by DNA sequencing. DNA sequencing data showed 2 nucleotide substitutions, however, it was a synonymous mutation that made no change in amino acid sequence (**Figure 5.40**). Expression of pLVX::*FLAG-mCherry* was also verified in HEK293T cells. Using fluorescence detection, FLAG-mCherry protein could be strongly expressed in HEK293T cells at 24 h.p.t. (**Figure 5.41**). It was confirmed that the irrelevant interacting protein control could be produced in the mammalian cells.

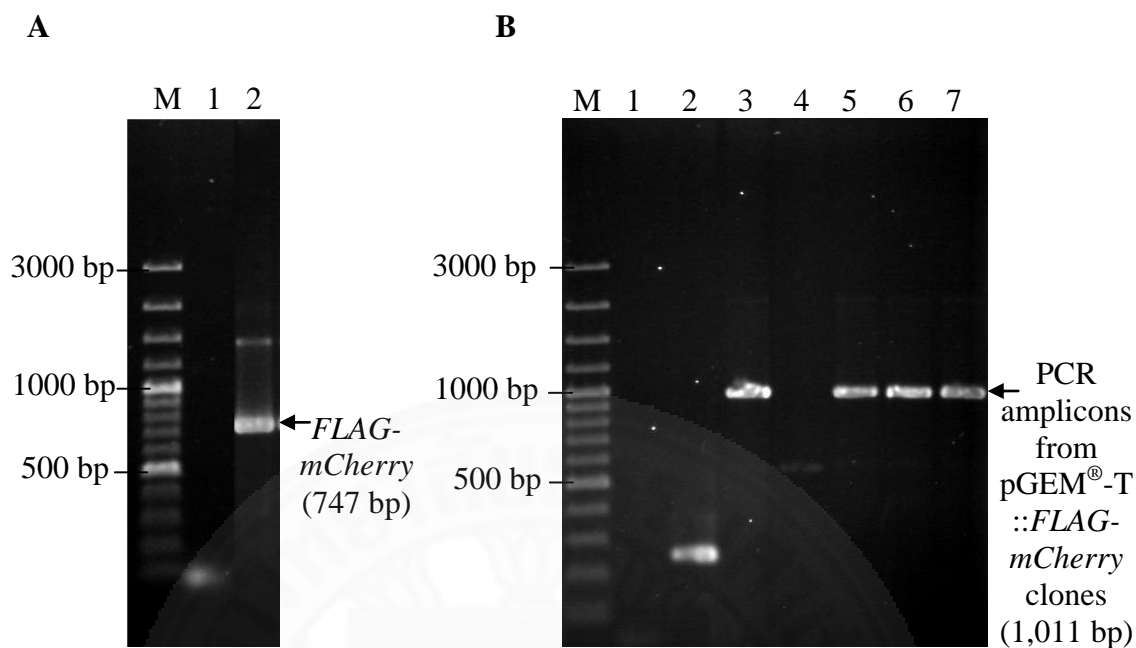


**Figure 5.38** Agarose gel electrophoresis of *FLAG-mCherry* amplification (**A**) and clone selection of *FLAG-mCherry* inserted in pGEM<sup>®</sup>-T Easy vector (pGEM<sup>®</sup>-T::*FLAG-mCherry*) by colony PCR (**B**). **A**; lane M; 100 bp Plus DNA ladder (in base pairs, bp), lane 1; non- template control, lane 2; PCR amplicons of *FLAG-mCherry* (747 bp). **B**; lane M; 100 bp Plus DNA ladder (in base pairs, bp), lane 1; non-template control, lane 2; PCR amplicons from blue colony or pGEM<sup>®</sup>-T without insert (264 bp), lanes 3-7; PCR amplicons from 5 randomly selected colonies of the transformed *E. coli*, respectively. Four out of five colonies as shown in lanes 3, and 5-7 were positive transformants producing PCR amplicons at size of 1,011 bp which is *FLAG-mCherry* with flanking region from the vector. The sizes of molecular weight are indicated on the left of the figure. The sizes of the bands of interest are indicated by arrow on the figure.

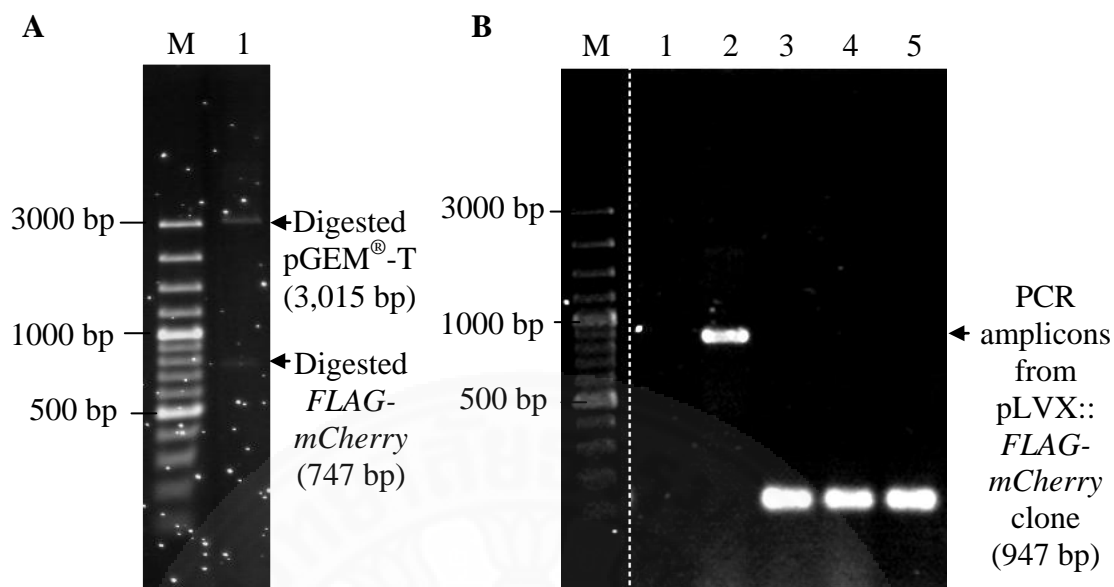


**Figure 5.39** Agarose gel electrophoresis of the pGEM<sup>®</sup>-T::*FLAG-mCherry* double-digested by *Xho*I and *Xba*I endonucleases (**A**) and clone selection of *FLAG-mCherry* inserted in pLVX-Puro vector (pLVX::*FLAG-mCherry*) by colony PCR (**B**). **A**; Lane M; 100 bp Plus DNA ladder (in base pairs, bp), lane 1; Digested pGEM<sup>®</sup>-T::*FLAG-mCherry* showing 2 bands including digested pGEM<sup>®</sup>-T (3,105 bp) and digested *FLAG-mCherry* (747 bp). **B**; lane M; 100 bp Plus DNA ladder (in base pairs, bp), lane 1; non-template control, lanes 2-5; PCR amplicons amplified from 4 randomly selected colonies of the transformed *E. coli*, respectively. One out of four colonies was positive transformant producing PCR amplicons at size of 947 bp which is *FLAG-mCherry* with flanking region from the vector. The sizes of molecular weight are indicated on the left of the figure. The sizes of the bands of interest are indicated by arrow on the figure.

A

```

FLAG-mCherry ATGGATTACAAGGATGACGATGACAAGGTGAGCAAGGGCGAGGAGGATAACATGGCCATCATCAAGGAGTTCATGCGCTT
Template -----c-t-----

FLAG-mCherry CAAGGTGCACATGGAGGGCTCCGTGAACGGCCACGAGTTCGAGATCGAGGGCGAGGGCGAGGGCCGCCCTACGAGGGCA
Template -----

FLAG-mCherry CCCAGACCGCCAAGCTGAAGGTGACCAAGGGTGGCCCCCTGCCCTTCGCCTGGGACATCCTGTCCCTCAGTTCATGTAC
200
Template -----

FLAG-mCherry GGCTCCAAGGCCTACGTGAAGCACCCCGCGACATCCCGACTACTTGAAGCTGTCTTCCCCGAGGGCTTCAAGTGGGA
Template -----

FLAG-mCherry GCGCGTGATGAACCTCGAGGACGGCGCGTGGTGACCGTGACCCAGGACTCCTCCCTGCAGGACGGCGAGTTCATCTACA
Template -----

FLAG-mCherry AGGTGAAGCTGCGCGGCACCAACTTCCCCTCCGACGGCCCCGTAATGCAGAAGAAGACCATGGGCTGGGAGGCTCCTCC
Template -----

FLAG-mCherry GAGCGGATGTACCCCGAGGACGGCGCCCTGAAGGGCGAGATCAAGCAGAGGCTGAAGCTGAAGGACGGCGGCCACTACGA
Template -----

FLAG-mCherry CGCTGAGGTCAAGACCACCTACAAGGCCAAGAAGCCCGTGCAGCTGCCCGGCCCTACAACGTCAACATCAAGTTGGACA
Template -----

FLAG-mCherry TCACCTCCACAACGAGGACTACACCATCGTGGAACAGTACGAACGCGCCGAGGGCGCCACTCCACCGCGGCATGGAC
Template -----

FLAG-mCherry GAGCTGTACAAGTAA
Template -----

```

B

```

FLAG-mCherry MDYKDDDDKVSKEEDNMAIIKEFMRFKVHMEGSVNGHEFEIEGEGEGRPYEGTQTAKLKVTKGGPLPFAWDILSPQFMY
Template -----

FLAG-mCherry GSKAYVKHPADIPDYLKLSFPEGFKWERVMNFEDGGVVTVTQDSSLQDGEFIYKVKLRGTFNPSDGFVMQKKTMGWEASS
Template -----

FLAG-mCherry ERMYPEDGALKGEIKQRLKLDGGHYDAEVKTTYKAKKPVQLPGAYNVNIKLDITSHNEDYTIVEQYERAEGRHSTGGMD
Template -----

FLAG-mCherry ELYK
Template -----

```

**Figure 5.40** Alignment of the verified *FLAG-mCherry* sequence with sequence of *mCherry* template. Nucleotide sequence (A) and the deduced amino acid sequence (B). The identical residues of the aligned nucleotide or amino acid were represented with dashes (-).

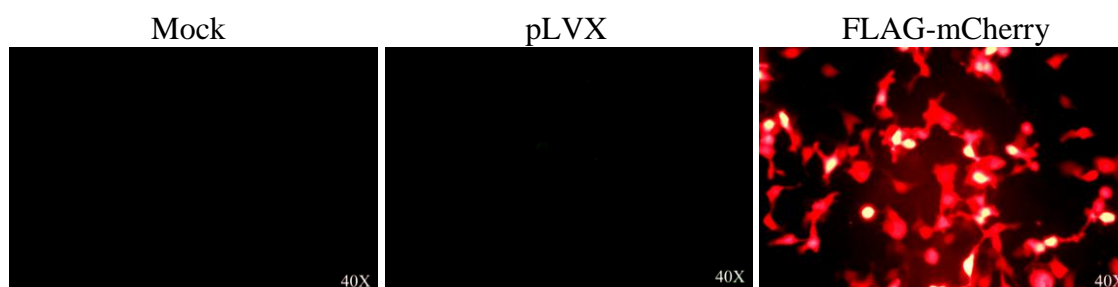


**Figure 5.41** Micrographs of FLAG-mCherry protein expressed in HEK293T cells visualized by fluorescence microscopy. The expression of FLAG-mCherry in the transfected HEK293T cells was determined at 24 h.p.t. Cells transfected with pLVX-Puro vector and only transfection reagent served as negative and mock control, respectively.

### 5.5.2 Confirmation of direct interaction between EV-A71 3A and PRSS3 protein interaction by co-immunoprecipitation assay

Scale of expression of each protein was adjusted according to its level of expression in HEK293T cells. Total proteins of each sample were measured and loaded at the highest volume capacity per well for western blot analysis. Cell lysate of FLAG-mCherry was loaded 10  $\mu$ g per well, while FLAG-3A-mCherry and FL-PRSS-Myc were loaded 30  $\mu$ g per well. Detection of FLAG fusion proteins using anti-FLAG antibody showed that the band of FLAG-mCherry appeared at its molecular weight (28 kDa). FLAG-3A-mCherry appeared as doublet bands with approximately 26-27 kDa which were lower than its molecular weight (38 kDa). Meanwhile, FL-PRSS3-Myc detected by anti-cMyc antibody appeared at correct molecular weight (29.5 kDa) (**Figure 5.42**). Using this adjusted scale of expression, amounts of target proteins were roughly fair to be used for co-immunoprecipitation.

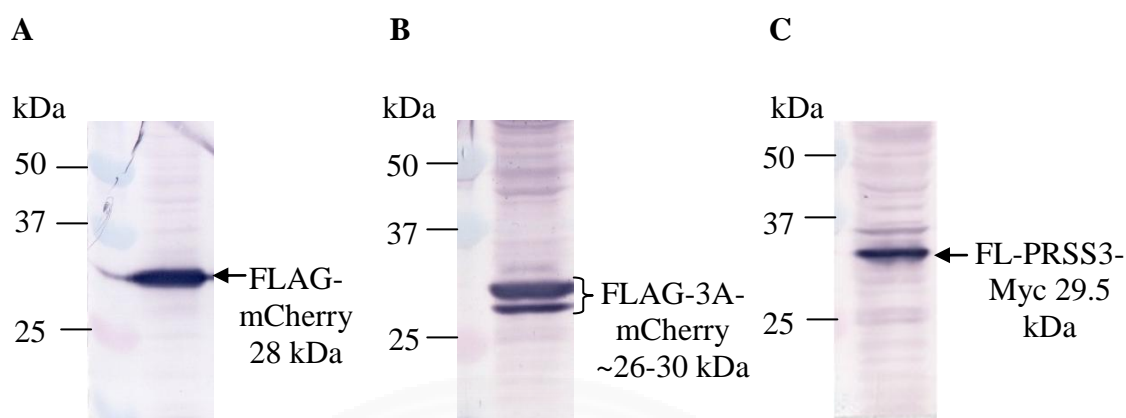
Firstly, to examine specific binding of anti-Myc magnetic beads to Myc tagged protein, cell lysates prepared from untransfected HEK293T cells and pLVX::*FL-PRSS3-Myc*-transfected cells were incubated with the beads. As a result of elution by SDS sample buffer and boiling, the mouse anti-Myc antibody captured on the beads (as shown only 25 kDa light chain) was also co-eluted and detected by secondary antibody goat anti-mouse IgG labeled with alkaline phosphatase (AP) in immunoblotting. It was showed that there was some protein background in

untransfected cell fractions (**Figure 5.43A**) while in PRSS3-Myc protein fractions, the PRSS3-Myc could be detected in eluate at correct relative molecular size (29.5 kDa) (**Figure 5.43B**), suggesting specific binding of the beads.

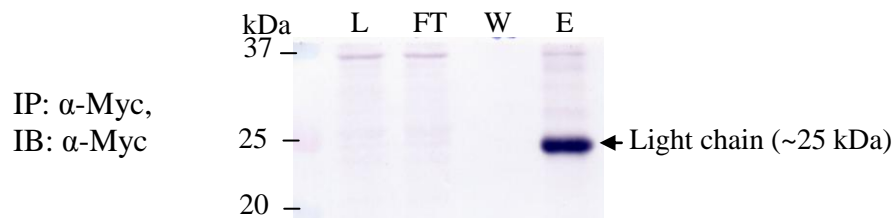
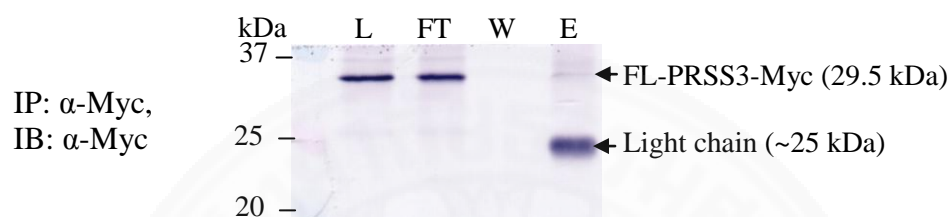
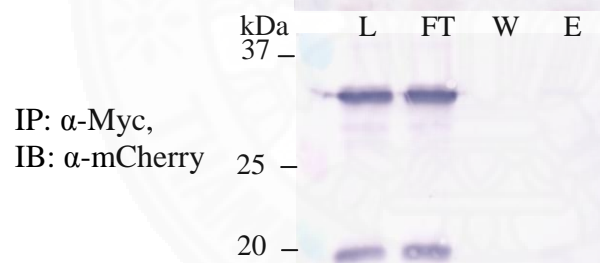
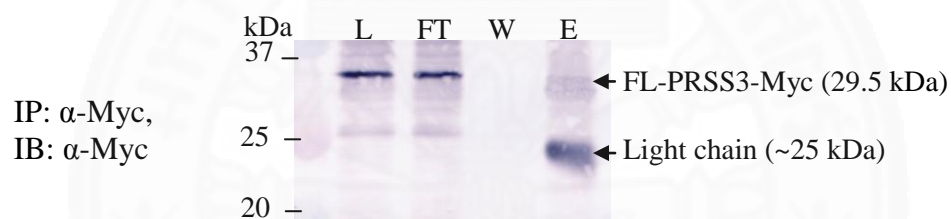
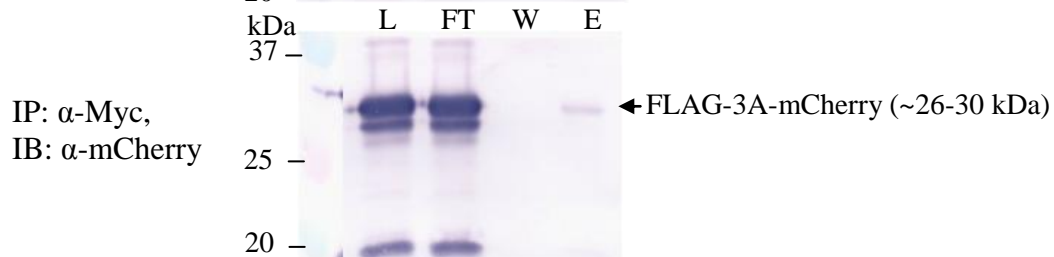
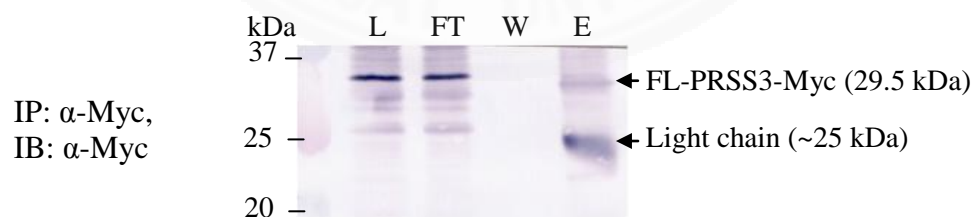
To confirm interaction of EV-A71 3A and PRSS3 proteins, immunoprecipitation reactions were done at 1:1 protein-protein amount ratio and mixed with anti-Myc magnetic beads. The eluate fractions were resolved by 12% SDS-PAGE and the target proteins were examined by western blot analysis using rabbit anti-mCherry antibody. It was found that only the FLAG-3A-mCherry (~26-30 kDa), but not FLAG-mCherry, was co-purified with FL-PRSS3-Myc protein as it was detected in the eluted fraction, suggesting specifically physical interaction of the proteins (**Figure 5.43C and D**). It has been definitely confirmed that the EV-A71 3A protein directly interacts with PRSS3 variant 3 protein in the human SH-SY5Y neuronal cells. The direct protein-protein interaction suggesting the essential role of the PRSS3 protein in viral replication.







**Figure 5.42** Western blot analysis of FLAG-mCherry (A), FLAG-3A-mCherry (B), and FL-PRSS3-Myc (C) expressed in HEK293T cells. FLAG-mCherry (molecular weight = 28 kDa) and FLAG-3A-mCherry proteins (molecular weight = 38 kDa, migratory size ~ 26-30 kDa) were immunoblotted with mouse monoclonal anti-FLAG<sup>®</sup> M2 antibody. FL-PRSS3-Myc protein (molecular weight = 29.5 kDa) was immunoblotted with mouse monoclonal anti-cMyc antibody. The bands of target protein were indicated by arrows or bracket. The molecular mass markers (in kilodaltons, kDa) are indicated to the left of the membranes.

**A; Cell lysates prepared from HEK293T cells****B; FL-PRSS3-Myc****C; FL-PRSS3-Myc + FLAG-mCherry****D; FL-PRSS3-Myc + FLAG-3A-mCherry**

(See figure legend on next page)

**Figure 5.43** Co-immunoprecipitation (IP) assay for determining direct protein-protein interaction of FLAG-3A-mCherry and FL-PRSS3-Myc. The FLAG-mCherry served as irrelevant interacting protein. The protein complex was precipitated (IP) by mouse anti-Myc magnetic beads ( $\alpha$ -Myc) and the eluted proteins were detected by western blot analysis (IB) using either  $\alpha$ -Myc or rabbit anti-mCherry polyclonal antibody ( $\alpha$ -mCherry). M; protein standard marker, L; cell lysates, FT, flow-through fractions, W; wash fractions, E; eluate fractions.

### 5.6 Role of PRSS3 in EV-A71 replication

Prior to use in the subsequent experiments, permissiveness of HEK293T cells to EV-A71 infection was tested in comparison to those of RD cells using CCID50 method. With EV-A71 viral stock starting at  $10^{6.125}$  CCID50/100  $\mu$ L, it was found testing in RD cells was corresponding to the titer of the stock while testing in HEK293T cells gave  $10^{4.24}$  CCID50/100ul (**Figure 5.44**). As a result, HEK293T cells are permissive to EV-A71 infection, but less strongly than tested in RD cells approximately 100 times. When RD cells require MOI 0.1 for infection, therefore, EV-A71 at MOI 10 was used for infecting HEK293T cells. It could be suggested that HEK293T cells were suitable for studying role of PRSS3 in EV-A71 replication.

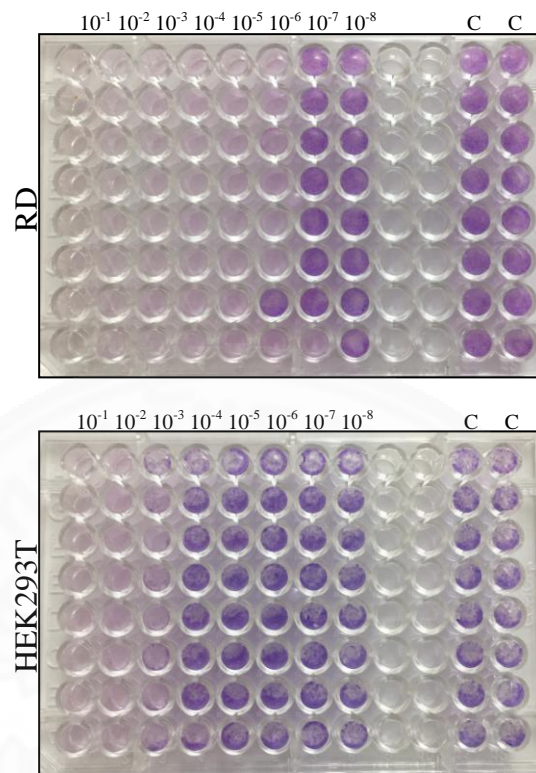


**Figure 5.44** Determination of permissiveness of HEK293T cells to EV-A71 infection by comparing CCID50 with those of RD cells. Dilutions of the tested EV-A71 viral stock ( $10^{-1}$  to  $10^{-8}$ ) were indicated above each row of 96-well plate. Monolayer cells were stained with Giemsa dye. Wells with cell detachment showing clear well or less stained cells were positive for CPE. C; Cell control.

Over-expression of recombinant PRSS3 protein in EV-A71-infected HEK293T cells caused a nearly 2-fold increase in viral RNA replication which was significantly different from the pLVX-transfected- and untransfected cells (**Figure 5.45**) while viral RNA replication in pLVX-transfected HEK293T cells was not significantly different from the untransfected cells. It was concluded that overexpression the neuron-derived PRSS3 could enhance EV-A71 replication.

Since endogenous PRSS3 has very low level of expression in HEK293T cells (**Figure 5.24**). First, to determine if it could be silenced by siRNA. HEK293T cells were transfected with either three-pooled siRNAs targeting *PRSS3* (siPRSS3) or siGAPDH which was served as control for siRNA transfection and irrelevant gene knockdown for EV-A71 infection. It was found that silencing of *PRSS3* (**Figure 5.46A**) and *GAPDH* (**Figure 5.46B**) using siRNA was successful. Next, to assess the role of PRSS3 in EV-A71 replication, HEK293T cells were transfected with siPRSS3 or siGAPDH followed by EV-A71 infection at MOI 10. It was found that knockdown of *GAPDH* did not significantly affect EV-A71 replication while *PRSS3* knockdown resulted in reduction of EV-A71 RNA (**Figure 5.46C, D and E**). EV-A71 proteins from the same samples were also detected by western blot analysis using anti-EV71 antibody which is specific to viral capsid protein VP0 and VP2 which is the cleaved form of the VP0. It was found that detection of EV-A71 proteins confirmed the decrease of EV-A71 production (**Figure 5.46F**). Using Image lab program to estimate protein intensity of VP0 showed that the protein in PRSS3 knockdown sample was lesser than EV71-infected and EV71-infected siGAPDH-treated cells for 4.5 and 5 times, respectively. Thus, silencing of *PRSS3* resulting in reduction of EV-A71 replication.

Taken together, it could be concluded that the EV-A71 3A protein directly interacts with PRSS3 variant 3 protein in human neuronal cells and the PRSS3 plays essential role in the EV-A71 replication.

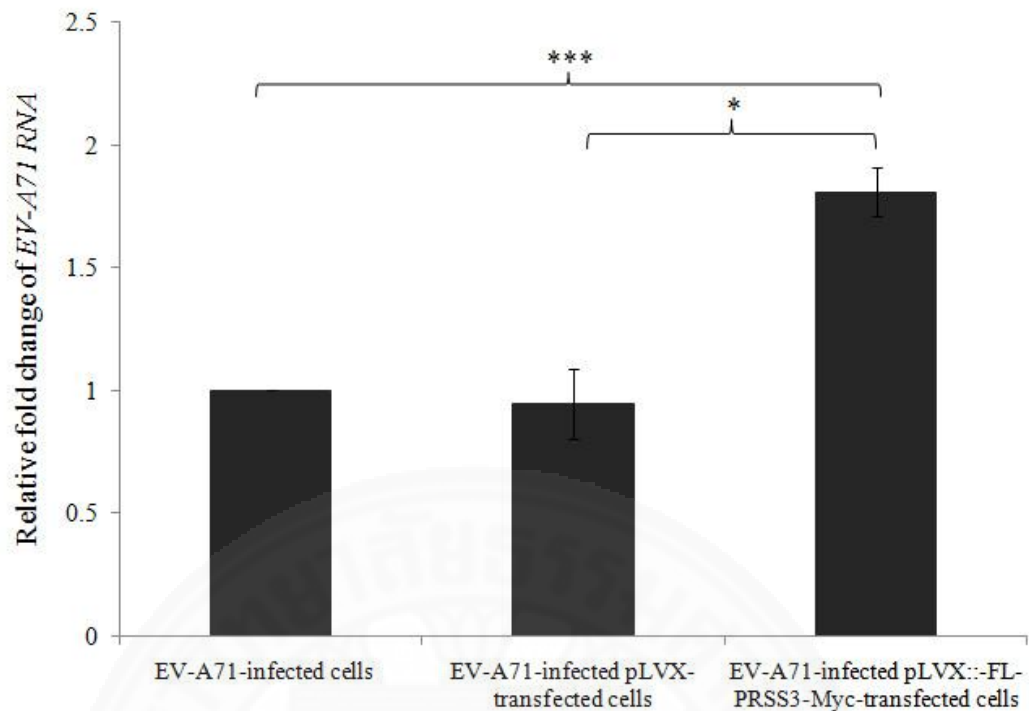
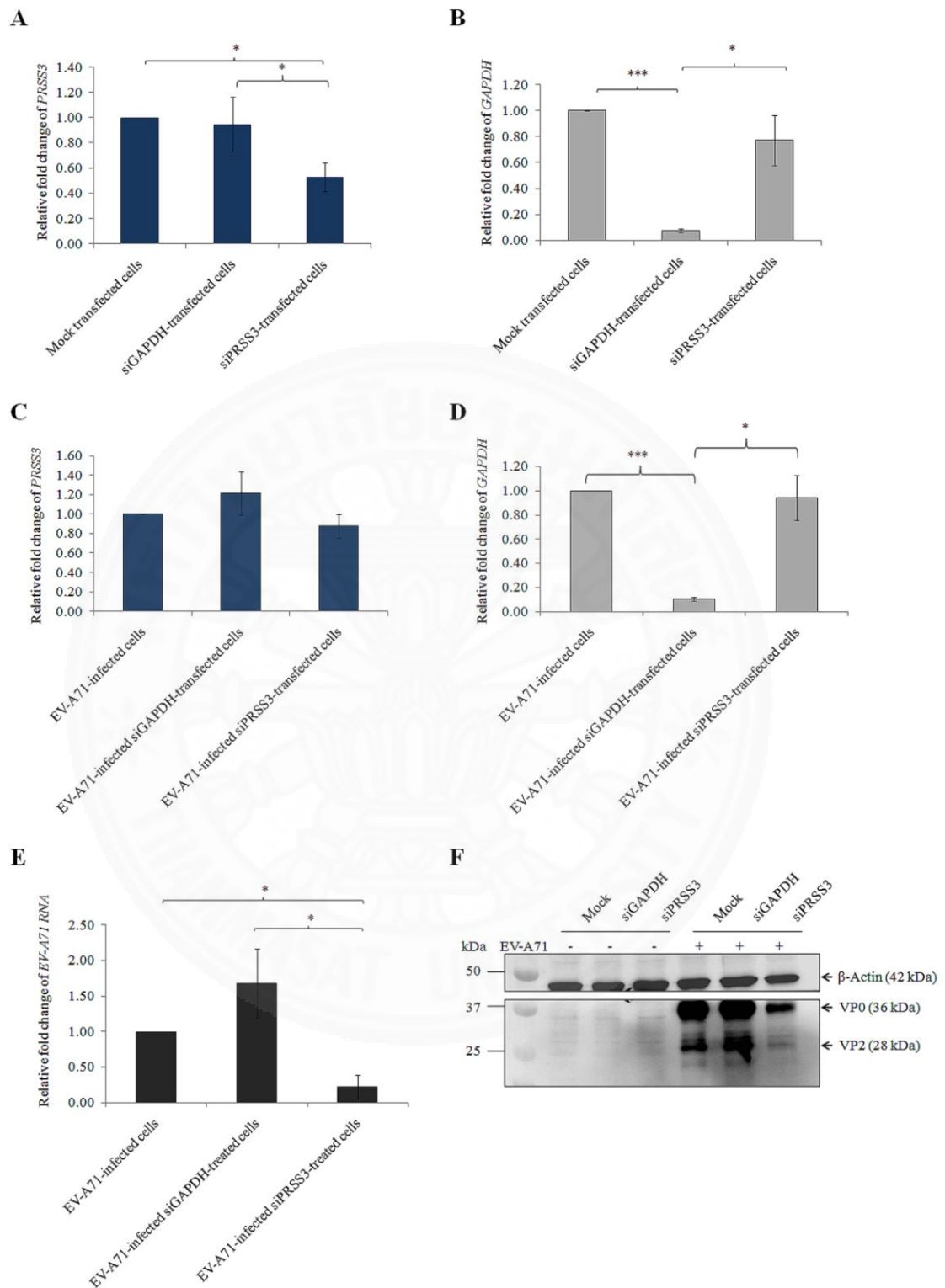


**Figure 5.45** Determination of relative fold-change of *EV-A71 RNA* copy number by semi-quantitative real-time RT-PCR in response to overexpression of neuron-derived PRSS3 in pLVX::*FL-PRSS3-Myc*-transfected HEK293T cells. The pLVX::*FL-PRSS3-Myc*-transfected HEK293T cells infected with EV-A71 was designated as EV-A71-infected pLVX::*FL-PRSS3-Myc*-transfected cells. Mock transfected and pLVX-transfected HEK293T cells infected with EV-A71 served as infection control and empty vector control, respectively. Data were expressed by mean  $\pm$  SD from three independent experiments in triplicate measurements (N=9). Statistical analysis was done by One-way ANOVA with post-hoc tests. Level of statistically significant difference at  $p < 0.05$  and  $p < 0.001$  was indicated by \* and \*\*\*, respectively.



(See figure legend on next page)



**Figure 5.46** Determination of relative fold-change of *EV-A71 RNA* copy number by semi-quantitative real-time RT-PCR in response to the knockdown of *PRSS3*. The siPRSS3-transfected HEK293T cells infected with EV-A71 were designated as EV-A71-infected siPRSS3-treated cells. Fold-change of gene expression of *PRSS3* (**A**), *GAPDH* (**B**) in the siRNAs-transfected non-infected cells was relative to mock transfected non-infected cells. Determination of *PRSS3* (**C**) and *GAPDH* (**D**) expression in EV-A71-infected siRNAs transfected cells. Determination of EV-A71 RNA in EV-A71-infected siRNAs transfected cells (**E**). Western blot analysis for EV-A71 and  $\beta$ -Actin (**F**). EV-A71 proteins detected by anti-EV-A71 antibody are VP0 (MW=36 kDa) and VP2 (MW = 28 kDa). MW of  $\beta$ -Actin = 42 kDa. Data were expressed by mean  $\pm$  SD from three independent experiments in triplicate measurements (N=9). Statistical analysis was done by One-way ANOVA with post-hoc tests. Level of statistically significant difference at  $p < 0.05$  and  $p < 0.001$  was indicated by \* and \*\*\*, respectively.

## CHAPTER 6

### DISCUSSION

Enterovirus A71 (EV-A71) infection can culminate in neurological complications such as meningitis, acute flaccid paralysis, neurologic cardiopulmonary failure and even death.<sup>18</sup> So far, there is no specific treatment or vaccine for EV-A71 infection. Understanding viral neuropathogenesis might provide more strategies to prevent or mitigate deleterious effects from the virus.

Enterovirus nonstructural proteins; 2B-2C, and 3A-3D, play several roles in viral replication cycle. To establish successful infection, the virus has to produce a number of viral progenies throughout time of infection, and at the same time, virus has to evade or protect itself from recognition by intracellular immune sensing. Enterovirus has evolved strategies to survive in host cell by reorganizing host cellular proteins and lipids to build up platforms for negative-sense viral RNA (vRNA) synthesis and viral assembly termed as replication complexes (RCs) or replication organelles (ROs). It has been reported that enterovirus nonstructural 3A protein (3A) is the key player who mediates the RO formation.<sup>24, 25, 69</sup> The virally modified platforms were reported to promote vRNA replication by concentrating the co-opted host factors and viral proteins, and providing the proper milieu for vRNA synthesis. Moreover, ROs are served as shelter protecting the double-stranded RNA intermediate from host immune detection. It seems like composition of ROs is diverse depending on host organelle donor, preferential location of RO formation, and host cell that the virus infects. It was reported that enterovirus ROs are originated from ER followed by *trans*-Golgi network upon infection.<sup>110</sup>

To date, neuropathogenesis of enterovirus A71 is poorly understood. The role of EV-A71 3A protein in infected neuronal cells remains unknown. Since 3A protein plays role in RO formation, investigating its interacting counterpart would provide more understanding about viral replication in neuronal cells and the promising host candidate to be a target for generation of EV-A71 specific treatment and development of biomarker for prognosis.

## 6.1 The use of human SH-SY5Y neuroblastoma and HEK293T cells as models in CNS-associated EV-A71 infection

EV-A71 infection causes hand, foot, and mouth disease (HFMD) implicated with serious neurological complications such as meningitis, encephalitis, etc. Detection of EV-A71 antigens and RNA in CNS tissue sections from EV-A71-induced encephalitis patients showed exclusive localization of the virus in neuronal cells at the inflamed areas consisting of spinal cord, medulla, pons, midbrain, hypothalamus, dentate nucleus area of cerebellum, and motor cortex.<sup>111</sup> The finding of localization of EV-A71 in human neuronal cells was corresponding to the studies in animal models.<sup>112, 113</sup> To scrutinize EV-A71 neuropathogenesis, the *in vitro* study conducted in neuronal cells has been developed. Even though the use of primary cells derived from CNS tissues might provide an accurate recapitulation of the neuronal cell properties *in vivo*. The isolation and culture of the primary cells is challenging. The ethical approval is also required. In addition, primary cells are generally known as difficult-to-transfect cells. To overcome the limitations, human neuroblastoma cell lines have been used not only for studying neurological disorders but also for neurotropic virus infection. Two commonly used neuronal-like cell lines are SH-SY5Y and SK-N-MC (also known as HTB-10). Human SH-SY5Y is a thrice-subcloned cell line derived from the parental SK-N-SH neuroblastoma cell line originated from metastatic cells in bone marrow, while SK-N-MC neuroepithelioma is originated from supra-orbital region. Determination of the neuronal cell marker genes by RNA-sequencing in these two cell lines showed higher expression level of the genes in SH-SY5Y than SK-N-MC, indicating high neuronal-like properties of SH-SY5Y.<sup>114</sup> Human SH-SY5Y cells have been used in many studies in both neurodegenerative diseases such as Parkinson's disease, and neurotropic virus infection such as enterovirus A71 (EV-A71), enterovirus D68 (EV-D68), poliovirus, rabies virus, japanese encephalitis virus (JEV), zika virus (ZIKV), dengue virus (DENV), and herpes simplex virus.<sup>107, 114-129</sup> Even though SK-N-MC was also used in the viral study and it has been reported that both SH-SY5Y and SK-N-MC cells express SCARB2, the entry receptor for EV-A71.<sup>123</sup> In this study, it was found that only SH-SY5Y cells are permissive to EV-A71 infection determined by CCID50

method, thus, suitable for studying *in vitro* interaction between human neuronal cells and EV-A71. However, human SH-SY5Y cells still have limitation in some aspects in which the cells have low transfection efficiency. To solve this problem in transfection-based experiments including studying role of PRSS3, the identified 3A-interacting protein, in EV-A71 replication, by gain-of-function experiment i.e. determination of EV-A71 replication in response to overexpression of recombinant PRSS3 protein and loss-of-function experiment i.e. determination of EV-A71 replication in response to PRSS3 gene knockdown using siRNA, HEK293T cells which is one of twelve tribes of HEK293 cell line were used as model instead. It has been reported that the HEK293 cell line harbors multitude of immature neuronal cell-specific genes as a consequence of transformation by adenovirus.<sup>130, 131</sup> In addition, HEK293T cells are permissive to EV-A71 infection. Taken together, SH-SY5Y and HEK293T cells were eligible for studying role of EV-A71 3A and its interacting counterpart in EV-A71 replication.

## 6.2 Molecular cloning of EV-A71 nonstructural 3A coding sequence

Nonstructural 3A proteins are conserved among enteroviruses. It was found that the cloned EV-A71 3A protein in this study showed high nucleotide sequence identity not only among the strains (97.67% to 100% identity) but also across members in genus *Enterovirus* such as coxsackievirus A2 (98% identity), A10 (100% identity), and A16 (100% identity) (**Figure 5.5**). All of them are etiological agents of hand, foot, and mouth disease similar to the EV-A71. However, the information about structure and function of the enteroviral 3A proteins are still limited. Hence, in this study, the finding of cellular factors interacting with the EV-A71 3A protein would be beneficial for further investigations on biological functions and structural biology as well as host cellular and molecular pathways involved. The data gained from this thesis research could be applicable to the closely related enteroviruses.

Recombinant EV-A71 3A protein was produced as a bait aiming to study the role and the counterparts in human neuronal cells using pull-down assay. At present, there is no antibody specific to EV-A71 3A protein commercially available.

Therefore, FLAG epitope tag which is one of the protein tags that commonly used was N-terminally fused to the 3A protein, generating FLAG-3A, to facilitate immunoprecipitation using anti-FLAG<sup>®</sup> M2 magnetic beads. However, it was found that FLAG-3A protein could only be expressed in HEK293T cells; the effective cells for transfection and mammalian expression system, but not our target cell of study which is human neuronal SH-SY5Y cells (**Figure 5.11**). Fusion of the viral nonstructural proteins with fluorescent protein tags at N- or C-terminal ends were demonstrated in several studies. It was shown that fusion with fluorescent proteins did not only benefit protein detection, but also improved level of protein expression in mammalian cell. Moreover, it did not interfere the biological functions of the proteins.<sup>107</sup> Thus, EV-A71 3A protein was N-terminally fused with FLAG tag and C-terminally fused with mammalian codon optimized red fluorescent mCherry protein. It was found that FLAG-3A-mCherry protein could be expressed in both HEK293T and SH-SY5Y cells (**Figure 5.20**). By using Lipofectamine<sup>™</sup> 3000 reagent, transfection efficiencies suggested by manufacturer for HEK293T and SH-SY5Y cells yield >80 % and <30 %, respectively. In our study, it was found that transfection efficiency of HEK293T was as suggested, but of SH-SY5Y cells was only 4% (**data not shown**) as determined by flow cytometry. Anyway, this problem could be overcome by increasing numbers of duplicate transfected cells and employing a highly sensitive assay or instruments to measure the outputs of the assays experimented with the 3A protein. Therefore, the FLAG-3A-mCherry protein produced in SH-SY5Y which was comparable to quantity expressed in HEK293T cells as determined by western blot analysis was sufficient (**Figure 5.21**). Interestingly, migration of FLAG-3A-mCherry protein in SDS-PAGE did not correlate to its formula molecular weight which is 38 kDa but appeared at approximately 26-30 kDa with 2-3 distinct bands. The causes of anomalous migration of FLAG-3A-mCherry in SDS-PAGE were discussed; (i) degradation of the protein in preparation; the transfected cells were lysed by ice-cold 1× lysis buffer supplemented with 1× protease inhibitor cocktail and subjected to brief ultrasonication to complete cell lysis. The cell lysate was then collected by high-speed centrifugation at 4 °C, before storing at -20 °C for a few days prior to western blot analysis. The same pattern of relative migration of FLAG-3A-mCherry was detected by both monoclonal

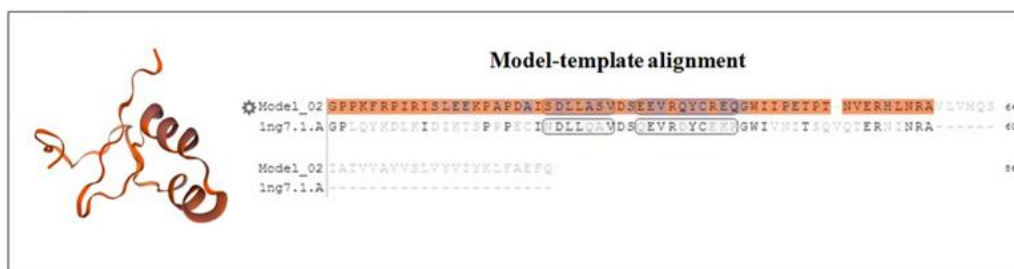
anti-FLAG antibody and polyclonal anti-mCherry antibody suggesting no degradation. Thus, gel shifting of FLAG-3A-mCherry might not be caused by protein preparation. (ii) interaction of EV-A71 3A and human trypsinogen PRSS3 protein; even though PRSS3 is a proactive form of trypsin, autoactivation of human trypsinogen has been reported.<sup>132, 133</sup> Cleavage sites of trypsin on recombinant FLAG-3A-mCherry were predicted using PeptideCutter program (<https://www.expasy.org/resources/peptidecutter>). It was found that there are 39 cleavage sites on FLAG-3A-mCherry sequence generating a number of small fragments which none of them corresponds to the apparent molecular weight in SDS-PAGE (**Appendix G**). However, *in vitro* analysis is required to confirm proteolytic reaction. (iii) anomalous migration of membrane protein; it has been reported that helical membrane protein can cause anomalous SDS-PAGE migration or gel shifting as a result of altered SDS loading at hydrophobic region. The proteins tested showed gel shift ranging from -46% (migration faster than molecular weight) to +48% (migration slower than molecular weight).<sup>134</sup> By BLASTx analysis, conserved domain analysis, and sequence alignment, it was found that EV-A71 3A is 86 amino acids long and has structure homology to poliovirus 3A protein-like domain or P3A (accession number pfam08727). The EV-A 71 3A protein was predicted for containing soluble N-terminal domain, hydrophobic C-terminal domain, and additional residues which located at amino acid residues 1-58, 59-80, and 81-85, respectively (**Figure 5.6C**). Hence, the aberrant electrophoretic mobility of the FLAG-3A-mCherry in SDS-PAGE seemed to be result of altered SDS loading at hydrophobic region of the 3A molecule. It was reported that the structure of P3A (also known as 3A-N) determined by NMR spectroscopy consists of 2 alpha-helices spanning at residues 23-29 and 32-41 spaced with loop bending 180° to form a helical hairpin. Molecular modeling of the cloned EV-A71 3A protein by Swiss-Model demonstrated that it could be modeled with P3A accession number 1NG7. The model of secondary structure of the cloned EV-A 71 3A protein was predicted to contain two amphipathic alpha-helices at amino acid positions 22-28 and 31-40 on the EV-A71 3A, respectively (**Figure 6.1A**). It has been reported that the N-terminal region of enteroviral 3A protein is involved with biological function and interaction while C-terminal hydrophobic region is responsible for membrane anchoring. Poliovirus 3A



was reported to exist as homodimer (**Figure 6.1B**).<sup>26, 135</sup> In this study, recombinant EV-A71 3A protein was fused with FLAG at N-terminus and with mCherry at C-terminus producing the larger molecular size of the protein (~38kDa), yet, the migration of the protein showed faster than its molecular weight (~26-30 kDa) while FLAG-mCherry was appeared at correct molecular size. Detection of 3A protein from poliovirus-infected cells showed the band size ~10 kDa according to its formula molecular weight.<sup>136</sup> Additionally, in spite of without mentioning about relative molecular weight in SDS-PAGE migration of recombinant EV-A71 3A fused with green fluorescent protein (GFP) expressed by 293T cells, it was showed that the band of EV-A71 3A-GFP appeared slightly higher than GFP (28 kDa), suggesting increasing of molecular size by protein fusion.<sup>137</sup> Even though the 3A-GFP and FLAG-mCherry showed no changes in migration, fusion of EV-A71 3A with FLAG and mCherry causes alteration of SDS loading leading to anomalous SDS-PAGE migration is still questioning. (iv) post-translational modifications (PTMs); some EV-A71 proteins were modified upon viral infection such as SUMOylation of 3D<sup>pol</sup> RNA-dependent RNA polymerase (RdRp) to facilitate viral replication, myristoylation of VP4 to increase infectivity and membrane interaction.<sup>105, 138</sup> These modifications showed increase in molecular weight of the proteins resolved in SDS-PAGE. Even though myristoylation was found in 3A proteins of Aichi virus and kobuvirus, EV-A71 3A was predicted as non-myristylated protein. And, so far, there is no report of any modification of enterovirus 3A. Thus, PTMs might not be the cause of anomalous migration. Collectively, production of FLAG-3A-mCherry protein in human SH-SY5Y neuronal cells was successful and could be subsequently studied its interacting counterparts, and the causes of anomalous SDS-PAGE migration of FLAG-3A-mCherry is required elucidation.



A



B

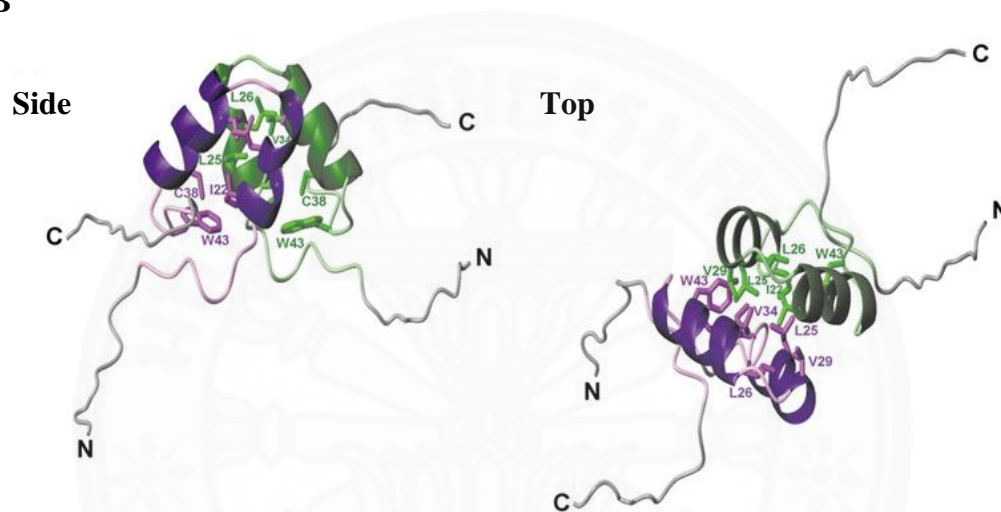


**Figure 6.1** Prediction of EV-A71 3A protein structure compared to the poliovirus 3A-N.<sup>26</sup> Amino acids 1-58 of EV-A71 3A (orange shaded residues) were modeled with core protein P3A accession 1NG7 (PDB 1ng7.1.A). Two amphipathic alpha-helices were predicted at amino acid positions 22-28 and 31-40 on the EV-A71 3A, respectively (orange shaded residues indicated by boxes) (A). The ribbon diagram of P3A structure in homodimer form viewed from top side and top (B). One monomer is shown in purple while another is shown in green. N; N-terminus. C; C-terminus.

### 6.3 pull-down and protein identification by liquid chromatography with tandem mass spectrometry (LC-MS/MS) and analysis

FLAG-3A-mCherry protein was used as a bait for fishing out the cellular proteins that directly interact with EV-A71 3A protein by anti-FLAG<sup>®</sup> M2 magnetic beads. The eluates from FLAG pull-down were resolved in 12% SDS-PAGE compared to the protein background controls including cell lysate prepared from

untransfected SH-SY5Y cells, cell lysate prepared from pLV-mCherry-transfected SH-SY5Y cells, and washing fraction. The gel was stained with colloidal Coomassie brilliant blue and counterstained with silver solution to enhance the sensitivity. In **Figure 5.22**, five differential protein bands presented in eluates of FLAG pull-down, compared to the controls, were selected and estimated for molecular weight using Gene Tools program. The estimated molecular weights were 22-26 kDa (data not shown). Then, the selected protein bands were excised and subjected to trypsin digestion and protein identification by LC-MS/MS. It was found that the potentially identified proteins at 95% confidence were human trypsinogens (PRSS1 and PRSS3), putative protein N-methyltransferase FAM86B1, and proteasome subunit alpha type-7. Human trypsinogens were detected in all selected bands. It might be due to degradation of the proteins, cleavage of trypsinogen transforming to mature trypsin, or various band sizes resulting from reducing condition. Based on Mascot scores and the estimated molecular weight, human trypsinogens (PRSS1 and PRSS3) were in our interest. It has been reported that cationic trypsinogen (PRSS1) was identified from human glioblastoma cell line T98G as one of the cellular proteins that were associated with EV-A71 IRES.<sup>109</sup> Moreover, PRSS3 plays a role in cell entry of influenza A virus.<sup>103</sup> Since PRSS1 and PRSS3 shows high sequence homology as analyzed by sequence alignment (**Figure 5.23**). Therefore, the generated peptide sequences by LC-MS/MS shown in **Table 5.2**, were interpreted as PRSS1 and PRSS3 proteins. Thus, human trypsinogens were further characterized in subsequent experiments.

To elucidate which isoform of the PRSS that was likely to be EV-A71 3A-interacting protein in SH-SY5Y cells. Expression profiles of human *PRSS* genes consisting of *PRSS1*, *PRSS2* and *PRSS3* were determined in SH-SY5Y cells compared to HEK293T cells which were shown to express all 3 isoforms serving as positive control.<sup>103</sup> It was found that the *PRSS3* was conclusively expressed in the SH-SY5Y cells (**Figure 5.24**). The result was confirmed by detecting endogenous PRSS3 protein by fluorescence microscopy using PRSS3 specific antibody (**Figure 5.25**). Expression of PRSS3 has been reported in pancreas and brain, and also known as human mesotrypsinogen or brain trypsinogen.<sup>139</sup> It contains 4 transcript variants that encode for N-terminally different sub-isoforms. Thus, full-length cDNA of each

transcript variant of *PRSS3* was determined in SH-SY5Y cells. Only *PRSS3* transcript variant 3 (*PRSS3-v3*) were able to be amplified by RT-PCR (**Figure 5.26**). The nucleotide sequence was also verified by DNA sequencing and bioinformatic analysis (**Figure 5.28 and 5.29**). To confirm direct interaction of EV-A71 3A and *PRSS3* proteins by co-immunoprecipitation assay, the nucleotide sequence of *PRSS3-v3* derived from SH-SY5Y cells were cloned by fusion with Myc tag at C-terminus (as named FL-*PRSS3*-Myc) and expressed in HEK293T cells. Cell lysate of FL-*PRSS3*-Myc was incubated with cell lysate of FLAG-3A-mCherry or FLAG-mCherry which served as irrelevant interacting protein control at 1:1 amount protein-protein ratio, and precipitated by anti-Myc magnetic beads. It was found that only FLAG-3A-mCherry, but not FLAG-mCherry, was co-precipitated with FL-*PRSS3*-Myc confirming specifically direct interaction of EV-A71 3A and *PRSS3* proteins (**Figure 5.43**). It was confirmed that *PRSS3* variant 3 was neuronal-specific interacting protein of EV-A71 3A protein.

#### 6.4 Role of *PRSS3* in EV-A71 replication

Positive-sense RNA (+RNA) viruses have intriguing strategies for establishing viral replication by reorganizing intracellular membrane to serve as platforms for viral RNA synthesis, viral assembly, and also shielding virus products from host immune recognition. The platforms are termed as replication complexes (RCs) or replication organelles (ROs). Enteroviruses, the +RNA viruses in the *Picornaviridae* family, use viral nonstructural 3A proteins to recruit cellular proteins and lipids to generate efficient milieu for viral replication upon time of infection. It has been reported that membrane donor organelles utilized by enteroviruses for RO formation are ER and *trans*-Golgi network.<sup>110</sup> To maintain RO biogenesis, host proteins, and lipids might be recruited independently and differentially upon stages of infection. In this study, it was found that EV-A71 3A protein had direct interaction with *PRSS3* (**Figure 5.43**) suggesting that the 3A protein might recruit this host cellular protein to serve some aspects in viral replication in human neuronal cells. Due to low transfection efficiency of SH-SY5Y cells, the role of neuron cell-derived *PRSS3* in EV-A71 replication was subsequently studied in the susceptible HEK293T

cells. Overexpression of neuronal cell-derived recombinant PRSS3 variant 3 resulted in nearly 2-fold increase in EV-A71 RNA production in the infected HEK293T cells relative to the infected mock cells (**Figure 5.45**). The involvement of PRSS3 in RNA replication was confirmed by *PRSS3* gene knockdown using siRNA. It was shown that transient silencing of *PRSS3* significantly caused reduction of EV-71 production (**Figure 5.46**).

Trypsinogen is a proactive precursor of trypsin which is one of the important serine proteases. Characterized by isoelectric points (pI), human trypsinogens have been classified into 3 major isoforms; PRSS1 (cationic trypsinogen), PRSS2 (anionic trypsinogen), and PRSS3 (mesotrypsinogen). They were initially isolated from human pancreatic juice.<sup>140</sup> Later, it was found that trypsinogens are also expressed in several tissues as well as central nervous system (CNS).<sup>139,141</sup> There is an increasing body of evidence that human trypsinogens are implicated with virus infection e.g. human PRSS1 (cationic trypsinogen) is one of the EV-A71 IRES-associated proteins in human glioblastoma T98G cells, cleavage of hemagglutinin (HA) by activated human trypsinogen (PRSS3) enhanced influenza A virus infection.<sup>103, 109</sup> As the function of viral 3A is to recruit host cellular proteins or lipids to generate replication organelles (ROs), the interacting counterparts of 3A might provide some benefits for viral replication. One of the reported 3A-interacting partners is cholesterol which regulates membrane-dependent polyprotein processing of viral 3CD protease and facilitates viral replication.<sup>25</sup> Even though virus has its own proteases, it has been found that calpains, the host cellular papain-like cysteine proteases which are expressed as proenzyme in cytoplasm and activated by an increasing of intracellular  $Ca^{2+}$ , could cleave polyprotein of enterovirus B at VP3-VP1 interface *in vitro*.<sup>142</sup> And despite being proactive enzyme, autoactivation of trypsinogens was reported in PRSS1 and PRSS2.<sup>132, 133</sup> The trypsin cleavage sites of the PRSS on the amino acid sequence of EV-A71 polyprotein were predicted by PeptideCutter program (**Appendix G**). It was shown that there are tentative 194 trypsin cleavage sites on the EV-A71 polyprotein. Interestingly, the predicted trypsin cleavage site at position 69 was corresponded to VP4-VP2 junction, so-called VP0 cleavage site.<sup>143</sup> In viral assembly, viral capsid precursor P1 is primarily cleaved by viral 3CD<sup>pro</sup> into VP0, VP1 and VP3 which are assembled into 5S protomer, then five

protomers are combined to form 14S pentamer. The viral  $2C^{ATPase}$  then recruits 14S pentamers to replication organelles (ROs). To achieve virion maturation, the VP0 is cleaved into VP2 and VP4 changing the capsid conformation. In EV-A71 study, it has been found that  $2A^{pro}$  and  $3C^{pro}$  proteins are not participated in VP0 cleavage.<sup>143</sup> So far, the speculated mechanism of cleavage of VP0 is RNA-dependent autocatalytic action. Since viral proteases also play important roles at ROs to facilitate viral replication, cleavage sites of both EV-A71 proteases;  $2A^{pro}$  and  $3C^{pro}$ , on the 3A-interacting PRSS3 protein were evaluated. It was found that there are one cleavage site of  $2A^{pro}$  at amino acid position 164 and two cleavage sites of  $3C^{pro}$  at position 182 and 225 (**Appendix G**). Thus, it could be postulated that PRSS3 are recruited to ROs by EV-A71 3A protein might be cleaved by the viral proteases to get maturation and then turn to facilitate viral replication. At the ROs, the mature PRSS3 might be involved with membrane-dependent viral polyprotein processing or maturation of viral assembly by cleavage of VP0 to facilitate viral replication. These notions and postulated mechanism of PRSS3 facilitate the EV-A71 replication remains to decipher.

Serine proteases are involved in many biological processes such as proteolytic processing of the protein, food digestion, signal transduction, and immune response.<sup>144</sup> In the CNS, it has been reported that serine proteases are widely expressed and play diverse roles including structural plasticity, neural development, regulation of neuronal survival, neurodegeneration, and neuroregeneration.<sup>145–148</sup> For brain trypsinogens, the study in rat tissue model showed that PRSS2 (anionic trypsinogen) secreted by activated microglial cells promotes generation of white matter neurons.<sup>149</sup> Trypsinogens function as a signaling agent by cleaving extracellular N-terminus of protease-activated receptors (PARs) resulting in activation of signal cascades via MAPK/ERK pathway leading to promotion of cell growth and survival. In addition, it has been reported that treatment of primary neuronal cells with trypsin renders the protective effect against glutamate excitotoxicity.<sup>150</sup> Hence, trypsinogens exert crucially physiological functions in CNS. Trypsinogens are secreted proteins, thus, destined to be transported via cellular secretory pathway. In this study, the interaction of PRSS3 trypsinogen with EV-71 3A might cause retention of the protein at viral replication organelles (ROs). Importantly, one of the

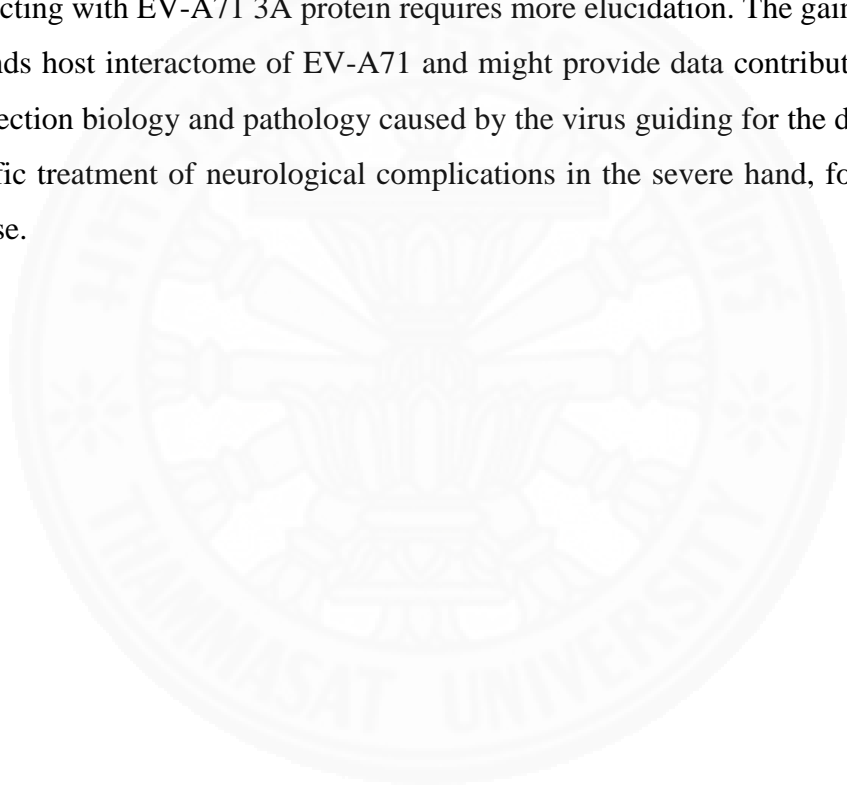
pathological features of neurodegenerative diseases such as Alzheimer's disease (AD), Amyotrophic lateral sclerosis (ALS), and Parkinson's disease (PD) is intracellular protein toxicity caused by accumulation or mislocalization of the toxic protein.<sup>151–153</sup> Therefore, retention of PRSS3 trypsinogen in human neuronal cells might be one of pathological mechanisms in EV-A71 infection. This notion warrants further investigations.



## **CHAPTER 7**

### **CONCLUSION AND RECOMMENDATION**

In this study, the human brain PRSS3 (mesotrypsinogen) was identified as a novel EV-A71 3A-interacting protein in human neuronal cells. Investigation of the role of human PRSS3 in EV-A71 infected cells revealed the positive implication of the protein with EV-A71 replication. Mechanism of human PRSS3 for enhancing viral replication and role in neuropathogenesis as well as the binding domains for interacting with EV-A71 3A protein requires more elucidation. The gained knowledge expands host interactome of EV-A71 and might provide data contributing to insights in infection biology and pathology caused by the virus guiding for the development of specific treatment of neurological complications in the severe hand, foot, and mouth disease.





## REFERENCES

1. Zhang Y, Tan X-J, Wang H-Y, Yan D-M, Zhu S-L, Wang D-Y, et al. An outbreak of hand, foot, and mouth disease associated with subgenotype C4 of human enterovirus 71 in Shandong, China. *J Clin Virol*. 2009;44(4):262–7.
2. Yang F, Ren L, Xiong Z, Li J, Xiao Y, Zhao R, et al. Enterovirus 71 Outbreak in the People's Republic of China in 2008. *J Clin Microbiol*. 2009;47(7):2351–2.
3. Ma E, Chan KC, Cheng P, Wong C, Chuang SK. The enterovirus 71 epidemic in 2008—public health implications for Hong Kong. *Int J Infect Dis*. 2010;14(9):e775–80.
4. Wang J-R, Tuan Y-C, Tsai H-P, Yan J-J, Liu C-C, Su I-J. Change of Major Genotype of Enterovirus 71 in Outbreaks of Hand-Foot-and-Mouth Disease in Taiwan between 1998 and 2000. *J Clin Microbiol*. 2002;40(1):10–5.
5. Fujimoto T, Chikahira M, Yoshida S, Ebira H, Hasegawa A, Totsuka A, et al. Outbreak of Central Nervous System Disease Associated with Hand, Foot, and Mouth Disease in Japan during the Summer of 2000: Detection and Molecular Epidemiology of Enterovirus 71. *Microbiol Immunol*. 2002;46(9):621–7.
6. Shekhar K, Lye MS, Norlijah O, Ong F, Looi LM, Khuzaiah R, et al. Deaths in children during an outbreak of hand, foot and mouth disease in Peninsular Malaysia--clinical and pathological characteristics. *Med J Malaysia*. 2005;60(3):297–304.
7. Shah VA, Chong CY, Chan KP, Ng W, Ling AE. Clinical characteristics of an outbreak of hand, foot and mouth disease in Singapore. *Ann Acad Med Singapore*. 2003;32(3):381–7.
8. Wu Y, Yeo A, Phoon MC, Tan EL, Poh CL, Quak SH, et al. The largest outbreak of hand; foot and mouth disease in Singapore in 2008: The role of enterovirus 71 and coxsackievirus A strains. *Int J Infect Dis*. 2010;14(12):e1076–81.
9. Khanh TH, Sabanathan S, Thanh TT, Thoa LPK, Thuong TC, Hang V thi T, et al. Enterovirus 71-associated Hand, Foot, and Mouth Disease, Southern Vietnam, 2011. *Emerg Infect Dis*. 2012;18(12):2002–5.
10. Horwood PF, Andronico A, Tarantola A, Salje H, Duong V, Mey C, et al. Seroepidemiology of Human Enterovirus 71 Infection among Children, Cambodia. *Emerg Infect Dis*. 2016;22(1):92–5.
11. Chatproedprai S, Theanboonlers A, Korkong S, Thongmee C, Wananukul S, Poovorawan Y. Clinical and molecular characterization of hand-foot-and-mouth disease in Thailand, 2008-2009. *Jpn J Infect Dis*. 2010;63(4):229–33.

12. Samphutthanon R, Kumar Tripathi N, Ninsawat S, Duboz R. Spatio-Temporal Distribution and Hotspots of Hand, Foot and Mouth Disease (HFMD) in Northern Thailand. *Int J Environ Res Public Health*. 2014;11(1):312–36.
13. Linsuwanon P, Puenpa J, Huang S-W, Wang Y-F, Mauleekoonphairoj J, Wang J-R, et al. Epidemiology and seroepidemiology of human enterovirus 71 among Thai populations. *J Biomed Sci*. 2014;21(1):16.
14. Puenpa J, Mauleekoonphairoj J, Linsuwanon P, Suwannakarn K, Chieochansin T, Korkong S, et al. Prevalence and Characterization of Enterovirus Infections among Pediatric Patients with Hand Foot Mouth Disease, Herpangina and Influenza Like Illness in Thailand, 2012. *PLoS one*. 2014;9(6):e98888.
15. Mauleekoonphairoj J, Vongpunsawad S, Puenpa J, Korkong S, Poovorawan Y. Complete genome sequence analysis of enterovirus 71 isolated from children with hand, foot, and mouth disease in Thailand, 2012-2014. *Virus Genes*. 2015;51(2):290–3.
16. Podin Y, Gias EL, Ong F, Leong Y-W, Yee S-F, Yusof MA, et al. Sentinel surveillance for human enterovirus 71 in Sarawak, Malaysia: lessons from the first 7 years. *BMC Public Health*. 2006;6:180.
17. Chen S-C, Chang H-L, Yan T-R, Cheng Y-T, Chen K-T. An Eight-Year Study of Epidemiologic Features of Enterovirus 71 Infection In Taiwan. *Am J Trop Med Hyg*. 2007;77(1):188–91.
18. Hand Foot and Mouth Disease | Home | HFMD | CDC [Internet]. [cited 2016 Jul 7]. Available from: <http://www.cdc.gov/hand-foot-mouth/>
19. Rhoades RE, Tabor-Godwin JM, Tsueng G, Feuer R. Enterovirus Infections of the Central Nervous System Review. *Virology*. 2011;411(2):288–305.
20. Liu Y, Wang C, Mueller S, Paul AV, Wimmer E, Jiang P. Direct Interaction between Two Viral Proteins, the Nonstructural Protein 2CATPase and the Capsid Protein VP3, Is Required for Enterovirus Morphogenesis. *PLoS Pathog* [Internet]. 2010 Aug [cited 2016 Jul 7];6(8). Available from: <http://www.ncbi.nlm.nih.gov/pmc/articles/PMC2928791/>
21. Feng Q, Langereis MA, Lork M, Nguyen M, Hato SV, Lanke K, et al. Enterovirus 2Apro Targets MDA5 and MAVS in Infected Cells. *J Virol*. 2014;88(6):3369–78.
22. Wang L-C, Chen S-O, Chang S-P, Lee Y-P, Yu C-K, Chen C-L, et al. Enterovirus 71 Proteins 2A and 3D Antagonize the Antiviral Activity of Gamma Interferon via Signaling Attenuation. *J Virol*. 2015;89(14):7028–37.
23. Tang F, Xia H, Wang P, Yang J, Zhao T, Zhang Q, et al. The identification and characterization of nucleic acid chaperone activity of human enterovirus 71 nonstructural protein 3AB. *Virology*. 2014;464–465:353–64.

24. Belov GA, Altan-Bonnet N, Kovtunovych G, Jackson CL, Lippincott-Schwartz J, Ehrenfeld E. Hijacking components of the cellular secretory pathway for replication of poliovirus RNA. *J Virol.* 2007;81(2):558–67.
25. Ilnytska O, Santiana M, Hsu N-Y, Du W-L, Chen Y-H, Viktorova EG, et al. Enteroviruses Harness the Cellular Endocytic Machinery to Remodel the Host Cell Cholesterol Landscape for Effective Viral Replication. *Cell Host Microbe.* 2013;14(3):281–93.
26. Strauss DM, Glustrom LW, Wuttke DS. Towards an Understanding of the Poliovirus Replication Complex: The Solution Structure of the Soluble Domain of the Poliovirus 3A Protein. *J Mol Biol.* 2003;330(2):225–34.
27. Chen H, Zhang Y, Yang E, Liu L, Che Y, Wang J, et al. The effect of enterovirus 71 immunization on neuropathogenesis and protein expression profiles in the thalamus of infected rhesus neonates. *Virology.* 2012;432(2):417–26.
28. Solomon T, Lewthwaite P, Perera D, Cardosa MJ, McMinn P, Ooi MH. Virology, epidemiology, pathogenesis, and control of enterovirus 71. *Lancet Infect Dis.* 2010;10(11):778–90.
29. Jiang P, Liu Y, Ma H-C, Paul AV, Wimmer E. Picornavirus Morphogenesis. *Microbiol Mol Biol Rev.* 2014;78(3):418–37.
30. Combelas N, Holmblat B, Joffret M-L, Colbère-Garapin F, Delpyroux F. Recombination between Poliovirus and Coxsackie A Viruses of Species C: A Model of Viral Genetic Plasticity and Emergence. *Viruses.* 2011;3(8):1460–84.
31. Choe SS, Dodd DA, Kirkegaard K. Inhibition of cellular protein secretion by picornaviral 3A proteins. *Virology.* 2005;337(1):18–29.
32. Deitz SB, Dodd DA, Cooper S, Parham P, Kirkegaard K. MHC I-dependent antigen presentation is inhibited by poliovirus protein 3A. *Proc Natl Acad Sci U S A.* 2000;97(25):13790–5.
33. Brown BA, Oberste MS, Alexander JP, Kennett ML, Pallansch MA. Molecular Epidemiology and Evolution of Enterovirus 71 Strains Isolated from 1970 to 1998. *J Virol.* 1999;73(12):9969–75.
34. Cardosa MJ, Perera D, Brown BA, Cheon D, Chan HM, Chan KP, et al. Molecular Epidemiology of Human Enterovirus 71 Strains and Recent Outbreaks in the Asia-Pacific Region: Comparative Analysis of the VP1 and VP4 Genes. *Emerg Infect Dis.* 2003;9(4):462–8.
35. Huang P-N, Shih S-R. Update on enterovirus 71 infection. *Curr Opin Virol.* 2014;5:98–104.
36. Puenpa J, Theamboonlers A, Korkong S, Linsuwanon P, Thongmee C, Chatproedprai S, et al. Molecular characterization and complete genome analysis of

human enterovirus 71 and coxsackievirus A16 from children with hand, foot and mouth disease in Thailand during 2008-2011. *Arch Virol.* 2011;156(11):2007–13.

37. Ehrenfeld E, Domingo E, Roos RP, editors. *The Picornaviruses*. 1 edition. Washington, DC: ASM Press; 2010. 536 p.

38. Belov GA, Sztul E. Rewiring of Cellular Membrane Homeostasis by Picornaviruses. *J Virol.* 2014;88(17):9478–89.

39. Lei X, Sun Z, Liu X, Jin Q, He B, Wang J. Cleavage of the Adaptor Protein TRIF by Enterovirus 71 3C Inhibits Antiviral Responses Mediated by Toll-Like Receptor 3. *J Virol.* 2011;85(17):8811–8.

40. Schneider WM, Chevillotte MD, Rice CM. Interferon-Stimulated Genes: A Complex Web of Host Defenses. *Annu Rev Immunol.* 2014;32:513–45.

41. Zheng Z, Li H, Zhang Z, Meng J, Mao D, Bai B, et al. Enterovirus 71 2C Protein Inhibits TNF- $\alpha$ -Mediated Activation of NF- $\kappa$ B by Suppressing I $\kappa$ B Kinase  $\beta$  Phosphorylation. *J Immunol.* 2011;187(5):2202–12.

42. Lu J, Yi L, Zhao J, Yu J, Chen Y, Lin MC, et al. Enterovirus 71 Disrupts Interferon Signaling by Reducing the Level of Interferon Receptor 1. *J Virol.* 2012;86(7):3767–76.

43. Yamayoshi S, Fujii K, Koike S. Receptors for enterovirus 71. *Emerg Microbes Infect.* 2014;3(7):e53.

44. Lin Y-W, Lin H-Y, Tsou Y-L, Chitra E, Hsiao K-N, Shao H-Y, et al. Human SCARB2-Mediated Entry and Endocytosis of EV71. *PLoS one* [Internet]. 2012 Jan 17 [cited 2016 Jul 7];7(1). Available from: <http://www.ncbi.nlm.nih.gov/pmc/articles/PMC3260287/>

45. Lin H-Y, Yang Y-T, Yu S-L, Hsiao K-N, Liu C-C, Sia C, et al. Caveolar endocytosis is required for human PSGL-1-mediated enterovirus 71 infection. *J Virol.* 2013;87(16):9064–76.

46. Laszik Z, Jansen PJ, Cummings RD, Tedder TF, McEver RP, Moore KL. P-selectin glycoprotein ligand-1 is broadly expressed in cells of myeloid, lymphoid, and dendritic lineage and in some nonhematopoietic cells. *Blood.* 1996;88(8):3010–21.

47. Granger DN, Senchenkova E. *Inflammation and the Microcirculation* [Internet]. San Rafael (CA): Morgan & Claypool Life Sciences; 2010 [cited 2016 Jul 11]. (Integrated Systems Physiology—From Cell to Function). Available from: <http://www.ncbi.nlm.nih.gov/books/NBK53373/>

48. Nishimura Y, Shimojima M, Tano Y, Miyamura T, Wakita T, Shimizu H. Human P-selectin glycoprotein ligand-1 is a functional receptor for enterovirus 71. *Nat Med.* 2009;15(7):794–7.

49. Nishimura Y, Lee H, Hafenstein S, Kataoka C, Wakita T, Bergelson JM, et al. Enterovirus 71 Binding to PSGL-1 on Leukocytes: VP1-145 Acts as a Molecular Switch to Control Receptor Interaction. *PLoS Pathog.* 2013;9(7):e1003511.
50. Nishimura Y, Wakita T, Shimizu H. Tyrosine Sulfation of the Amino Terminus of PSGL-1 Is Critical for Enterovirus 71 Infection. *PLoS Pathog.* 2010;6(11):e1001174.
51. Kataoka C, Suzuki T, Kotani O, Iwata-Yoshikawa N, Nagata N, Ami Y, et al. The Role of VP1 Amino Acid Residue 145 of Enterovirus 71 in Viral Fitness and Pathogenesis in a Cynomolgus Monkey Model. *PLoS Pathog* [Internet]. 2015 [cited 2016 Jul 7];11(7). Available from: <http://www.ncbi.nlm.nih.gov/pmc/articles/PMC4504482/>
52. Yamayoshi S, Iizuka S, Yamashita T, Minagawa H, Mizuta K, Okamoto M, et al. Human SCARB2-Dependent Infection by Coxsackievirus A7, A14, and A16 and Enterovirus 71. *J Virol.* 2012;86(10):5686–96.
53. Yamayoshi S, Koike S. Identification of a Human SCARB2 Region That Is Important for Enterovirus 71 Binding and Infection . *J Virol.* 2011;85(10):4937–46.
54. Jiao X-Y, Guo L, Huang D-Y, Chang X-L, Qiu Q-C. Distribution of EV71 receptors SCARB2 and PSGL-1 in human tissues. *Virus Res.* 2014;190:40–52.
55. Zhang Y, Cui W, Liu L, Wang J, Zhao H, Liao Y, et al. Pathogenesis study of enterovirus 71 infection in rhesus monkeys. *Lab Invest.* 2011;91(9):1337–50.
56. Dang M, Wang X, Wang Q, Wang Y, Lin J, Sun Y, et al. Molecular mechanism of SCARB2-mediated attachment and uncoating of EV71. *Protein Cell.* 2014;5(9):692–703.
57. Chen P, Song Z, Qi Y, Feng X, Xu N, Sun Y, et al. Molecular Determinants of Enterovirus 71 Viral Entry. *J Biol Chem.* 2012;287(9):6406–20.
58. Wang X, Peng W, Ren J, Hu Z, Xu J, Lou Z, et al. A sensor-adaptor mechanism for enterovirus uncoating from structures of EV71. *Nat Struct Mol Biol.* 2012;19(4):424–9.
59. Hussain KM, Leong KLJ, Ng MM-L, Chu JJH. The Essential Role of Clathrin-mediated Endocytosis in the Infectious Entry of Human Enterovirus 71. *J Biol Chem.* 2011;286(1):309–21.
60. Zachos C, Blanz J, Saftig P, Schwake M. A Critical Histidine Residue Within LIMP-2 Mediates pH Sensitive Binding to Its Ligand  $\beta$ -Glucocerebrosidase. *Traffic.* 2012;13(8):1113–23.
61. Yamayoshi S, Ohka S, Fujii K, Koike S. Functional Comparison of SCARB2 and PSGL1 as Receptors for Enterovirus 71. *J Virol.* 2013;87(6):3335–47.



62. Fricks CE, Hogle JM. Cell-induced conformational change in poliovirus: externalization of the amino terminus of VP1 is responsible for liposome binding. *J Virol*. 1990;64(5):1934–45.
63. Ren J, Wang X, Hu Z, Gao Q, Sun Y, Li X, et al. Picornavirus uncoating intermediate captured in atomic detail. *Nat Commun* [Internet]. 2013 Jun 3 [cited 2016 Jul 11];4. Available from: <http://www.ncbi.nlm.nih.gov/pmc/articles/PMC3709478/>
64. Lyu K, Ding J, Han J-F, Zhang Y, Wu X-Y, He Y-L, et al. Human Enterovirus 71 Uncoating Captured at Atomic Resolution. *J Virol*. 2014;88(6):3114–26.
65. Martínez-Salas E, Francisco-Velilla R, Fernandez-Chamorro J, Lozano G, Diaz-Toledano R. Picornavirus IRES elements: RNA structure and host protein interactions. *Virus Res*. 2015;206:62–73.
66. Pilipenko EV, Viktorova EG, Guest ST, Agol VI, Roos RP. Cell-specific proteins regulate viral RNA translation and virus-induced disease. *EMBO J*. 2001;20(23):6899–908.
67. Sun D, Chen S, Cheng A, Wang M. Roles of the Picornaviral 3C Proteinase in the Viral Life Cycle and Host Cells. *Viruses*. 2016;8(3):82.
68. Blom N, Hansen J, Blaas D, Brunak S. Cleavage site analysis in picornaviral polyproteins: discovering cellular targets by neural networks. *Protein Sci Publ Protein Soc*. 1996;5(11):2203–16.
69. Hsu N-Y, Ilnytska O, Belov G, Santiana M, Chen Y-H, Takvorian PM, et al. Viral Reorganization of the Secretory Pathway Generates Distinct Organelles for RNA Replication. *Cell*. 2010;141(5):799–811.
70. Egger D, Teterina N, Ehrenfeld E, Bienz K. Formation of the Poliovirus Replication Complex Requires Coupled Viral Translation, Vesicle Production, and Viral RNA Synthesis. *J Virol*. 2000;74(14):6570–80.
71. Dorobantu CM, Albuлесcu L, Harak C, Feng Q, Kampen M van, Strating JRPM, et al. Modulation of the Host Lipid Landscape to Promote RNA Virus Replication: The Picornavirus Encephalomyocarditis Virus Converges on the Pathway Used by Hepatitis C Virus. *PLoS Pathog*. 2015;11(9):e1005185.
72. Prentice E, Jerome WG, Yoshimori T, Mizushima N, Denison MR. Coronavirus replication complex formation utilizes components of cellular autophagy. *J Biol Chem*. 2004;279(11):10136–41.
73. Miller DJ, Schwartz MD, Ahlquist P. Flock House Virus RNA Replicates on Outer Mitochondrial Membranes in *Drosophila* Cells. *J Virol*. 2001;75(23):11664–76.
74. Lazarow PB. Viruses exploiting peroxisomes. *Curr Opin Microbiol*. 2011;14(4):458–69.

75. Belov GA, van Kuppeveld FJ. (+)RNA viruses rewire cellular pathways to build replication organelles. *Curr Opin Virol.* 2012;2(6):740–7.
76. Shulla A, Randall G. (+) RNA virus replication compartments: a safe home for (most) viral replication. *Curr Opin Microbiol.* 2016;32:82–8.
77. Wessels E, Duijsings D, Niu T-K, Neumann S, Oorschot VM, de Lange F, et al. A Viral Protein that Blocks Arf1-Mediated COP-I Assembly by Inhibiting the Guanine Nucleotide Exchange Factor GBF1. *Dev Cell.* 2006;11(2):191–201.
78. Wessels E, Duijsings D, Lanke KHW, Melchers WJG, Jackson CL, van Kuppeveld FJM. Molecular Determinants of the Interaction between Coxsackievirus Protein 3A and Guanine Nucleotide Exchange Factor GBF1. *J Virol.* 2007;81(10):5238–45.
79. Belov GA, Fogg MH, Ehrenfeld E. Poliovirus Proteins Induce Membrane Association of GTPase ADP-Ribosylation Factor. *J Virol.* 2005;79(11):7207–16.
80. Lei X, Xiao X, Zhang Z, Ma Y, Qi J, Wu C, et al. The Golgi protein ACBD3 facilitates Enterovirus 71 replication by interacting with 3A. *Sci Rep [Internet].* 2017 Mar 17 [cited 2017 Mar 24];7. Available from: <http://www.ncbi.nlm.nih.gov/pmc/articles/PMC5356004/>
81. Greninger AL, Knudsen GM, Betegon M, Burlingame AL, DeRisi JL. ACBD3 Interaction with TBC1 Domain 22 Protein Is Differentially Affected by Enteroviral and Kobuviral 3A Protein Binding. *mBio [Internet].* 2013 Apr 9 [cited 2016 Jul 7];4(2). Available from: <http://www.ncbi.nlm.nih.gov/pmc/articles/PMC3622926/>
82. Greninger AL, Knudsen GM, Betegon M, Burlingame AL, DeRisi JL. The 3A Protein from Multiple Picornaviruses Utilizes the Golgi Adaptor Protein ACBD3 To Recruit PI4KIII $\beta$ . *J Virol.* 2012;86(7):3605–16.
83. Altan-Bonnet N, Balla T. Phosphatidylinositol 4-kinases: hostages harnessed to build panviral replication platforms. *Trends Biochem Sci.* 2012;37(7):293–302.
84. Strating JRPM, van der Linden L, Albuлесcu L, Bigay J, Arita M, Delang L, et al. Itraconazole Inhibits Enterovirus Replication by Targeting the Oxysterol-Binding Protein. *Cell Rep.* 2015;10(4):600–15.
85. Mesmin B, Bigay J, Moser von Filseck J, Lacas-Gervais S, Drin G, Antony B. A Four-Step Cycle Driven by PI(4)P Hydrolysis Directs Sterol/PI(4)P Exchange by the ER-Golgi Tether OSBP. *Cell.* 2013;155(4):830–43.
86. Goluszko P, Nowicki B. Membrane Cholesterol: a Crucial Molecule Affecting Interactions of Microbial Pathogens with Mammalian Cells. *Infect Immun.* 2005;73(12):7791–6.



87. Dodd DA, Giddings TH, Kirkegaard K. Poliovirus 3A Protein Limits Interleukin-6 (IL-6), IL-8, and Beta Interferon Secretion during Viral Infection. *J Virol*. 2001;75(17):8158–65.
88. Robinson SM, Tsueng G, Sin J, Mangale V, Rahawi S, McIntyre LL, et al. Coxsackievirus B Exits the Host Cell in Shed Microvesicles Displaying Autophagosomal Markers. *PLoS Pathog*. 2014;10(4):e1004045.
89. Bird SW, Maynard ND, Covert MW, Kirkegaard K. Nonlytic viral spread enhanced by autophagy components. *Proc Natl Acad Sci*. 2014;111(36):13081–6.
90. Feng Z, Hensley L, McKnight KL, Hu F, Madden V, Ping L, et al. A pathogenic picornavirus acquires an envelope by hijacking cellular membranes. *Nature*. 2013;496(7445):367–71.
91. Takahashi M, Yamada K, Hoshino Y, Takahashi H, Ichiyama K, Tanaka T, et al. Monoclonal antibodies raised against the ORF3 protein of hepatitis E virus (HEV) can capture HEV particles in culture supernatant and serum but not those in feces. *Arch Virol*. 2008;153(9):1703–13.
92. Owens RJ, Limn C, Roy P. Role of an Arbovirus Nonstructural Protein in Cellular Pathogenesis and Virus Release. *J Virol*. 2004;78(12):6649–56.
93. Feng Z, Li Y, McKnight KL, Hensley L, Lanford RE, Walker CM, et al. Human pDCs preferentially sense enveloped hepatitis A virions. *J Clin Invest*. 2015;125(1):169–76.
94. Chen Y-H, Du W, Hagemeyer MC, Takvorian PM, Pau C, Cali A, et al. Phosphatidylserine Vesicles Enable Efficient En Bloc Transmission of Enteroviruses. *Cell*. 2015;160(4):619–30.
95. Mao L, Wu J, Shen L, Yang J, Chen J, Xu H. Enterovirus 71 transmission by exosomes establishes a productive infection in human neuroblastoma cells. *Virus Genes*. 2016;52(2):189–94.
96. Picornaviruses- Enteroviruses and general features of picornaviruses [Internet]. [cited 2016 Jul 7]. Available from: <http://www.microbiologybook.org/virol/picorna.htm>
97. Phyu WK, Ong KC, Wong KT. A Consistent Orally-Infected Hamster Model for Enterovirus A71 Encephalomyelitis Demonstrates Squamous Lesions in the Paws, Skin and Oral Cavity Reminiscent of Hand-Foot-and-Mouth Disease. *PLoS ONE* [Internet]. 2016 Jan 27 [cited 2016 Jul 11];11(1). Available from: <http://www.ncbi.nlm.nih.gov/pmc/articles/PMC4729525/>
98. Chen C-S, Yao Y-C, Lin S-C, Lee Y-P, Wang Y-F, Wang J-R, et al. Retrograde Axonal Transport: a Major Transmission Route of Enterovirus 71 in Mice. *J Virol*. 2007;81(17):8996–9003.

99. Taylor MP, Enquist LW. Axonal spread of neuroinvasive viral infections. *Trends Microbiol.* 2015;23(5):283–8.
100. Wang Y-F, Yu C-K. Animal models of enterovirus 71 infection: applications and limitations. *J Biomed Sci.* 2014;21(1):31.
101. Wong KT, Munisamy B, Ong KC, Kojima H, Noriyo N, Chua KB, et al. The Distribution of Inflammation and Virus in Human Enterovirus 71 Encephalomyelitis Suggests Possible Viral Spread by Neural Pathways. *J Neuropathol Exp Neurol.* 2008;67(2):162–9.
102. Organization WH. Polio laboratory manual. 2004 [cited 2021 May 5]; Available from: <https://apps.who.int/iris/handle/10665/68762>
103. Hayashi H, Kubo Y, Izumida M, Takahashi E, Kido H, Sato K, et al. Enterokinase Enhances Influenza A Virus Infection by Activating Trypsinogen in Human Cell Lines. *Front Cell Infect Microbiol* [Internet]. 2018 Mar 23;8. Available from: <https://www.ncbi.nlm.nih.gov/pmc/articles/PMC5876233/>
104. Rao X, Huang X, Zhou Z, Lin X. An improvement of the  $2^{-\Delta\Delta CT}$  method for quantitative real-time polymerase chain reaction data analysis. *Biostat Bioinforma Biomath.* 2013;3(3):71–85.
105. Cao J, Qu M, Liu H, Wan X, Li F, Hou A, et al. Myristoylation of EV71 VP4 is Essential for Infectivity and Interaction with Membrane Structure. *Viol Sin.* 2020;35(5):599–613.
106. Moscufo N, Simons J, Chow M. Myristoylation is important at multiple stages in poliovirus assembly. *J Virol.* 1991;65(5):2372–80.
107. Supasorn O, Tongtawe P, Srimanote P, Rattanakomol P, Thanongsaksrikul J. A nonstructural 2B protein of enterovirus A71 increases cytosolic Ca<sup>2+</sup> and induces apoptosis in human neuroblastoma SH-SY5Y cells. *J Neurovirol.* 2020;26(2):201–13.
108. Wessels E, Notebaart RA, Duijsings D, Lanke K, Vergeer B, Melchers WJG, et al. Structure-function analysis of the coxsackievirus protein 3A: identification of residues important for dimerization, viral rna replication, and transport inhibition. *J Biol Chem.* 2006;281(38):28232–43.
109. Xi J, Ye F, Wang G, Han W, Wei Z, Yin B, et al. Polypyrimidine Tract-Binding Protein Regulates Enterovirus 71 Translation Through Interaction with the Internal Ribosomal Entry Site. *Viol Sin.* 2019;34(1):66–77.
110. Melia CE, Peddie CJ, de Jong AWM, Snijder EJ, Collinson LM, Koster AJ, et al. Origins of Enterovirus Replication Organelles Established by Whole-Cell Electron Microscopy. *mBio.* 2019;10(3).
111. Wong KT, Ng KY, Ong KC, Ng WF, Shankar SK, Mahadevan A, et al. Enterovirus 71 encephalomyelitis and Japanese encephalitis can be distinguished by

topographic distribution of inflammation and specific intraneuronal detection of viral antigen and RNA. *Neuropathol Appl Neurobiol.* 2012;38(5):443–53.

112. Kc O, M B, S D, Kl L, Mj C, Kt W. Pathologic characterization of a murine model of human enterovirus 71 encephalomyelitis [Internet]. *Journal of neuropathology and experimental neurology.* 2008 [cited 2021 May 29]. Available from: <https://pubmed.ncbi.nlm.nih.gov/18520772/>

113. N N, T I, Y A, Y T, A H, Y S, et al. Differential localization of neurons susceptible to enterovirus 71 and poliovirus type 1 in the central nervous system of cynomolgus monkeys after intravenous inoculation [Internet]. *The Journal of general virology.* 2004 [cited 2021 May 29]. Available from: <https://pubmed.ncbi.nlm.nih.gov/15448361/>

114. Contemporary Circulating Enterovirus D68 Strains Have Acquired the Capacity for Viral Entry and Replication in Human Neuronal Cells [Internet]. *mBio.* [cited 2021 Jun 10]. Available from: <https://journals.asm.org/doi/abs/10.1128/mBio.01954-18>

115. Fm L, R S, Ml da F, A Z-F, Cb M, As P, et al. Comparison between proliferative and neuron-like SH-SY5Y cells as an in vitro model for Parkinson disease studies [Internet]. *Brain research.* 2010 [cited 2021 Jun 10]. Available from: <https://pubmed.ncbi.nlm.nih.gov/20380819/>

116. Ramalingam M, Huh Y-J, Lee Y-I. The Impairments of  $\alpha$ -Synuclein and Mechanistic Target of Rapamycin in Rotenone-Induced SH-SY5Y Cells and Mice Model of Parkinson's Disease. *Front Neurosci* [Internet]. 2019 [cited 2021 Jun 10];13. Available from: <https://www.frontiersin.org/articles/10.3389/fnins.2019.01028/full>

117. Tr T-W, Cl LM, Ja D, Cf D, Dp S. Recapitulating Parkinson's disease pathology in a three-dimensional human neural cell culture model [Internet]. *Disease models & mechanisms.* 2019 [cited 2021 Jun 10]. Available from: <https://pubmed.ncbi.nlm.nih.gov/30926586/>

118. M B, E Y, M RD, M P, M G-H, M S, et al. MiR-193b deregulation is associated with Parkinson's disease [Internet]. *Journal of cellular and molecular medicine.* 2021 [cited 2021 Jun 10]. Available from: <https://pubmed.ncbi.nlm.nih.gov/34018309/>

119. Modification of the Untranslated Regions of Human Enterovirus 71 Impairs Growth in a Cell-Specific Manner [Internet]. *Journal of Virology.* [cited 2021 Jun 10]. Available from: <https://journals.asm.org/doi/abs/10.1128/jvi.00069-11>

120. Xu L-J, Jiang T, Zhang F-J, Han J-F, Liu J, Zhao H, et al. Global Transcriptomic Analysis of Human Neuroblastoma Cells in Response to Enterovirus Type 71 Infection. *PLoS ONE.* 2013;8(7):e65948.

121. Liu Z-W, Zhuang Z-C, Chen R, Wang X-R, Zhang H-L, Li S-H, et al. Enterovirus 71 VP1 Protein Regulates Viral Replication in SH-SY5Y Cells via the mTOR Autophagy Signaling Pathway. *Viruses*. 2019;12(1).
122. Hu Y, Xu Y, Huang Z, Deng Z, Fan J, Yang R, et al. Transcriptome sequencing analysis of SH-SY5Y cells infected with EV71 reveals the potential neuropathic mechanisms. *Virus Res*. 2020;282:197945.
123. Chang C-S, Liao C-C, Liou A-T, Chou Y-C, Yu Y-Y, Lin C-Y, et al. Novel Naturally Occurring Mutations of Enterovirus 71 Associated With Disease Severity. *Front Microbiol*. 2020;11:610568.
124. Mm S, Ca M, Cv K, Ml S. Differentiated Human SH-SY5Y Cells Provide a Reductionist Model of Herpes Simplex Virus 1 Neurotropism [Internet]. *Journal of virology*. 2017 [cited 2021 Jun 10]. Available from: <https://pubmed.ncbi.nlm.nih.gov/28956768/>
125. Ahmad W, Li Y, Guo Y, Wang X, Duan M, Guan Z, et al. Rabies virus co-localizes with early (Rab5) and late (Rab7) endosomal proteins in neuronal and SH-SY5Y cells. *Virol Sin*. 2017;32(3):207–15.
126. M C, G G, A M, Ce W, K I, Y O, et al. Upregulated expression of the antioxidant sestrin 2 identified by transcriptomic analysis of Japanese encephalitis virus-infected SH-SY5Y neuroblastoma cells [Internet]. *Virus genes*. 2019 [cited 2021 Jun 10]. Available from: <https://pubmed.ncbi.nlm.nih.gov/31292858/>
127. Mukherjee S, Sengupta N, Chaudhuri A, Akbar I, Singh N, Chakraborty S, et al. PLVAP and GKN3 Are Two Critical Host Cell Receptors Which Facilitate Japanese Encephalitis Virus Entry Into Neurons. *Sci Rep*. 2018;8(1):1–16.
128. Sánchez-San Martín C, Li T, Bouquet J, Streithorst J, Yu G, Paranjpe A, et al. Differentiation enhances Zika virus infection of neuronal brain cells. *Sci Rep*. 2018;8(1):1–10.
129. Sharma A, Vasanthapuram R, Venkataswamy MM, Desai A. Prohibitin 1/2 mediates Dengue-3 entry into human neuroblastoma (SH-SY5Y) and microglia (CHME-3) cells. *J Biomed Sci*. 2020;27(1):1–17.
130. G S, S M, M A, Fl G. Preferential transformation of human neuronal cells by human adenoviruses and the origin of HEK 293 cells [Internet]. *FASEB journal : official publication of the Federation of American Societies for Experimental Biology*. 2002 [cited 2021 May 28]. Available from: <https://pubmed.ncbi.nlm.nih.gov/11967234/>
131. Yuan J, Xu WW, Jiang S, Yu H, Poon HF. The Scattered Twelve Tribes of HEK293. *Biomed Pharmacol J*. 2018;11(2):621–3.

132. Kukor Z, Tóth M, Sahin-Tóth M. Human anionic trypsinogen: properties of autocatalytic activation and degradation and implications in pancreatic diseases. *Eur J Biochem.* 2003;270(9):2047–58.
133. Szmola R, Kukor Z, Sahin-Tóth M. Human Mesotrypsin Is a Unique Digestive Protease Specialized for the Degradation of Trypsin Inhibitors\*. *J Biol Chem.* 2003;278(49):48580–9.
134. Rath A, Glibowicka M, Nadeau VG, Chen G, Deber CM. Detergent binding explains anomalous SDS-PAGE migration of membrane proteins. *Proc Natl Acad Sci.* 2009;106(6):1760–5.
135. W X, A C, D H, K K, E W. Complete protein linkage map of poliovirus P3 proteins: interaction of polymerase 3Dpol with VPg and with genetic variants of 3AB [Internet]. *Journal of virology.* 1998 [cited 2021 Jun 10]. Available from: <https://pubmed.ncbi.nlm.nih.gov/9658121/>
136. Arita M. Mechanism of Poliovirus Resistance to Host Phosphatidylinositol-4 Kinase III  $\beta$  Inhibitor. *ACS Infect Dis.* 2016;2(2):140–8.
137. Enterovirus 3A Facilitates Viral Replication by Promoting Phosphatidylinositol 4-Kinase III $\beta$ -ACBD3 Interaction [Internet]. *Journal of Virology.* [cited 2021 Jun 10]. Available from: <https://journals.asm.org/doi/abs/10.1128/JVI.00791-17>
138. Y L, Z Z, B S, J M, Y Z, C Z, et al. SUMO Modification Stabilizes Enterovirus 71 Polymerase 3D To Facilitate Viral Replication [Internet]. *Journal of virology.* 2016 [cited 2021 Jun 10]. Available from: <https://pubmed.ncbi.nlm.nih.gov/27630238/>
139. Tóth J, Siklódi E, Medveczky P, Gallatz K, Németh P, Szilágyi L, et al. Regional Distribution of Human Trypsinogen 4 in Human Brain at mRNA and Protein Level. *Neurochem Res.* 2007;32(9):1423–33.
140. Haverback BJ, Dyce B, Bundy H, Edmondson HA. Trypsin, trypsinogen and trypsin inhibitor in human pancreatic juice: Mechanism for pancreatitis associated with hyperparathyroidism. *Am J Med.* 1960;29(3):424–33.
141. Unconventional translation initiation of human trypsinogen 4 at a CUG codon with an N-terminal leucine. [cited 2021 May 5]; Available from: <https://febs.onlinelibrary.wiley.com/doi/epdf/10.1111/j.1742-4658.2007.05708.x>
142. Laajala M, Hankaniemi MM, Määttä JAE, Hytönen VP, Laitinen OH, Marjomäki V. Host Cell Calpains Can Cleave Structural Proteins from the Enterovirus Polyprotein. *Viruses* [Internet]. 2019 Nov 28;11(12). Available from: <https://www.ncbi.nlm.nih.gov/pmc/articles/PMC6950447/>



143. Cao J, Liu H, Qu M, Hou A, Zhou Y, Sun B, et al. Determination of the cleavage site of enterovirus 71 VP0 and the effect of this cleavage on viral infectivity and assembly. *Microb Pathog.* 2019;134:103568.
144. Owen CA. SERINE PROTEINASES. In: Laurent GJ, Shapiro SD, editors. *Encyclopedia of Respiratory Medicine* [Internet]. Oxford: Academic Press; 2006. p. 1–10. Available from: <https://www.sciencedirect.com/science/article/pii/B0123708796002647>
145. Wagh AR, Bose K. Emerging Roles of Mitochondrial Serine Protease HtrA2 in Neurodegeneration. In: Chakraborti S, Dhalla NS, editors. *Proteases in Physiology and Pathology* [Internet]. Singapore: Springer Singapore; 2017. p. 325–53. Available from: [https://doi.org/10.1007/978-981-10-2513-6\\_15](https://doi.org/10.1007/978-981-10-2513-6_15)
146. Wang Y, Luo W, Reiser G. Trypsin and trypsin-like proteases in the brain: proteolysis and cellular functions. *Cell Mol Life Sci CMLS.* 2008;65(2):237–52.
147. Shiosaka S. Serine proteases regulating synaptic plasticity. *Anat Sci Int.* 2004;79(3):137–44.
148. Fuster Lluch O, Galindo MF, Ceña V, Jordán J. [The serine proteases and their function in neuronal death processes]. *Rev Neurol.* 2004;38(5):449–57.
149. Nikolakopoulou AM, Dutta R, Chen Z, Miller RH, Trapp BD. Activated microglia enhance neurogenesis via trypsinogen secretion. *Proc Natl Acad Sci.* 2013;110(21):8714–9.
150. Am N, A G, Nk R. Presenilin 1 promotes trypsin-induced neuroprotection via the PAR2/ERK signaling pathway. Effects of presenilin 1 FAD mutations [Internet]. *Neurobiology of aging.* 2016 [cited 2021 Jun 10]. Available from: <https://pubmed.ncbi.nlm.nih.gov/27143420/>
151. S P, A J, Q L, B A, C M, J A, et al. Mutant Presenilin 1 Dysregulates Exosomal Proteome Cargo Produced by Human-Induced Pluripotent Stem Cell Neurons [Internet]. *ACS omega.* 2021 [cited 2021 Jun 10]. Available from: <https://pubmed.ncbi.nlm.nih.gov/34056454/>
152. Daigle JG, Lanson NA, Smith RB, Casci I, Maltare A, Monaghan J, et al. RNA-binding ability of FUS regulates neurodegeneration, cytoplasmic mislocalization and incorporation into stress granules associated with FUS carrying ALS-linked mutations. *Hum Mol Genet.* 2013;22(6):1193–205.
153. Rockenstein E, Nuber S, Overk CR, Ubhi K, Mante M, Patrick C, et al. Accumulation of oligomer-prone  $\alpha$ -synuclein exacerbates synaptic and neuronal degeneration in vivo. *Brain.* 2014;137(5):1496–513.
154. Saeed M, Kapell S, Hertz NT, Wu X, Bell K, Ashbrook AW, et al. Defining the proteolytic landscape during enterovirus infection. *PLoS Pathog.* 2020;16(9):e1008927.





**APPENDICES**



## APPENDIX A

### OLIGONUCLEOTIDE NUCLEOTIDE SEQUENCES

#### 1. Primers used for detection of EV-A71 genomic RNA

<b>Primer name</b>	<b>5' to 3' sequence</b>
EV-F2760	ATGGKTATGYWAAAYTGGGACAT
EV-R3206	CCTGACRTGYTTMATCCTCAT

#### 2. Primers used for molecular cloning of EV-A71 nonstructural 3A coding sequence

<b>Primer name</b>	<b>5' to 3' sequence</b>
Outer1-MamNS3A	ATGAATTCATGGATTACAAGGATGAC GATGACAAGGGCCCCGCCCAAGTTC
R-pQE30pGEX4T1-NS3A	ATGTGCACCTATTGAAACCCCGCAA GAG
Inner1-mCherry-3A-Reverse	CTTCTCCTTTACTCATTTGAAACCCCG CAAAGAG
Inner2-3A-mCherry-Forward	AGCTCTTTGCGGGGTTTCAAATGGTG AGCAAGGGCGAGGAGGATAACATG
Outer2-mCherry-Reverse	TCTAGATTACTTGTACAGCTCGTCCAT
pLVX-Puro-Forward	ACACCGACTCTACTAGAGGA
pLVX-Puro-Reverse	CACTTGTGTAGCGCCAAGTG

#### 3. Primers used for determination of PRSS gene expression

<b>Primer name</b>	<b>5' to 3' sequence</b>
PRSS1-F	CCACCCCAATACGACAGGAA
PRSS1-R	TAGTCGGCGCCAGAGCTCGC
PRSS2-F	CCACCCCAATACAACAGCCG
PRSS2-R	GGGTAGTCGGCACCAGAACTCAG
PRSS3-F	CGCCACCCTAAATACAACAGGGA
PRSS3-R	TGGGTAGTCAGCACCAAAGCTCAG

**4. Primers used for determination of PRSS3 transcript variant**

<b>Primer name</b>	<b>5' to 3' sequence</b>
PRSS1-Forward	GCCTCGAGATGAATCCACTCCTGATCCT
PRSS1-Reverse	CCTCTAGATTAGCTATTGGCAGCTATGG
PRSS3-V1-Forward	GCCTCGAGATGTGCGGACCTGACGACAG
PRSS3-V2-Forward	GCCTCGAGATGAATCCATTCCTGATCCT
PRSS3-V3-Forward	GCCTCGAGATGCACATGAGAGAGACAAG
PRSS3-V4-Forward	GCCTCGAGATGGGACCTGCGGGGGAGGT
PRSS3 Common-Reverse	CCTCTAGATTAGCTGTTGGCAGCGATGG

**5. Primers used for construction of full-length PRSS3 transcript variant 3 in-frame with Myc at 3-end**

<b>Primer name</b>	<b>5' to 3' sequence</b>
1-prss3v3-forward	CTCGAGATGCACATGAGAGAGACAAGT
783-Myc-prss3v3-reverse	TCTAGATTACAGATCCTCTTCTGAGATG AGTTTCTGCTCGCTGTTGGCAGCGATGG TGTC

**6. Primers used for determination of GAPDH and Beta actin using qRT-PCR**

<b>Primer name</b>	<b>5' to 3' sequence</b>
GAPDH-F	CAAGGTCATCCATGACAACTTTG
GAPDH-R	GTCCACCACCCTGTTGCTGTA
Human ACTB-F	GAGCGGGAAATCGTGCGTGACATT
Human ACTB-R	GAAGGTAGTTTCGTGGATGCC

## 7. siRNA information

**Part Number (P/N):** 4392420

**Product line, siRNA type:** Silencer<sup>®</sup> Select, Pre-designed (ThermoFisher Scientific, US)

**Locus ID:** 5646, Target gene symbol: PRSS3, Gene alias(es): MTG, PRSS4, T9, TRY3, TRY4

siRNA ID	Strand	5' to 3' sequence
s194719	Sense	AGAUCAUCCGCCACCCUAAtt
	Anti-sense	UUAGGGUGGCGGAUGAUCUtg
s11259	Sense	CUCUGAGCUUUGGUGCUGAtt
	Anti-sense	UCAGCACCAAAGCUCAGAGtg
s11260	Sense	GGGAGAGCACAACAUCAAAtt
	Anti-sense	UUUGAUGUUGUGCUCUCCCag

Sequences of Silencer<sup>®</sup> Select Negative Control #1 siRNA (cat. 4390843, ThermoFisher Scientific, US) and Silencer<sup>®</sup> Select GAPDH siRNA (cat. 4390849, ambion<sup>®</sup>, life technologies<sup>™</sup>) are not provided by manufacturer.

## **APPENDIX B**

### **BACTERIAL CULTURE MEDIA**

#### **1. Luria-Bertani (LB) broth or agar**

Luria-Bertani (LB) broth contains 10 g of tryptone type-1 (HIMEDIA, Mumbai, India), 5 g of yeast extract powder (HIMEDIA, Mumbai, India), and 5 g of NaCl (Univar, NSW, AUS). For LB agar, 15 g of agar powder (bacteriological grade) (HIMEDIA, Mumbai, India) was also added. All components were dissolved in 1 liter of DW. The broth or agar were sterilized by autoclaving. The LB broth was kept at room temperature while the LB agar solution was cooled down in 50 °C using water bath. Approximate 25 mL of the agar solution were poured into sterile 90-mm petri dishes. The agar plates were left at room temperature for 30 minutes to solidify and air-dried in biosafety cabinet. The plates were stored at 4°C until use.

#### **2. LB-Ampicillin (LB-A) broth**

LB-A broth was freshly prepared before use. The stock ampicillin solution (General drug house, Thailand) was added to LB broth to final concentration 100 µg/mL.

#### **3. LB-A agar**

LB agar solution was prepared as previously described. After cooling down, the stock ampicillin solution was added to final concentration 100 µg/mL. The agar solution was mixed by swirling and poured 25 mL into sterile 90-mm petri dishes. The plates were left at room temperature for 30 minutes for solidify. The plates were air-dried in biosafety cabinet before storing at 4 °C until use.

#### **4. LB-A agar supplemented with IPTG/X-Gal**

Prior to bacterial transformation, 100 µL of 100 mM IPTG and 40 µL of 5% (w/v) X-Gal were spread on moist LB-A agar, and allowed to dry at room temperature. The agar plates were then ready to use.

## APPENDIX C

### CHEMICAL REAGENTS FOR IMMUNOFLUORESCENCE

#### 1. **4% paraformaldehyde (PFA) solution**

Two grams of paraformaldehyde were dissolved in 40 mL of 1× PBS and mixed gently on magnetic stirrer hot plate. 1N NaOH was gradually added until the PFA solution became clear. Volume was filled up to 50 mL with 1× PBS. The solution was sterilized by filtration and kept as aliquots in  $-20\text{ }^{\circ}\text{C}$ .

#### 2. **0.1% Triton X-100 solution**

Fifty microliters of 100% Triton X-100 were added into 50 mL of 1× PBS and mixed thoroughly using vortex. The solution was sterilized by filtration and kept at room temperature

#### 3. **5% bovine serum albumin (BSA) solution**

Bovine serum albumin (Capricorn scientific, USA) 2.5 g were dissolved in 1× PBS and mixed using vortex. The 5% BSA solution was sterilized by filtration and kept at  $4\text{ }^{\circ}\text{C}$ .

#### 4. **1% bovine serum albumin (BSA) solution**

The solution was prepared by diluting 1 in 5 of 5 % BSA in 1× PBS and kept at  $4\text{ }^{\circ}\text{C}$ .

## APPENDIX D

### CHEMICAL REAGENTS FOR PROTEIN ASSAYS

#### 1. **6× SDS-gel reducing loading buffer**

To prepare 10 mL of 6× SDS-gel reducing loading buffer, the components including 0.6 mg of SDS, 0.5 mg of bromophenol blue, 3.75 mL of 0.5 M Tris-HCl, pH 8.8, 4.6 mL of glycerol, and 1.5 mL of β-mercaptoethanol (BME) were mixed on magnetic stirrer. The volume of the preparation was made up to 10 mL by adding UDW. The complete 6× sample buffer was kept in a 1 mL-aliquot at -20 °C. For SDS-PAGE, one part of 6× sample buffer was diluted with five parts of sample and heated at 100 °C for 5 minutes before loading to the gel.

#### 2. **2× buffer G (50 mM Na-HEPES, 150 mM NaCl, 1 mM EDTA, pH 7.4)**

To prepare 500 mL of 2× buffer G, the components including 50 mL of 1 M Na-HEPES, pH 7.4, 50 mL of 3 M NaCl, and 2 mL of 0.5 M EDTA were mixed on magnetic stirrer. The volume was filled up to 500 mL with UDW. The buffer solution was sterilized by filtration and kept at 4 °C.

#### 3. **1× lysis buffer (1× buffer G, 0.5% Triton X-100, 10% glycerol)**

The buffer was prepared by adding 25 mL of 2×buffer G, 0.25 mL of 100% Triton X-100, 6.25 mL of 80% glycerol. The volume was filled up to 50 mL by UDW. Protease inhibitor cocktail (50×) (Promega) was added to the desired volume of 1× lysis buffer at final concentration 1× when use.

#### 4. **Wash buffer 1 (1× buffer G, 0.5% Triton X-100, 5% glycerol)**

The buffer was prepared freshly by adding 25 mL of 2×buffer G, 0.25 mL of 100% Tritox X-100, and 3.125 mL of 80% glycerol. The volume was filled up to 50 ml by UDW.



**5. Wash buffer 2 (1× buffer G, 5% glycerol)**

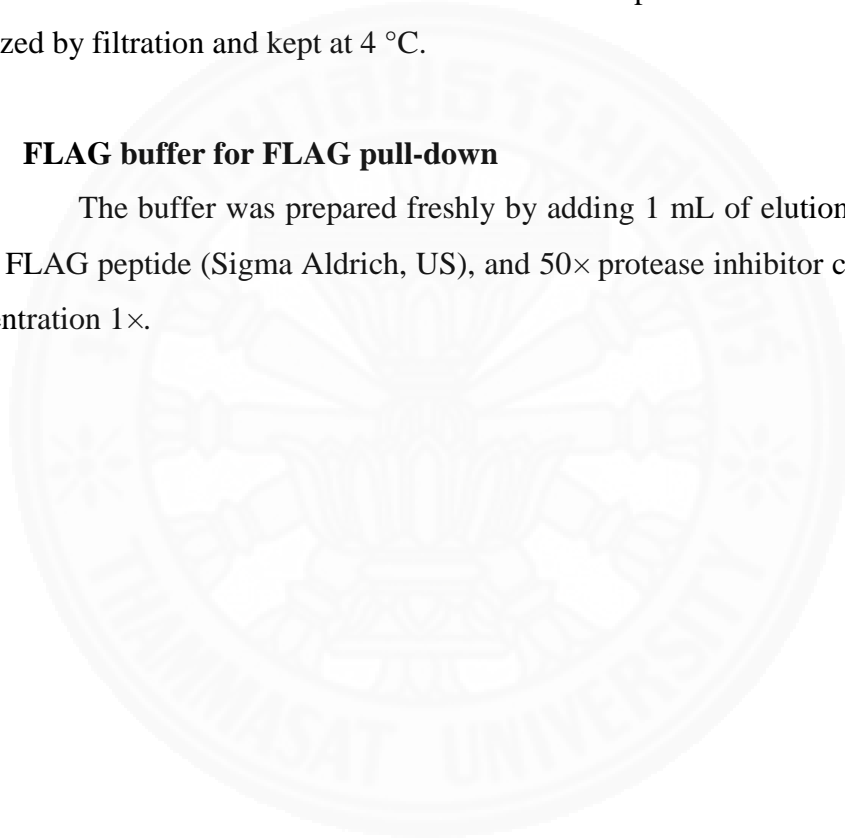
The buffer was prepared freshly by adding 25 mL of 2×buffer G and 3.125 mL of 80% glycerol. The volume was filled up to 50 mL by UDW.

**6. Elution buffer for FLAG pull-down (25 mM Na-HEPES, 100 mM NaCl, pH 7.4)**

The buffer was prepared by adding 2.5 mL of 1 M Na-HEPES and 3.33 mL of 3 M NaCl solution. The volume was filled up to 100 mL. The buffer was sterilized by filtration and kept at 4 °C.

**7. FLAG buffer for FLAG pull-down**

The buffer was prepared freshly by adding 1 mL of elution buffer, 40 µL of 3× FLAG peptide (Sigma Aldrich, US), and 50× protease inhibitor cocktail to final concentration 1×.



## APPENDIX E

### BASIC TECHNIQUES IN MOLECULAR BIOLOGY

#### 1. Conventional polymerase chain reaction (PCR)

PCR master mixture was prepared as follows.

Component	Volume
Ultrapure distilled water (UDW)	Top up to 20 $\mu$ L
10 $\times$ Reaction buffer	2 $\mu$ L
20 mM MgCl <sub>2</sub>	2 $\mu$ L
10 mM dNTPs (2.5 mM each)	2 $\mu$ L
Forward primer (10 pmol/ $\mu$ L)	1 $\mu$ L
Reverse primer (10 pmol/ $\mu$ L)	1 $\mu$ L
<i>Taq</i> or <i>ProFi Taq</i> DNA polymerase (5 units/ $\mu$ L)	0.1 $\mu$ L
DNA template	1-500 ng

Thermal cycles of the PCR were performed as follows.

Step	Temperature ( $^{\circ}$ C)	Time	Cycle
Pre-denaturation	95	5 minutes	1 cycle
Denaturation	95	30-60 seconds	} 30 cycles
Annealing	45-65	30-60 seconds	
Extension	68	1 minute/kb	
Final extension	68	3-5 minutes	1 cycle

#### 2. Agarose gel electrophoresis

Agarose powder (AXYGEN, Spain) was dissolved in 0.5 $\times$  TBE buffer in the desired percentage concentration and melted by using microwave. The polymerization of agarose was allowed to occur in gel casting apparatus at room temperature. Samples were prepared in 10 $\times$  DNA loading dye and loaded into well. The gel electrophoresis was performed in 0.5 $\times$  TBE buffer at 100 voltages. Then, the

gel was stained with ethidium bromide solution, rinsed with reverse osmosis (RO) water, and visualized under UV light using SYNGENE Gene Flash Bio Imaging gel documentation.

### **3. Gel purification**

The DNA fragments were resolved in 1% agarose gel running at 100 voltages. The expected band of the fragment was excised from agarose gel and purified following AccuPrep<sup>®</sup> Gel Purification Kit protocol (Bioneer, Korea). The purified DNA fragments were detected using agarose gel electrophoresis and ethidium bromide staining.

### **4. Preparation of competent *E. coli* (calcium chloride treatment)**

A bacterial starter was prepared by inoculating a single bacterial colony of JM109 *E. coli* into 2 mL of Luria-Bertani (LB) broth (**Appendix B**) supplemented with ampicillin at final concentration 100 µg/mL (LB-A) and growing at 37 °C for 16 hours with shaking at 250 rpm. One percentage (v/v) of the bacterial culture was prepared by adding 200 µL of the saturated culture of bacterial starter into 20 mL of LB-A at 37 °C with shaking at 250 rpm until the optical density (OD) at A<sub>600nm</sub> was approximately 0.4-0.6 which is at log phase of bacteria. The culture was kept on ice for 15-20 minutes before harvesting by centrifugation at 7,000 rpm for 5 minutes at 4 °C. After decanting the supernatant, the bacterial cells were resuspended in 10 mL of 100 mM ice-cold magnesium chloride (MgCl<sub>2</sub>) and recovered the bacterial cells by centrifugation at 7,000 rpm for 5 minutes at 4 °C. Then, the bacterial cells were resuspended in 2 mL of 100 mM ice-cold calcium chloride (CaCl<sub>2</sub>) and kept on ice for 1 hour. At this point, the competent cells could be directly used for transformation or kept as 100 µL/aliquot in 20% (v/v) sterile glycerol at -80 °C.

### **5. Transformation of competent *E. coli* and clone selection**

The JM109 *E. coli* competent cells were transformed by heat-shock method. Ten microliters of ligation reaction were added into 100 µL of the bacterial competent cells. After mixing gently, the tube was kept on ice for 30 minutes. The tube was transferred to a floating rack placed in water bath with conditioned

temperature at 42 °C and incubated for 2 minutes exactly. Then, the tube was immediately transferred to ice bath and incubated for 30 minutes. Following that, 1 mL of LB broth was added into the tube and incubated at 37 °C with gently shaking allowing bacteria to recover and express an antibiotic resistant marker encoded by the plasmid. To select transformant, 100 µL of the transformed competent *E. coli* was spread on LB-A agar plate as a low bacterial density plate, while the remaining 900 µL of the transformed competent *E. coli* was centrifuged at 13,000 rpm for 2 minutes, decanted the supernatant, and spread the resuspended bacterial cells on the LB-A agar plate as a high bacterial density plate. Thereafter, the plates were incubated at 37 °C for 16 hours. Additionally, for plasmid containing *lacZ* promotor, LB-A agar was supplemented with IPTG and X-Gal (**Appendix B**) for blue-white screening. The presence of the inserted DNA fragment was screened by direct colony PCR using plasmid specific primers prepared as shown in the below table, together with making replica plate for further use. The positive clones from screening were inoculated in 2 ml of LB-A broth and incubated at 37 °C with shaking at 250 rpm for 16 hours to keep as bacteria stocks in 20% (v/v) sterile glycerol stored in –80 °C.

## **6. Preparation of recombinant plasmid DNA**

A single colony from a streaked bacterial plate was inoculated in LB-A broth and incubated at 37 °C with shaking at 250 rpm for 16 hours. Three to five milliliters of bacterial culture was harvested for plasmid extraction using AccuPrep<sup>®</sup> Nano-Plus Plasmid Mini Extraction Kit protocol (Bioneer, Korea). The integrity of the extracted recombinant plasmid DNA was detected using 0.8% (w/v) agarose gel electrophoresis and ethidium bromide staining. The purity and concentration of the plasmid were measured by spectrophotometry.

## APPENDIX F

### 1. Pull down of FLAG-3A-mCherry protein in SH-SY5Y cells

Protein fractions including cell lysate prepared from pLVX::FLAG-3A-mCherry transfected SH-SY5Y cells (L), flow through (FT), last washing fraction (W), and elutes 1-3 (E1-E3, respectively), were resolved in 12% SDS-PAGE followed by western blot analysis using mouse monoclonal anti-FLAG<sup>®</sup> M2 antibody (**Figure F.1**). The faint bands of FLAG-3A-mCherry present in cell lysate corresponding to relative migration of the protein in denaturing condition (~26-30 kDa) as described in **Section 5.3.6** were indicated by red bracket. After pull down, only one distinct band of FLAG-3A-mCherry at approximately 26 kDa was detected in eluate fractions indicated by arrow. Thus, FLAG-3A-mCherry could be precipitated by anti-FLAG<sup>®</sup> M2 magnetic beads and could be further examined for 3A-interacting proteins by LC-MS/MS.

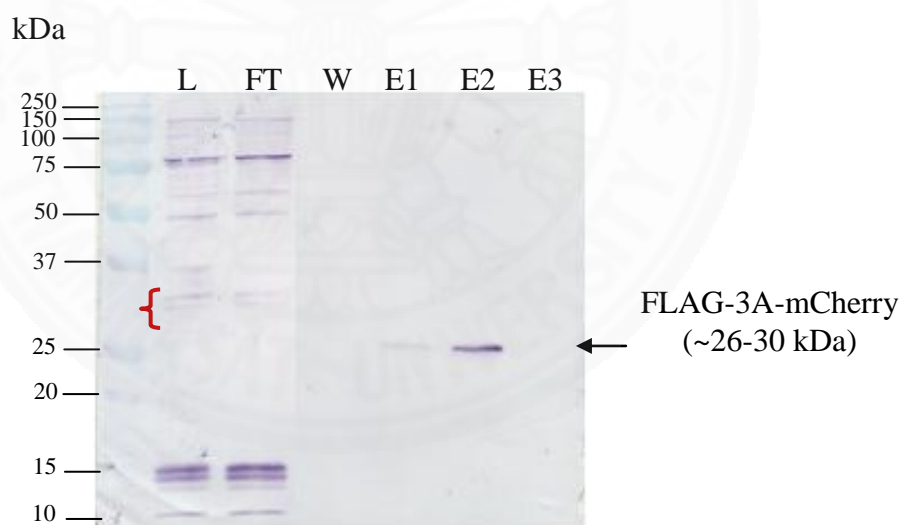


**Figure F.1** Detection of FLAG-3A-mCherry protein from pull down. L; cell lysate prepared from pLVX::FLAG-3A-mCherry transfected SH-SY5Y cells, FT; flow through, W; last washing fraction, E1-E3, eluates 1-3, respectively. The protein fractions were resolved in 12% SDS-PAGE and immunoblotted with mouse monoclonal anti-FLAG<sup>®</sup> M2 antibody. The molecular mass markers (in kilodaltons, kDa) are indicated to the left of the membranes.

## APPENDIX G

### 1. Prediction of trypsin cleavage sites of FLAG-3A-mCherry sequence by PeptideCutter program

#### Amino acid sequence of FLAG-3A-mCherry (331 aa)

```

1   MDYKDDDDKG PPKFRPIRIS LEEKPAPDAI SDLLASVDSE
41  EVRQYCREQG WIIPETPTNV ERHLNRAVLV MQSIATVVAV
81  VSLVYVIYKL FAGFQMVSKG EEDNMAIIKE FMRFKVHMEG
121 SVNGHEFEIE GEGEGRPYEG TQTAKLKVTK GGPLPFAWDI
161 LSPQFMYGSK AYVKHPADIP DYLKLSFPEG FKWERVMNFE
201 DGGVVTVTQD SSLQDGEFIY KVKLRGTNFP SDGPVMQKKT
241 MGWEASSERM YPEDGALKGE IKQRLKLDKG GHYDAEVKTT
281 YKAKKPVQLP GAYNVNIKLD ITSHNEDYTI VEQYERAAGR
321 HSTGGMDELY K

```

#### Amino acid position

```

1-9      =   FLAG
10-95    =   EV-A71 3A
96-331   =   mCherry

```

There were 39 positions in the FLAG-3A-mCherry sequence that were predicted as trypsin cleavage sites. The predicted positions, amino acid sequences, lengths and masses of the cleaved peptides were listed in **Table G.1**.

**Table G.1** Prediction of trypsin cleavage sites on FLAG-3A-mCherry by PeptideCutter

Position of cleavage site	Resulting peptide sequence	Peptide length [aa]	Peptide mass [Da]
4	MDYK	4	555.647
9	DDDDK	5	606.544
13	GPPK	4	397.475

**Table G.1** Prediction of trypsin cleavage sites on FLAG-3A-mCherry by PeptideCutter (cont.)

<b>Position of cleavage site</b>	<b>Resulting peptide sequence</b>	<b>Peptide length [aa]</b>	<b>Peptide mass [Da]</b>
18	FRPIR	5	687.843
43	ISLEEKPAPDAISDLL ASVDSEEVR	25	2683.949
47	QYCR	4	568.648
62	EQGWIIPETPTNVER	15	1768.944
66	HLNR	4	538.607
89	AVLVMQSIATVVAVVS LVYVIYK	23	2466.061
99	LFAGFQMVSK	10	1127.367
109	GEEDNMAIIK	10	1119.255
113	EFMR	4	581.687
115	FK	2	293.366
145	VHMEGSVNGHEFEIEG EGEGRPYEGTQTAK	30	3275.467
147	LK	2	259.349
150	VTK	3	346.427
170	GGPLPFAWDILSPQFM YGSK	20	2211.563
174	AYVK	4	479.577
184	HPADIPDYLK	10	1168.315
192	LSFPEGFK	8	924.064
195	WER	3	489.531
221	VMNFEDGGVVTVTQDS SLQDGEFIYK	26	2879.145
223	VK	2	245.322
225	LR	2	287.362



**Table G.1** Prediction of trypsin cleavage sites on FLAG-3A-mCherry by PeptideCutter (cont.)

<b>Position of cleavage site</b>	<b>Resulting peptide sequence</b>	<b>Peptide length [aa]</b>	<b>Peptide mass [Da]</b>
238	GTNFPSDGPVMQK	13	1377.535
239	K	1	146.189
249	TMGWEASSER	10	1153.232
258	MYPEDGALK	9	1023.169
262	GEIK	4	445.516
264	QR	2	302.333
266	LK	2	259.349
268	LK	2	259.349
278	DGGHYDAEVK	10	1090.114
282	TTYK	4	511.576
284	AK	2	217.268
298	KPVQLPGAYNVNIK	14	1540.826
316	LDITSHNEDYTIVEQY ER	18	2225.353
320	AEGR	4	431.449
	HSTGGMDELYK	11	1237.350

**2. Prediction of trypsin cleavage sites of EV-A71 polyprotein by PeptideCutter program**

Amino acid sequence of EV-A71 polyprotein (2193 aa)

```

1    MGSQVSTQRS GSHENSNSAT EGSTINYTTI NYKDSYAAT
41   AGKQSLKQDP DKFANPVKDI FTEMAAPLKS PSAEACGYSD
81   RVAQLTIGNS TITTQEAANI IVGYGEWPSY CSDDDATAVD
121  KPTRPDVSVN RFYTLDTKLW EKSSKGWYWK FPDVLTETGV
161  FGQNAQFHYL YRSGFCIHVQ CNASKFHQGA LLVAILPEYV
201  IGTVAGGTGT EDSHPPYKQT QPGADGFELQ HPYVLDAGIP
241  ISQLTICPHQ WINLRTNNCA TIIIVPYMNTL PFDSALNHCN
281  FGLLVVPISP LDFDQGATPV IPITITLAPM CSEFAGLRQA
321  VTQGFPTPEK PGTNQFLTTD DGVSAPILPN FHPTPCIHIP
361  GEVRNLLLELC QVETILEVNN VPTNATSLME RIRFPVSAQA
401  GKGELCAVFR ADPGRNGPWQ STLLGQLCGY YTQWSGSLEV
441  TFMFTGSFMA TGKMLIAYTP PGGPLPKDRA TAMLGTHVIW
481  DFGLQSSVTL VIPWISNTHY RAHARDGVFD YYTTGLVSIW
521  YQTNVVPVPIG APNTAYIIAL AAAQKNFTMK LCKDTSHILQ
561  TASIQGDRVA DVIESSIGDS VSRALTRALP APTGQNTQVS
601  SHRLDTGEVP ALQAAEIGAS SNTSDESMIE TRCVLNHSHST
641  AETTLDSFFS RAGLVGEIDL PLEGTTPNG YANWDIDITG
681  YAQMRRKVEL FTYMRFDAEF TFVACTPTGE VVPQLLQYMF
721  VPPGAPKPDS RESLAWQTAT NPSVFVKLTD PPAQVSVPFM
761  SPASAYQWFY DGYPTFGEHK QEKDLEYGAC PNNMMGTFSV
801  RTVGSSSKSKY PLVVRIYMRM KHVRAWIPRP MRNQNYLFKA
841  NPNYAGNSIK PTGTSRTAIT TLGKFGQQSG AIYVGNFRVV
881  NRHLATHNDW ANLVWEDSSR DLLVSSTTAQ GCDTIARCDC
921  QTGVYYCNSK RKHYVVSFSK PSLIYVEASE YYPARYQSHL
961  MLAAGHSEPG DCGGILRCQH GVVGIVSTGG NGLVGFADVR
1001 DLLWLDEEAM EQGVSDYIKG LGDAFGTGFT DAVSREVEAL
1041 RNHLIGSDGA VEKILKNLIK LISALVIVIR SDYDMVTLTA
1081 TLALIGCHGS PWAWIKAKTA SILGIPIAQK QSASWLKFFN
1121 DMASAAKGLE WISNKISKFI DWLREKIVPA AREKAEFLTN

```

1161 LKQLPLENQ ITNLEQSAAS QEDLEAMFGN VSYLAHFCRK  
 1201 FQPLYATEAK RYVYLEKRMN NYMQFKSKHR IEPVCLIIRG  
 1241 SPGTGKSLAT GIIARAIADK YHSSVYSLPP DPDHFDGYKQ  
 1281 QVVTVMDDLC QNPDGKDMSL FCQMVSTVDF IPPMASLEEK  
 1321 GVSFTSKFVI ASTNSSNIIV PTVSDSDAIR RRFYMDCDIE  
 1361 VTDSYKTDLG RLDAGRAAKL CSENNTANFK RCSPLVCGKA  
 1401 IQLRDRKSKV RYSVDTVVSE LIREYNSRSA IGNTIEALFQ  
 1441 GPPKFRPIRI SLEEKPAFDA ISDLLASVDS EEVRQYCREQ  
 1481 GWIIPETPIN VERHLNRAVL VMQSIATVVA VVSLVYVIYK  
 1521 LFAGFQGAYS GAPKQVLRKP VLRTATVQGP SLDFALSLLR  
 1561 RNIRQVQTDQ GHFTMLGVRD HLAVLPRHAQ PGKTIWVEHK  
 1601 LVNVLDAREL VDEQGVNLEL TLVTLDTNEK FRDITKFIPE  
 1641 TISGASDATL VINTEHMPSM FVPVGDVVQY GFLNLSGKPT  
 1681 HRTMMYNFPT KAGQCGGVVT SVGKIVGIHI GGNGRQGFCA  
 1721 GLKRSYFASV QGEIQWVKS N KETGRLNING PTRTKLEPSV  
 1761 FHDVFKGSKE PAVLTSKDPR LEVDFEQALF SKYVGNVLHE  
 1801 PDEYVTQAAL HYANQLKQLD INTSKMSMEE ACYGTENLEA  
 1841 IDLCTSAGYP YSALGIKKRD ILDPVTRDVS KMKFYMDKYG  
 1881 LDLPYSTYVK DELRPLDKIK KGKSRLIEAS SLNDSVYLRM  
 1921 TFGHLYEVFH ANPGTVTGS A VGCNPDVFW S KLPILLPGSL  
 1961 FAFDYSGYDA SLSPVWFRAL EVVLREIGYT EEAVSLIEGI  
 2001 NHTHHVYRNK TYCVLGGMPS GCSGTSIFNS MINNIIIRTL  
 2041 LIKTFKGIDL DELNMVAYGD DVLASYPFPI DCLELAKTGK  
 2081 EYGLTMTPAD KSPCFNEVTW ENATFLKRGF LPDHQFPFLI  
 2121 HPTMPMREIH ESIRWTKDAR NTQDHVRS LC LLAWHNGKDE  
 2161 YEKFVSTIRS VPVGKALAI P SFENLRRNWL ELF

**Amino acid position of each viral mature protein**

1-69 = VP4  
 70-323 = VP2  
 324-565 = VP3  
 566-862 = VP1

863-1012	=	2A
1013-1111	=	2B
1112-1440	=	2C
1441-1526	=	3A
1527-1548	=	3B
1549-1731	=	3C
1732-2193	=	3D

There were 194 positions in amino acid sequence of EV-A71 polyprotein that were predicted as trypsin cleavage sites. The predicted positions, amino acid sequences, lengths and masses of the cleaved peptides were listed in **Table G.2**.

**Table G.2** Prediction of trypsin cleavage sites on EV-A71 polyprotein by PeptideCutter

Position of cleavage site	Resulting peptide sequence	Peptide length [aa]	Peptide mass [Da]
9	MGSQVSTQR	9	993.103
34	SGSHENSNSATEGSTI NYTTINYYK	25	2738.817
43	DSYAATAGK	9	882.926
47	QSLK	4	474.558
52	QDPDK	5	601.614
58	FANPVK	6	674.798
69	DIFTEMAAPLK	11	1235.461
81	SPSAEACGYSDR	12	1242.282
131	VAQLTIGNSTITTQEA ANIIVGYGEWPSYCSD DDATAVDKPTRPDVSV NR	50	5340.818
138	FYTLDTK	7	887.000
142	LWEK	4	574.677

**Table G.2** Prediction of trypsin cleavage sites on EV-A71 polyprotein by PeptideCutter (cont.)

<b>Position of cleavage site</b>	<b>Resulting peptide sequence</b>	<b>Peptide length [aa]</b>	<b>Peptide mass [Da]</b>
145	SSK	3	320.346
150	GWYWK	5	738.844
172	FPDVLLETGVFGQNAQ FHYLYR	22	2602.888
185	SGFCIHVQCNASK	13	1393.598
218	FHQGALLVAILPEYVI GTVAGGTGTEDSHPPY K	33	3438.885
255	QTQPGADGFELQHPYV LDAGIPISQLTICPHQ WINLR	37	4157.716
318	TNNCATIIVPYMNTLP FDSALNHCNFGLLVVP ISPLDFDQGATPVIPI TITLAPMCSEF AGLR	63	6749.893
364	QAVTQGFPTPEPKPGTN QFLTDDGVVSAPILPN FHPTPCIHIPGEVR	46	4926.538
391	NLLELCQVETILEVNN VPTNATSLMER	27	3044.485
393	IR	2	287.362
402	FPVSAQAGK	9	904.034
410	GELCAVFR	8	894.056
415	ADPGR	5	514.539
453	NGPWQSTLLGQLCGYY TQWSGSLEVTFMFTGS FMATGK	38	4195.748
467	MLIAYTPPGGPLPK	14	1454.791
469	DR	2	289.291

**Table G.2** Prediction of trypsin cleavage sites on EV-A71 polyprotein by PeptideCutter (cont.)

<b>Position of cleavage site</b>	<b>Resulting peptide sequence</b>	<b>Peptide length [aa]</b>	<b>Peptide mass [Da]</b>
501	ATAMLGTHVIWDFGLQ SSVTLVIPWISNTHYR	32	3615.167
505	AHAR	4	453.501
545	DGVFDYYTTGLVSIWY QTNYVVPIGAPNTAYI IALAAAQK	40	4368.953
550	NFTMK	5	639.767
568	LCKDTSHILQTASIQG DR	18	1986.230
583	VADVIESSIGDSVSR	15	1533.656
587	ALTR	4	459.546
603	ALPAPTQNTQVSSHR	16	1663.811
632	LDTGEVPALQAAEIGA SSNTSDESMIETR	29	2993.203
651	CVLNSHSTAETTLDSF FSR	19	2115.302
685	AGLVGEIDLPLEGTTN PNGYANWDIDITGYAQ MR	34	3666.033
686	R	1	174.203
687	K	1	146.189
695	VELFTYMR	8	1058.261
731	FDAEFTFVACTPTGEV VPQLLQYMFVPPGAPK PDSR	36	3956.543
747	ESLAWQTATNPSVFVK	16	1777.995
780	LTDPPAQVSVPFMSPA SAYQWFYDGYPTFGEH K	33	3735.141

**Table G.2** Prediction of trypsin cleavage sites on EV-A71 polyprotein by PeptideCutter (cont.)

<b>Position of cleavage site</b>	<b>Resulting peptide sequence</b>	<b>Peptide length [aa]</b>	<b>Peptide mass [Da]</b>
783	QEK	3	403.436
801	DLEYGACPNMMGTFS VR	18	2005.266
807	TVGSSK	6	577.635
809	SK	2	233.268
815	YPLVVR	6	745.920
819	IYMR	4	581.731
821	MK	2	277.382
824	HVR	3	410.476
832	AWIPRPMR	8	1026.268
839	NQNYLFK	7	926.040
856	ANPNYAGNSIKPTGTS R	17	1747.885
864	TAITTLGK	8	803.954
878	FGQSGAIYVGNFR	14	1543.702
882	VVNR	4	486.572
900	HLATHNDWANLVWEDS SR	18	2151.282
917	DLLVSSTTAQGCDTIA R	17	1750.941
930	CDCQTGVYYCNSK	13	1483.649
931	R	1	174.203
932	K	1	146.189
955	HYPVSEFSKPSLIYVEA SEYYPAR	23	2704.034



**Table G.2** Prediction of trypsin cleavage sites on EV-A71 polyprotein by PeptideCutter (cont.)

<b>Position of cleavage site</b>	<b>Resulting peptide sequence</b>	<b>Peptide length [aa]</b>	<b>Peptide mass [Da]</b>
977	YQSHMLAAGHSEPGD CGGILR	22	2312.603
1000	CQHG VVGIVSTGGNGL VGFADVR	23	2242.538
1019	DLLWLDEEAMEQGVSD YIK	19	2254.493
1035	GLGDAFGTGFTDAVSR	16	1570.679
1041	EVEALR	6	715.805
1053	NHLIGSDGAVEK	12	1239.351
1056	ILK	3	372.508
1060	NLIK	4	486.612
1070	LISALVIVIR	10	1096.422
1096	SDYDMVTLTATLALIG CHGSPWAWIK	26	2850.300
1098	AK	2	217.268
1110	TASILGIPIAQK	12	1211.467
1117	QSASWLK	7	818.928
1118	K	1	146.189
1127	FNDMASAAK	9	954.066
1135	GLEWISNK	8	946.071
1138	ISK	3	346.427
1144	FIDWLR	6	849.000
1146	EK	2	275.305
1152	IVPAAR	6	625.769
1154	EK	2	275.305
1162	AEFLTNLK	8	935.088

**Table G.2** Prediction of trypsin cleavage sites on EV-A71 polyprotein by PeptideCutter (cont.)

<b>Position of cleavage site</b>	<b>Resulting peptide sequence</b>	<b>Peptide length [aa]</b>	<b>Peptide mass [Da]</b>
1200	QLPLLENQITNLEQSA ASQEDLEAMFGNVSYL AHFCRK	38	4309.835
1210	FQPLYATEAK	10	1167.327
1211	R	1	174.203
1217	VYVLEK	6	749.905
1218	R	1	174.203
1226	MNNYMQFK	8	1075.265
1228	SK	2	233.268
1230	HR	2	311.344
1239	IEPVCLIIIR	9	1055.344
1246	GSPGTGK	7	602.645
1255	SLATGIIAR	9	901.074
1260	AIADK	5	516.595
1279	YHSSVYSLPPDPDHF D GYK	19	2224.371
1296	QQVVTVMDDL CQNP DG K	17	1890.113
1320	DMSLFCQMVSTVDFIP P MASLEEK	24	2719.193
1327	GVSFTSK	7	724.812
1350	FVIASTNSSNIIVPTV S DSDAIR	23	2406.675
1352	RR	2	330.390
1366	FYMDCDIEVTD SYK	14	1728.906
1371	TDLGR	5	560.608
1376	LDAGR	5	530.581

**Table G.2** Prediction of trypsin cleavage sites on EV-A71 polyprotein by PeptideCutter (cont.)

<b>Position of cleavage site</b>	<b>Resulting peptide sequence</b>	<b>Peptide length [aa]</b>	<b>Peptide mass [Da]</b>
1379	AAK	3	288.347
1390	LCSENNTANFK	11	1240.353
1391	R	1	174.203
1399	CSPLVCGK	8	806.006
1404	AIQLR	5	599.731
1406	DR	2	289.291
1407	K	1	146.189
1409	SK	2	233.268
1411	VR	2	273.335
1423	YSVDTVVSELIR	12	1380.561
1428	EYNSR	5	667.676
1444	SAIGNTIEALFQGPPK	16	1642.872
1449	FRPIR	5	687.843
1474	ISLEEKPA PD A I S D L L ASVDSEEV R	25	2683.949
1478	QYCR	4	568.648
1493	EQGW I I P E T P I N V E R	15	1780.998
1497	HLNR	4	538.607
1520	AVLVMQSIATVVAVVS LVYVIYK	23	2466.061
1534	LFAGFQ G A Y S G A P K	14	1413.596
1538	QVLR	4	514.625
1543	KPVL R	5	611.786
1560	TATVQGPSLDFALSLL R	17	1789.062

**Table G.2** Prediction of trypsin cleavage sites on EV-A71 polyprotein by PeptideCutter (cont.)

<b>Position of cleavage site</b>	<b>Resulting peptide sequence</b>	<b>Peptide length [aa]</b>	<b>Peptide mass [Da]</b>
1561	R	1	174.203
1564	NIR	3	401.466
1579	QVQTDQGHFTMLGVR	15	1716.932
1587	DHLAVLPR	8	920.079
1593	HAQPGK	6	636.709
1600	TIWVEHK	7	912.056
1630	LVNVLDAVELVDEQGV NLELTLVTLDTNEK	30	3296.717
1632	FR	2	321.379
1636	DITK	4	475.542
1682	FIPETISGASDATLVI NTEHMPSMFVPVGDVV QYGFLNLSGKPTR	46	4974.681
1691	TMMYNFPTK	9	1132.358
1704	AGQCGGVVTSVGK	13	1162.326
1715	IVGIHIGNGR	11	1092.266
1723	QGFCAGLK	8	822.977
1724	R	1	174.203
1738	SYFASVQGEIQWVK	14	1641.844
1741	SNK	3	347.371
1745	ETGR	4	461.475
1753	LNINGPTR	8	884.003
1755	TK	2	247.294
1766	LEPSVFHDVFK	11	1317.507
1769	GSK	3	290.319

**Table G.2** Prediction of trypsin cleavage sites on EV-A71 polyprotein by PeptideCutter (cont.)

<b>Position of cleavage site</b>	<b>Resulting peptide sequence</b>	<b>Peptide length [aa]</b>	<b>Peptide mass [Da]</b>
1777	EPAVLTSK	8	843.976
1780	DPR	3	386.408
1792	LEVDFEQALFSK	12	1425.601
1817	YVGNVLHEPDEYVTQA ALHYANQLK	25	2873.174
1825	QLDINTSK	8	918.015
1857	MSMEEACYGTENLEAI DLCTSAGYPYSALGIK	32	3431.864
1858	K	1	146.189
1859	R	1	174.203
1867	DILDVTR	8	928.053
1871	DVSK	4	447.489
1873	MK	2	277.382
1878	FYMDK	5	702.823
1890	YGLDLPYSTYVK	12	1418.609
1898	DELRPLDK	8	985.105
1900	IK	2	259.349
1901	K	1	146.189
1903	GK	2	203.241
1905	SR	2	261.281
1919	LIEASSLNDSVYLR	14	1579.770
1951	MTFGHLYEVFHANPGT VTGSAVGCNPDVFSK	32	3469.894
1978	LPILLPGSLFAFDYSG YDASLSPVWFR	27	3032.488

**Table G.2** Prediction of trypsin cleavage sites on EV-A71 polyprotein by PeptideCutter (cont.)

<b>Position of cleavage site</b>	<b>Resulting peptide sequence</b>	<b>Peptide length [aa]</b>	<b>Peptide mass [Da]</b>
1985	ALEVVL	7	798.981
2008	EIGYTEEA	23	2667.918
	AVSLIEGIN		
	HTHHVYR		
2010	NK	2	260.293
2038	TYCVLGGMP	28	2949.466
	SGCSGTS		
	IFNSMINNIIIR		
2043	TLLIK	5	586.773
2046	TFK	3	394.471
2077	GIDLDELNM	31	3400.860
	VAYGDDV		
	LASYPFPIDCLELAK		
2080	TGK	3	304.346
2091	EYGLTMT	11	1225.379
	PKADK		
2107	SPCFNEVT	16	1886.109
	WENATFLK		
2108	R	1	174.203
2127	GFLPDHQ	19	2281.721
	FPFLIHPTM		
	PMR		
2134	EIHESIR	7	882.972
2137	WTK	3	433.508
2140	DAR	3	360.370
2147	NTQDHVR	7	868.905
2158	SLCLLAW	11	1241.473
	HNGK		
2163	DEYEK	5	682.685
2169	FVSTIR	6	721.855
2175	SVPVGK	6	585.701
2186	ALAI	11	1230.429
	PSFENLR		
2187	R	1	174.203
	NWLELF	6	820.943

### 3. Prediction of EV-A71 2A<sup>pro</sup> and 3C<sup>pro</sup> cleavage sites on human trypsinogen PRSS3 variant 3 (PRSS3-V3)

#### Amino acid sequence of PRSS3-V3 (261 aa)

```

1   MHMRETSGFT LKKGRSAPLV FHPPDALIAV PFDDDDKIVG
41  GYTCEENSLP YQVSLNSGSH FCGGSLISEQ WVVSAAHCYK
81  TRIQVRLGEH NIKVLEGNEQ FINAAKIIRH PKYNRDTLDN
121 DIMLIKLSPP AVINARVSTI SLPTAPPAAG TECLISGWGN
161 TLSFGADYPD ELKCLDAPVL TQAECKASYP GKITNSMFCV
201 GFLEGGKDSC QRDSGGPVVC NGQLQGVVSW GHGCAWKNRP
241 GVYTKVYNYV DWIKDTIAAN S

```

EV-A71 2A<sup>pro</sup> and 3C<sup>pro</sup> proteins are chymotrypsin-like proteases. The consensus motifs for enzymatic cleavage of the proteins are defined as P1 and P1' position. For EV-A71 2A<sup>pro</sup>, the preferential amino acid residues at P1 are threonine (T), tyrosine (Y), and phenylalanine (F) while amino acid at P1' is strict for glycine (G). For EV-A71 3C<sup>pro</sup>, P1 position is specific for glutamine (Q) while P1' is for glycine (G) > alanine (A) > serine (S).<sup>154</sup> Evaluation of cleavage sites of the EV-A71 proteases on PRSS3-V3 found that there are 1 cleavage site of 2A<sup>pro</sup> at amino acid position 164 (F-G) and 2 cleavage sites of 3C<sup>pro</sup> at position 182 (Q-A) and 225 (Q-G). The sequences, lengths and masses of the cleaved peptides were shown in **Tables G.3.1 and G.3.2**. The peptide masses were analyzed by DNAMAN program.



**Table G.3.1** Prediction of EV-A71 2A<sup>pro</sup> cleavage site on PRSS3-V3

Position of cleavage site	Resulting peptide sequence	Peptide length [aa]	Peptide mass [Da]
164	MHMRETSGFTLKKGRSAPLV FHPPDALIAVPFDDDDKIVG GYTCEENSLPYQVSLNSGSH FCGGSLISEQWVVSAAHCYK TRIQVRLGEHNIKVLEGNEQ FINAAKIIIRHPKYNRDTLDN DIMLIKLSPPAVINARVSTI SLPTAPPAAGTECLISGWN TLSF	164	17,900
	GADYPDELKCLDAPVLTQAE CKASYPGKITNSMFCVGFLE GGKDSCQRDSGGPVVCNGQL QGVVSWGHCACWKNRPGVYT KVYNYVDWIKDTIAANS	97	10,422

**Table G.3.2** Prediction of EV-A71 3C<sup>pro</sup> cleavage site on PRSS3-V3

Position of cleavage site	Resulting peptide sequence	Peptide length [aa]	Peptide mass [Da]
182	MHMRETSGFTLKKGRSAPLV FHPPDALIAVPFDDDDKIVG GYTCEENSLPYQVSLNSGSH FCGGSLISEQWVVSAAHCYK TRIQVRLGEHNIKVLEGNEQ FINAAKIIIRHPKYNRDTLDN DIMLIKLSPPAVINARVSTI SLPTAPPAAGTECLISGWN TLSFGADYPDELKCLDAPVL TQ	182	19,828
225	AECKASYPGKITNSMFCVGF LEGGKDSCQRDSGGPVVCNG QLQ	43	4,460
	GVVSWGHCACWKNRPGVYTK VYNYVDWIKDTIAANS	36	4,034

## BIOGRAPHY

**Name** Miss Pathaya Rattanakomol

**Date of Birth** 10<sup>th</sup> July 1992

**Place of Birth** Nonthaburi, Thailand

### Educational Attainment

2010-2013 Bachelor of Science (Medical Technology)  
with 1<sup>st</sup> class honor,  
Department of Medical Techonology,  
Faculty of Allied Health Sciences,  
Thammasat University, Thailand

2014-Present Ph.D. candidate in Doctor of Philosophy  
(Biomedical Sciences),  
Graduate Program in Biomedical Sciences,  
Faculty of Allied Health Sciences,  
Thammasat University, Thailand

**Scholarship** Ph.D. Scholarship, Thammasat University,  
Fiscal Year 2015-2018

**Home Address** 19/1 Moo 1, Prayabunlue, Ladbualuang,  
Phra Nakhon Si Ayutthaya, Thailand, 13230

**E-mail Address** k\_iis-z@hotmail.com

### Publication

1. Supasorn O, Tongtawe P, Srimanote P, **Rattanakomol P**, Thanongsaksrikul J. A nonstructural 2B protein of enterovirus A71 increases cytosolic Ca<sup>2+</sup> and induces apoptosis in human neuroblastoma SH-SY5Y cells. J Neurovirol. 2020 Apr 1;26(2):201–13.

**License**

1. License on Medical Technologist from The Medical Technology Council of Thailand (2014-Present)

**Training attended**

1. Student Intern (Medical Technology) at Nakhon Pathom Hospital, Nakhon Pathom, Thailand (January-March 2014)
2. Biosafety Training in Guidelines for Biological safety (Basic Course) , 26<sup>th</sup> March 2016, Thammasat University, Rangsit Campus, Pathum Thani, Thailand
3. Animal Ethics Training in Occupational Health and Safety in Laboratory Animal Care and Use, 20<sup>th</sup> January 2017, Thammasat University, Rangsit Campus, Pathum Thani, Thailand
4. Training Course on Digital EDGE Technology in Cell Imaging, 28<sup>th</sup> April 2017, Bangkok, Thailand
5. Training Course on Fluorescence Imaging for Material and Biomedical Sciences, 20<sup>th</sup>-21<sup>st</sup> July 2017, Bangkok, Thailand
6. Training Course on Diagnostic Techniques for Investigation of Influenza and Other Respiratory Viruses: Molecular Diagnosis, Virus Isolation, and Immunological Assay, 1<sup>st</sup> August 2017, Bangkok, Thailand
7. Training Course on Basic to Advance of Cell Culture Techniques, 27<sup>th</sup>-28<sup>th</sup> September 2017, Bangkok, Thailand

**Oral Presentation**

1. Patthaya Rattanakomol. Genes involved in prostaglandin synthesis and apoptosis in cholangiocarcinoma cells following exposure to cyclooxygenase inhibitors. Joint Symposium of BK21 PLUS of CUK and Thammasat University, College of Medicine, Catholic University of Korea, South Korea. January 2013.

**Poster Presentation**

1. Patthaya Rattanakomol, Thanuwat Boonmak, Peeraya Pladket, Jeeraphong Thanongsaksrikul. Determination of mitochondrial electron transport chain gene expression and apoptosis in EV-71-infected human neuronal cells. The 27<sup>th</sup> Thai Viro

meeting by The Virology Association (Thailand), Bangkok , Thailand. The 23<sup>rd</sup>-24<sup>th</sup> November 2017.

2. Patthaya Rattanakomol. Cell factory for producing enterovirus A71 nonstructural 3A protein. The 5<sup>th</sup> Joint Symposium of Thammasat University, BK21 PLUS of CUK and National Defense Medical Center, Thammasat University, Rangsit Campus, Pathum Thani, Thailand, 2018.

